




UNIVERSITAT POLITÈCNICA
DE CATALUNYA
BARCELONATECH



Proceedings of the
2012 Barcelona Forum on Ph.D. Research in
Communication and Information Technologies

**Departament de Teoria de Senyal
i Comunicacions**

Departament d'Enginyeria Electrònica

**Departament d'Arquitectura de
Computadors**

Departament d'Enginyeria Telemàtica

**Departament de Llenguatges
i Sistemes Informàtics**

October 15th, 2012
Campus Nord UPC—Aula Master—Edifici A3

<http://phdbarcelonaforum.upc.edu/>

Proceedings of the 2012 Barcelona Forum on Ph.D. Research in Communication and Information Technologies

October 15th, 2012

Campus Nord UPC—Aula Màster—Edifici A3

<http://phdbarcelonaforum.upc.edu/>

Editors: Xavier Masip, Xavier Aragonès, Jordi Forné, José Luis Balcázar, Alejandro Rodríguez-Gómez

Departament de Teoria de Senyal i Comunicacions

Departament d'Enginyeria Electrònica

Departament d'Arquitectura de Computadors

Departament d'Enginyeria Telemàtica

Departament de Llenguatges i Sistemes Informàtics

UNIVERSITAT POLITÈCNICA DE CATALUNYA - Barcelona Tech

Barcelona, October 2012

ISBN: 978-84-615-9915-8

© 2012 Universitat Politècnica de Catalunya.

Table of Contents

Foreword	
Thread Assignment of Network Applications in Multithreaded Processors: A Statistical Approach	1
Author: Petar Radojković, Thesis Director: Francisco J. Cazorla Thesis Advisers: Javier Verdú, Alex Pajuelo, Mario Nemirovsky	
Dynamic Data Partitioning for Distributed Graph Databases	3
Author: Xavier Martinez-Palau, Thesis Advisor(s): Josep Lluís Larriba-Pey, David Dominguez-Sal	
On the Scalability Limits of Communication Networks at the Nanoscale	5
Author: Ignacio Llatser, Thesis Advisors: Eduard Alarcón and Albert Cabellos-Aparicio	
CPU Accounting in the Multi-core and Multi-threaded Era	7
Author: Carlos Luque, Thesis Director: Francisco J. Cazorla Thesis Advisor(s): Miquel Moreto and Mateo Valero	
Characterization, design and re-optimization on multi-layer optical networks	9
Author: Marc Ruiz, Thesis Advisor(s): Luis Velasco	
Resonant Inductive Coupling Wireless Power Transfer	11
Author: Elisenda Bou Balust, Thesis Advisor(s): Eduard Alarcón Cot, Jordi Gutierrez Cabello	
Quality of Service Strategies for Heterogeneous Backbone Networks	13
Author: Joana Sócrates-Dantas, Thesis Advisor(s): Davide Careglio and Wilson Vicente Ruggiero Thesis Co-Advisor(s): Regina Melo Silveira and Josep Solé-Pareta	
Speech-in-speech hiding based on a bio-inspired model	15
Author: Dora Maria Ballesteros, Thesis Advisor: Juan Manuel Moreno Aróstegui	
A Contribution to Unobtrusive Measurement Methods For Sleep Monitoring using Magnetic Induction	17
Author: Hadiseh Mahdavi, Thesis Advisor: Prof. Javier Rosell Ferrer	
Opportunities for RF nanoelectronic integrated circuits using carbon-based technologies	19
Author: Gerhard M. Landauer, Thesis Advisor: José Luis Gonzalez	
Efficient implementation with FIR filters of operators based on B-splines to represent and classify signals of one and two dimensions	21
Author: Lluís Ferrer-Arnau, Thesis Advisor: Vicenç Parisi-Baradad	
Hardware Model of Large Spiking Neural Networks using Parallel NoCs	23
Author: Andres Gaona Barrera, Thesis Advisor: Manuel Moreno Arostegui	

2D/3D Simulation of Solar Cells.....	25
Author: David Carrió, Thesis Advisor(s): Ramon Alcubilla (Thesis Tutor), Pablo Ortega, Isidro Martín	
The Imbalance Element and Artificial Nervous System Design.....	27
Author: Paul Olivier, Thesis Advisor: Juan Manuel Moreno Aróstegui	
Study of energy efficiency in DC/AC grid-connected converters using multiplexed switches and adaptive control techniques.....	29
Author: R. Pérez Delgado, Thesis Advisor(s): M. Román Lumbreras, G. Velasco Quesada	
On Graphene Circuits.....	31
Author: Mario Iannazzo, Thesis Advisors: Eduard Alarcón (UPC), Max Lemme (KTH Stockholm)	
Design and Rapid Prototyping of Low-cost CMOS-MEMS Accelerometers.....	33
Author: Piotr Michalik, Thesis Advisors: Jordi Madrenas Boadas, Daniel Fernández Martínez	
Application of SIMD hardware implementations to bio-inspired systems.....	35
Author: Giovanni Sánchez Rivera, Thesis Advisor: Jordi Madrenas Boadas	
Multi-Phase Fault Tolerant Converters, Modulation Strategies and Fault Detection Schemes.....	37
Author: Mehdi Salehifar, Thesis Advisor(s): Juan Manuel Moreno, Vicent Sala	
Determining the state of charge and state of health of batteries.....	39
Author: Victòria Júlia Ovejas Benedicto, Thesis Advisor(s): Àngel Cuadras	
Assessment of trends in the cardiovascular system from time interval measurement using physiological signals obtained at the limbs.....	41
Author: Joan Gomez-Clapers, Thesis Advisors: Ramon Casanella, Ramon Pallas-Areny	
Fault Tolerant Vector Control of Five-Phase Permanent Magnet Motors.....	43
Author: Ramin Salehi Arashloo, Thesis Advisor: Prof. José Luis Romeral Martínez	
Satellite for Health: An architecture to provide E2E quality of service guarantees.....	45
Author: Elizabeth Rendón-Morales, Thesis Advisors: Jorge Mata-Díaz and Juanjo Alins	
Contribution to develop a communication framework for vehicular ad-hoc networks in urban scenarios.....	47
Author: Carolina Tripp Barba, Thesis Advisor: Mónica Aguilar Igartua	
Layer Discovery in the Recursive InterNetwork Architecture.....	49
Author: Eleni Trouva, Thesis Advisors: Eduard Grasa, Xavier Hesselbach Serra	
Privacy Protection of User Profiles in Personalized Information Systems.....	51
Author: Javier Parra-Arnau, Thesis Advisors: Jordi Forné, David Rebollo-Monedero	

Analytical Models for Architectural Exploration of Many-core Chip Multiprocessors.....	53
Author: Nikita Nikitin, Thesis Advisor: Jordi Cortadella	
Spectral Feature Detection For Spectrum Sensing.....	55
Author: Eva Lagunas, Thesis Advisor(s): Montse Najar	
GNSS Array-based Acquisition: Theory and Implementation.....	57
Author: Javier Arribas Lázaro Thesis Advisor: Carles Fernández-Prades	
Elastic transponders for optical direct detection OFDM systems based on the FHT.....	59
Author: Laia Nadal Reixats, Thesis Advisor(s): Michela Svaluto Moreolo and Gabrient Junyent	
Characterization and design of coherent optical OFDM transmission systems based on Hartley Transform.....	61
Author: Marcin Chochol, Thesis Advisor(s): Josep M. Fàbrega, Gabriel Junyent	
Multi-Antenna Diversity Techniques For Fbmc/Oqam Systems In Wireless Communications.....	63
Author: Màrius Caus López, Thesis Advisor: Ana I. Pérez Neira	
On the resource abstraction, partitioning and composition for virtual GMPLS-controlled multi-layer optical networks.....	65
Author: Ricard Vilalta, Thesis Advisor: Raül Muñoz (CTTC)	
Automatic representative keyframe selection for video by using a Random Walk algorithm.....	67
Author: Carles Ventura Thesis Advisor(s): Verónica Vilaplana, Xavier Giró-i-Nieto, Ferran Marqués	
Context Discovery in Cognitive Radio Networks.....	69
Author: Liliana Bolea, Thesis Advisors: Ramon Agustí Comes, Jordi Pérez-Romero	
Network Stability Assurance in the Context of Autonomic Management.....	71
Author: Antonio Astorga, Thesis Advisor(s): Joan Serrat	
Multi-Agent based Reinforcement Learning for Dynamic Resource Allocation in Next Generation Virtual Networks.....	73
Author: Rashid Mijumbi. Thesis Advisors: Joan Serrat and Juan-Luis Gorricho	
Atmospheric compensation experiments on advanced free-space optical coherent communication systems.....	75
Author: Esdras Anzuola, Thesis Advisor(s): Aniceto Belmonte	
Contributions to Radio Frequency Interference Detection and Mitigation in Earth Observation.....	77
Author: Giuseppe Francesco Forte, Thesis Advisor: Adriano Camps Carmona	
Simulation, detection and classification of vessels in maritime SAR images.....	79
Author: Luis E. Yam Ontiveros, Thesis Advisor: Jordi J. Mallorquí	

Contributions to Free-Space Optical Communications through the Turbulent Atmosphere	81
Author: Ricardo Barrios, Thesis Advisor: Federico Dios	
A Framework for the Design of Pilot Sequences and Precoders in Multiple-Antenna Systems	83
Author: Adriano Pastore, Thesis Advisor: Javier Rodríguez Fonollosa	
Demand-Side Management via Distributed Energy Generation and Storage Optimization	85
Author: Italo Atzeni, Thesis Advisors: Javier R. Fonollosa, Luis G. Ordóñez	
MOSAIC: Multilateral agreements for clinical data exchange	87
Author: Magí Lluch-Ariet and Albert Brugués de la Torre, Thesis Advisors: Josep Peguerols-Vallés and Francesc Vallverdú-Bayes	
The Doctoral Programme in Computer Architecture	89
The Doctoral Program in Computing	91
The Doctoral Program in Electronic Engineering	93
The Doctoral Programme in Telematics Engineering	95
The Doctoral Programme in Signal Theory and Communications	97
The Doctoral Programme in Artificial Intelligence	99

Foreword

It is our pleasure to introduce the Proceedings of the 3rd edition of the Barcelona Forum on Ph.D. Research in Information and Communication Technologies, organized by the Universitat Politècnica de Catalunya – BarcelonaTech. This Forum aims to be a showcase for the research activity developed by the different research groups in the ICT area, as well as a contact point for PhD students and private companies. In this compilation you will find a selection –about 10%- of the PhD research works currently on progress in the ICT area of our University, together with short overviews of the PhD Programs involved, and related research groups.

With about 850 new R+D projects and contracts, 80 patents and over 2000 papers in scientific journals per year, UPC-BarcelonaTech is a leading university in engineering research, which is confirmed by its privileged positions in reference university rankings as ARWU or QS. As such, UPC has a highest potential to create innovation and transfer it in benefit of the society and economic progress. Innovation, the generation of new ideas based on knowledge and the application of these ideas for the benefit of society, must be the main tools to create future in our economic context. UPC – BarcelonaTech, as a leading generator and transmitter of knowledge, must be positioned as a significant player in this process, and the collaboration with companies, defining common goals and providing the necessary training, is necessary and inexcusable. As the highest academic degree, Doctors are trained to innovate in their field, to be able to expand the frontiers of knowledge. In this sense, Doctors should have a leading role in a knowledge-based economic recovery, should be *innovation catalysts for the industry*.

This Forum edition has prepared a number of activities around this concept. A panel with representatives of local companies will debate about how the industry benefits from the innovation created by PhDs, and the valorization of thesis works and PhD training by companies. Previously a keynote speaker will explain his success story and personal experience on creating a spin-off company from his research. These topics, entrepreneurship and innovation, will have further insight in the afternoon when representatives and managers of spin-offs in the ICT area will share their experience, and advice, with the audience. Also in the afternoon, the Vice-Rector of Research will address companies and faculty on the convenience and opportunities to develop PhDs in private companies. Around these activities, PhD students will have the opportunity to present their research works in poster sessions and selected oral presentations, enabling interaction with visitors and other related researchers.

Xavier Aragonès Alejandro Rodríguez José Luis Balcázar

Xavier Masip Jordi Forné

Program Committee

Thread Assignment of Network Applications in Multithreaded Processors: A Statistical Approach

Author: Petar Radojković

Thesis Director: Francisco J. Cazorla

Thesis Advisers: Javier Verdú, Alex Pajuelo, Mario Nemirovsky

contact email: {petar.radojkovic, francisco.cazorla, mario.nemirovsky}@bsc.es, {jverdu, mpajuelo}@ac.upc.edu

I. Introduction

Multithreaded processors comprised of several cores, where each core supports several simultaneously running threads, have different *levels of resource sharing* [6]. For example, in a multicore processor where each core supports concurrent execution of several threads, all threads simultaneously running on the processor share global resources such as the last level of the cache memory or the Input/Output devices. In addition to this, threads running in the same core share the core resources, such as the execution units. Therefore, the way that threads are assigned to cores determines which resources they share, which may significantly affect the system performance. In processors with several levels of resource sharing, thread scheduling comprises two steps. In the first step, usually called *workload selection*, the OS selects the set of threads (workload) that will be executed on the processor in the next time slice, from a set of ready-to-run threads. In the second step, called *thread assignment*, each thread in the workload is assigned to a hardware context of the processor.

In multithreaded processors that comprise a large number of cores and that have several levels of resource sharing, finding a good thread assignment is an intractable problem. As the number of possible thread assignments is vast (e.g. 10^{50}) [4], it is unfeasible to do an exhaustive search in order to find the thread assignment with the highest (optimal) performance. Also, the analytical analysis of the optimal thread assignment is an NP-complete problem [3]. Moreover, the performance of the best possible thread assignment is unknown, thus the room for improvement of current thread-assignment algorithms cannot be determined.

Our research focuses on the thread assignment of applications running on multithreaded processors with several levels of resource sharing. The main contributions of our study are:

(1) We present a statistical method that estimates the performance of the optimal thread assignment based on the measured performance of a sample of random thread assignments [5].

(2) We show that running a sample of several hundred or thousand random thread assignments most probably captures an assignment with a performance very close to the optimal ones [5].

II. Our study

II.A. Estimation of the optimal system performance

The performance of the best-performing thread assignment is unknown, thus the room for improvement of current thread assignment algorithms cannot be

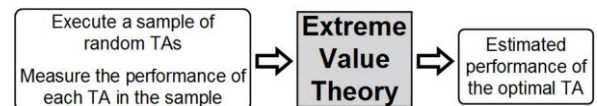


Figure 1. Estimation of the optimal thread assignment (TA) performance: A schematic view.

determined. This is a major problem for the industry because it may lead to:

(1) A waste of time and resources if excessive effort is devoted to improving a thread assignment algorithm that already provides a performance that is close to the optimal one.

(2) Significant performance loss if insufficient effort is devoted to improving poorly-performing thread assignment algorithms.

We propose a method that, estimates the performance of the optimal thread assignment based on the measured performance of a sample of random assignments. The schematic view of the method is shown in Fig. 1. First, the user should simply execute a sample of independent and identically distributed (i.i.d.) random thread assignments on the target processor and measure the performance of each assignment. The measured performance of the sample of thread assignments are the input to the statistical analysis. The analysis is based on Extreme Value Theory (EVT), a branch of statistics that studies extreme deviations from the median of distributions. EVT can be used to statistically estimate (with a given confidence level) the performance of the best-performing thread assignment, i.e. the optimal system performance for a given workload.

II.B. Random thread assignment approach

The probability that a sample of random assignments selected from a vast population contains the assignment with the best performance is low. However, it is not clear what the probability is that a sample of random thread assignments contains at least one of the assignments with a *good* performance. In order to address this problem, we analyze the probability that a sample of n randomly selected thread assignments contains at least one from the $P\%$ (e.g. $P=1\%$ or 2%) of the best-performing assignments [5]. The given probability can be computed as:

$$Probability = 1 - \left(\frac{100-P}{100}\right)^n$$

Using the presented formula, we can compute that a sample of several hundred random observations is sufficient to capture at least one of 1% or 2% of the best-performing thread assignments with a very high

probability (over 99%). This means that, if we assume that 1% or 2% of the best-performing assignments have a good performance, simply running several hundred or several thousand randomly selected thread assignments is sufficient to capture at least one assignment with a good performance.

The designer can also use Extreme Value Theory to estimate the performance of the optimal thread assignment. If the difference between the estimated optimal performance and the measured performance of the best thread assignment in the random sample is not acceptable, the designer can simply increase the sample size and repeat the analysis. This removes the need for any application profiling or to understand the increasingly complex multithreaded architectures.

II.C. Experimental environment and results

The presented statistical approach is successfully applied to thread assignment of multithreaded network applications. The experiments are executed in a real industrial environment based on network servers that comprise UltraSPARC T2 processor [1] and Netra DPS lightweight runtime environment [2].

Our results show that running several thousand random thread assignments provided enough information for the precise estimation of the performance of the optimal thread assignment. Also, several thousand thread assignments were sufficient to capture the assignments with performance very close to the optimal ones. In all the experiments, the detected performance loss was below 2.5%. The execution of the random thread assignments on the target processor required only two hours in the worst case.

III. Commercial and industrial application

Numerous problems in computer science are intractable. It is formally proven that many problems related to network design, program optimization, data storage and retrieval, process scheduling, and automata theory, are NP-complete [3]. Also, since many problems have a vast exploration space, it is unfeasible to do an exhaustive search in order to find a solution with the optimal performance. Currently, intractable problems in computer science are usually addressed by using different heuristics-based approaches. Design of heuristics-based approaches requires significant effort. Also, since the performance of the optimal solution of intractable problems is unknown, the room for the improvement of heuristics-based approaches cannot be determined. Thus, it is difficult to decide whether a given approach should be enhanced, or it has already determined a close-to-the-optimal solution.

The statistical approach that is presented in this paper can be easily applied to different intractable problems. The approach can be used to estimate the optimal system performance by using random sampling and Extreme Value Theory. Moreover, random sampling itself can be an effective approach to find good solutions from a vast exploration space.

In order to apply the statistical approach to any problem, the user should generate random samples and measure the performance of each of them. The statistical analysis of the sample of measurements is independent of the problem that is addressed. Thus, the analysis that is presented in our previous study [5] can be directly (without any change) applied to other

problems. We have already successfully applied the statistical analysis based on Extreme Value Theory to the problem related to the compilation of multithreaded applications. The scientific article that summarizes our work in this field is currently under submission.

IV. Conclusions

Our research focuses on the thread assignment of multithreaded network applications in multithreaded processors with several levels of resource sharing. We propose a statistical approach to this problem. We present a method that estimates the performance of the optimal thread assignment based on the measured performance of a sample of random thread assignments. The performance of the optimal thread assignment is the most important piece of information when a system designer has to decide whether a given thread assignment algorithm should be enhanced. We also show that, in environments in which the workload infrequently changes, the system designer can simply execute a sample of several hundred or thousand random thread assignments of a given workload and measure the performance of each assignment. With a very high probability, the performance of the best observed assignment exhibits a performance that is close to the optimal one.

In the research that is summarized in this paper, we analyze the thread assignment problem being focused on the overall system performance. As a part of future work, we plan to enhance our analysis by considering different criteria such as the utilization of the hardware resources or the energy consumption. We also plan to apply random sampling and optimal performance estimation on other intractable problems in the computer science.

V. Acknowledgments

This work has been supported by the Ministry of Science and Technology of Spain under contract TIN-2007-60625. Petar Radojković holds the FPU grant (Programa Nacional de Formación de Profesorado Universitario) under contracts AP2008-02370 of the Ministry of Education of Spain.

VI. References

- [1] *UltraSPARC T1 Supplement to the UltraSPARC Architecture 2005*. Sun Microsystems, Inc, 2006.
- [2] *Netra Data Plane Software Suite 2.0 Update 2 User's Guide*. Sun Microsystems, Inc, 2008.
- [3] M. R. Garey, D. S. Johnson. *Computers and Intractability: A Guide to the Theory of NP-Completeness*. W.H. Freeman and Company, 1979.
- [4] P. Radojković *et al.* "Thread to strand binding of parallel network applications in massive multi-threaded systems". In PPOPP-2012: Proceedings of the 15th ACM SIGPLAN Symposium on Principles and Practice of Parallel Programming, 2010.
- [5] P. Radojković *et al.* "Optimal task assignment in multithreaded processors: A statistical approach". In ASPLOS-2012: Proceedings of the 17th International Conference on Architectural Support for Programming Languages and Operating Systems, 2012.
- [6] V. Čakarević, *et al.* "Characterizing the resource-sharing levels in the UltraSPARC T2 processor". In MICRO-42: Proceedings of the 42nd Annual IEEE/ACM International Symposium on Microarchitecture, 2009.

Dynamic Data Partitioning for Distributed Graph Databases

Author: Xavier Martinez-Palau, Thesis Advisor(s): Josep Lluís Larriba-Pey, David Dominguez-Sal
 {xmartine,larri,ddomings}@ac.upc.edu

I. Introduction

Database Systems are specialized software solutions to manage large data volumes. Databases are widely used in all areas where there is the need to store large amounts of data. Since they are a very important tool, there is a lot of scientific research focused on databases.

The need of very efficient database systems has motivated the development of database systems specialized in the storage of specific sets of data. We work with a special kind of database named graph database, which specializes in the storage of graph structured data.

Graph databases have lots of direct applications; for example, a social network like Facebook can be interpreted as a graph. Each vertex corresponds to a user, and an edge that joins two vertices indicates friendship between two users. A graph database is used to analyze the existing relationships in the graph. For example, perform community detection to detect groups of friends or groups of people with similar interests.

A distributed database is a database that is stored using several storage devices in different computers that do not share physical components. Each of these computers is called a node. The most immediate gain is an improvement of performance, that is, distributed databases are able to execute queries at rates much greater than systems that only use one node. Other important advantages are increased availability and reliability. This means that there is a continuous operation of the system and, if one computer becomes unavailable, the system is not affected. Distributed systems also allow to keep important data physically closer to the final user, for example in social networks or email service providers, by having servers in several countries. Finally, distributed systems are able to store and process amounts of data several orders of magnitude larger than those possible with single computer systems.

Distributed systems are widely used and there is a lot of research literature on the subject. However, there is very little research focused on distributed graph databases. Whereas generic approaches are applicable, it is possible to develop methods specific to graph databases to achieve better results.

The main work of the thesis is DistriDEX, a distributed graph database. In this system, the data access patterns are monitored and the information is used to partition data in a way that minimizes the time used by the system to solve queries. This partitioning of data is updated dynamically and adapts to the changes of the query workload of the system. This way, the distribution of data is maintained in an optimal state independently of the query workload.

II. State of the Art

There are several distributed systems described in the literature. Some of those systems, such as Yahoo! PNUTS, are based on the widely used relational data model, while other systems, such as Google BigTable,

are based on key-value data models. The technology used on these systems is not always directly applicable to graph databases due to the differences in the structure of the data stored. Other systems adapted to the particularities of graphs achieve better performance.

There are some frameworks designed to performed analysis of data on massive graphs. One of these frameworks is Google Pregel. Pregel takes an approach different than that of graph databases: it is used to perform operations on large graphs one at a time. On the other hand, graph databases are systems that are always online with data loaded in memory and resolve different types of queries on the graph. Systems like Pregel have the disadvantage that writing new queries for the system is more complex than writing queries for graph databases.

III. Thesis Overview

As part of the thesis, we developed a distributed graph database. The system works like a regular graph database but uses several computers, named nodes, to store and access the data. This allows the storage of larger databases and faster execution of queries.

The main objective is to develop a distributed database that configures itself automatically in order to achieve the maximum possible performance.

The system monitors the data access patterns to balance the amount of work performed by each node by assigning each piece of data to different nodes. Different aspects of this distributed system are described in the following subsections.

III.A. Data Partitioning and Load Balancing

Data partitioning consists on assigning different pieces of data to different nodes. There are two objectives of partitioning: one is that the majority of operations are done in main memory, which is faster than reading from secondary storage. The second objective is to balance load among nodes: if all nodes do approximately the same amount of computations, the results are obtained faster.

The system uses a compressed matrix to store information on the patterns of data access. This information is used to partition the data. This means that each piece of data is assigned to a particular node, and that node is the only one that performs operations using the piece of data.

The algorithm that partitions the data ensures that the solution found is one that minimizes the amount of network communication in the system, achieving faster execution times.

The partitioning of the data is updated periodically, as new information is obtained as the system executes queries. This allows to balance the load of the system among the nodes at all times, maintaining the system in an optimal state that allows the fastest times for query execution.

III.B. Query Routing

The queries executed in our system are divided in several phases. During each phase, each node accesses the data that is assigned to itself by the data partitioning and performs the calculations needed to solve the query. Between each two consecutive phases, there is a network communication step where nodes exchange information.

During each network communication step, each node sends each piece of data to the corresponding node according to the data partitioning. Once this network communication step ends, each node has the information needed to start executing the next phase of the query.

III.C. Data Replication

Data replication consists on storing several copies of the data stored in the system, each copy in a different node. Data replication is a very important feature of any distributed system, as it allow the continued operation of the system in the event of a power failure on one or more nodes. Another effect of data replication is increased throughput: if there are several copies of the data that is most frequently accessed, queries that access the same data can be executed simultaneously.

At this point, data replication has not been yet implemented on DistriDEX. There are several desirable features of data replication. One of these features is that the system automatically selects which data is replicated according to the usage of the system at any given time.

III.D. Write support

Having write support in a system means that the data stored in it can be added, updated or deleted. This is a desirable feature because most systems are not static, they change with time. For example, a system that stores bibliographic information is updated on a daily basis, as new authors and publications appear.

Having write support on a distributed system is more complicated than on a single machine system because of replication. Each time that a piece of data is added, changed, or deleted, the distributed system has to decide when to update all replicas. If the replicas are updated instantaneously, the system is said to be in a consistent state, as all nodes see the same data at the same time.

While consistency is a desirable property of any system, systems without consistency can achieve better performance and scalability.

IV. Preliminar Results

The system described in Sections III.A and III.B has been implemented on top of DEX [1,2], a high performance scalable graph database management system that uses one machine to execute. DistriDEX is compared to a traditional distributed system, that partitions data in a static way, without considering the query workload as DistriDEX does.

The distributed systems store a large random graph with more than 37 million vertices and one billion edges. The experiment is repeated with 1, 2, 8 and 32 nodes.

Figure 1 shows the throughput of both the traditional system and DistriDEX. The throughput measures the number of edges visited each second in a system that is operating continuously. Throughput is inversely proportional to the time needed by the system to

execute a query. As such, the larger the value of the throughput, the better. The figure shows that DistriDEX achieves much higher throughput, up to 9 times in the best case, with 32 machines, meaning that DistriDEX is able to use the available resources in a much more efficient manner.

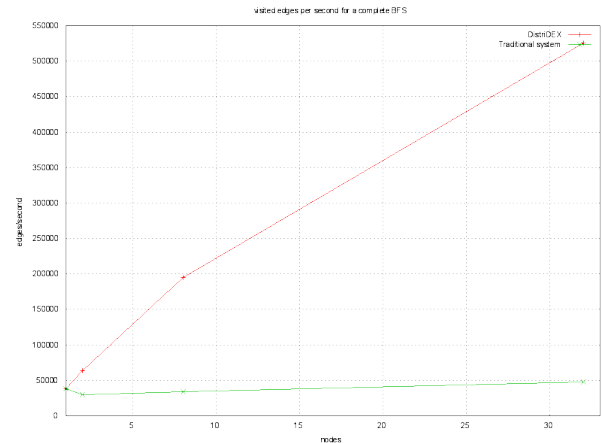


Figure 1. Throughput of DistriDEX and a traditional distributed graph database.

V. Conclusions

The thesis focuses on distributed graph databases. Graph databases have a wide range of applications, they store social networks, protein interaction networks, bibliographical networks, etc. Also, graph databases are capable of performing very fast analysis on said networks.

The large quantity of information to be stored, and the increasing growing rate of it demands the use of more resources to be able to cope with it. This means that distributed systems play an essential role in these cases.

The aim of this thesis is to develop a distributed graph database that is able to improve the performance of regular graph databases while maintaining all of its features: being able to analyze huge networks and process queries on very large graphs.

VI. Acknowledgments

The members of DAMA-UPC thank the Ministry of Science and Innovation of Spain and Generalitat de Catalunya, for grant numbers TIN2009-14560-C03-03 and SGR-1187 respectively.

VII. References

- [1] N. Martínez-Bazan, V. Muntés-Mulero, S. Gómez-Villamor, J. Nin, M. Sánchez-Martínez, and J. Larriba-Pey. *Dex: high-performance exploration on large graphs for information retrieval*. In Proceedings of the 16th ACM Conference on Information and Knowledge Management (CIKM), pages 573–582. ACM, 2007.
- [2] N. Martínez-Bazan, V. Muntés-Mulero, S. Gómez-Villamor, M.A. Águila-Lorente, D. Domínguez-Sal and J-L. Larriba-Pey. *Efficient Graph Management Based On Bitmap Indices*. In Proceedings of the 16th Symposium on International Database Engineering & Applications (IDEAS). ACM, 2012.
- [3] L. Bargaño, V. Muntés-Mulero, D. Domínguez-Sal, and P. Valduriez. *ParallelGDB: a parallel graph database based on cache specialization*. In Proceedings of the 15th Symposium on International Database Engineering & Applications (IDEAS), pages 162–169. ACM, 2011.

On the Scalability Limits of Communication Networks at the Nanoscale

Author: Ignacio Llatser, Thesis Advisors: Eduard Alarcón and Albert Cabellos-Aparicio
contact e-mail: llatser@ac.upc.edu

I. Introduction

Nanotechnology is enabling the development and manufacture of *nanosystems*, entities that take advantage of the unique properties of nanomaterials and are able to perform very simple tasks at the nanoscale, including computing, data storage, sensing, actuation and communication. Despite their promising capabilities, because of their tiny size (a few μm), the operation range of nanosystems is limited to their close nano-environment. In consequence, a huge number of them will be required to perform meaningful tasks in a real scenario.

Nanonetworks, the interconnection of nanosystems, provide means for cooperation and information sharing among them, allowing nanosystems to cover larger areas and fulfill more complex tasks [1]. Nanonetworks will greatly expand the capabilities of a single nanosystem and they are expected to revolutionize many fields of science and engineering, bringing new opportunities in fields as diverse as ICT, biomedicine or environmental sciences. For instance, some of the envisaged applications of nanonetworks include Wireless Nanosensor Networks, i.e., networks of small sensors that can measure magnitudes with unprecedented nanoscale accuracy, and Graphene-enabled Wireless Network-on-Chips, which allow the efficient implementation of wireless communication among the different cores in a multicore processor.

As we will see next, nanonetworks cannot be implemented by merely downscaling current wireless networks; on the contrary, classical communication mechanisms need to undergo a profound revision before being applied to this new scenario.

Consequently, important research challenges need to be addressed before nanonetworks can become a reality. Indeed, several techniques have recently been proposed to interconnect nanosystems, leading to two novel network paradigms at the nanoscale: molecular communication and graphene-enabled wireless communications.

II. Molecular Communication

Molecular communication is a new paradigm inspired by communication among living cells. Among the diverse techniques that have been proposed to implement molecular communication, Diffusion-based Molecular Communication (DMC) is the most widely studied, since it allows modeling several communication processes in biology, such as calcium signaling, quorum sensing and pheromonal communication.

A DMC network can be described as a set of nanosystems which communicate by means of molecular diffusion in a fluid medium. It is composed of three main phases: emission, propagation and reception. First, transmitter nanosystems encode the information to be sent into the release pattern of molecules. The emitted molecules cause a variation in their local concentration, which then propagates throughout the medium due to a diffusion process. Finally, receivers are able to estimate the concentration of molecules in their neighborhood. This measurement

activates specific signal transducing mechanisms which allow the receivers to decode the transmitted information. Fig. 1 illustrates a conceptual DMC network with multiple transmitters and receivers.

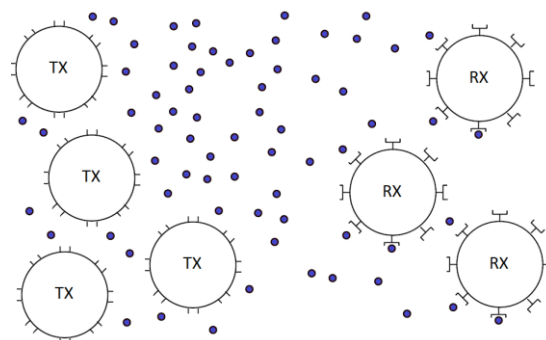


Figure 1. Conceptual diagram of a nanonetwork using Diffusion-based Molecular Communication (DMC).

III. Graphene-enabled Wireless Communications

Another option that has been investigated to communicate nanosystems is by means of electromagnetic (EM) waves. In this case, there are doubts about the feasibility of scaling down current metallic antennas, mainly because metallic nano-antennas resonate in the optical range (several hundreds of THz). Such a high resonant frequency would result in a huge channel attenuation which would greatly limit the transmission range of nanosystems. Graphene-enabled Wireless Communications (GWC) aim to overcome this fundamental limitation by means of graphene-based plasmonic nano-antennas, also known as *graphennas*.

Graphene, a flat monolayer of carbon atoms tightly packed in a two-dimensional honeycomb lattice, has recently attracted the attention of the research community due to its novel mechanical, thermal, chemical, electronic and optical properties. By taking advantage of the unique properties of graphene, GWC are envisaged to allow the implementation of wireless communications among nanosystems.

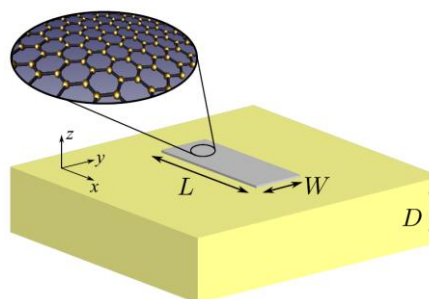


Figure 2. Schematic diagram of a graphene-based plasmonic nano-antenna, or *graphenna*.

The main novelty of graphennas with respect to metallic nano-antennas is that they are predicted to resonate in the terahertz band (0.1-10 THz), up to two orders of magnitude below their metallic counterparts. A

graphenna, as shown in Fig. 2, is composed of a finite-size graphene layer mounted over a metallic flat surface (the ground plane), with a dielectric substrate in between. Fig. 3 displays a conceptual diagram of a GWC network.

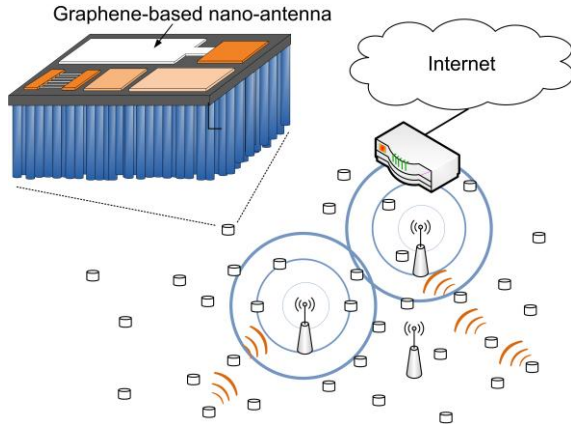


Figure 3. Conceptual diagram of a nanonetwork using Graphene-enabled Wireless Communications (GWC). The upper left corner shows a magnified individual nanosystem.

IV. Summary of the Thesis

Considering that no experimental results of communication among nanosystems have been reported to date, a key question naturally arises: do nanonetworks have the potential of becoming a tangible reality in the near future? The purpose of our thesis is to answer this question by studying the scalability limits of communication networks when their size is reduced to the nanoscale, which will allow determining the *feasibility* of nanonetworks. We focus in the analysis of the main performance metrics in a communication network, such as the throughput, the transmission delay and the energy consumption.

In order to perform this study, and considering the uniqueness of the physical layer of nanonetworks, we first need to characterize the physical channel of both DMC and GWC. On the one hand, in a DMC network, the information is encoded by means of molecules which are physically transported from the transmitters to the receivers. On the other hand, in GWC, graphennas offer excellent conditions for the propagation of Surface Plasmon Polariton (SPP) waves in the terahertz band; thus, SPP waves allow graphennas to resonate at a much lower frequency than metallic nano-antennas. As a consequence of these fundamental differences, the communication metrics of nanonetworks may be significantly different to their equivalent in current communication networks.

In order to analyze the physical channel of DMC, we propose a simple pulse-based modulation scheme, which we use to derive analytical expressions of important communication metrics in this scenario [2]. Interestingly, Table 1 shows that all the obtained metrics in DMC scale differently with respect to their equivalent in wireless EM communications. These results confirm the unique nature of the physical channel of DMC.

Finally, we investigate the propagation of SPP waves in graphennas. Due to the particular dispersion relation of SPP waves in graphene, the resonant frequencies of graphennas show a very different

Metric	DMC	Wireless EM
Pulse delay	$\Theta(r^2)$	$\Theta(r)$
Pulse amplitude	$\Theta(1/r^2)$	$\Theta(1/r^2)$
Pulse width	$\Theta(r^2)$	$\Theta(1)$
Pulse energy	$\Theta(1/r)$	$\Theta(1/r^2)$
Pulse duration	$\Theta(r^2)$	$\Theta(1)$

Table 1. Comparison of the scalability of communication metrics as a function of the transmission distance r in DMC and wireless EM communications.

behavior with respect to metallic antennas. We observe in Fig. 4 that, in the terahertz range, not only the resonant frequency of a graphenna is lower than that of a metallic antenna with the same size, but it also scales better as the antenna size is reduced [3]. In consequence, graphennas with a length of a few μm will resonate in the terahertz band, at much lower frequencies than metallic nano-antennas with the same size. This unique scalability trend turns out to be one of the strongest factors that motivate the use of graphennas to implement wireless communications among nanosystems.

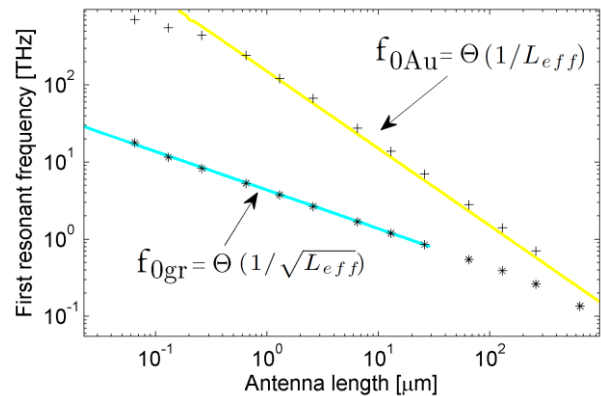


Figure 4. Scalability of the resonant frequency of graphennas (blue line) and metallic nano-antennas (yellow line) as a function of their length. The simulation results for graphene (stars) and metallic (crosses) antennas are also shown.

In conclusion, in this thesis, we aim to prove the feasibility of nanonetworks by studying the scalability limits of communication networks at the nanoscale. With this purpose, we analyze how their unique physical channel will impact the performance of nanonetworks. The results of this study will provide guidelines that may prove useful for designers of future nanonetworks.

V. Acknowledgments

This thesis has been partially supported by the FPU grant of the Spanish Ministry of Education and the German Academic Exchange Service (DAAD).

VI. References

- [1] I. F. Akyildiz, J. M. Jornet, M. Pierobon, "Nanonetworks: A New Frontier in Communications," *Communications of the ACM*, vol. 54, no. 11, pp. 84–89, Nov. 2011.
- [2] I. Llatser, E. Alarcón and M. Pierobon, "Diffusion-based Channel Characterization in Molecular Nanonetworks," in *Proc. of IEEE MoNaCom* (held within IEEE INFOCOM), 2011.
- [3] I. Llatser, C. Kremers, A. Cabellos-Aparicio, J. M. Jornet, E. Alarcón and D. N. Chigrin, "Graphene-based Nano-patch Antenna for Terahertz Radiation," *Photonics and Nanostructures - Fundamentals and Applications*, doi:10.1016/j.photonics.2012.05.011, May 2012.

CPU Accounting in the Multi-core and Multi-threaded Era

Author: Carlos Luque,

Thesis Director: Francisco J. Cazorla

Thesis Advisor(s): Miquel Moreto and Mateo Valero

contact email: {carlos.luque, francisco.cazorla}@bsc.es, {mmoreto, mateo}@ac.upc.edu

I. Introduction

An Operating System (OS) is a software application that acts as an interface between user and the computer hardware. Its major responsibilities are to manage and ensure proper operations of the hardware resources. Moreover, OS provides the user with an abstraction of the hardware resources. The user application perceives this abstraction as if it is using the complete hardware while, in fact, the OS shares hardware resources among the user applications. Hardware resources can be shared *temporally* and *spatially*. Hardware resources are time shared between users when each application can make use of a resource for a limited amount of time (for example, the exclusive use of a CPU). Orthogonally, hardware resources can be shared spatially when each application makes use of a limited amount of resources, such as cache memory or I/O bandwidth.

In single-threaded processors the execution time of an application depends on the other applications it runs with, since the OS time shares the CPU(s) between running applications. However, the time accounted to each application is roughly the same since the OS takes into account those periods in which the application is not scheduled onto a CPU.

Currently, the limitation imposed by Instruction-Level Parallelism (ILP) has motivated the use of Thread-Level Parallelism (TLP) as a common strategy for improving processor performance. This strategy has led to a wide range of Multi-Threaded (MT) processor architectures, including Simultaneous Multithreading (SMT) processors [7] Chip MultiProcessors (CMP) [6] and also SMT+CMP processors, i.e., chip multiprocessors in which every core is a SMT such as IBM POWER7 [8], Sun UltraSPARC T4 [10], and Intel Core i7 [9].

The MT processors introduce complexities into the process of measuring CPU utilization, since the progress of an application does not only depend on the time an application is scheduled onto a CPU, but also on the amount of hardware resources it receives during that period, which in fact depends on the workload¹. Thus, in MT processors the CPU time accounted to an application depends on the workload it executes. This is undesirable because the same application with the same data input set may be accounted differently depending on the workload it executes. The inaccuracy measuring per-task CPU utilization may affect several key aspects of a system such as OS statistics or the charging mechanism in data centers.

II. Our Approach

The aim of this thesis is to investigate a mechanism to propose an accurate measurement of CPU

accounting in SMT and CMP architectures, both at hardware level and software level. We research on a hardware mechanism ensuring a low overhead. After collecting accuracy information from hardware level, we investigate the adoption of this information into the software level. The target of the thesis is a CPU accounting mechanism that will allow measuring the CPU utilization in MT processors achieving a good accuracy.

The main objectives of this thesis are the following:

(1) To achieve breakthrough in techniques for the CPU accounting measurement in multi-core and multi-threaded processors so that we improve the accuracy when measuring the CPU utilization. The mechanisms will report with a high accuracy the progress of each application in the MT processors. This mechanism must have good behaviour in the different models of MT processors, such as SMT, CMP and SMT+CMP. This goal can be breakdown into the following steps: (1) Achieving a CPU accounting mechanism in CMP architectures. This mechanism [1,3] is novel, because there are no previous papers for CMP architecture. (2) Investigating the different mechanisms [4,5] to measure CPU accounting in SMT processors, proposing a new one if required. (3) To discover new CPU accounting proposals for SMT+CMP architectures. We will combine our CPU accounting proposal for CMP processors with some CPU accounting mechanism proposed by SMT processors, proposing a new one if required.

(2) We will study how software level has to be adapted to use the new hardware mechanisms to accomplish improvement in the distribution of CPU time between applications in a system.

III. CPU Accounting for CMP Processors

Throughout this paper, we refer to *inter-task* resource conflicts to those resource conflicts that a task suffers due to the interference of the other tasks running at the same time. For example, a given task X suffers an inter-task L2 cache miss when it accesses a line that was evicted by another task, but would have been in cache, if X had run in isolation. Likewise, *intra-task* resource conflicts denote those resource conflicts that a task suffers even if it runs in isolation. These are conflicts inherent to the task.

The target of our proposal, Inter-Task Conflict Aware (ITCA) accounting [2], is to accurately estimate the CPU time accounted to a task in CMPs. The basic idea of ITCA is to account to a task only those cycles in which the task is not stalled due to an inter-task L2 cache miss. In other words, a task is accounted CPU cycles when it is progressing or when it is stalled due to an intra-task L2 miss. The next paragraphs provide a detailed discussion of when the accounting of a task is stopped and resumed.

L2 data misses: We consider a task is in one of the following states: (s1) It has no L2 (data) cache misses or

¹ A workload is a set of applications running, simultaneously, in a system

it has only intra-task L2 misses in flight; (s2) It has only inter-task L2 misses in flight; and (s3) It has both inter-task and intra-task L2 misses in flight simultaneously. We take care of the lost opportunity of extracting MLP by stopping the accounting of a task if the instruction in the top of the ROB is an inter-task L2 miss and the register renaming stage is stalled. We call this condition state (s4).

L2 instruction misses: ITCA also stops accounting to a task when the ROB is empty because of an inter-task L2 cache instruction miss (s5). In our processor setup instruction cache misses do not overlap with other instruction cache misses. That is, at every instant, there is at most one in flight instruction miss per task. Hence, on an inter-task L2 instruction miss we consider that the task is not progressing because of an inter-task conflict, and hence, we stop its accounting.

Figure 1 illustrates the accounting decision in the defined five states. Note that state (s5) is part of state (s1), since when the ROB is empty, no L2 data cache miss can be in flight. Finally, state (s4) can only occur when there are some inter-task L2 data misses in flight and, consequently, is contained in states (s2) and (s3).

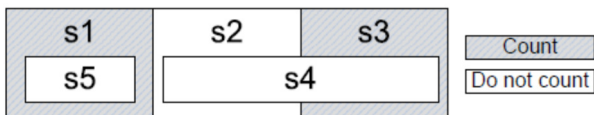


Figure 1 Accounting decision for all possible states

The cycles accounted to each task in each core are saved into a special purpose register per core, denoted *Accounting Register* or *AR*, which can be communicated to the OS. This register is a read-only register and can be managed by the OS similarly to the Time Stamp Register in Intel architectures

We improve our CPU accounting mechanism, *Improved ITCA* (I^2TCA) [3]. The basic conceptual difference between ITCA and I^2TCA is the accounting decision for state (s2). In state, there are only inter-task data misses in flight and the register renaming is not stopped. I^2TCA decides to account cycles in this state. Though the task is not progressing at full speed, actual work is being done so these cycles should be accounted to the task. As a result, the overhead of I^2TCA logic is reduced.

So far, we have assumed that the CPU time accounted to a task should be equal to the execution time of the task when it runs in isolation in the system. On the one hand, this is the natural extension of the concept of CPU utilization in single-threaded uniprocessor systems. On the other hand, this accounting mechanism accomplishes with the principle of accounting, meaning that a task should be always accounted the same regardless of the workload in which it runs. Thus, we explore different *reference accountings* alternative. We propose a reference accounting in which we consider that a task should be accounted the time it would require to run with $1/N$ of the processor hardware resources, where N is the number of cores. In the case of a CMP with a shared cache, we have to assign $1/N$ of the cache space to the task. In this new scenario, an L2 miss when running in isolation with $1/N$ of the shared cache might become a hit when running with the whole shared cache. It is called an *inter-task L2 hit*. As a result, a task might be quicker than the task running in isolation with $1/N$ of the shared cache. We do few

changes to I^2TCA to adapt it this new reference accounting without losing accuracy.

III.A. Simulator Description

We use the MPsim simulator [1] to evaluate the performance of our proposals and existed approaches. This simulation tool includes a trace driven SMT+CMP simulator that is a highly flexible cycle-accurate simulator. It provides an accurate cycle timing simulation of the program execution, considering the delays of the pipeline stages, the possible dependency among instructions, etc.

IV. Software Support for CPU Accounting

Our goal is to adapt the software in particular the OSes to utilize our CPU accounting hardware mechanisms and study their effect. We will investigate the OS scheduler in depth because it is one of the most important tasks in OS that indirectly makes use of CPU accounting. The OS scheduler is in charge of allocating CPU time to different applications within the operating system and selects the best application to assign to all CPUs present in the system.

V. Acknowledgments

This work has been supported by the Ministry of Science and Technology of Spain under contract TIN-2007-60625 and grants BES-2008-003683, by the HiPEAC Network of Excellence (IST-004408) and a Collaboration Agreement between IBM and BSC with funds from IBM Research and IBM Deep Computing organizations. The authors are grateful to Pradip Bose, Chen-Yong Cher, and Alper Buyuktosunoglu from IBM, to Enrique Fernández from the University of Las Palmas de Gran Canaria, to Jaume Abella from BSC, and to Roberto Gioiosa from Pacific Northwest National Laboratory for their technical support.

VI. References

- [1] C. Acosta et al., "The MPsim Simulation Tool," Computer Architecture Dept., UPC, Technical Report UPC-DAC-RR-CAP-2009-15, 2009.
- [2] C. Luque et al., "ITCA: Inter-task Conflict-Aware CPU Accounting for CMPs," in Proc. 18th Int'l Conf. Parallel Architecture and Compilation Techniques (PACT), 2009, pp. 203--213.
- [3] C. Luque et al., "CPU Accounting for Multicore Processors," IEEE Trans. Comput., 61, 2 (February 2012), 251-264
- [4] S. Eyerhan and L. Eeckhout, "Per-thread cycle accounting in SMT processors," in ASPLOS, 2009
- [5] B. Gibbs et al. "Advanced POWER Virtualization on IBM eServer p5 Servers: Architecture and Performance Considerations," in IBM Redbook, 2005.
- [6] K. Olukotun et al., "The case for a single-chip multiprocessor," in SIGPLAN Not., 31, 1996.
- [7] D. M. Tullsen et al., "Simultaneous Multithreading: Maximizing On-Chip Parallelism", in ISCA, 1995.
- [8] M. Broyles et al., "IBM EnergyScale for POWER7 processor-based systems", in IBM J. Res. Dev., May 2011.
- [9] E. Rotem et al. "Power Management Architecture of the 2nd Generation Intel Core microarchitecture, formerly codenamed Sandy Bridge", in Hot Chips, August 2011.
- [10] Oracle 2012, "White Paper, Oracle's SPARC T4-1, SPARC T4-2, SPARC T4-4, and SPARC T4-1B Server Architecture," Technical Report, Oracle, 2012.

Characterization, design and re-optimization on multi-layer optical networks

Author: Marc Ruiz, Thesis Advisor(s): Luis Velasco

contact email: mruiz@ac.upc.edu

I. Introduction

The explosion of IP traffic due to the increase of IP-based multimedia services (HDTV, video conferencing, etc.) poses new challenges to network operators to provide a cost-effective data transmission. Although Wavelength Division Multiplexing (WDM) meshed transport networks support high-speed optical connections, these networks lack the flexibility to support sub-wavelength switching leading to poor bandwidth usage. To cope with the transport of that huge and heterogeneous amount of traffic, multilayer networks are the most accepted architectural solution.

Multilayer optical networks allow optimizing network capacity by means of packing several low-speed traffic streams into higher-speed optical connections (lightpaths). During this operation, a dynamic virtual topology is created and modified the whole time. Because new connections are dynamically allocated in the network, and connection holding times are typically random, a suboptimal allocation of resources may exist at any time. In this context, a periodical resource reallocation could be deployed in the network, aiming at improving network resource utilization. This dynamic connection capability in multilayer optical networks has been enhanced with the advent of the Automatically Switched Optical Network (ASON) architecture. To accomplish such dynamicity, a control plane responsible for establishing and releasing connections is deployed over the optical transport plane. In this regard, Generalized Multiprotocol Label Switching (GMPLS) protocols are commonly used.

This thesis is devoted to the characterization, planning, and re-optimization of next-generation multilayer networks from an integral perspective including physical layer, optical layer, virtual layer, and control plane optimization. To this aim, statistical models, mathematical programming models and meta-heuristics are developed.

II. Contributions on multilayer optical networks

In this section, three of the main contributions of this thesis are briefly described.

II.A. Statistical Q-factor computation for online IA-RWA

The Routing and Wavelength Assignment (RWA) problem is one of the most important problems in designing optical networks. Among different versions, Impairment-aware RWA (IA-RWA) algorithms include the Q-factor evaluation in their decisions on whether to establish or block new optical connections. Nevertheless, Q-factor computation presents some drawbacks that make difficult its use in on-line (dynamic) IA-RWA algorithms. Specifically, the long computation times inherent to calculate Q values drastically increases lightpath set-up times.

Since the exact computation of the Cross-phase Modulation (XPM) effect is the bottleneck of the Q-factor computation (in terms of time), we propose a statistical model to estimate it. Being the XPM of a lightpath affected independently by each single busy wavelength

channel in a certain interfering distance, we propose a *restricted polynomial* model consisting in finding a polynomial equation to estimate the XPM of wavelength channels. The restricted polynomial model opens the possibility to compute XPM values from solving a simple mathematical operation. The use of this model in the Q-factor formula in addition to other approximations defines the statistical Q-factor computation.

II.B. Survivable IP/MPLS-over-WDM network design

The virtual topology of a multilayer optical network can be carefully designed and dimensioned to exploit the capacity of the optical network keeping some Quality-of-Service requirement (e.g.: availability). In this thesis, we present the novel Survivable IP/MPLS-over-WDM Multilayer Network problem (SIMULTANEO) as a capital expenditures (CAPEX) minimization problem, considering hierarchical grooming together with survivability against IP/MPLS node, opto-electronic (OE) port, and optical link failures.

From the architectural point of view, the SIMULTANEO problem can be solved applying a conventional solution (*overlay approach*) based on designing a single virtual topology and duplicating backbone IP/MPLS nodes and lightpaths. Aiming at reducing the expected CAPEX of the solution, we propose a new approach (*joint approach*) based on over-dimensioning IP/MPLS devices and lightpath connectivity and recovery.

With the aim to evaluate the benefits of our proposed approach, we define Integer Linear Program (ILP) formulations for both joint and overlay approaches. However, due to the complexity of the problem (it can be proved to be NP-hard) exact solutions cannot be obtained for real-size instances. For this reason we develop a meta-heuristic algorithm to efficiently solve this problem obtaining near-optimal solutions.

II.C. Re-optimization in dynamic multi-layer networks

As introduced above, some re-optimization could be periodically performed in dynamic traffic scenarios as a consequence of set-up and tear-down lightpath processes according to the traffic demand lead to a non-optimal use of network resources. One of the most expensive resources in an optical network are OE ports.

In this work, we introduce the Optical Resources Optimization (ORO) problem as an online re-optimization problem, proposing an ILP model to solve it. Due to the complexity of the problem, the time needed to solve ORO (even in small networks) trend to be very long, and thus, that method may be not applicable to real-time problems. For this reason, we present several meta-heuristic algorithms to improve resources utilization.

III. Illustrative numerical results

III.A. XPM and Q-factor model fitness

The restricted polynomial model has been obtained from exact XPM values. Figure 1 depicts both exact and statistical XPM values of wavelength channels for three

different lengths of links. Specifically, the effect of the first neighboring channel (i.e.: the one with the highest XPM influence) is shown. As can be observed, the polynomial model fits with high accuracy ($\pm 2.5\%$ for worst predictions) the set of exact values. Note that, since the time needed to execute this operation is negligible, the use of this statistical model in on-line IA-RWA algorithms provides a fast and accurate method to compute XPM values.

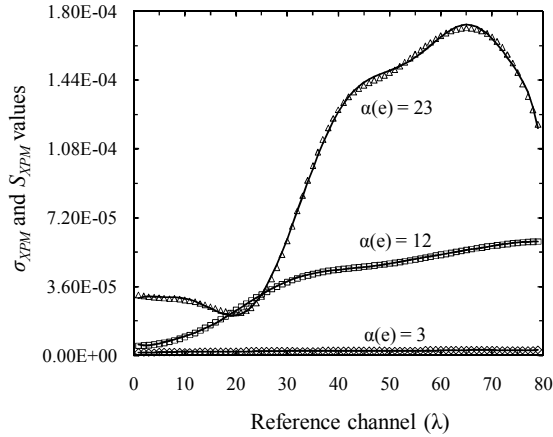


Figure 1. Analytical (markers) vs. statistical (lines) XPM models

For validating the statistical Q-factor model, we generate lightpaths of different lengths and number of links and, for each one of them, we compute both exact and statistical Q-factors (pairs depicted in Figure 2 within the dotted lines of the 95% confidence interval). In light of these results, we can conclude that our statistical Q-factor based on a polynomial XPM model provides a valid impairment computation method for online IA-RWA problems.

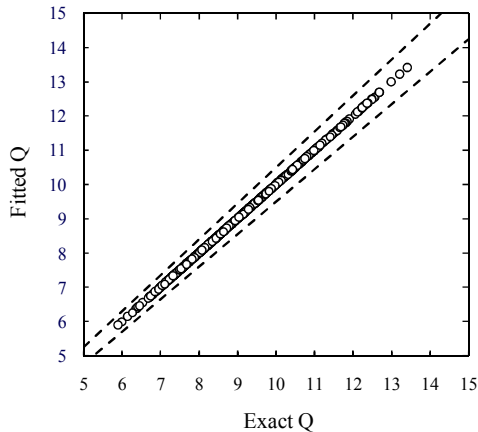


Figure 2. Exact vs. Fitted Q-factor

III.B. Multilayer approaches comparison

We have solved the SIMULTANEO problem using our heuristics for several real core networks and with real costs for IP/MPLS devices. Figure 3 shows, for one of those networks the expected CAPEX savings of using our proposed joint approach instead of the overlay one for different lightpath costs. For a fair value of these costs, we conclude that the joint approach leads to significant CAPEX savings ($\approx 24\%$) compared with the overlay approach. Moreover, operational expenditures and energy savings are also expected with the joint approach, since the number of IP/MPLS nodes and the

number of switched-on OE ports is lower with respect to the overlay approach.

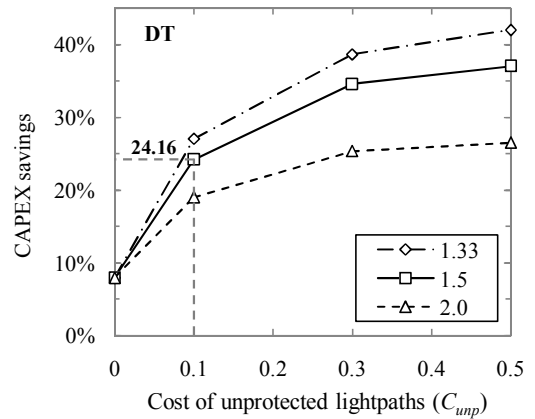


Figure 3. CAPEX saving of joint w.r.t overlay approach

III.C. ORO performance

After testing and tuning all heuristic algorithms, we chose the best of them and we have implemented it in the Network Management System (NMS) of an ASON/GMPLS test-bed for solving ORO in real networks. Figure 4 illustrates the obtained blocking probability with and without applying ORO with a certain periodicity. As can be observed, the relative gain of offered load at the reference blocking probability level of 1% is more than 10%, which represents a significant increase for validating the usefulness of ORO.

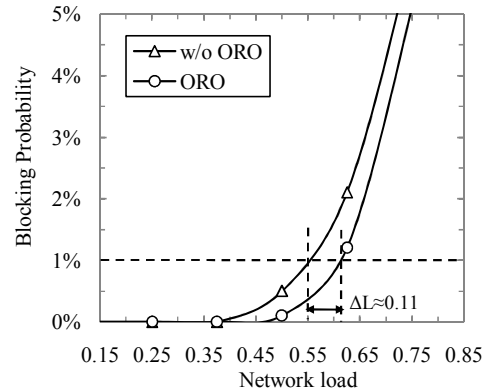


Figure 4. ORO performance in ASON/GMPLS test-bed

IV. Conclusions

In this work we propose problems and approaches oriented to improve the design and performance of multilayer optical networks. By means of statistical models, mathematical programming, and meta-heuristics to solve them, we obtain significant benefits in terms of network cost reduction and capacity efficiency increasing.

V. References

- [1] L. Velasco et al., "Statistical Approach for Fast Impairment-Aware Provisioning in Dynamic All-Optical Networks", IEEE/OSA J. Opt. Commun. Netw. (JOCN), 4, 2012.
- [2] M. Ruiz et al., "Survivable IP/MPLS-over-WSON Multilayer Network Optimization," IEEE/OSA J. Opt. Commun. Netw. (JOCN), 3, 2011.
- [3] M. Ruiz et al., "Resources optimization in GMPLS-based optical multilayer networks", European Conference on Networks and Optical Communications (NOC), 2009.

Resonant Inductive Coupling Wireless Power Transfer

Author: Elisenda Bou Balust, Thesis Advisor(s): Eduard Alarcón Cot, Jordi Gutierrez Cabello
contact email: elisenda.bou@upc.edu

I. Introduction

Recent research on wireless power transfer (WPT) using resonant inductive coupling has demonstrated very promising efficiencies (above 80%) [1] at large distances compared to the antenna dimensions (more than three times the receiver/transmitter diameters). Due to the number of applications that could benefit from WPT: from electric vehicles to sensor networks, commercial electronic devices, health equipment, biomedical implants, in-space systems and so on, the development and optimization of this technology is of great interest. Since RIC is still a very novel technology, different models should be proposed to analyze and predict the behavior of these systems and to increase the overall efficiencies and transmission ranges.

II. RIC and EM Wireless Power Transfer

II.A. Electromagnetic Wireless Power Transfer (WPT)

EM Wireless Power Transfer consists on the transmission of electric energy through electromagnetic fields. These fields experiment behavioral changes, predicted by Maxwell's equations, which define two terms of electric and magnetic fields (radiative and non-radiative). Maxwell's equations state that the electric fields produced by changes in charge distribution are different from those produced by a change in magnetic field. Similarly, the behavior of magnetic fields produced by changes in electric currents is different from the ones produced by a change in electric fields. For these reasons, in the spatial region very close to currents and charge distributions, the EM field is dominated by electric and magnetic components produced directly by currents and changes in charge distributions. This is called the electromagnetic near-field region.

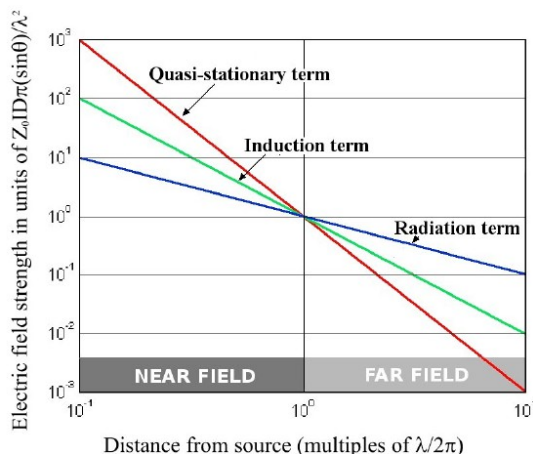


Figure 1. Radiative & Non-radiative behaviors of EM fields.

On the other hand, at distances far from there the EM field becomes dominated by the electric and magnetic fields indirectly produced by the change in the other type of field, and thus the effects of the charges and currents at the EM source are negligible. This part

of the EM field predominantly radiative constitutes the far-field. Both behaviors can be observed in Fig. 1.

II.B. Resonant Inductive Coupling (RIC)

The transmission of wireless power transfer using electromagnetic induction was first demonstrated in the early 20th century by Nikola Tesla. Since then, electromagnetic induction (EMI) has been used for the powering of artificial hearts and implantable devices. While the early systems used non-resonant links, later systems increased their efficiency by implementing resonant transmitter coils thus creating a resonant inductive coupled link. In such a link, each coil is capacitively loaded forming a tuned LC resonating at a common frequency, which allows to transmit significant power over a wider ranges. The equivalent circuit of the link is shown in Fig.2.

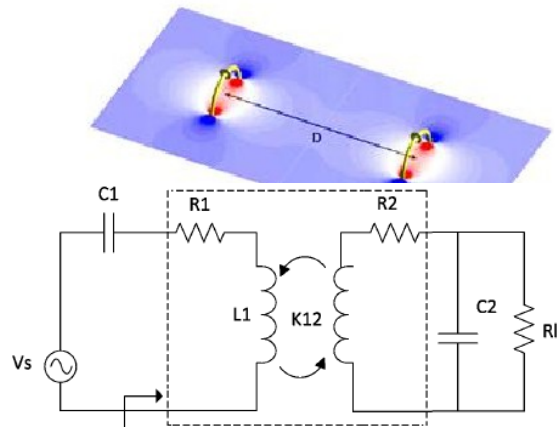


Figure 2. RIC & Equivalent Circuit

III. Objectives & Thesis Work

Because RIC is a very multidisciplinary field, different analysis have been performed from the physical theory, the antenna theory and the circuit theory. One of the main objectives of this thesis is to develop a unified, design-oriented, scalable model that can predict accurately the behavior of RIC systems under different conditions.

In this thesis, we developed a model that merges these three different points of view, showing a complete agreement between theories under optimal conditions and steady-state analysis. Also, we demonstrated that the circuital analysis is the only one that can predict the behavior of this systems under transitory state.

Finally, the optimal parameters to achieve maximum power transfer efficiency have been found and introduced into the model as design-oriented guidelines towards maximum efficiencies: optimal input frequency, resonant frequency, distance between transmitter and receiver antennas, source equivalent resistance and optimal load resistance. The effects of an unmatched load onto the PTE are shown in Fig.3.

Once the theoretical maximum efficiencies and optimal parameters are found, it is necessary to explore different adaptation techniques (frequency and impedance) to force these systems to work under optimal conditions.

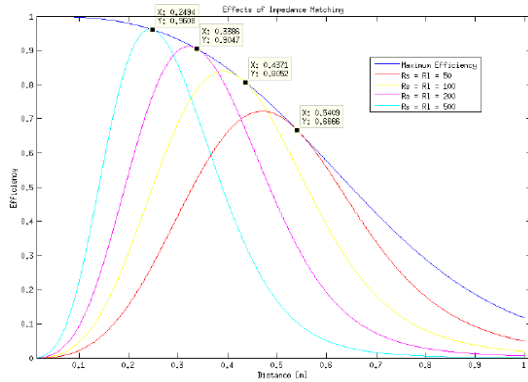


Figure 3. RIC Impedance Matching Techniques

Finally, this thesis aim is to explore techniques such as RIC SIMO/MIMO systems and power-and-data systems to apply this concepts on two different applications: Fractionated Spacecraft and Active Energy Harvesting.

IV. Applications

IV.A. Fractionated Spacecraft

Fractionated spacecraft (Fig. 4) is a type of satellite architecture that distributes the capabilities of a conventional spacecraft across multiple independent modules. These modules are not physically connected but, because they need to act cooperatively, it is necessary to implement a wireless power-and-data bus.

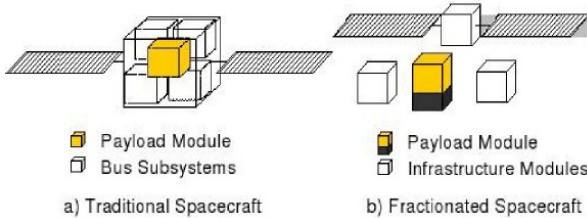


Figure 4. Traditional versus fractionated spacecraft.

For the application of RIC to this fractionated spacecraft bus, different solutions should be developed to cope with the in-space special requirements and limitations.

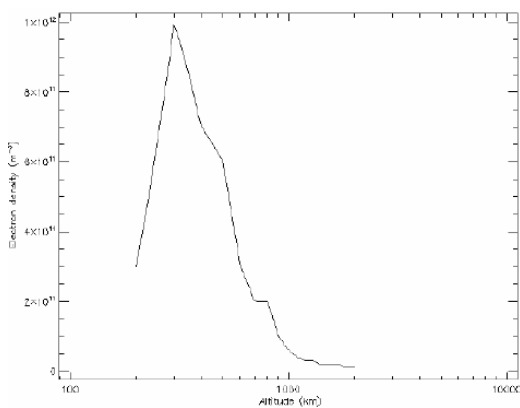


Figure 5. Electron density (plasma effect) Analysis.

This research includes analyzing the plasma effects on near-field wireless power transfer (shown in Fig. 5), increasing the coil performance (magnetic field and coupling) without incurring in mass increments, transmitting power and data simultaneously (space power and telemetry), EM compatibility/potential effects and developing adaptive impedance matching and frequency tuning techniques.

Some of this concepts as well as the interactions between plasma and near-field RIC will be explored by a payload placed inside the UPC Cubesat, project led by Adriano Camps (TSC) and Roger Jové.

IV.B. Active Energy Harvesting

One of the main constrains/problems that wireless sensor networks have is the requirement to individually power each sensor or node. Different energy harvesting techniques have been performed to use ambient energy to power them, but the challenges of powering these devices using the most ubiquitous form of energy (EM energy) are still unsolved. To circumvent this situation, we propose to increase ambient energy by actively adding an inductive EM field and using on-chip RIC spirals to harvest the energy.

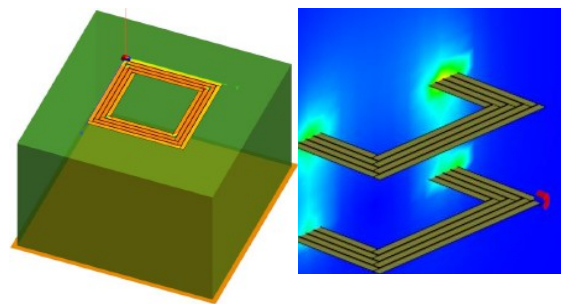


Figure 7. Characterization of on-chip inductors.

V. Acknowledgments

Work partially funded by Thales Alenia Space.

VI. References

[1] André Kurs, Aristeidis Karalis et al, "Wireless Power Transfer via Strongly Coupled Magnetic Resonances," *Science*, vol. 317, no. 5834, pp. 83-86, July, 2007.
 [2] Mehdi Kiani, Uei-Ming Jow, Maysam Ghovanloo, "Design and Optimization of a 3-Coil Inductive Link for Efficient Wireless Power Transmission", *IEEE Transactions on Biomedical Circuits and Systems*, vol. 5 no6, December 2011.
 [3] Elisenda Bou, Eduard Alarcon, Jordi Gutierrez, "A comparison of analytical models for Resonant Inductive Wireless Power Coupling". *PIERS*, August 2012.

Quality of Service Strategies for Heterogeneous Backbone Networks

Author: Joana Sócrates-Dantas, Thesis Advisor(s): Davide Careglio and Wilson Vicente Ruggiero
Thesis Co-Advisor(s): Regina Melo Silveira and Josep Solé-Pareta
contact email: joana@ac.upc.edu

I. Introduction

On a backbone network, carriers serve Internet Service Providers (ISP) with long-haul data transport. The service provided must guarantee a minimum supply quality stipulated in a Service Level Agreement (SLA). In order to be able to offer different service levels for each client, backbone network managers must rely on Quality of Service (QoS) strategies.

Currently, the main type of QoS mechanisms available for backbone networks are pre-emption policies described by MPLS architecture [1] and extended to GMPLS architecture [2]. In preemption mechanisms higher priority demands may use the resources used by a lower priority active connection that would be torn down.

A backbone network connection transmits a large volume of data belonging to diverse end users connections and therefore should ideally not be disconnected. Besides the aforementioned drawback, preemption strategies tend to cause network instability [3], not tolerable on large complex networks, as is the case of backbone networks. Furthermore, service class types are defined locally by each autonomous systems' management, and are usually disregarded when a connection crosses to a new domain.

This research aims on proposing a QoS strategy for backbone networks based on differentiated distribution of resources. The proposed strategy will focus on Wavelength Division Multiplexing (WDM) and Optical Orthogonal Frequency Division Multiplexing (OOFDM) technologies, as they are mostly suitable for backbone networks. This research will also consider the Path Computation Element (PCE) as the architecture adopted for the centralised routing task for the backbone network scenario. In this work will we also assess the multi-domain problem of service class-types and propose a solution where class-type values can be globally interpreted.

II. Our Proposal

The main objective of this research is the development of a QoS strategy for backbone networks. This QoS strategy will be based on the different distribution of resources according to demands' class-types and will be implemented through a resource distribution constraint model. Since backbone networks are by default optical networks, this research will focus on the distribution of resources on channels resulted from WDM and OOFDM technologies. Due to the multi-domain characteristic of backbone networks, this study will consider path computation and resource assignment to be centralised and provided by the PCE architecture.

Fig. 1 presents a scheme where this research scenario can be appreciated: a backbone network is represented comprising its sub-networks with respective border routers and control planes. The figure illustrates a hierarchical PCE architecture where PCE devices communicate with each other. The image's hatched area refers to the specific focus of this research.

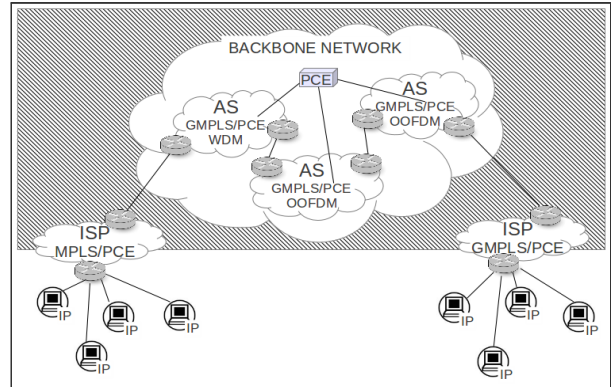


Figure 1. Backbone network and its components

This work relies on the Russian Dolls Model (RDM) as the resources distribution constraint model implemented [4]. In RDM, the maximum bandwidth usage allowed in a link is achieved by the accumulation of successive Class-Types (CTs) bandwidth constraints (BW). For example, CT7 may use resources up to BC7 limit, while CT6 shares its BC6 constraint with CT7, CT5 shares its BC5 constraint with CT6 and CT7 and so on as can be observed in Fig. 2.

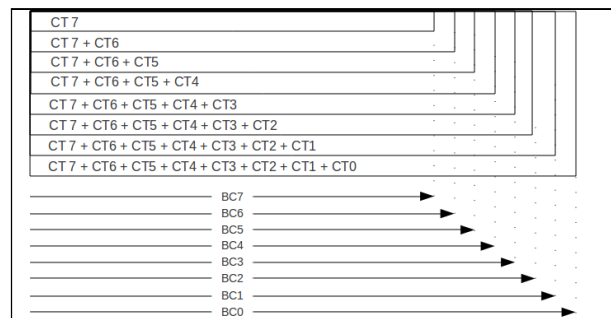


Figure 2. Russian Dolls Model - resource distribution constraint

The differentiated distribution of resources mechanism proposed in this research needs to be tested and analysed in both static and dynamic routing scenarios.

The aim of the testing is to assess the performance of the proposed mechanism in comparison to the currently available technologies. In order to do so, a Mixed Integer Linear Programming (MILP) function and a simulator will be developed as tools for measuring performance.

II.A. Metrics

The metrics that will be outputted by the ad-hoc Java simulator will be used to assess the proposed QoS strategy performance in comparison to the standardized mechanism. The metrics that will be used for evaluation purposes will be:

- Number of demands processed per interval of time;

- Number of ERO messages exchanged per interval of time;
- Number of NOPATH messages exchanged per interval of time;
- Number of demands not served per number of demands processed per interval of time;
- Amount of served bandwidth per Set-up priority and holding priority per demands served per interval of time;
- Number of tear-down connections per interval of time;
- Amount of tear-down bandwidth per interval of time.

III. Contributions

III.A. Algorithm

The research process have, so far, developed an algorithm of the proposed mechanism to be implemented by a PCE in a multi-domain WDM network. Which summarized procedure is described as follows:

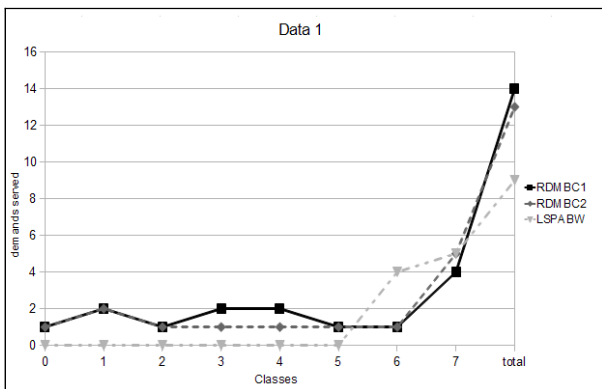
A Path Computation Request (PCReq) message is received. If demand's requested bandwidth is greater than Bandwidth Constraint (BC) for the demand's CT value PCE sends Path Computation Reply (PCRep) with NOPATH object. Otherwise if there is an available wavelength throughout selected route PCE sends PCRep informing the computed light-path. If there is not a whole wavelength available PCE checks if there is a wavelength for the same selected route and with same source destination nodes pair. In case there is PCE sends PCRep message informing light-path and assuming electronic grooming at the route's edge nodes. The grooming would follow the RDM model in case there is not enough available resource in the selected wavelength.

III.B. Preliminary Results

We have tested the principle of our proposed QoS strategy on an off-line Routing and Wavelength Assignment (RWA) scenario, where the distribution of available bandwidth is determined by the Russian Dolls Model (RDM) [5].

We solved, in CPLEX IBM solver, analytical models based on MILP functions for both the standard scenario (from now on referred to as control scenario) and a scenario where the proposed strategy is implemented (from now on referred to PCE RDM scenario).

From the comparison of results it is



possible to observe the following.

Figure 3. Number of demands Served per Class-Type

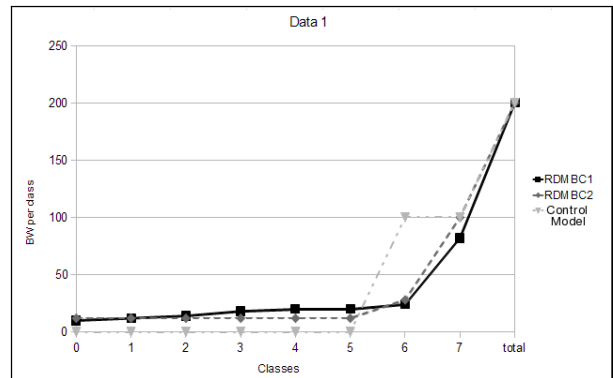


Figure 4. Resource distribution per Class-Type

In PCE RDM scenario at least one demand is served for each CT (Fig. 3). Also it presents a higher level of distribution of resources throughout Class-Types compared to the control scenario (Fig. 4).

Finally, the total number of demands assigned a connection is higher for PCE RDM than on the control model.

III.C. Standards enhancement suggestions

In order to perform the specific tasks of our proposed model, we had to propose some enhancements to the current standardized mechanisms.

For the PCE we propose a third possibility of reply message where the path suggested relies on the usage of the constraint model resulting resources and not the resources demanded originally by the request message.

In order for the PCE to be able to compute paths based on priorities for connection the TED must contain information on the class-type values of all current connection and their respective Bandwidth Constraint values.

IV. Acknowledgments

The authors would like to thank Erasmus Mundus Brazilian Windows II program for mobility programs scholarships and Capes Brazilian PhD student scholarship. This work has been partially supported by the Spanish Ministry of Science and Innovation through the DOMINO project (TEC2010-18522).

V. References

- [1] Le Faucheur, Ed., "Protocol Extensions for Support of DiffServ-aware MPLS Traffic Engineering" IETF, RFC4124, June, 2005.
- [2] Mannie, E., "Generalized multi-protocol label switching (GMPLS) architecture," IETF, RFC 3945, 2004.
- [3] de Oliveira, J.C. and Scoglio, C. and Akyildiz, I.F. and Uhl, G., "New Preemption Policies for DiffServ-Aware Traffic Engineering to Minimize Rerouting in MPLS Networks", in IEEE/ACM Transactions on Networking, vol. 12(4), pp. 733-745, August 2004.
- [4] Le Faucheur, F. and others, "Russian Dolls Bandwidth Constraints Model for Diffserv-aware MPLS Traffic Engineering," IETF, RFC 4127, June 2005.
- [5] Socrates Dantas, J., Careglio, D., Melo Silveira, R., Ruggiero, W.V. and Sole-Pareta, J., "Pce algorithm for traffic grooming and qos in multilayer/multi-domain IP over WDM networks," in (ICTON), 2011 13th International Conference on Transparent Optical Networks.

Speech-in-speech hiding based on a bio-inspired model

Author: Dora Maria Ballesteros, Thesis Advisor: Juan Manuel Moreno Aróstegui

contact email: dora.maria.ballesteros@upc.edu

I. Introduction

The growing of the information transmission using digital media has been accompanied by the development of techniques and protocols which protect the content of data. One choice to transmit data in a secure way is to hide the secret message within a host signal. This technique is known as steganography. Typically in a steganography model, the secret messages like text, speech and image, are hidden into host signals like audio and images, but the techniques to hide a speech signal into another speech signal have not been widely researched in the past. The most important hurdle is that the secret message can have up to the same time-scale of the host signal, and therefore the number of bits to hide can be significantly high.

There are three features to satisfy in a steganography system: the transparency of the output (stego) signal, the hiding capacity (number of bits hidden) and the robustness of the stego signal against signal manipulations such as lossy compression and filtering [1]. The most important feature is the transparency which is referred to the ability to not create suspicion about the existence of the secret message. This is satisfied if the stego signal is highly similar to the host one. Nevertheless, in the case of speech-in-speech hiding, the hiding capacity plays an important role in the steganography model.

In this work, we present a bio-inspired model of speech-in-speech hiding that has a good trade-off between transparency, hiding capacity and robustness. Our model is known as Efficient Wavelet Masking (EWM) [2] and it is based on the ability of adaptation of the speech signals [3].

II. Ability of adaptation of Speech Signals

The ability of adaptation of speech signals is the core of the Efficient Wavelet Masking scheme. One of the examples of adaptation in nature it is the ability to modify the color of an animal so that it resembles the surrounding environment. It is known as camouflage. In this context, the secret message can be adapted to another speech signal in which the "target" speech signal is not sensitive information. Then, the secret message is camouflaged so that it resembles the target speech one.

For example, the secret message "my secret key is 1234" can be adapted to the target speech signal "good morning everybody". So, if the camouflaged secret message is received by a non-authorizer user, the sensitive information is not revealed. To reverse the process of camouflaging, it is necessary to know the key. A deterministic method to obtain the key has been described in [3].

Figure 1 shows the secret message and the target speech signal of the previous example. Together with that it is shown the camouflaged speech signal.

It is worth noting that the ability of adaptation is true if the requirements in [3] are satisfied even if the gender (or language) of the secret message and the target

speech signal are not the same, or even if one of them is a vowel signal and the other is a voice signal.

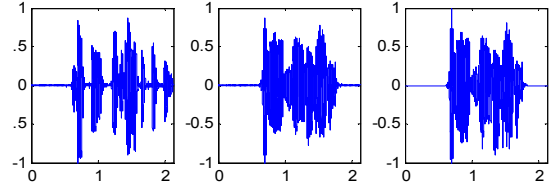


Figure 1(a b c). Secret, Host and Camouflaged secret

To evaluate the similarity between the target speech signal and the camouflaged secret message it can be used the speech distortion index, ρ^2 [4]. If ρ^2 is close to 1, it means that the similarity between the speech signal and the camouflaged speech signal is high, but if this value is close to 0, the signals are highly dissimilar. It is expected that speech distortion index will be close to 1 if the ratio of the non-silent time of the signals is 1.

In the current example, the value of ρ^2 is 0.9745 and the ratio of the non-silent time is 1.0262.

III. Efficient Wavelet Masking

The proposed speech-in-speech hiding scheme, EWM, uses the ability of adaptation of the speech signals, explained in Section II, and it takes advantage of the masking property of the Human Auditory System (HAS) in which one sound may be masked by another if the first one produces high levels while the latter remains faint. The steps to obtain the stego signal are described as follows (Figure 2):

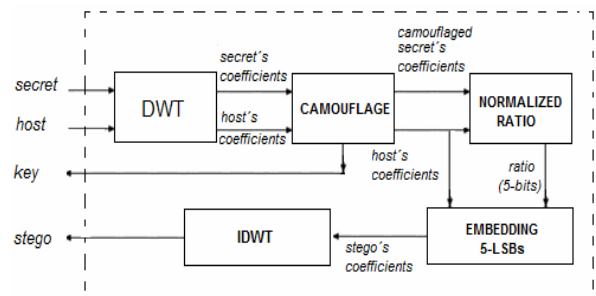


Figure 2. Embedding module of the EWM scheme.

a) Both the secret message and the host signal are decomposed by using the Discrete Wavelet Transform (DWT).

b) The secret's coefficients are camouflaged so that they resemble the host's coefficients by using the ability of adaptation of the speech signals. The *key* is related to the original positions of the secret's coefficients.

c) The normalized ratio between every pair of coefficients (camouflaged secret's coefficient divided by the host's coefficient) is encoded to 5-bits; i.e. the stream 11111 means that the ratio is 1.

d) The 5-least-significant-bits (5-LSBs) of every host's coefficient are replaced to the ratio obtained in the previous step.

e) The Inverse Discrete Wavelet Transform (IDWT) of the modified host's coefficients is applied and the stego signal is obtained.

Since only 5-LSBs of the host's coefficients are changed, the stego signal is close to the host signal.

To recover the secret message, the following steps are applied (Figure 3):

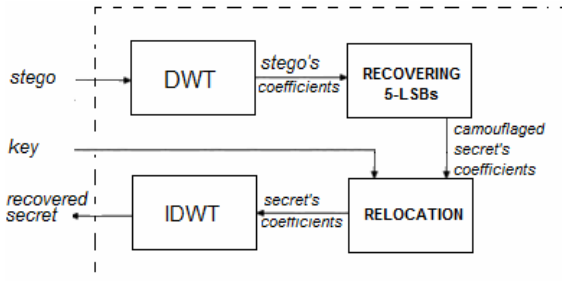


Figure 3. Extraction module of the EWM scheme.

a) The stego signal is decomposed by the DWT.

b) The 5-LSBs of the stego's coefficients are extracted. The normalized ratio is multiplied by the stego's coefficients and the result is the recovered camouflaged secret's coefficient.

c) Once all of the camouflaged secret's coefficients have been recovered they are relocated according to the information of the *key*. The result is the recovered secret's coefficients.

d) The IDWT is applied and it is obtained the recovered secret message.

The recovered secret message is close to the original secret message.

IV. Results

In order to illustrate the performance of the proposed scheme, we show the statistical transparency of the stego signal and the quality of the recovered secret message. The results of the proposed model are compared to the obtained from the Frequency Masking (FM) scheme. The host signal and the secret message are the same as used in Section II.

IV.A. Transparency

One of the methods to analyze the statistical transparency consists on calculate the logarithm of the stego signal. If the histogram from the stego signal is close to the histogram from the host signal, the statistical transparency is satisfied, otherwise, the stego signal is not statistically transparent.

In Figure 4, the blue bars correspond to the host signal behavior while the green bars to the stego signal obtained with the studied schemes. It is clear that the histogram of the first case is more similar to the host's histogram than the second one. It means that the stego signal obtained with the EWM scheme is statistically more transparent than the obtained with the FM scheme.

IV.B. Quality of the recovered secret message

The recovered signals are shown in Figure 5. The quality of the speech signal obtained by the EWM scheme is significantly higher than the obtained by the FM scheme. In the first case the index of distortion between the secret message (Figure 1a) and the

recovered secret message is $\rho^2=0.994$, while in the second case is $\rho^2=0.475$.

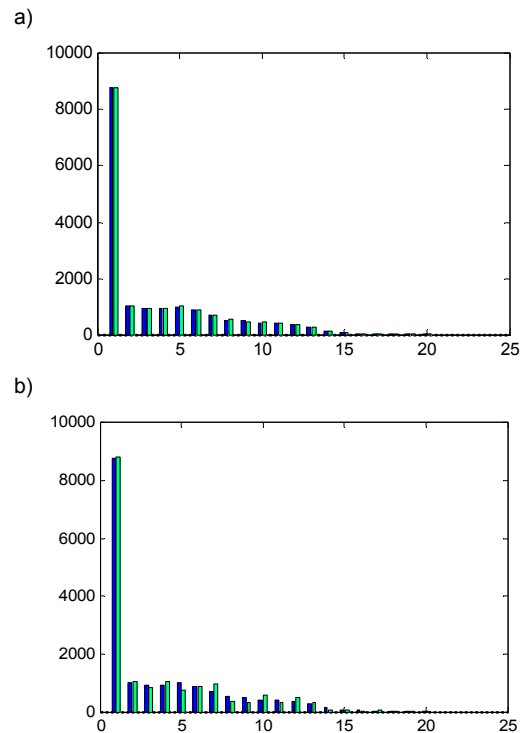


Figure 4. histogram with a) EWM scheme, b) FM scheme

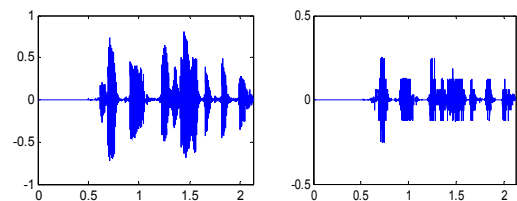


Figure 5(a,b). Recovered secret messages from EWM, FM.

In conclusion, the EWM scheme has higher statistical transparency and better quality of the recovered secret message than the FM scheme. Nevertheless, both schemes are based on the masking concept. In future work, the ability of adaptation of speech signals can be used in other security models.

V. Acknowledgments

The author would like to acknowledgment her sponsor, the University Military Nueva Granada.

VI. References

- [1] Anderson, R. J., & Petitcolas, F. A. P. "On the limits of steganography," *Selected Areas in Communications, IEEE Journal on*, 16(4), 474-481, 1998.
- [2] Ballesteros, D.M., Moreno, J.M., "Highly transparent steganography model of speech signals using Efficient Wavelet Masking," *Expert Systems with Applications*, vol. 39, pp. 9141-9149, Aug 2012, doi: 10.1016/j.eswa.2012.02.066
- [3] Ballesteros, D.M., Moreno, J.M., "On the ability of adaptation of speech signals and data hiding", *Expert Systems with Applications*, doi: 10.1016/j.eswa.2012.05.027.
- [4] Benesty, J., Jingdong, C., & Yiteng, H. (2008). "On the Importance of the Pearson Correlation Coefficient in Noise Reduction. Audio", *Speech, and Language Processing, IEEE Transactions on*, 16(4), 757-765.

A Contribution to Unobtrusive Measurement Methods For Sleep Monitoring using Magnetic Induction

Author: Hadiseh Mahdavi, Thesis Advisor: Prof. Javier Rosell Ferrer

Contact email: hadiseh.mahdavi@upc.edu

I. Introduction

Sleep consumes 1/3 of our lives and it is essential for a person's health and well-being. Yet millions of people do not get enough sleep and many suffer from lack of sleep [1]. The cumulative effects of sleep loss and sleep disorders represent an under-recognized public health problem and have been associated with a wide range of health consequences including an increased risk of hypertension, diabetes, obesity, depression, heart attack, and stroke [2]. Almost 20% of all serious car crash injuries in the general population are associated with driver sleepiness. Hundreds of billions of dollars a year are spent on direct medical costs related to sleep disorders such as doctor visits, hospital services, prescriptions, and over-the-counter medications [2]. The effects of sleep loss on work performance may cost 18 billion in lost productivity [1]. Therefore, the contribution of sleep monitoring, for diagnosing sleep problems to live free of preventable disease, disability, injury, and premature death has been given lot of attention.

Sleep monitoring requires a method of supervising a patient without interfering with his natural state.

The assessment of sleep-related disturbances is traditionally performed by Polysomnography. While this method provides a rich data set like breathing, heart rate, blood pressure, etc., it can be done only in the clinic environment with the use of wired sensors and skin electrodes. Another approach is by actigraphy and wearing devices which is a relatively unobtrusive method. The problem is that they are rather expensive devices and still the user needs to wear the device.

Applying optical methods, textiles embedded electrodes, microwave Doppler radar techniques, instrumenting the mattress pad with different types of pressure sensors and magnetic induction monitoring are other different approaches that have been used for sleep monitoring. To name some drawbacks of the stated methods, we could mention the complex installation process, measurements' high dependency on the mattress and bed parameters, movements of the patient and his orientations regarding the receiver systems, etc.

An ideal sensor for these applications would be non-invasive, minimally restrictive, robust enough to compensate for patient movement, and would function without relying on patient cooperation.

Apart from sleep monitoring, the necessity of a non-invasive, unobtrusive system for monitoring vital signals is a subject of interest in other medical issues. In home health care applications, patients with conditions that can be perturbed or worsened by contact sensors include neonates, infants at risk of sudden infant health syndrome and burn victims; a non-contact heart and respiration rate monitoring could provide the necessary data without affixed electrodes for these patients.

The main purpose of this thesis is to develop an unobtrusive and contactless system based on *Magnetic Induction Spectroscopy* for detecting vital signals of a patient on the bed. The data detected by the system

would be subject to further analysis for assessment of sleep and vital sign monitoring.

II. Method and Material

When a conductive object is placed in a time varying magnetic field, eddy currents are induced in the body and perturb the magnetic field in the vicinity. These currents, which are in accordance with the laws of Faraday and Lenz, produce a magnetic field that can be detected by a properly designed receiver system. This fact has been verified theoretically and experimentally and has been used extensively for nondestructive testing of metals. By injecting a time-varying current to an excitation antenna (coil), a magnetic flux, also called the primary magnetic field is produced. The magnetic field induces eddy currents in conductive materials.

The amplitude of the eddy current is proportional to the magnetic flux density and the conductivity of the material. This induced eddy currents generates itself a further magnetic field call secondary magnetic field which could be measured by a suitable receiver antenna. This measured signal is a function of the conductivity, geometry of the tissue and the geometry of the excitation and detection antennas.

II.A. Simulation

An anatomical 3D model of the human trunk (lungs and heart) was designed with COMSOL MULTYPHYSICS (Figure 1). A current carrying coil is located in front of the chest as an excitation coil.

Regarding to meshing limitations, the model have been designed considering simplification. By using the parametric sweep tools of the software, different solutions were obtained for various coil positions, inflation and deflation of the lungs, conductivity changes due to the inspiration and expiration and frequency.

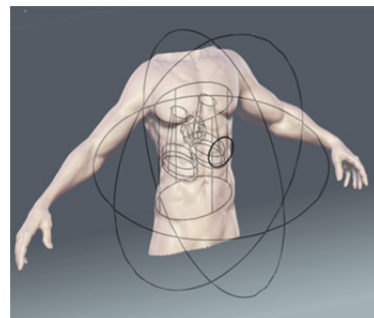


Figure 1. General view of the geometry

Multiple parameters in trunk are changing while breathing, such as geometry and size of the lungs, dimensions of the chest and electrical conductivity of the lung tissue. In addition, since obtaining the convenient location of the coil regarding to the chest is of great interest especially for safety issues and compatibility

with national and international standards, coil distance from the body was defined as a variable parameter.

III. Results and Discussions

Specific absorption rate (SAR) is a measure of the rate at which energy is absorbed by the body when exposed to a radio frequency (RF) electromagnetic field; which is an important limitation that affect the whole system design. As a result, it should be studied both in simulation and experiments to be compatible with the main safety standards [3].

As expected, the SAR value is highest close to the surface of the body (Figure 2) and the absorption rate decreases by increasing the distance while it is rising by the frequency increment.

According to the ICNIRP basic restrictions for localized SAR for head and trunk [3], the maximum of absorption is 2 (W/Kg) and for the whole body is 0.08 (W/Kg), which in our case is orders of magnitude less than the standard limitations.

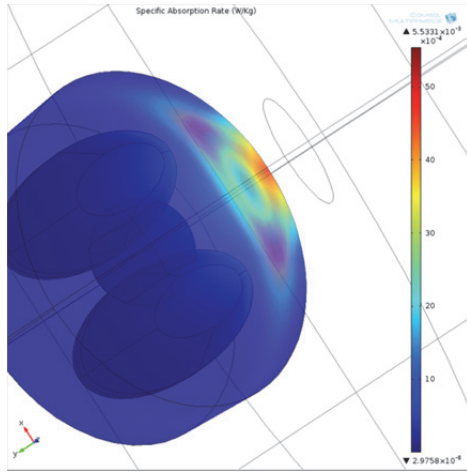


Figure 2. Specific absorption rate (W/Kg) at body surface at 1MHz

In general, the secondary magnetic field (ΔB) will have real and imaginary components representing the permittivity (ϵ) and conductivity (σ) of the sample respectively. For biological tissues, the conductivity (imaginary) component will normally be dominant [4]:

$$\Delta B/B \propto \omega(\omega\epsilon_0\epsilon_r - j\sigma)$$

The secondary magnetic field at different frequencies at a distance of 5 cm from the chest (driven from simulation) is shown in figure 3.

The secondary magnetic field detected at the same plane where the excitation coil is located, increases as frequency rises. The dotted lines are the induced magnetic field values while the lungs are inflated.

Since the conductivity of lungs is lower when inflated, the secondary magnetic field is lower.

The secondary signal should be amplified in order to enabling further studies regarding the breathing and cardiac activity.

In further studies the secondary magnetic field will be obtained in other places to find out the best locations for the detection coil.

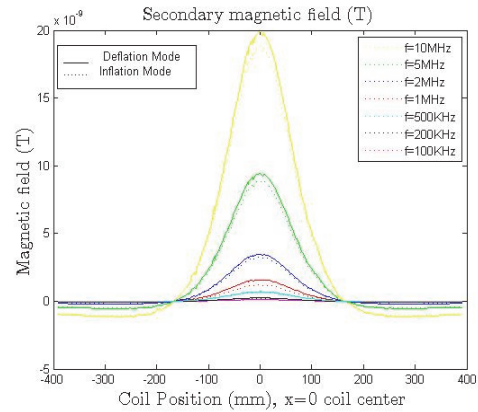


Figure 3. Secondary Magnetic Field vs. Frequency

IV. Conclusions

Sleep and vital sign monitoring are of special interest for a variety of biomedical applications. The objective of this thesis is to use the magnetic induction method to unobtrusively measure and monitor these signals and states.

Since vital signs monitoring needs continuous methods of measurement and monitoring, people would be exposed to magnetic fields continuously and as a result the human safety issues would have significant importance in the design process. Results demonstrate that regarding the national and international standards, the system is safe for a one turn coil with a diameter of 10 (cm) carrying a current up to 1 (A) and the desired limitations has been fulfilled.

V. Acknowledgments

This thesis has been funded by the Help4Mood project from the European Union's Seventh Framework Program.

VI. References

- [1] L. M. Swanson, J. T. Arnedt, M. R. Rosekind, G. Belenky, T. J. Balkin, and C. Drake, "Sleep disorders and work performance: findings from the 2008 National Sleep Foundation Sleep in America poll.," *Journal of Sleep Research*, vol. 20, no. 3, pp. 487-494, 2011.
- [2] M. W. Mahowald, "Book Review Sleep Disorders and Sleep Deprivation: An Unmet Public Health Problem By the Committee on Sleep Medicine and Research. Edited by Harvey R. Colten and Bruce M. Altevogt. 404 pp., illustrated. Washington, DC, National Academies Press, 2006. 48.," *New England Journal of Medicine*, vol. 356, no. 2, pp. 199-200, 2007.
- [3] International Commission on Non-Ionizing Radiation, "ICNIRP Guidelines for Limiting Exposure to Time-Varying Electric, Magnetic and Electromagnetic Fields (up to 300 GHz)," *Health Physics*, vol. 74, no. 4, pp. 494-522, 1998.
- [4] H. Griffiths, "Magnetic induction tomography," *Measurement Science and Technology*, vol. 12, no. 8, pp. 1126-1131, 2001.

Opportunities for RF nanoelectronic integrated circuits using carbon-based technologies

Author: Gerhard M. Landauer, Thesis Advisor: José Luis Gonzalez
 contact email: gerhard.landauer@upc.edu

I. Graphene and carbon nanotubes for future integrated circuits

The last decades electronics has developed from the first transistors towards high performance integrated circuits with billions of switching devices. This development was made possible by scaling the size of the transistors down to today's several tenths of nanometers. However, the downsizing of the classical silicon-based complementary metal-oxide-semiconductor (CMOS) technology will reach fundamental physical limits during the next decade and the scientific community has started to search for alternative technologies. Promising candidates among them are the graphene field-effect transistor (GFET) and the carbon-nanotube field-effect transistor (CNFET), which have awakened significant interest during the last years [1], [2].

Graphene is a single-atom-thick layer of carbon atoms arranged in a honeycomb lattice. It has outstanding physical and electronic properties, e.g. extremely high mobility of charge carriers. Carbon nanotubes (CNT) are an alternative carbon-based material, which can be viewed as slices of graphene rolled up to tubes with diameters of about 1 to 3 nm. Today the fabrication of both these materials is still immature. The digital parts of integrated circuits with their high device density require tight manufacturing tolerances, which cannot be fulfilled and make it unlikely that carbon-based devices for digital circuitry will arrive at the point of market insertion in the near future. However, for the analog building blocks of systems-on-chip these tolerances are more relaxed. This makes GFETs and CNFETs a realistic medium-term choice for low-cost radiofrequency (RF) applications with excellent performance.

The research on carbon-based is still in its early stages, with the first demonstrations of CNFETs and GFETs in the years 1998 and 2004, respectively. Therefore, there is a lack of comprehensive studies

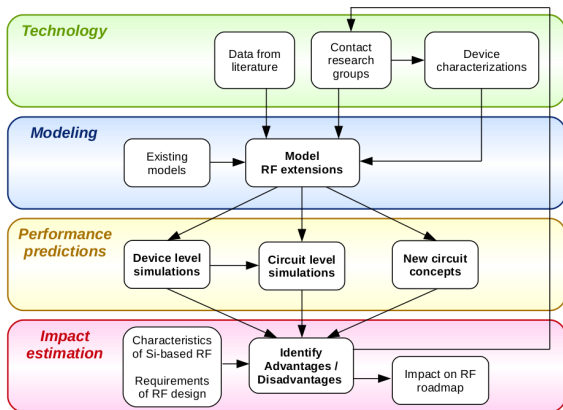


Figure 1. Methodology applied in our research: Existing device models are complemented with RF extensions to be able to do RF performance predictions. This allows identifying advantages and disadvantages of the novel technologies and their impact on the RF technology roadmap.

weighing up their advantages and disadvantages for RF applications. In our work we aim for developing transistor models, characterizing manufactured devices, and doing performance benchmarking on device and circuit level. This allows us to finally compare carbon-based with conventional silicon-based technologies, evaluate their impact on the RF technology roadmap, and explore their use for innovative high-performance electronics (Fig. 1).

II. Modeling of CNFETs

An obstacle to investigations on the RF-CNFET is the lack of suitable compact models. In particular, existing compact models do not consider noise, which is yet crucial for analog applications. Furthermore, process variations have to be taken into account. We have added these additional functionalities to the Stanford CNFET compact model [3], which enables us to do extensive simulations of the CNFET's analog behavior.

II.A. CNFET variability model

Today's CNT growth processes are immature and the tubes' diameters are subject to strong statistical variation (Fig. 2.a). As the diameter directly defines the CNT's electrical properties, this uncertainty in diameter results in a variation of the band gap and conduction type, i.e. metallic or semiconducting character (Fig. 2.b). Therefore, the array of aligned CNTs of the CNFET channel includes metallic tubes in parallel to the semiconducting ones, which can significantly degrade performance (Fig. 2.c). These metal shorts can be removed by an additional process step (e.g. by electrical burning), which however unintentionally also damages a part of the semiconducting tubes (Fig. 2.d). This procedure of obtaining a realistic device channel is repeated multiple times in form of Monte-Carlo simulations to obtain results with statistical significance.

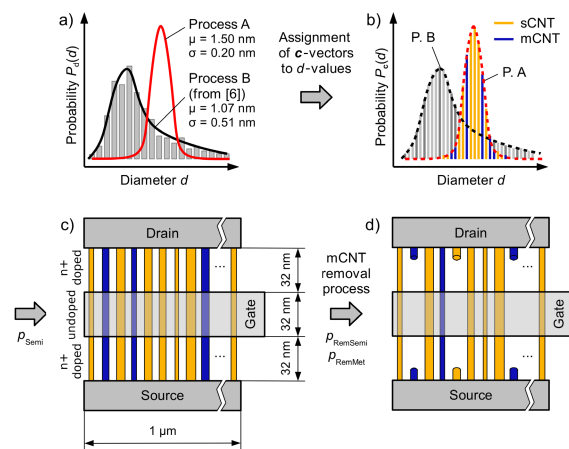


Figure 2. CNFET variability model [4]; a) Diameter distribution of different CNT growth processes. b) Chirality vector distribution resulting in semiconducting and metallic CNTs (sCNTs and mCNTs, respectively). c) CNFET with multi-tube channel including metallic shorts. d) CNFET after applying a metal tube removal process.

II.B. CNFET noise model

Fig. 3 depicts the CNFET's equivalent circuit diagram including different types of noise sources. In addition to suppressed channel shot noise occurring in ballistic devices, we consider flicker noise, which has been reported to be extraordinarily high in this type of devices, thermal noise sources in the extrinsic ohmic resistances and shot noise at the Schottky barriers at the CNT-metal contacts. An estimation of channel-induced gate noise completes the noise model.

III. CNFET performance projections

A wide spectrum of simulations of RF figures-of-merit has been performed. The main results can be summarized as follows:

- **Speed:** In its optimum biasing point the CNFET shows the excellent peak cut-off frequency $f_T = 1.75$ THz (Fig. 4). The peak maximum oscillation frequency is $f_{max} = 8.59$ THz. Therefore, the CNFET may be used for applications with operating frequencies as high as several hundreds of GHz.
- **Gain:** Due to good electrostatic control of the one-dimensional channel, the CNFET is insensible to short-channel effects. This translates to a low output resistance and high intrinsic gain.
- **Noise:** Even though the minimum noise figure $NF_{min} = 0.087$ dB of the CNFET is low (Fig. 4), it is difficult to realize the required source impedance matching near the open-circuit point. In addition, the device shows extraordinarily high flicker noise with an impact up to several GHz. This has severe consequences for circuits with noise up-conversion such as oscillators, mixers or frequency doublers.
- **Variability:** The high number of tubes in the channel results in an averaging effect, which avoids problems due to tube diameter variability. However, in order to obtain the CNFET's predicted excellent performance, an efficient metal tube removal step or high-purity semiconducting tube growth process are required.

IV. Conclusion

The GFET and CNFET are possible alternatives to the conventional silicon-CMOS technology and may replace it in future high-performance integrated circuits. Especially carbon-based analog circuits are a promising candidate to find their way into industry, as compared to the digital part of integrated circuits the manufacturing tolerances are relaxed.

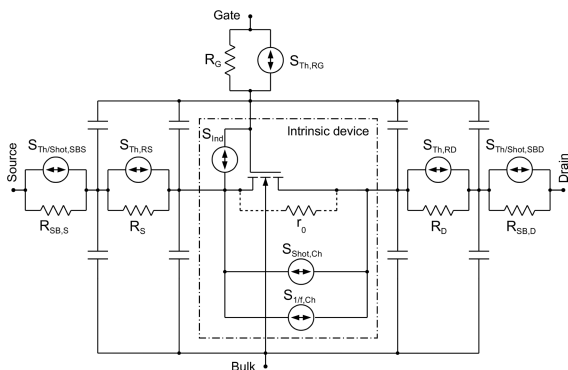


Figure 3. CNFET equivalent circuit including noise sources [4]

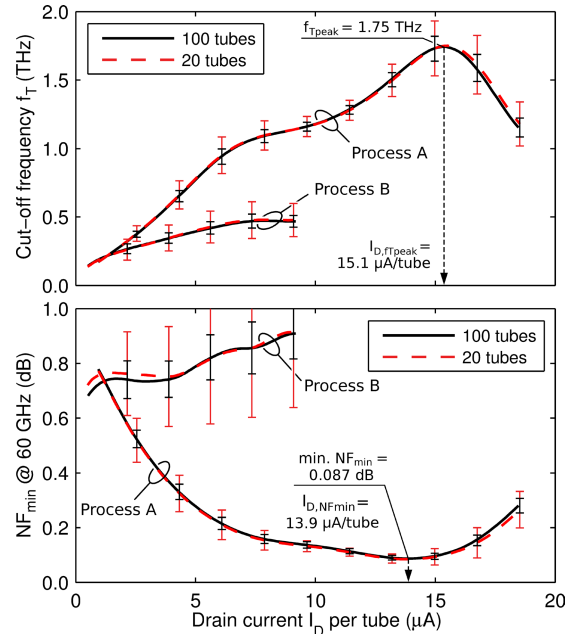


Figure 4. CNFET figures-of-merit: Dependence of cut-off frequency f_T and minimum noise figure NF_{min} on drain biasing current I_D . The error bars indicate the standard deviation due to tube diameter variability [4].

Our work focuses on evaluating the RF potential of these novel technologies, and in this paper we highlighted recent progress in adding variability and noise to an existing CNFET compact model. Subsequently we determined the CNFET's analog behavior, ranging from device speed and gain to noise and process variability. It shows excellent performance in all areas, except of high flicker noise. Circuits with noise-upconversion such as oscillators or mixers would have low performance due to this flicker noise, but low-noise or power amplifiers may experience a significant performance boost when using CNFET technology.

As a further step we will extend our research to GFET devices and circuits. This will allow us to obtain an overall view on carbon-based RF electronics for future low-cost high-performance applications.

V. Acknowledgments

This research work was supported by the Spanish Ministry of Science and Innovation (MICINN) through the project TEC2008-01856 with additional participation of FEDER funds and the European TRAMS project, FP7 248789. G.M. Landauer acknowledges the support of an FI grant of the Generalitat de Catalunya and the European Social Fund.

VI. References

- [1] F. Schwierz, "Graphene Transistors," *Nature Nanotechnol.*, vol. 5, no. 7, pp. 487-496, May 2012.
- [2] C. Rutherglen, D. Jain, and P. Burke, "Nanotube electronics for radiofrequency applications," *Nature Nanotechnol.*, vol. 4, no. 12, pp. 811-819, Nov. 2009.
- [3] J. Deng and H.-S.P. Wong, "A Compact SPICE Model for Carbon-Nanotube Field-Effect Transistors Including Nonidealities and Its Application - Part II: Full Device Model and Circuit Performance Benchmarking," *IEEE Trans. Electron Devices*, vol. 54, no. 12, pp. 3195-3205, Dec. 2007.
- [4] G.M. Landauer and J.L. González, "Carbon Nanotube FET Process Variability and Noise Model for Radiofrequency Investigations," in *12th Int. Conf. Nanotechnology (IEEE NANO)*, Aug. 2012, *accepted for publication*.

Efficient implementation with FIR filters of operators based on B-splines to represent and classify signals of one and two dimensions

Author: Lluís Ferrer-Arnau, Thesis Advisor: Vicenç Parisi-Baradad
 contact email: luis.jorge.ferrer@upc.edu

I. Introduction

Digital signals have a lot of advantages: facility in storage, compression, easy to operate numerically, but they have disadvantages, too. For example, operations relative to differential calculus like derivatives, integration, etc., are not well defined. In this thesis a way to solve this problem is presented. First, digital signals are converted into a continuous signal using polynomial spline interpolation, and then, the derivatives and others operators are calculated in the same way as in the continuous signals. Another main objective is to find the most efficient way to implement these operators with digital FIR filters.

The splines are curves or functions defined piecewise by polynomials of different degrees. The splines of order 1 are straight lines that connect the different samples. The junction points of the polynomial are called knots and at this point the splines have the characteristic of having continuity in the curve as well as in derivatives up to one order less than the spline. For example with cubic splines the continuity in the knots of polynomials is insured up to the second derivative. In Fig.1 it's shown an example of interpolation with linear splines. Fig. 2 shows the same points but interpolated with cubic splines. As it can be seen with cubic splines a curve much smoother than with linear splines is achieved.

In the case of cubic splines, to find each coefficient of each spline polynomial is necessary to solve a system of three equations per point to interpolate. In this thesis we proposed to solve this by applying a digital FIR filter.

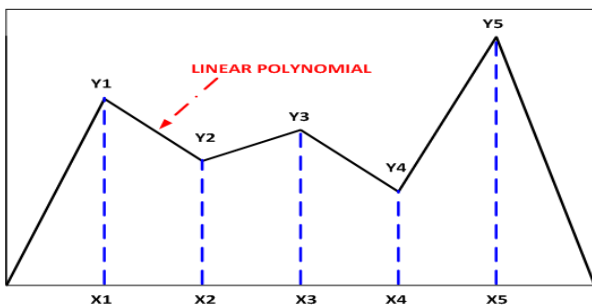


Figure 1. Example of interpolation with linear splines.

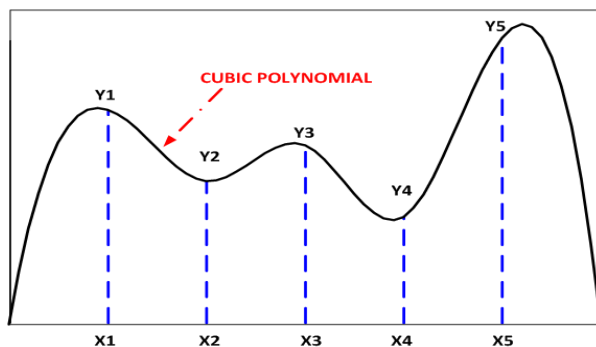


Figure 2. Example of interpolation with cubic splines.

One of the first reference works on the spline is [1]. At first, it was applied in the field of graphic design and basically to define continuous curves, interpolating or approximating specific points, without needing that these points be evenly spaced.

It was in early 1990's when Michael Unser, professor and director of research group "Biomedical Imaging group" of the Federal Polytechnic School of Lausanne, who developed much of the mathematical theory to apply B-splines in signal processing [2], [3]. This imply to have equidistant samples and normalized period ($T=1$).

The B-spline function of order zero is a rectangle defined in the real domain between $[-0.5$ and $+0.5]$. The B-spline of order n is a function that has compact support and can be generated by convolving the B-spline of order zero $n+1$ times with itself. Any polynomial spline can be represented by a linear combination of B-spline functions displaced. In figures 3 and 4 the B-splines functions of order 0, 1, 2 and 3 respectively are shown.

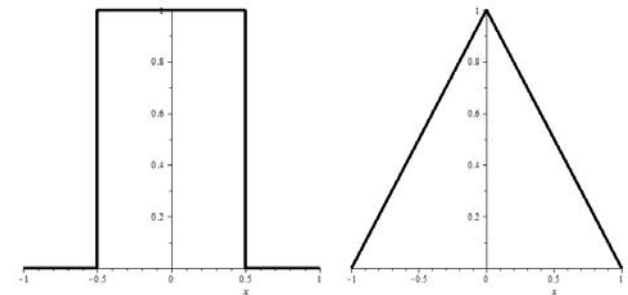


Figure 3. B-spline of order 0 (left), and order 1 (right).

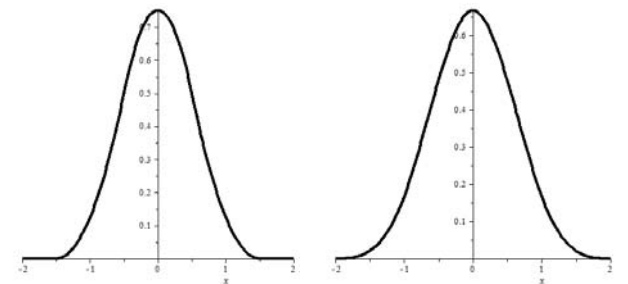


Figure 4. B-spline of order 2 (left), and order 3 (right).

II. Methodology applied

Spline interpolation needs to solve a large set of equations. In this thesis we show how to implement operators based on B-splines using digital FIR filters.

As an example of magnitude, interpolating 16 samples would involve solving a linear system of 48 equations, and interpolating 100 samples implies solving a system of 300 equations. In this paper we have solved this equation system for different numbers of samples, and experimentally, by simple observation, we have concluded that the polynomial coefficients can be calculated using the discrete convolution between the

samples and coefficients that can be represented perfectly by an anticausal FIR filter. The inverse matrix method was used to solve the equation system. To find the stability of the solution the equation system has been solved for different numbers of samples. Table I shows the result of the filter coefficients to calculate the first derivative with cubic splines in periodic form, interpolating between 16 and 32 samples respectively. In this thesis we apply this method of solving the corresponding equation system to find the most efficient implementation with FIR filters of the different operators based on B-splines.

		with 16 knots	with 32 knots
k=0		0	0
k=+/-1	+/-	0,80384757	0,803847577
k=+/-2	-/+	-0,21539028	-0,215390309
k=+/-3	+/-	0,057713549	0,057713659
k=+/-4	-/+	-0,015463918	-0,015464328
k=+/-5	+/-	0,004142121	0,004143654
k=+/-6	-/+	-0,001104566	-0,001110289
k=+/-7	+/-	0,000276141	0,000297501

Table I. Coefficients of the first derivative operator based on cubic splines.

Another objective is to detect the exact localization of the singular points of a signal, which typically are associated with the maximums of the first derivative or the zero crossings of the second derivative. These points may not match the sampling points.

To avoid the high frequency components of the signal, first it's necessary to filter the signal. In this thesis we proposed to use the B-spline function to filter and to calculate the derivatives. In Fig. 5 is shown a B-spline of order 4 and its first derivative, formed with B-splines of order 3, and its second derivative, formed with B-splines of order 2.

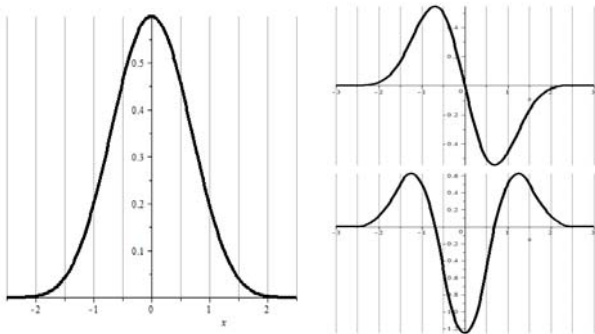


Figure 5. B-spline of order 4 and its first derivative (top right of the figure), and its second derivative (bottom right of the figure).

III. Results, conclusions and applications

In this work we propose a procedure to obtain a temporal and frequency representation of the operators that are applied to calculate the derivatives of different orders of discrete signals, based on cubic splines. In Fig. 8 the continuous representation of the first derivative of the discrete signal of the Fig. 6, calculated using filters based on cubic splines, is shown.

We also propose [4] a way of obtaining the FIR approximation of the cubic spline interpolator. By using only 10 coefficients (10 additions and 5 multiplications), the accuracy is as high as 99.9 %. One of the many applications of converting a discrete signal into a

continuous signal is to be able to calculate the exact frequency of a signal by determining its zero crossings.

These operations are usually needed in a lot of fields, like power quality measurements, nonintrusive load monitoring, etc.

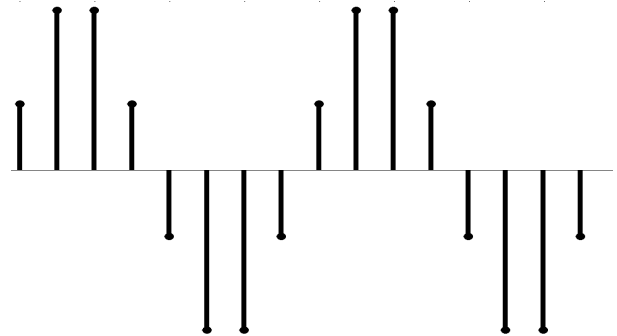


Figure 6. Example of discrete signal obtained by sampling a continuous sine wave of 50 Hz. The sampling frequency is 400 Hz.

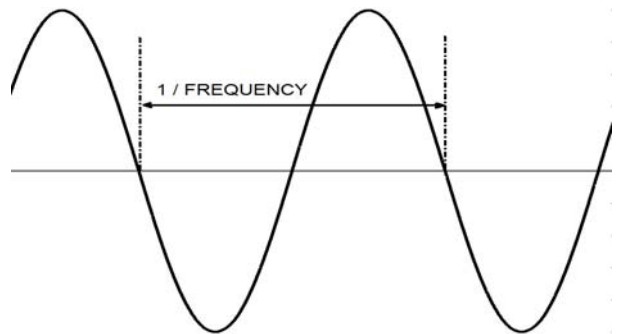


Figure 7. Continuous signal obtained by interpolating with cubic splines the discrete signal of Fig. 6. In this continuous representation is possible to determine the exact zero crossings and the exact frequency.

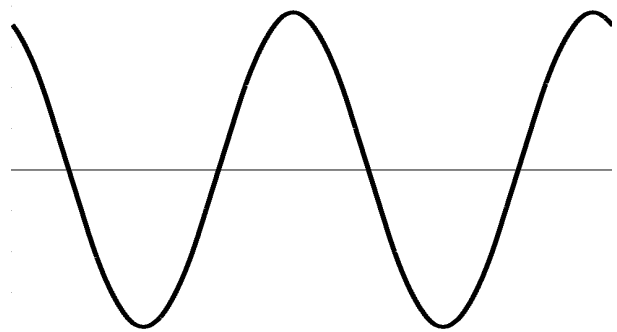


Figure 8. The continuous representation of the first derivative of the discrete signal of the Fig. 6.

IV. References

- [1] C. de Boor, A practical guide to splines. New York: Springer-Verlag, 1978.
- [2] M. Unser, A. Aldroubi and M. Eden, "B-spline signal processing: Part I-theory," IEEE Trans. Signal Processing, vol. 41, no. 2, pp. 821-833, 1993.
- [3] M. Unser, A. Aldroubi and M. Eden, "B-spline signal processing: Part II-efficient design and applications," IEEE Trans. Signal Processing, vol. 41, no. 2, pp. 834-848, 1993.
- [4] Ll. Ferrer-Arnau, R. Reig-Bolaño, P. Martí-Puig, A. Manjabacas, V. Parisi-Baradad, "Efficient cubic spline interpolation implemented with FIR filters", International Journal of Computer Information Systems and Industrial Management Applications. ISSN 2150-7988, vol. 5, pp. 098-105, 2012

Hardware Model of Large Spiking Neural Networks using Parallel NoCs

Author: Andres Gaona Barrera, Thesis Advisor: Manuel Moreno Arostegui

andres.eduardo.gaona@upc.edu, aegaona@udistrital.edu.co

I. Introduction

Large Scale Spiking Neural Networks (LSSNN) have been recently studied in computational neuroscience because they can simulate the brain dynamics of a particular cortex or interactions among neuron populations at mesoscopical scales [1]. Each neuron can be analyzed as an independent MISO (multiple input, single output) system, where the output can be connected both to other neurons and to its own inputs. The connection between neurons is called synapse and it allows the transmission of spikes (neural impulses) from a source neuron to a target neuron. Additionally, the connectivity pattern is probabilistic, so that these networks are nearer to a chaotic model.

The main problems of the hardware implementations of the LSSNN are the high-level connectivity and the multiple concurrencies of spikes. For example, let's consider a possible LSSNN composed of 10^7 neurons and an average grade of connectivity of about 10^5 synapses per neuron. If the above network is completely mapped it would implement up to 10^{12} point to point connections; therefore, the routing issue would have a hard solution with the current technologies. Another important restriction is the high computational load, since the neuronal spiking frequency is approximately 100 Hz causing large delays in long synapses.

Some hardware models of LSSNN have been investigated based on Networks on Chip (NoCs). The Embrace architecture uses a bi-dimensional array of neural tiles; this model can generate feedforward neural networks of two layers [2]. According with [3], a neuron-router set is grouped in each tile and the communication between routers is done using packet switching. In [4], the interconnection of Spinnaker chips is presented, each chip has 1000 neurons communicated with two NoCs, and the first one communicates the synapses of its neurons, while the second transmits information about particular synaptic weights. The NoCs employed inside Spinnaker are configured with packet switching and routing tables for point-to-point connections. Similarly, a VLSI system for implementing neural networks (512 neurons and 10^{14} synapses) has also been presented. An initial model contains a NoC organized in bus, then a hybrid network whose routers use packet and circuit switching was also proposed [5].

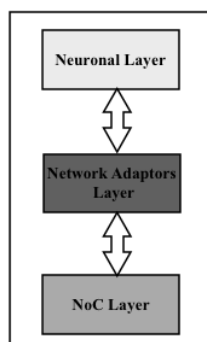


Figure 1. Layers of Sepelyns

Making use of the concept of Networks on Chip (NoCs) operating in parallel, the architecture for hardware implementation of LSSNN, termed as *Sepelyns* (SEpals and PETals providing Large densities of sYnapses in Neural Structures), is proposed to communicate millions of neurons and thousand of synapses per neuron [6]. The communication infrastructure is developed as a generic and scalable model for a possible implementation on dedicated (ASIC) or programmable (FPGA) devices. Additionally, the NoCs decrease the complexity of the routing processes and several of them give redundancy to manage the model dimensions. Some capabilities of *Sepelyns* are its scalability, programmability, redundancy of the communication links and biologically-plausible. The *Sepelyns* architecture is briefly presented in the section II, while the section III is focused to the layer of Network Adaptors (NA). Finally, some implementation results of the NA are showed in the section IV.

II. Sepelyns Architecture

The *Sepelyns* architecture is organized in three functional layers according with the abstraction level of the model, as shown in Figure 1. The highest block corresponds to the neuronal layer, where each neuron is localized and operated independently. Either output spikes or input spikes of the neuronal layer are sent to/from layer of network adaptors, respectively, hence this layer is the interface between the neurons and the communication infrastructure. The sepals and petals are two kinds of NoCs and they permit to manage all synapses of the LSSNN, both are contained in the NoC layer. A petal is a bi-dimensional array of routers for traffic BE (Best Effort), so that short synapses, or distance between near neurons, are configured to pass by only BE routers. Likewise, GS (Guaranteed Service) traffic is defined for long synapses and it is routed through of the sepals, being the sepal a NoC with truncated pyramid topology of GS routers.

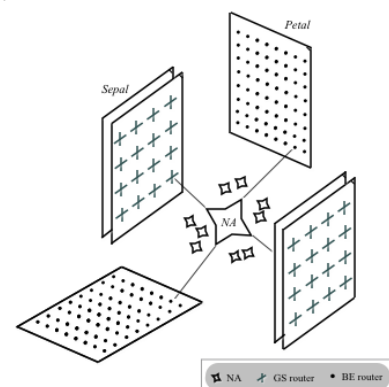


Figure 2. Interaction between NA and the NOC layer

An example of how the NAs interact with the NoC layer is illustrated in the Figure 2. In this case, there are two sepals and two petals in the NoC layer and they are connected to the highlighted NA using the links

associated with the BE or GS routers. It is important to see that an NA has assigned the same router inside of the petals or sepals.

III. Structure of the NAs

A NA can group a set of neurons; furthermore there are at least one sepal and one petal connected to the NAs. The most important functions of the NAs are summarized below.

- Transform the input spikes of a source neuron in one or multiple packets to transmit through of the NoC layer. In the Figure 3 is showed a circuit for implementing this functionality, named packetization. The circuit is split in two parts, most and least significant blocks, and the LSR_b register is loaded with one block through the output multiplexer. The identifier of the target neuron ($NA_Addr + i$) corresponds to the most significant part of the packet, where i denotes the neuron in the target NA (NA_Addr). The least significant part is a bit more complex because it contains a memory array; in this example there are 8 memories, where all synaptic targets of one neuron are stored in the same memory. The control unit chooses the memory and increases one counter for a common address bus of the memories. The dotted lines correspond to signals of the control unit.

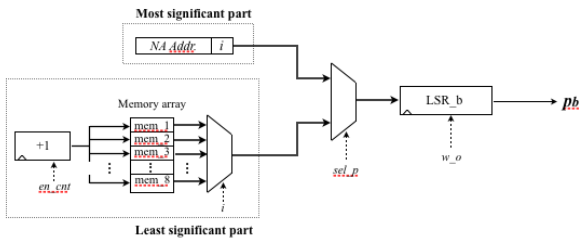


Figure 3. Circuit for packetization process

- Receive a packet of the NoC layer, identify the target neuron and generate the output spike to the neuron source. The circuit of the Figure 4 is designed according to the above depacketization process. The SHR register is loaded bit to bit using the i_x_y line. When the entire packet is stored, then it is transferred to the REG register, where the target neuron is identified comparing the i value with the constant of the comparator.

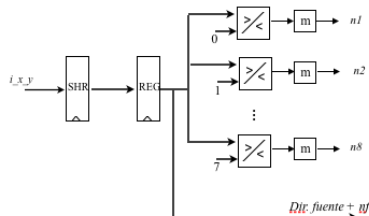


Figure 4. Circuit for depacketization

IV. Implementation results

The table I shows the resources/frequency comparisons of the NA model implemented in three FPGA, assuming that the memory array is external to NA block. The packets have a length of 40 bits, where each block can handle up to 17 bits for the NA addresses. The 6 bits remaining correspond to the identifier of the source and target neurons. Groups of

eight neurons per NA have been demonstrated as a near optimal value in Sepelyns for a neural network with one million of neurons [6].

Kind of FPGA	Maximum Operating Frequency (MHz)	Resources (slices)
Virtex 6 (xc6vlx75t)	215.77	91/93120
Spartan 3E (xc3s1660e)	68.83	123/14752
Statix II (ep2s15f484)	161.81	94/12480

Table I Results of synthesis on FPGAs

In the three cases presented in the table I, the quantity of resources for the developed NA is less than 1% in all of FPGAs, this is a evidence of the simplicity of the proposed design. However, the operation frequency of the NAs is highly correlated with selected technology. The best operation frequency is 215MHz in a FPGA of the Virtex 6 family, while the worst case is almost four times lower in a Spartan 3, which value is 68MHz.

V. Conclusions

We presented the most relevant characteristics of the Sepelyns architecture that can emulate a large-scale neural network. To perform biologically realistic simulations in order to connections and dimensions of a neural model, the organization considered by Sepelyns can be a good alternative in neurodynamic modeling approaches or neuroscience applications. Specifically, this paper focused on describing two processes executed by the NAs: packetization and depacketization. These processes provide to the adaptor network layer of the facilities for serving of bridge between the neurons and the NoCs, sepals and petals. Important tradeoffs about NAs implementation are the hardware cost and the operating frequency, a simple scheme of datapath and control unit can achieve for a balance in the NA. Therefore, the memory array size will have an important contribution to the size of the NA and read operations will increase the overall delay of this block in Sepelyns.

VI. Acknowledgments

The author would like to acknowledgement his sponsor, the District University Francisco Jose de Caldas.

VII. References

- Misra J. and Saha J., "Artificial neural networks in hardware: A survey of two decades of progress", Journal Neurocomputing, vol. 74, pp. 239 – 255, december 2010.
- Harkin J., Morgan F., et al., "A Reconfigurable and Biologically Inspired Paradigm for Computation Using Network-On-Chip and Spiking Neural Networks", International Journal of Reconfigurable Computing, 2009.
- Carrillo S., Harbin J., et al., "An Efficient, High-Throughput Adaptive NoC Router for Large Scale Spiking Neural Network Hardware Implementations", ICES Conference 2010, York, UK. Springer-Verlag, 2010.
- Rast, A. D., Yang, S., Khan, M. et al, "Virtual Synaptic Interconnect using an Asynchronous Network-on-Chip, IEEE IJCNN 2008, pp. 2727-2734, 2008.
- Fieres J., Schemmel J. and Meier K., "Realizing Biological Spiking Network Models in a Configurable Wafer-Scale Hardware System", IEEE IJCNN 2008, pp. 969-976, 2008.
- Gaona A. and Moreno M., "A Communication Infrastructure for Emulating Large- scale Neural Networks Models", 22nd ICANN Conference, Laussane, Switzerland, 2012.

2D/3D Simulation of Solar Cells

Author: David Carrió, Thesis Advisor(s): Ramon Alcubilla (Thesis Tutor), Pablo Ortega, Isidro Martín
 contact email: david.carrio@gmail.com

I. Introduction

The new solar cells structures seek to achieve higher efficiencies that are characterized by optical and electrical behavior in more than one dimension. This multidimensional behavior involves an analysis of the results in two and three dimensions. These types are looking for improved efficiency in the conversion of solar energy to electrical energy by different design strategies. The multidimensional behavior adds greater complexity in the analysis of the results and modelling to simulation tools to predict and adjust the design parameters. Therefore we must develop a methodology for the simulation of adjusted models to the particular characteristics of these types of solar cells which have a complexity related to the different strategies of efficiency improvement.

The main objective is oriented to the development of this methodology for modelling and simulation of these types of solar cells taking into account its specific characteristics, in order to have a prediction tool, understanding of analytical results and thus forward in setting the design and parameterization of these structures. Therefore, this study seeks to develop modeling and simulation techniques of these types of solar cells whose design stands out from the conventional conception.

Once the main objective of this study is explained, an important element is the simulation tool, which in this study, it is employed the TCAD Sentaurus Device which provides the ability to simulate and analyze the electronic and optical behavior in 2 or 3 dimensions. The TCAD software Sentaurus Device is a powerful tool which includes the main numerical models such as the carrier transport, recombination and generation, mobility, semiconductor band structure. Also it includes the optical generation models.

The first step in this study is the selection and adjustment of the models and the definition of their parameters in order to obtain a more accurate resolution. In other words, the validation and the verification of the models and resolution system by means the use of the analytical data must be a prior and unavoidable step of optimization.

Moreover, this work so far has focused on developing and adjusting models and values of them, validating and verifying the results that are obtained with analytical results. An example, it is the Auger recombination model adjustment [1] [2] which has modified by PMI (Physical Modeling Interface) Sentaurus Device tool. A particular case is the incident solar spectrum adjustment, which the standard spectrum AM1.5G is parameterised according to the reflectance of the textured frontal region of the solar cells.

Two types of these solar cells are presented in this paper, which are analyzed for to characterize their behavior in specific boundary conditions. A previous study has been focused on to normalize and to adjust the models, their parameters and boundary conditions.

In particular, these two types are the IBC solar cells (Interdigitated Back Contact) and the DoppaCell. In the next section these solar cells are presented.

II. Solar cells structure

In this section, these two types are presented:

II.A. IBC solar cells (Interdigitated Back Contact)

These solar cells have the contacts in the rear side. The advantages are:

- The shading is removed by the absence of metallic bus bar in the front side, that generates an increase of short circuit current (I_{sc}).
- The reduction of the metallic bus bar series resistances. The contacts and fingers are in the rear side, so they may have unlimited width because there aren't shading effects.
- The integration between several modules of solar cells is easier

Due to the absence of the metallic bus bar in the front side, this region can be optimized according to the capture area, the passivation in the surface by means the reduction of the surface recombination. The collect union, which is in the rear and the front, is very well passivated. The minority carriers, which are generated mainly at the front, it should be diffused towards the union rear. So it requires an optimal relationship between the diffusion length and the thickness of the solar cell.

The basic concept of this type of solar cells is based on achieving better efficiency by means passivation techniques, so a greater number of collected photons arrive to generate power, and above all to expand the capture area of photons, since the contacts and metallic fingers are the rear side. It requires an asymmetric structure where the base and emitter contacts are located in the rear side.

The p-type semiconductor region is the greater part of the structure, base region, and the n-type semiconductor region, emitter region, is a small area that is located above the emitter contact.

An important item is the pitch between base and emitter contacts, as well as on surface recombination contact both in the front side as the rear side.

Related to the simulation, the first step is the definition of the structure to simulate in order to minimize the calculations and the simulation time. The strategy is the search for symmetries according to reduce the structure of simulation. By means the Sentaurus Structure Editor (SDE) is defined the 3D structure according to a doping profile.

II.B. Doplacell solar cells

The second structure has a transparent contact in the front side, base contact, and the emitter doping profile and its contact is the same as the IBC solar cell. In addition, an optimal relationship between the diffusion length and the thickness of the solar cell is also required.

The transparent contact in the front side solves the problem of the shading effects, so the study of this structure is focused on the recombination rate of the passivated rear side. Equal to the IBC solar cells the p-type semiconductor region is the greater part of the structure, base region, and the n-type semiconductor region, emitter region, is a small area that is located above the emitter contact. These types of solar cells differ in the arrangement of the contacts, the base contact is in the front side and the emitter in the rear side.

Applying the same strategy as the IBC solar cell for the definition of the structure to simulate, the meshed structure is according to the minimal dimensions. In other words, it is applied the reduction of the part of structure that allows to expand the results.

III. Obtaining results

The purpose of the study is to verify and to validate analytical results by means a electronic and optical modeling of solar cells that have a 2D/3D behavior, and it develops new structures, using a TCAD software.

A previous study has been focused on to normalize the models and their parameters that will be used for two types of solar cells. The structure is solar cell with a transparent front emitter contact and a set of rear separated base contacts with a specified pitch. The symmetries, in order to minimize the calculations, allow a reduction of the simulation structure. A example of a result is the total density current in the x direction that is presented in the Figure [1].

Finally, in the other Figure [2] it is presented the Auger recombination that is obtained from a IBC solar cell simulation with the characteristics which have been mentioned in the previous section. You can see the effect on the base and emitter contacts, as well as the different ranges depending on the area of the structure, particularly in the rear side. Clearly there is a dependency with the geometry and layout of the base and emitter contacts, as well as other parameters such as the surface recombination of them.

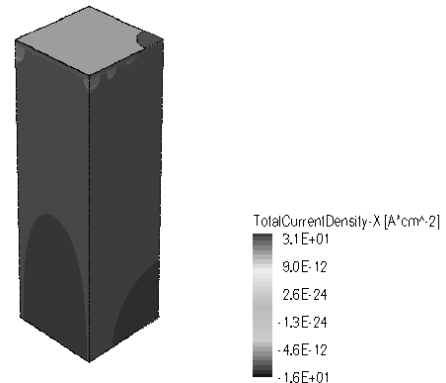


Figure 1. Total current density in the x direction, $v_{out} = 0,4$ V.

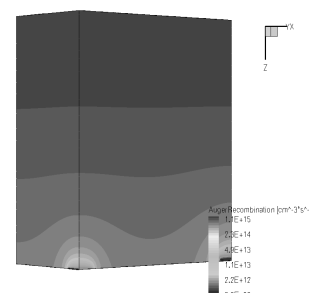


Figure 2. IBC Auger recombination, $v_{out} = 0,08$ V.

IV. Prior work

In the introduction. It was mentioned the first step, which is focused on the adjustment and selection of the models and parameters by means the validation and verification with analytical results.

The current work is dedicated to obtaining results for the interpretation of some sensitive parameters in the solar cell operation to the knowledge of their behavior due to the impossibility of knowing them by means another way. This study should allow the proposal of new variants of design for the improvement of efficiency and for the modeling and collection of studies prior to the physical implementation.

V. Acknowledgments

My acknowledgments to my thesis advisors of *MNT-DEE-UPC Group*.

VI. References

- [1] Mark J.Kerr and Andres Cuevas, "General parameterization of Auger recombination in crystalline silicon," *Journal of Applied Physics*, volume 91, number 4, 15 February 2002
- [2] Mark J. Kerr, Andres Cuevas and Patrick Campbell, "Limiting Efficiency of Crystalline Silicon Solar Cells Due to Coulomb-Enhanced Auger Recombination," *Progress in Photovoltaics Research and Applications, Prog. Photovolt: Res. Appl.* 2003; 11:97–104 (DOI: 10.1002/ppv.464)
- [3] U. W. Peter Wurfel, *Physics of Solar Cells: From Basic Principles to Advanced Concepts*, 2009.

The Imbalance Element and Artificial Nervous System Design

Author: Paul Olivier, Thesis Advisor: Juan Manuel Moreno Aróstegui

Contact email: paul.olivier@upc.edu

I. Introduction

Over the past several decades, nonindustrial robotics has seen a change in emphasis from trying to discover an artificial form of intelligence to drawing inspiration from biology. This has led to fields such as biomimetics, behavior-based robotics and evolutionary robotics. But looking at the robotic products out there today (vacuum and pool cleaners, lawnmowers, assisted surgery, bomb-disposal units, personal robotics) one does not find any strong biological features but rather an attempt to “industrialize” the environment and robot that enable the reuse of concepts from industrial robotics. Yet, instead of therefore discarding the notion of bio-inspired robotics, rather there is an ever increasing interest in reproducing biological behavior to some extent in nonbiological entities. It is as though we are convinced about the relevance of biological inspiration, even if we haven't been able to discover really how to unlock the biological secrets on how to build nonbiological products with a clear biological nature regarding their behavior.

Under the concept of strong biological features (in regards to behavior) one can consider behavioral features such as evolution, adaptation, learning and acting with a sense of meaning (that is, acting as an individual rather than being a mere human-command interpreter or tool). In biology these features are integrated into a single nervous system technology that covers the complete range of biological organisms. All biological nervous systems share the same foundation and, therefore, one can argue they share the same mechanisms to enable a network of cells to generate biological behavior with the prime objective being the survival of the species.

Yet, robotic products show no such harmony between systems of lower to higher complexity. Neither do we see anywhere, not even in research, the tight integration between these strong biological features as found in biology. It is easy to comprehend why it is so challenging to merge the worlds of the biological and the artificial (nonbiological), especially when we want to make, for example, a computer program produce biological behavior on a wheeled-robot with two infrared proximity sensors.

While some might think we are already on the right track (it is just a matter of time), perhaps we need to revise our understanding of the fundamentals of biological behavior. Are we trying to discover the mechanisms of biological behavior from the neuron level upwards or merely trying to mimic observed behavioral patterns? Surely, if we can correctly discover the mechanisms of biological behavior and abstract these mechanisms from biology's cellular implementation, then it has to be possible to develop a single technology to design behavior for nonbiological organisms in which strong biological features are integrated naturally.

II. A New Design Methodology

This is the goal of the thesis: to try and discover at least the initial steps of such a single technology, with its

associated design methodology for developing the behavior for a nonbiological organism. The current focus is about discovering the theory behind such a design methodology rather than a design for a particular product or application. However, the purpose of the theory is to form the basis for the development of commercial solutions in the future. All designs originating along the course of the thesis are implemented on a real-world device as opposed to simulations. For this purpose a small, peripheral-rich, mobile robot is used, called the e-puck (see Fig. 1).

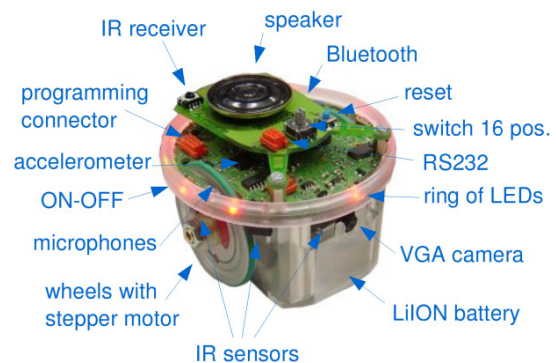


Figure 1. The e-puck robot.

It is important to understand that the research was originally not about a design methodology but about asking the question “Why?”. That is, “Why does the robot have to move? Why does the robot have to do anything? Why does a biological organism move? How is it that a biological organism can act purposefully, with sense to its actions without a computer program telling it what to do?”. Development of a plausible answer and its initial implementation in a real-world robot indicated that it might be possible to transform these initial concepts into a formal design methodology for the nervous system of nonbiological organisms. Thus, the initial results from the thesis are the concepts, processing elements and architecture that form the foundation of the design methodology.

The results from this initial phase has already led to successful, small designs that could already show features of adaptation and evolution [1][2]. Their low complexity, however, leads to minimal commercial application. It is predicted that the true potential of this design methodology lies in addressing problems that are hard to solve with current technologies. Typically these problems are those where humans either are not present (space exploration), cannot be present (radioactive environments) or cannot be present the whole time (satellites, ocean-floor observatories). Additionally, in line with biology, this design methodology will lead to substantial adaptation capabilities, in particular allowing the simplification of human-machine interfaces. As devices have become “smarter”, so have their interface and use become more complex, with an ever increasing list of configuration options. Furthermore, there are a vast number of systems and machines that can benefit from itself being able to perceive its own “health” and predict when it is about to break down. This would save on preventive maintenance costs and losses due to nonoperation

(e.g., home appliances). Evidently, such solutions would require a significant level of complexity. Therefore, the thesis is the initial phase of a long-term endeavor, given that the research results can show that reaching such complexity is viable.

III. Status

The current answer to the question “Why?” is the concept of the equilibrium-action cycle (Fig. 2). This concept says that there are elements (also, subsystems) in the nervous system that cycle through states of balance (equilibrium) and imbalance (disequilibrium). Particular inappropriate stimuli cause the element to change to a state of imbalance. During this state the element activates some signal that, according to the connections with the rest of the nervous system, will be involved directly or indirectly in action that will reestablish the appropriate stimuli. Consequently the element returns to a state of equilibrium. Sometimes this action leads to the organism acting upon its environment, which is the behavior we observe. Behavior is thus seen as being driven by imbalances in the nervous system as opposed to either being controlled or resulting from the execution of programmed instructions.

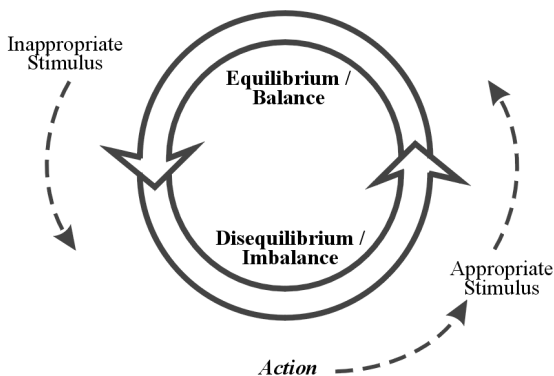


Figure 2. The equilibrium-action cycle.

The nervous system is the network of these imbalance elements. While some elements are directly associated with observable action (e.g., motor neurons), others perform functions such as information extraction (filtering, correlation, etc.), homeostasis and motivation. Since nowhere in the nervous system there is a unit for explicit generation of particular behaviors, all behaviors emerge from the actions between elements, and the elements with the environment (via the organism's body), all of which have the purpose of only restoring equilibrium. Hence, a nervous system that operates correctly with sufficient optimality represents an organism in equilibrium with its environment. For biological organisms this infers survival; for nonbiological organisms, that they are able to successfully perform their primary task or mission.

The sense we observe in the actions of biological organisms can therefore be explained since all behavior originate from the nervous system and have the particular purpose of maintaining equilibrium within the nervous system, which will have the effect of maintaining a healthy, fit individual within the population. Thus, the origin of all behavior (the reason for its appearance) has meaning firstly to the organism. The features of adaptation and learning stem from the nervous system containing a set of mechanisms through

which the nervous system can make changes that improve the equilibrium with the environment (that is, the fitness of the individual) [2]. We do not get born with this equilibrium. In the case of the just-born gazelle, its nervous system needs to adapt its muscle coordination as quickly as possible to run with the herd and avoid predators. Any excessive struggling (insufficient performance) for equilibrium could trigger adaptation. Evolution can be explained similarly except that the changes are made during reproduction at a genetic level [1]. Learning can be seen as the most complex form of adaptation in that it requires creativity and synthesis. Therefore, learning falls outside the scope of the thesis.

In terms of artificial nervous systems, the idea is to convert the equilibrium-action cycle into a basic model (the imbalance model), and then, using the neuron as reference, develop an element (the imbalance element) to serve as the ubiquitous processing element within the nervous system. Therefore, the imbalance element has features such as multiple-inputs-single-output, synaptic weights, excitatory and inhibitory inputs, and thresholds. The artificial nervous system design is the description of these elements and their connections that form the imbalance network (nervous system). This is the “application”, which is done with complete abstraction from any software. All software-specific aspects are contained within the implementation layer on top of which the application (that is, the design) executes. For software-based designs, this has meant using the concept of parallel emulation to be able to execute a parallel design on a CPU-based device. As a consequence, the same design will perform exactly in the same way (given the same stimuli) on a microcontroller, PC or FPGA.

In conclusion, the current results identify a generic mechanism for driving all behavior, artificial nervous system architecture, initial investigation into adaptation and evolution integration, and a solution for acting with a sense of meaning. The resulting designs were simple: a simple line follower to show design-evolution integration [1]; a simple obstacle-avoider to show an implementation of classical condition [2]; a mini sumo robot to show a multimodal implementation (line versus proximity sensors); and a preliminary design for an underwater autonomous vehicle with simple echolocation. The principal used for deciding robot sensor/motor complexity is to start with the simplest setup. That is, first only a single sensor, then two, then a line of sensors, and only then a two- or three-dimensional grid array (e.g., a camera). As with biology, the simplest and most complex organisms have the same neural fundamentals and it is argued that complex behavior (that is, based on complex sensory input) are not separate from the simplest behaviors. Instead, it is believed that complex nervous systems are an extension of simple nervous system. This necessary approach will delay immediate commercialization possibilities beyond mere games, toys and gadgets.

IV. References

- [1] Paul Olivier, Juan Manuel Moreno Aróstegui, “The Equilibrium-Action Cycle as a Mechanism for Design-Evolution Integration in Autonomous Behavior Design,” in AHS, 2012, In print
- [2] Paul Olivier, Juan Manuel Moreno Aróstegui, “Equilibrium-Driven Adaptive Behavior Design,” in IWANN, 2011, pp. 589-596

Study of energy efficiency in DC/AC grid-connected converters using multiplexed switches and adaptive control techniques

Author: R. Pérez Delgado, Thesis Advisor(s): M. Román Lumbreras, G. Velasco Quesada
 contact email: raul.perez-delgado@upc.edu

I. Introduction

The variability, more or less predictable, in electrical energy production based on renewable energies is a particularity of some distributed power generation systems. These variations, due to the nature of the power source, are further disadvantaged when considering the variability in energy demand. The fluctuations between energy generated and energy demanded makes it necessary to increase the use of power electronic systems in order to manage energy by storing the excess of energy during times of low demand and injecting to the grid when higher demand requires it.

This thesis is framed within the field of electrical energy conversion in power generation systems based on renewable and non-manageable energy resources. The research scope focuses on the impact in terms of cost and efficiency of grid connected power converters operating in case of variable power flow and possible improvements of these converters in order to maximize their efficiency.

Therefore, the thesis explores the energetic efficiency of DC/AC grid connected converters using switch multiplexed techniques and adaptive control strategies.

The parallel switch configurations based on discrete transistors improves the cost-per-ampere ratio of power switches [1]. The problem with such configurations is due to the unbalanced current sharing. To deal with this issue, several techniques have been presented by manufacturers and researchers [2] - [5].

II. Current sharing in parallel switches

One of the questions that this thesis aims to answer is how parallel switch configurations and a range of control strategies can affect the global efficiency of power converters.

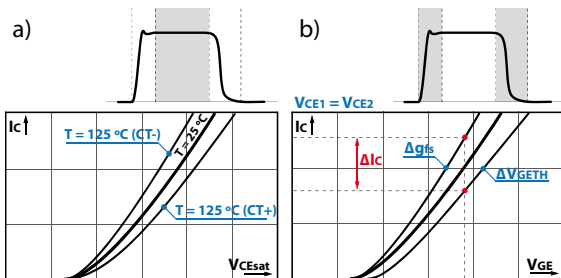


Figure 1. a) Static and b) dynamic current sharing in IGBT transistors. Technological parameters involved in current sharing.

In order to provide a satisfactory answer, special attention will be paid to the transistors technological parameters and which mechanisms are involved in the current sharing in parallel connected switches, especially power switches based on IGBT transistors.

Referring to the current sharing in parallel connected IGBT transistors, it is appropriate to differentiate between static and dynamic current sharing, particularly considering the collector current (I_c) of each transistor. Static current share is sensitive to collector-emitter voltage (V_{CE}) in conduction state (Fig.1a). Dynamic current share is sensitive to gate-emitter voltage (V_{GE}) and to the transistor transconductance (g_{fs}), as shown Fig.1b. According to the IGBT transistor technology (Punch Through or Non-Punch Through), the unbalanced current share is increased or decreased by temperature.

Obtaining good simulation models of converters whose switches are based on IGBT transistors connected in parallel, requires the selection of models which offer a better trade-off between speed and accuracy in the transient behavior of the transistor [6] – [8]. Finally, a balanced current sharing control strategy is proposed in case of multiple switch activation in power converters with this kind of architectures.

III. Results

In the present stage of the research, a current sharing control strategy for parallel connected IGBT has been proposed. By sensing the current of each transistor, this control scheme modifies the voltage level applied to the gate in order to share equally the flowing current through the transistors.

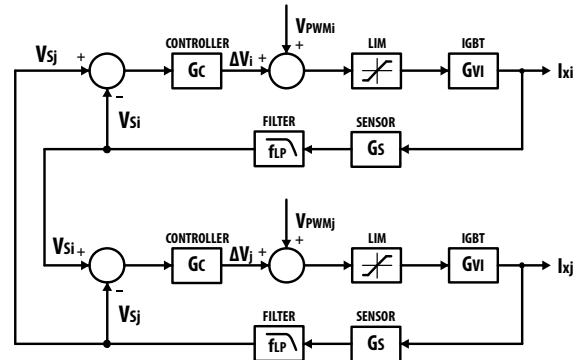


Figure 2. Balanced current sharing control strategy block diagram.

The control strategy that we are proposing is based on the setting of current cross references, grouping pairs of transistors as shown the block diagram in Fig.2. I_x refers to the collector current through the two parallel connected transistors, V_s is the filtered signal from the collector current measurement and ΔV is the voltage variation of the applied gate control signal referred to as V_{PWM} .

III.A. Simulation results

With the objective of validating this proposed control strategy, the current sharing scheme shown in Fig.2 has been simulated with *PSpice*. With this purpose, the

boost converter shown in Fig.3 has been used. In this case, different technological switch characteristics have been applied in order to obtain a heavy unbalanced current sharing through the parallel connected transistors.

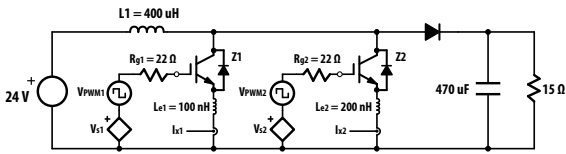


Figure 3. Boost converter with two parallel connected IGBT switches.

Fig.4a shows the current evolution in the transistors in case of applying the same voltage level in the gate control signal. An unbalanced sharing of current flowing through the transistors can be observed. On the other hand, Fig.4b shows a good current balance using the current control strategy proposed at the beginning of this section.

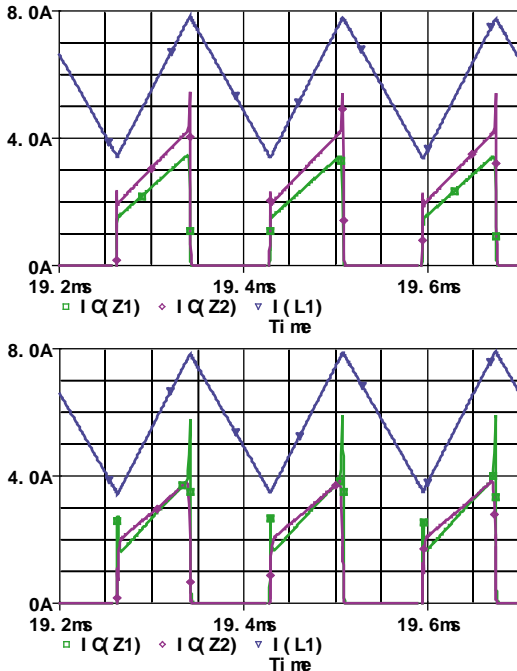


Figure 4. Inductive current sharing in two parallel connected transistors, a) without balanced current sharing control, b) with balanced current sharing control.

III.B. Experimental results

Two parallel connected IGBT switches have been implemented in order to validate the proposed balanced current control strategy. A schematic diagram for the boost converter is shown in Fig.3 and the system parameters are listed in Table 1.

Symbol	Description	Value
V_s	Input voltage	24 V
R_l	Load resistor	15 Ω
R_s	Shunt resistor	5 m Ω
L_1	Inductor	400 μ H
F_s	Switching frequency	6 kHz
Z_1, Z_2	IGBT transistors STGP7NC60HD	600 V/14 A

Table 1. Parameters for the test.

Fig.5 shows the current sharing under two different situations. The first one, shows the current through the parallel connected transistors without the use of a voltage level control technique (Fig.5a). The second shows a balanced current sharing in the transistors when the cross reference current sharing strategy is applied (Fig.5b).

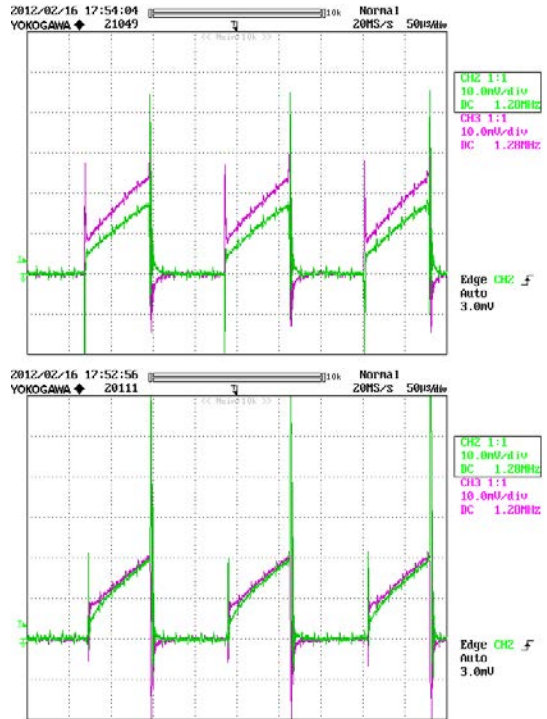


Figure 5. Experimental results, inductive current sharing in parallel connected transistors, a) without balanced current control strategy, b) with balanced current sharing control.

IV. Acknowledgments

This work has been developed in collaboration with the IE3P group at the Industrial Engineering College of Barcelona (EUETIB-UPC).

V. References

- [1] B. R. Pelly, "Choosing Between Multiple Discretes and High Current. Modules" International Rectifier.
- [2] International Rectifier "Application Characterization of IGBTs", AN-990 rev2, 2009.
- [3] Fairchild Semiconductor "Parallel and series connection of MOSFET, IGBT and SKiiPPACK modules", App. Manual, 2007.
- [4] H. Dehbonei, S.H. Ko, S.R. Lee, L. Borle and C. V. Nayar, "Current or Time Sharing Switches for High Efficiency Photovoltaic Power Systems", 32nd Annual Conference on IEEE Ind. Electronics (IECON 2006), Paris, France, Nov 2006.
- [5] N.Y.A. Shamma, R. Withanage, D. Chamund, "Review of series and parallel connection of IGBTs", IEE Proceedings – Circuits, Devices and Systems, vol. 153, pp. 34-39, Feb 2006.
- [6] K. Sheng, S.J. Finney and B.W. Williams, "Fast and accurate IGBT model for PSpice," *Electronics Letters*, vol. 32, no. 25, pp. 2294-2295, December 1996.
- [7] K. Sheng, S.J. Finney and B.W. Williams, "A new analytical IGBT model with improved electrical characteristics" in *IEEE Transactions on Power Electronics*, vol. 14, no. 1, pp. 98-107, January 1999.
- [8] K. Sheng, B.W. Williams and S.J. Finney, "A review of IGBT models" in *IEEE Transactions on Power Electronics*, vol. 15, no. 6, pp. 1250-1266, November 2000.

On Graphene Circuits

Author: Mario Iannazzo, Thesis Advisors: Eduard Alarcón (UPC), Max Lemme (KTH Stockholm)
 contact email: mario.iannazzo@gmail.com

I. Why Graphene?

I.A. Graphene vs Silicon

In Fig. 1.1 it is shown that III-V High Electron Mobility Transistors (HEMTs) Cut-off Frequency (f_t) doesn't increase anymore by reducing Gate Length (L_g). Silicon Field Effect transistors (FETs) f_t is still increasing but at lower pace than Graphene FETs. If Graphene performance keeps improving and Silicon performance keeps stagnating, Graphene could replace Silicon in long term.

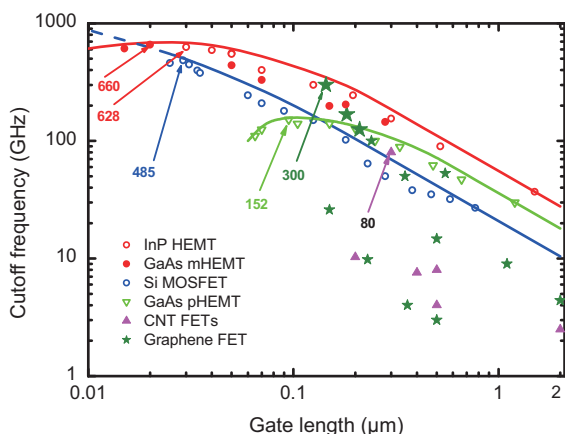


Figure 1.1. RF FETs [1]

I.B. Graphene nanoNetworks

Nanonetworking is an emerging field studying communication networks of nanosystems. These nanosystems (eg: nanosensors) require very small transceivers working at very high frequencies (THz), and Graphene could pave the way to these, so called, nanoTransceivers.

II. Graphene Semiconductors

Graphene is a new material discovered in 2004, a semi-metal or zero-gap semiconductor, one-atom-thick layer of carbon in a honeycomb lattice, with extraordinary properties like: transparency, flexibility, strength, high temperature conductivity, high carrier conductivity, high carrier velocity saturation, high current density, silicon compatibility and mass production suitability.

III. Graphene Transistors

III.A. Graphene FET (GFET)

GFETs (Fig. 3.1) high carrier mobility translates into high f_t , so they're good candidates to become THz transistors. But there are a few drawbacks to overcome: degraded carrier mobility caused by surrounding materials, low on-off current ratio which is not good for digital switching, and low current saturation which is not good for analog amplification. Technologists are developing new dielectrics (SiN, BN, Al_2O_3), contacts and substrates (DLC, SiC, BN) to improve such issues.

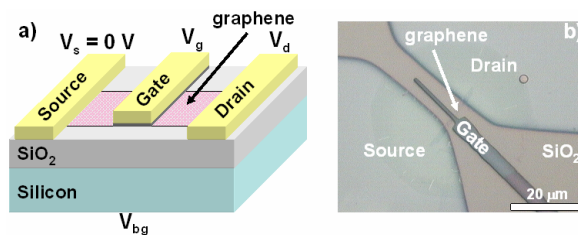


Figure 3.1. A GFET diagram (a) and layout (b) [2]

GFETs (Fig. 3.2) present a characteristic ambipolar behavior due to their lack of bandgap, so depending on bias, their channel can be N or P type. Such ambipolarity is exploited to implement new circuits.

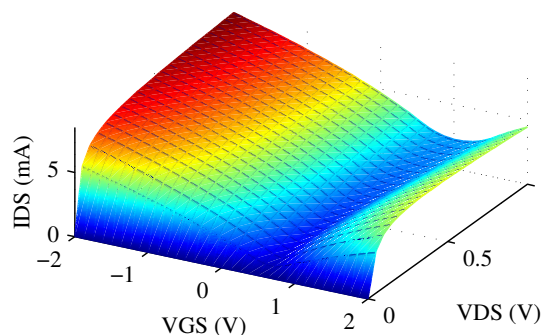


Figure 3.2. A simulated GFET I-V plot [3]

III.B. Other Graphene Transistors

Technologists are also developing new graphene transistors to improve even more on-off current ratio, current saturation and carrier mobility. A few examples are: Bilayer GFETs, Graphene Base Transistors (GBTs), Graphene Barristors and Graphene Nanoribbons.

IV. On Graphene Circuits

IV.A. State of Art

There's still little advances in graphene circuit design. Only single amplifiers, multipliers and mixers have been implemented. In Fig. 4.1 a GFET and two metal coils are used to implement a 10GHz mixer. That's the most complex graphene circuit nowadays. So there's plenty of room to innovate at this early stage.

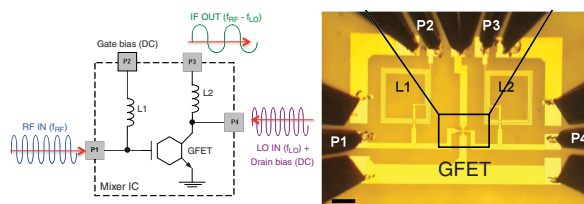


Figure 4.1. A GFET mixer schematic (left) and layout (right) [4]

IV.B. Thesis Objectives

Through analytical and empirical transistor models two approaches will be inter-twined with the objective of designing new graphene circuits. An horizontal approach will focus on device-circuit synergies and a vertical approach will focus on circuit-transceiver synergies. The horizontal approach consists in bandwidth, mismatch, noise, non-linearity circuit analysis and general circuit design like mirrors, references, amplifiers, multipliers, transconductors, comparators and oscillators... And the vertical approach consists in THz transceivers proposals and specific circuit design like, LNAs, PAs, regulators, filters, mixers and VCOs...

V. Towards Graphene nanoTransceivers

The targeted nanoTransceivers should work at THz because graphene nanoAntennas radiate at that frequency. NanoNetwork communications are short-range and low-power so using Ultra Wide Band (UWB) techniques seems the way to go.

V.A. THz Transceivers

Fig 5.1 shows clearly how difficult is to achieve high output power at THz frequencies in transmitters ($P_{out@820GHz} = -30dBm$). High noise figures are typical ($NF@820GHz = 50dB$) for receivers.

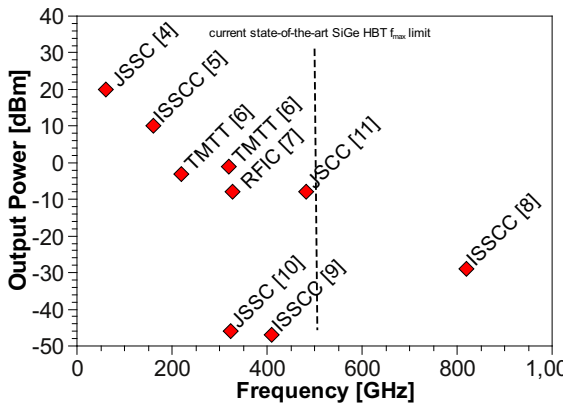


Figure 5.1. THz Transmitters in SiGe [5]

V.B. UWB Transceivers

Fig 5.2 shows that in these transceivers there's no need of oscillators, or mixers, which simplifies enormously the front-end design.

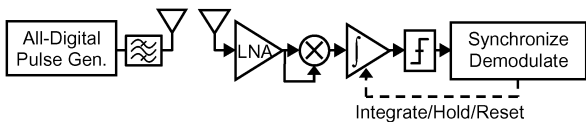


Figure 5.2. An UWB Transceiver [6]

VI. Graphene Applications

WNoC and WnSN are two applications based on nanonetworks.

VI.A. Wireless Network on Chip (WNoC)

WNoCs (Fig. 6.1) are connecting wirelessly thousands of nanoprocessors on the same die. The

main objective is to reduce communication latency between nanoprocessors using RF nanoTransceivers. Such multiprocessors could be used for big-data processing.

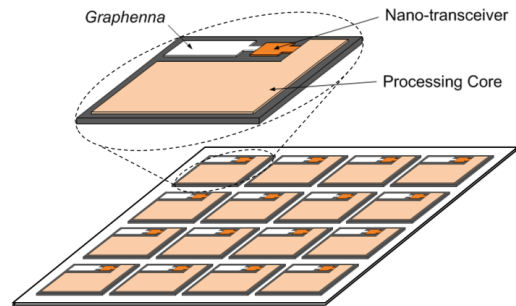


Figure 6.1. A WNoC [7].

VI.B. Wireless nanoSensor Network (WnSN)

The main objective for WnSNs (Fig. 6.2) is to locally communicate nanosensors. An application could be to measure low chemical concentrations inside the human body.

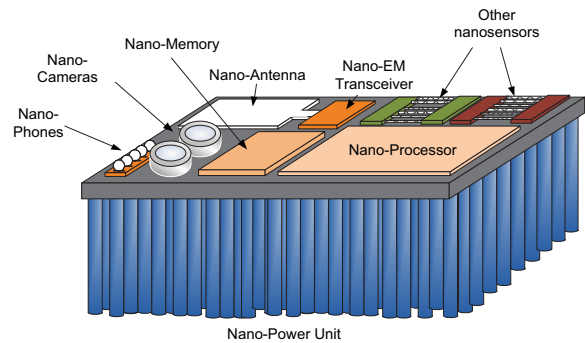


Figure 6.2. A WnSN nanosystem or mote [8].

VII. References

[1] Schwierz, F., "Graphene transistors 2011," VLSI Technology, Systems and Applications (VLSI-TSA), 2011 International Symposium on , vol., no., pp.1-2, 25-27 April 2011
 [2] Max C. Lemme, "Current Status of Graphene Transistors", *Solid State Phenomena*, Vols. 156-158 (2010) pp 499-509
 [3] Saul Rodriguez, Sam Vaziri, Mikael Ostling, Ana Rusu, Eduard Alarcon, Max C. Lemme, "RF Performance Projections of Graphene FETs vs. Silicon MOSFETs"
 [4] Yu-Ming Lin, Alberto Valdes-Garcia, Shu-Jen Han, Damon B. Farmer, Inanc Meric, Yanning Sun, Yanqing Wu, Christos Dimitrakopoulos, "Wafer-Scale Graphene Integrated Circuit", *Science* 10 June 2011: 332 (6035), 1294-1297
 [5] Pfeiffer, U.R.; , "Silicon CMOS/SiGe transceiver circuits for THz applications," *SiRF*, 2012 IEEE 12th Topical Meeting on , vol., no., pp.159-162, 16-18 Jan. 2012
 [6] Chandrakasan, A.P.; Lee, F.S.; Wentzloff, D.D.; Sze, V.; Ginsburg, B.P.; Mercier, P.P.; Daly, D.C.; Blazquez, R.; , "Low-Power Impulse UWB Architectures and Circuits," *Proceedings of the IEEE* , vol.97, no.2, pp.332-352, Feb. 2009
 [7] S. Abadal, A. Cabellos-Aparicio, "Graphene hybrid architectures for multiprocessors: bridging nanophotonics and nanoscale wireless communication," *ICTON 2012*
 [8] Jornet, Josep Miquel; Akyildiz, Ian F.; , "The internet of multimedia nano-things in the Terahertz band," 18th European Wireless Conference , vol., no., pp.1-8, 18-20 April 2012

Design and Rapid Prototyping of Low-cost CMOS-MEMS Accelerometers

Author: Piotr Michalik, Thesis Advisors: Jordi Madrenas Boadas, Daniel Fernández Martínez

contact email: piotr.michalik@upc.edu

I. Introduction

MEMS (Micro Electro Mechanical System) accelerometer market is currently experiencing a constant rapid growth (see Fig. 1) due to ubiquitous use of accelerometers in very fast-developing consumer electronic devices like smart phones, GPS, video game consoles, human interface devices (HID) etc., which are currently moving from premium and medium to the popular sector, where the total device price and size are the most critical factor.

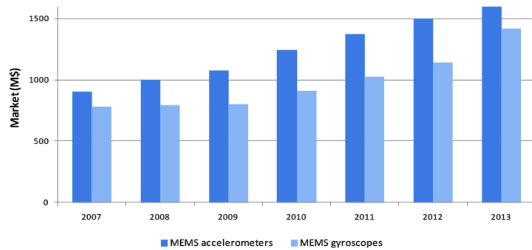


Figure 1. Global market for MEMS accelerometers and gyroscopes [1]

In very near future virtually every smartphone is going to contain six-degrees of freedom IMU (Inertial Measurement Unit) for position and motion sensing, containing 3-axis accelerometer and gyroscope. Probably the only possible way to compromise the challenge of small price and size with increasing system complexity is a full integration of multiple sensors not only with a CMOS read-out electronics, but also with other blocks like microprocessor or RF front-end on a single SoC (System on a Chip). However the full integration on one silicon die is perhaps not enough. The further goal is the integration of the MEMS and CMOS fabrication, so that a common process was used during the manufacture of the electronics and MEMS, with as few as possible additional steps for the latter.

Despite this clear need and long research in the field, the CMOS-MEMS integration industry standard does not exist yet. Accelerometers and gyroscopes available on the market are either built as multi-chip modules, where the electronic and mechanical parts are placed on separate chips or they are integrated on one silicon die, but the mechanical and electronic parts are produced in different fabrication processes. Both approaches require custom MEMS fabrication process what strongly limits the final price of the device.

II. CMOS-MEMS accelerometer

The goal of the project is to develop a CMOS-MEMS accelerometer IP-core that can be easily adjusted to demanded CMOS technology and ready to integrate in more complex System on a Chip. Apart from research on MEMS release process, the work requires preparation of the CMOS-MEMS design flow that includes MEMS device design and modeling as well as

development of an accelerometer readout CMOS circuitry that can be easily scaled-down to modern technology nodes.

II.A. CMOS-MEMS integration

The applied integration approach consists in using metal layers of CMOS process as a structural material for MEMS, and releasing them by isotropic etching of the silicon dioxide. Some simple elements like cantilevers and suspended plates have been already successfully released (see Fig. 2) from a CMOS chip in the Department of Electronic Engineering cleanroom [2]. The method does not need any disruptive complex fabrication steps. For this reason it can be very cost-effective.

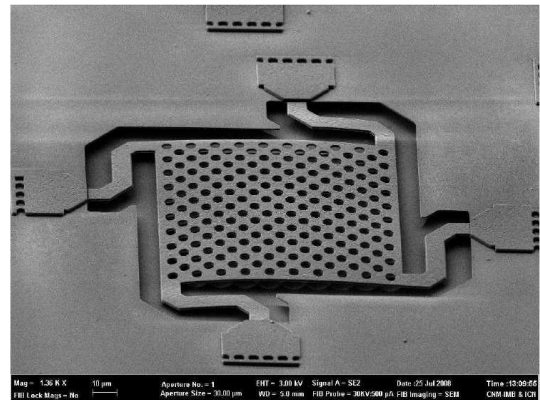


Figure 2. SEM image of a 100 μm x 100 μm electrostatic actuator released from a CMOS chip in UPC laboratory [2]. Similar structure can be employed as a z-axis accelerometer.

II.B. Technology-portable CMOS interface for accelerometers

The thesis is also concentrated on the circuits and architectures research for CMOS-MEMS monolithic accelerometers readout. The main aim is to benefit as much as possible from the electronics integration and design the architecture that provides digital output with fair resolution while contains limited amount of purely analog circuits, so that the whole design becomes easily portable between modern ultra-submicron CMOS technologies.

III. Main contributions

The MEMS part of the project is still on the experimental stage. Recently a collaboration with a CMOS foundry was established, so that the release is done in batch mode.

So far the main contribution is concentrated on the new mixed-signal architecture for capacitive sensors (see Fig. 3). The architecture consists of new type of relaxation oscillator for differential capacitive accelerometer, allows time-multiplexed electrostatic

actuation and applies time-to-digital converter (TDC) for precise digital frequency demodulation. The design contains only small amount of analog blocks and since it is dominated by the digital circuitry, it can be very easily transferred to another CMOS technology. The results are going to be published soon. During the architecture implementation a novel metastability-robust sampling method for coarse-fine TDCs was developed [3].

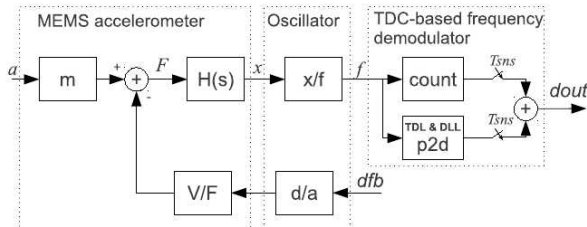


Figure 3. Block-level representation of the developed readout architecture.

IV. Acknowledgments

This work was supported in part by the Spanish Ministry of Science and Innovation under Projects TEC2008-06028 and TEC2011-27047, and the European Social Fund (ESF). Piotr Michalik holds an FPU scholarship of the Spanish Ministry of Education.

V. References

- [1] "MEMS accelerometer, gyroscope and IMU market 2008-2013." Yole Développement, www.yole.fr.
- [2] Daniel Fernández, Jordi Ricart, and Jordi Madrenas, "Experiments on the Release of CMOS-Micromachined Metal Layers," Journal of Sensors, 2010.
- [3] Piotr Michalik, Daniel Fernández, and Jordi Madrenas, "Result-consistent counter sampling scheme for coarse-fine TDCs," Electronics Letters 48, 2012.

Application of SIMD hardware implementations to bio-inspired systems

Author: Giovanni Sánchez Rivera, Thesis Advisor: Jordi Madrenas Boadas

Contact email: *giovanny.sanchez@upc.edu, jordi.madrenas@upc.edu*

I. Introduction

Bio-inspired systems employ artificial neural network models (ANNs) to solve complex systems. In particular, Spiking Neuronal Network models (SNN) have recently attracted great interest, SNNs fall into the third generation of neuronal network models and they are emerging as a plausible paradigm for characterizing neuronal dynamics in the cerebral cortex, due to the high level of realism in a neuronal simulation[1-3]. These models are also suitable for a physical hardware implementation [3-5]. Thus, the idea of implementing spiking neurons from nature in modern programmable digital systems becomes a very exciting and high impact research topic because they offer exceptional flexibility, re-configurability and scalability in number of neurons. In order to understand dynamics in the SNNs, and to use them in real-time applications such as in robotics, it is essential to implement large-scale network models that operate in almost near real time [6, 7]. Conventional processors and DSPs do not have enough parallelism and memory bandwidth for real-time simulation of SNNs [8]. Modern parallel architectures (such as clusters, super-computers, or high performance multi-processors) [9] promise powerful alternatives for speeding spiking network simulation, but incur high cost for purchase, maintenance and have size limitations. These digital architectures could implement a large SNN with a big amount of neurons (thousands to millions) with different number of connections per each one, working at real-time speeds.

This work focuses on the problem of developing efficient digital parallel hardware architectures and implementations that emulate in real time complex and biologically realistic spiking neural networks. The starting point of the work is the proposed multiprocessor architecture of the PERPLEXUS project [5]. The paper has been organized as follows: In Section II the multiprocessor has been described. Finally in Section III, relevant results have been presented.

II. The SIMD Digital Multi-Processor

The first version of this Single-Instruction, Multiple-Data processor customized for SNN emulation was proposed in [5]. Several models, such as Iglesias-Villa and Izhikevich [2, 10] have already been implemented successfully. During the last two years the performance of this Digital Multi-Processor version 1 (DMP_1) has been studied and the architecture bottlenecks have been detected from the simulation and implementation of several models [11]. Fig. 1 shows the DMP_1 architecture, which is constituted by four main building blocks: a programmable array, an AER block, a sequencer, and the external CPU interface. The configurable array is a regular, bi-dimensional arrangement of Processor Element (PE). The PE is the elementary block of the DMP_1 and consists of a 16-bit ALU with register banks. The microprocessor interface takes care of the communication between the DMP_1 and an external CPU. The memory controller manages

the interface of DMP with an external SRAM memory that stores the program executed by the sequencer and the data used by the PE. The sequencer is in-charge of the program execution and the control of PE array. The AER controller is the subsystem that carries out the physical implementation of the AER protocol. It is constituted by an AER encoder and a control unit that communicates with an AER decoder module provided with a CAM unit array with units corresponding to each PE. An external SRAM stores the instructions, constants and synaptic and neural parameters of each neuron. The DMP_1 emulates the SNN in two phases. In the first phase the sequencer executes the algorithm computing the synapse and neural parameters and generating the possible spikes. In the second phase the sequencer halts and scans the PE array for spikes. The spikes are fed to the AER controller and broadcasted. The AER decoder reads the same and the spikes are decoded by the internal Content Addressable Memory (CAM) of every corresponding PE. The matches are generated and stored in the external SRAM. The sequencer resumes the first phase of operation after all the matches get stored in the SRAM, in the positions corresponding to the respective neuron.

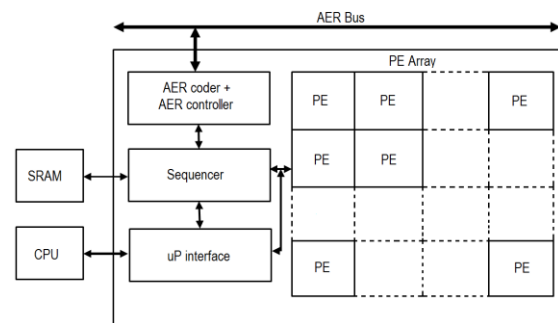


Figure 1. The DMP architecture

To boost the emulation performance of the original PERPLEXUS architecture, a new improved version of the Digital Multi-Processor version 2 (DMP_2) has been developed as a part of this PhD thesis. Three factors have been taken into account in order to achieve the objective; spike communication, memory system and data processing. The improved architecture possesses the following characteristics:

II.A. Processing

One of the aspects studied in the new version is the efficient number of bits required in fixed point representation in order to calculate the neural and synaptic parameters with precision, so that an optimal architecture and lower area consumption is achieved.

II.B. Communication

A spike distribution system that allows minimizing the number of clocks to process the incoming spikes has been developed. The pre-synaptic spikes are read

in parallel by the neurons, while in the initial version they were processed serially.

II.C. Memory system

Another main bottleneck considered is the memory system; the problems were caused by centralized memory access. So it has been proposed that a system of distributed memory be employed.

III. Results

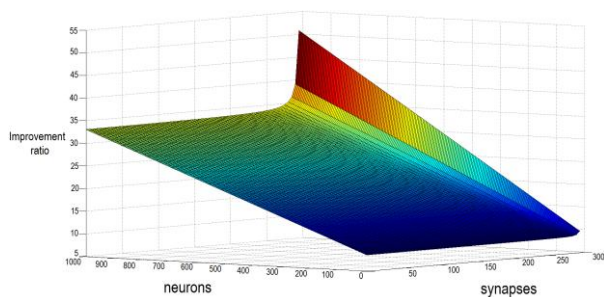


Fig. 2 Improvement ratio for the DMP_2 vs DMP_1

The DMP_2 is already complete and some improved estimations have been calculated in order to evaluate its performance and has been compared and contrasted with DMP_1's performance. Regarding the speed improvement-ratio for spike distribution is 600 (considering the worst case of 1000 neurons with 300 synapses each firing at the same time). Tremendous improvement in terms of processing speed was obtained taking into account the target criteria of 1000 neurons with 300 synapses each, the improvement is 52 times as is shown in Fig. 2.

Acknowledgments Giovanni Sanchez holds a research fellowship supported by the Catalan Department of Innovation, Universities and Companies, and the European Social Fund (ESF). This work was supported in part by the Spanish Ministry of Education and Science under Projects TEC2008-06028/TEC and TEC2011-27047, and by the ESF.

IV. References

- [1] W. Maass, "Networks of spiking neurons: The third generation of neural network models," *Neural Networks*, vol. 10, pp. 1659-1671, 1997.
- [2] E. M. Izhikevich, "Polychronization: Computation with Spikes," *Neural Comput.*, vol. 18, pp. 245-282, 2006.
- [3] S. Grossberg, "Spiking Neurons in Neuroscience and Technology," *Neural Networks*, vol. 14, pp. 6-7, 2001.
- [4] T. Lehmann and R. Woodburn, "Biologically-Inspired On-Chip Learning in Pulsed Neural Networks," *Analog Integrated Circuits and Signal Processing*, vol. 18, pp. 117-131, 1999.
- [5] A. Upegui, Y. Thoma, E. Sanchez, A. Perez-Urbe, J. M. Moreno, and J. Madrenas, "The Perplexus bio-inspired reconfigurable circuit," in *Adaptive Hardware and Systems, 2007. AHS 2007. Second NASA/ESA Conference on*, 2007, pp. 600-605.
- [6] A. Cassidy, A. G. Andreou, and J. Georgiou, "Design of a one million neuron single FPGA neuromorphic system for real-time multimodal scene analysis," in

- [7] *Information Sciences and Systems (CISS), 2011 45th Annual Conference on*, 2011, pp. 1-6.
- [8] M. J. Pearson, C. Melhuish, A. G. Pipe, M. Nibouche, L. Gilhespy, K. Gurney, and B. Mitchinson, "Design and FPGA implementation of an embedded real-time biologically plausible spiking neural network processor," in *Field Programmable Logic and Applications, 2005. International Conference on*, 2005, pp. 582-585.
- [9] M. A. Bhuiyan, V. K. Pallipuram, and M. C. Smith, "Acceleration of spiking neural networks in emerging multi-core and GPU architectures," in *Parallel & Distributed Processing, Workshops and Phd Forum (IPDPSW), 2010 IEEE International Symposium on*, 2010, pp. 1-8.
- [10] M. M. Khan, D. R. Lester, L. A. Plana, A. Rast, X. Jin, E. Painkras, and S. B. Furber, "SpiNNaker: Mapping neural networks onto a massively-parallel chip multiprocessor," in *Neural Networks, 2008. IJCNN 2008. (IEEE World Congress on Computational Intelligence). IEEE International Joint Conference on*, 2008, pp. 2849-2856.
- [11] J. Iglesias, J. Eriksson, F. Grize, M. Tomassini, and A. E. P. Villa, "Dynamics of pruning in simulated large-scale spiking neural networks," *Biosystems*, vol. 79, 2005.
- [12] G. Sanchez, J. Madrenas, and J. Moreno, "Performance Evaluation and Scaling of a Multiprocessor Architecture Emulating Complex SNN Algorithms," in *Evolvable Systems: From Biology to Hardware*. vol. 6274: Springer Berlin Heidelberg, pp. 145-156.

Multi-Phase Fault Tolerant Converters, Modulation Strategies and Fault Detection Schemes

Author: Mehdi Salehifar, Thesis Advisor(s): Juan Manuel Moreno, Vicent Sala

contact email: mehdi.salehifar@mcia.upc.edu

I. Introduction

Regarding their fault tolerant characteristics, five phase permanent magnet synchronous motors (PMSM) are gaining more interest in applications with high safety. In addition to being capable of continuing the operation with one or two faulty phases, their five phase structure allows to have lower amplitude of currents, reduced torque ripples and less operational noise [1] [2].

The concept of being fault tolerant is usually referred to have the capability of fault isolation, and remaining operational with minimum possible derating. In other words, a fault tolerant drive should have the ability of fault detection, converter reconfiguration, and control adaptation. This is essential in applications where safety is the most important objective; automotive industry, aerospace, power plants and military can be mentioned as good examples of these areas.

To achieve this concept, three main subjects for power converter should be investigated including:

- ✓ fault detection in power converter
- ✓ fault tolerant converter design
- ✓ optimized switching modulation

Aim of this thesis is to study aforementioned cases in a multi-phase fault tolerant PMSM drive.

As a result, the development of fault tolerant converters has been considered in previous conducted studies [3] [4].

Due to tremendous development of power converters in last 50 years, modulation methods as an indispensable part for this technology have been addresses in literature, since converter efficiency, final cost and performance are affected by modulation strategy as well.

Following objectives are considered in modulation strategy:

- Attain best waveforms with lowest possible losses
- Common mode voltage reduction
- Input dc voltage balancing
- Current harmonic minimization in input
- Low dv/dt
- Effective usage of dc link voltage

However achieving all these objectives at the same time is impossible, the optimized solution choose those with the highest importance for the special application [5], [6].

In order to maintain continuous operation of a fault tolerant converter, a fast fault detection scheme is of paramount importance, consequently investigation and developing of fault detection in power converter has been considered as part of this thesis. Using a fast and reliable method, damaging effects can be minimized and drive continuous operation is maintained [7], [8].

II. Methodology

To pursue with objectives described earlier following steps are done in order.

1-Review state of the art regarding three topics:

- multi-phase fault tolerant converters
- modulation strategies
- fault detection methods

Information about ongoing research in aforementioned topics is gathered in this part.

2- Simulation and analysis of topics given in part 1.

Purpose of this part is to understand appropriate fault tolerant converters, modulation methods and fault detection scheme.

3-Theoretical development of research topics

At this step, contributions to each part of research topics in step 1 are made.

4- Develop experimental setup

Finally, analyzed and simulated solutions in parts 1, 2, and 3 should be validated experimentally; so in this part appropriate hardware for each part is first prepared and then simulation is confirmed by experimental setup.

5-Drawing up the dissertation

As the final step, all done task in steps 1 to 3 is documented and conclusion is made.

Fig.1 shows a five phase fault tolerant drive which consists of three main parts as a fault tolerant five phase converter, a five phase PMSM, and field oriented control (FOC) strategy.

A supervisory control should be designed as shown in Fig. 2 in order to detect faults and reconfigure both converter configuration and control method. As seen in Fig. 2, under normal operation condition, there is a supervisory block which detects fault in converter, when a fault happens switch which is normally closed is changed to other state so that under faulty condition both control method and converter are reconfigured in order to maintain continuous operation of motor.

A fault tolerant converter is usually equipped with an extra leg. Under faulty mode, switch commands to faulty leg is firstly removed and then isolated from motor. Isolated phase is connected to extra leg. In this way, switching commands of faulty leg are replaced with extra leg. Control algorithm of converter is shown in Fig. 3.

As shown in Fig. 3, there is a fault detection part which plays an important role in control of drive. According to objectives of this thesis, aforementioned block is designed to detect power electronic converter faults which can be categorized in two main groups, including short circuit and open circuit. Since time between short circuit initialization fault and device failure is short, detection of this fault should be done very fast, i.e. less than 10 μ s in case of IGBT switch, detection and protection of this fault is done locally in driver circuit. In contrast, open switch faults are less destructive, different methods have been presented to detect this fault. Motor phase currents which are measured for control purpose are applied and analyzed to detect this kind of fault. Also, new approaches by analyzing multivariable IGBT's space (i.e., temperatures, desaturations, current levels, etc.) will be investigated. A pulsating torque with unequal stress of IGBT switches is the main feature of these kinds of faults.

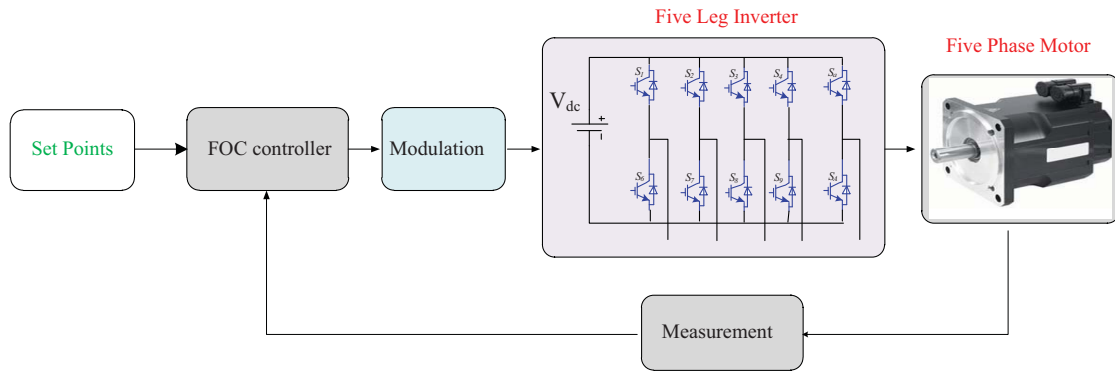


Figure 1. Five phase PMSM drive

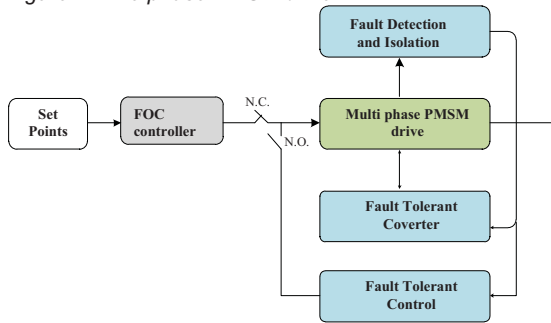


Figure 2. Supervisory block

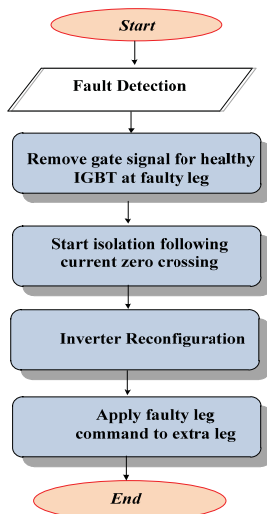


Figure 3. Control algorithm of converter

There are several advantages for using multi-phase converter in comparison with conventional three phase such as reduced per phase current, capability of multiple fault tolerant, and higher reliability. Using these advantages in combination with a multi-phase PMSM results in a reliable fault tolerant drive for applications whose continuous operation is critical, such as electric and hybrid electric vehicle, transportation, chemical industry, semiconductor manufacturing, more electric

aircraft, electric ship propulsion, aerospace industry, and railway traction.

III. Contributions of the thesis

Main contributions of the thesis are outlined as follows.

- Analysis, design and implementation of novel five phase fault tolerant converter for multi-phase PMSM
- Development of fault detection and localization methods in multi-phase converters.
- Development of fault tolerant modulation strategies.

IV. References

[1] L. Parsa and H. A. Toliyat, "Fault-tolerant five-phase permanent-magnet motor drives", *IEEE Trans. on Ind. App.*, Vol. 41, No. 1, 2005.

[2] P. Zheng, Y. Sui, J. Zhao, C. Tong, T.A. Lipo, A. Wang, "Investigation of a Novel Five-Phase Modular Permanent-Magnet In-Wheel Motor," *IEEE Trans. on Magnetics*, Vol. 47, No. 10, Oct. 2011.

[3] Ricardo Brian A. Welchko, Thomas A. Lipo, Thomas M. Jahns, and Steven E. Schulz, "Fault Tolerant Three-Phase AC Motor Drive Topologies: A Comparison of Features, Cost, and Limitations," *IEEE Trans. ON Power Electron.*, Vol. 19, No. 4, pp: 1108-1116, July 2004.

[4] Rammohan Rao Errabelli and Peter Mutschler, "Fault Tolerant Voltage Source Inverter for Permanent Magnet Drives," *IEEE Transactions on Power Electronics*, Vol. pp., No. 99, pp: 1-9, Feb. 2011.

[5] E. Roberto C. DA Silva, E. Cipriano Dos Santos, JR., and C. Brandao Jacobina, "Pulse Width Modulation Strategies," *IEEE Ind. Electron. Mag.*, pp: 37-45, JUNE 2011.

[6] D. Grahame Holmes, Thomas A. Lipo, T. A. Lipo, "Pulse width modulation for power converters: principles and practice," *Wiley-IEEE*, 2003.

[7] F. W. Fuchs, "Some diagnosis methods for voltage source inverters in variable speed drives with induction machines—A survey," in *Proc. IEEE Ind. Electron. Conf.*, pp. 1378–1385, 2003.

[8] Bin Lu, and Santosh K. Sharma, "A Literature Review of IGBT Fault Diagnostic and Protection Methods for Power Inverters," *IEEE Trans. ON Ind. App.*, Vol. 45, No. 5, pp: 1770-1777, Oct. 2009.

Determining the state of charge and state of health of batteries

Author: Victòria Júlia Ovejas Benedicto, Thesis Advisor(s): Àngel Cuadras

Contact email: Victoria.julia.ovejas@upc.edu

I. Introduction

At present there is a worldwide growing proliferation of the use of portable electric devices, from basic watches, mobile phones, laptops, or even electric vehicles. In this context, batteries are considered the most convenient solution to feed these systems, mainly due to the lack of better alternatives for storing electrical energy. Therefore, improving capabilities, performance and reliability of batteries are issues that are constantly studied. However, the applications grow more quickly than batteries, so the battery recharging process becomes more frequent which causes an acceleration of its deterioration. Given that the cost of the battery system can be more than 30% - 40% of the total cost of the final product, taking care of them and also the efficiency are critical factors to ensure product durability.

Several interesting aspects to improve the performance of batteries and therefore the systems that feed arise for that reason. The processes of charging and discharging a battery should be optimized by adjusting them to achieve longer average life. Moreover, it is convenient to have a status indicator of battery state of charge (SoC), i.e., the available charge in the battery, and state of health (SoH), i.e., the decrease in performance of a cell with respect to a fresh battery. Unfortunately, these two problems have not been resolved effectively until now, specifically for lithium batteries, which are more common in portable systems since they have a higher energy density than other technologies. As an example, in Spain more than one billion batteries are used every year, so prolonging their life seems desirable and urgent.

In the literature there are various methods to determine SoC. In general, commercial charge indicators do not take into account the aging of the battery. This is a problem because indicators are no longer reliable as the batteries are used and as they store energy over time. The reliability of these devices is of vital importance in the case, for example, of electric vehicles.

Present research focuses on using combinations of different methods in order to consider the aging of the cells when determining the SoC. The methods found in literature seem low accurate or too complex to process. Although there are many people working on a solution to this problem, there is still not a method that definitely solves that issue and there is not a solution commercially extended.

II. The aim of this research

Simultaneous determination of SoC and SoH is a problem of special interest that is not solved. Furthermore, although present attention is focused on impedance as it seems to be a good parameter to study the evolution of both SoC and SoH, it is difficult to discriminate their respective contributions. Thus, an additional variable is necessary in order to differentiate

them. A parameter that is currently generating interest is the evolution of entropy in batteries during operation.

The hypothesis of my dissertation is to demonstrate that the combined analysis of the impedance and the entropy of the battery, allows discriminating the effects of SoC and SoH.

III. Materials and methods

Thermal and electrical measurements will be carried out to different batteries with several capacities and chemical compounds.

III.A. Batteries

Low, medium and high capacity cells for different applications will be tested (Fig. 1). It is important to have enough data to generalize and validate the results.



Figure 1. Some portable applications with different capacity needs

For preliminary results, two 750 mAh capacity Varta Microbattery (LIP 533048 AJ) with different SoH were tested:

Battery reference	Percentage of capacity with respect to nominal capacity
Fresh cell	100 %
Degraded cell	80 %

Table 1. Cells that have been compared

III.B. Thermal and electrical behavior of the cells

We want to discriminate the effects of SoC and SoH of the cells from their thermal and electrical behavior. In particular, impedance and entropy have to be measured and calculated.

Entropy is a thermodynamic property of a system that accounts for the energy not available for work. In a microscopic scale, it describes the disorder or randomness of the particles in a system or structure. It can be obtained from voltage, current and temperature measurements.

Moreover, impedance is obtained by EIS (Electrochemical Impedance Spectroscopy) that works with very small excitation amplitudes to not disturb the cell and, therefore, permits to be working in the linear range of the battery (Fig. 2).

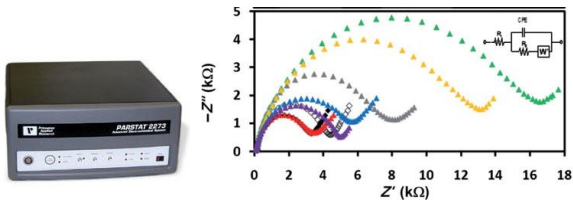


Figure 2. Potentiostat/galvanostat to measure impedance from very low frequency (left). Example of Nyquist plot of impedance obtained by EIS method (right).

III.C. Cycling

The recommended method for charging lithium batteries is constant current-constant voltage method (CC-CV) during charge and constant current (CC) during discharge.

While cycling lithium batteries, temperature has to be monitored for security purposes. For that reason, some of those batteries come with an internal thermistor. Temperature measurements will be done taking advantage of these sensors, when possible.

IV. Results and discussions

During the first research year of the Ph.D, some impedance measurements were carried out. It was obtained a clear evolution of the impedance with both SoC and SoH (Fig. 3 and Fig. 4, respectively), as expected. The frequency range of the measurements was 4 mHz to 1 kHz.

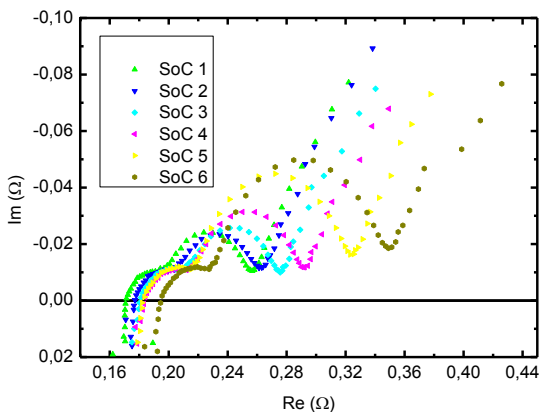


Figure 3. Impedance evolution of the degraded cell with SoC (SoC 1 means totally charged and SoC 6 totally discharged).

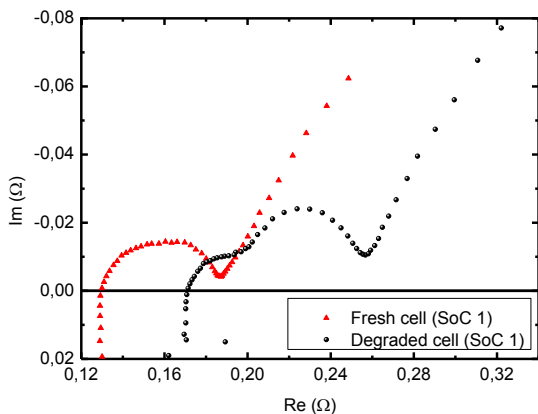


Figure 4. Impedance evolution of two cells of the same model and with same SoC but different aging or SoH.

In the case of SoC evolution, there is a global increase of the impedance when discharging the battery from 100% to 0% SoC. Although it seems that impedance could be a good SoC estimator, it also depends on the battery's degradation (Fig. 4). Therefore, as mentioned above, impedance is not enough to discriminate the effect of SoC and SoH.

When comparing the temperature profiles of the fresh and cycled or degraded battery, it can be seen a different temperature evolution during charge (Fig. 5). For the fresh cell and at the beginning of the charge process, there is a decrease in temperature because the endothermic nature of the reaction prevails over the Joule Effect. This is not true for the degraded cell in which temperature starts to rise at the same time the current is injected. Note that on the last part of the charge process in Fig. 5, temperature always decreases. It is because the transition point between CC and CV is reached in that moment.

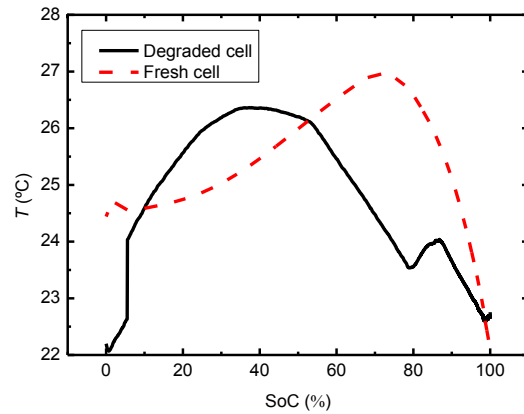


Figure 5. Temperature profiles during charge for fresh and degraded batteries.

Entropy depends on voltage, current and temperature. It is a promising parameter because depends on SoC, SoH and it can be obtained from parameters already available in these kind of systems in which voltage, current and temperature are constantly monitored.

V. Acknowledgments

This work was funded by the Spanish Government under contracts DPI2010-14829, TEC2011-27397 and by the European Regional Development Fund. We also acknowledge the financial support given by MICINN under the project CICYT NANO-EN-ESTO (MAT-2010-21510).

The research was supported by the European Regional Development Funds (ERDF, "FEDER Programa Competitivitat de Catalunya 2007-2013"). We also want to acknowledge the laboratory work performed by Francis Lopez.

Assessment of trends in the cardiovascular system from time interval measurement using physiological signals obtained at the limbs

Author: Joan Gomez-Clapers, Thesis Advisors: Ramon Casanella, Ramon Pallas-Areny
 contact email: joan.gomez-clapers@upc.edu

I. Introduction

The assessment of trends in the cardiovascular system has successfully increased life expectancy but it presents some serious drawbacks. Current procedures often rely on complex and expensive devices that require specialized staff to operate it, and the cost per capita cannot to be easily assumed by health-care providers. A new set of medical devices intended for in-home measurement has evolved from the need to extend the monitoring of cardiovascular parameters to broader population groups.

In-home healthcare devices are intended to be simple, noninvasive, robust and cost-effective so they can be integrated in patient's daily routine and used in different environments such as homes, gymnasiums or workplaces. The signals acquired under such circumstances usually show lower quality than those acquired in controlled environments, and they cannot be used as a surrogate for in-hospital measurements. Nevertheless, several parameters of interest can be obtained from them that can be used as a tool for early diagnose of diseases and alarm triggering when a malfunction is detected.

Non-invasiveness is an important factor to consider in devices intended for routine use. For this reason, the limbs are one of the most convenient body parts to acquire biosignals. They are often uncovered or easily accessible, hence less invasive or embarrassing for the patient. The best suited cardiovascular signals that can be obtained at the limbs in home settings are those based on electrical and mechanical measurements because they can be easily obtained from simple and cost-effective systems. For this reason, the target signals chosen for this work are the electrocardiogram (ECG), the impedance plethysmography (IPG) and the ballistocardiogram (BCG).

Even though useful information can be obtained from a single signal, more promising applications can be foreseen when the proposed signals are simultaneously acquired. Some events on the cardiac cycle are reflected in particular waves on the different signals and the time delay between these waves provides valuable information about cardiovascular performance.

The aim of this thesis is to assess trends based on time interval measurements between the proposed cardiovascular signals.

II. Methodology

II.A. Cardiovascular signals

The ECG is the recording of the electrical activity of the heart, normally at the surface of the body. It is one of the most accepted noninvasive tools for the evaluation of cardiac function and it can be acquired by measuring the electric potential difference between hands, feet or both. Multiple alterations on cardiac function can be diagnosed by simply evaluating the rate, regularity or shape of the signal on each heartbeat.

The IPG is the recording of changes in impedance caused by changes of volume in a current path. It is usually obtained by injecting a high frequency current between a pair of electrodes and measuring the voltage drop between another pair of electrodes. When it is measured at the limbs, the IPG shows a pulsatile shape caused by the circulation of blood through the arterial system. Blood pulse wave velocity depends on arterial stiffness which is an important parameter closely related to blood pressure and a direct marker for deterioration of the cardiovascular system.

The BCG is the recording of vertical forces caused by heart activity. On each heartbeat the heart pumps blood upward to the aorta and a downward reaction force arises. When the blood pulse propagates through the arterial tree, other forces arise. These forces can be measured from the strain gauges of a commercial electronics bathroom by amplifying and filtering the pulsatile part of the body weight. The origin of the ballistocardiogram is still controversial but it seems reasonable to think that it may contain information about heart strength and propagation of the blood pulse through the arterial tree.

Fig. 1 summarizes the cardiovascular signals acquired and the parts of the body where they will be measured.

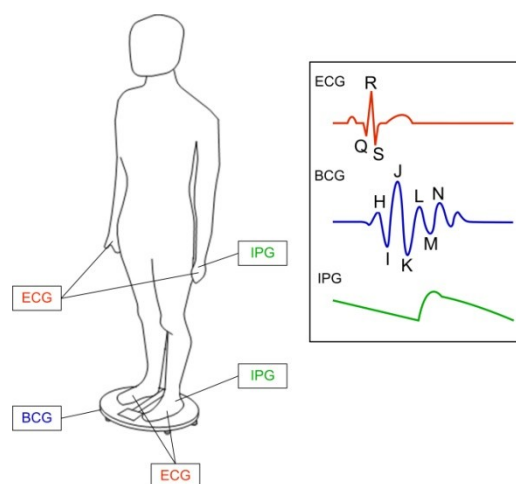


Figure 1. Cardiovascular signals acquired and measurement points

II.B. Data acquisition systems

The acquisition of cardiovascular signals for time interval measurement at the limbs in in-home environments requires the development of specific devices. The procedure poses some challenges that must be tackled without affecting the ability of the system to measure time intervals.

For the measurement at the hands our work is focused on handheld devices because they allow fast and noninvasive measurement. The ECG and the IPG can be acquired at the hands with dry and unattached electrodes but the signals obtained are expected to present higher levels of artifacts and electromyogram

interference (EMG) than usual recordings, because of the muscles that hold the device.

For the measurement at the feet we are targeting bathroom scales because they can be easily integrated in daily routine and are often used in bathrooms where the subject is sometimes barefoot hence the contact with the feet is easier. From a bathroom scale it is possible to acquire the IPG and the BCG with dry and unattached electrodes, but the ECG is more difficult to obtain. ECG records between feet are usually masked by EMG produced by the muscles of the legs. For this reason, we are also working in a bathroom scale combined with a handheld bar which enables the simultaneous acquisition of BCG, IPG and good quality ECG. It also allows the simultaneous acquisition of ECG between hands and feet that provides more information than the acquisition only between hands.

II.C. Time interval measurement and trends assessment

Several waves of the measured signals are related to specific cardiovascular events in the cardiac cycle. By studying the physiological basis of those events it is possible to develop hypothesis that relate the time intervals measured to cardiovascular parameters of interest.

Once hypothesis are established, the performance of our surrogates is compared to the parameters measured with standard procedures or commercial devices. Our systems are tested under hemodynamic changes induced in a few test subjects by applying maneuvers such as paced respiration, stand up movement or Valsalva.

In further stages, the markers developed will be tested in broader population groups under collaboration agreement with hospitals.

III. Results

Several devices for the acquisition of cardiovascular signals at the limbs have been developed. A handheld system for the acquisition of the ECG in in-home environments with a four electrode system has been presented. The signals acquired with this device can be used to perform fast diagnoses or screenings of large population groups based on the ECG shape or rhythm. A picture of the system it is shown on Fig. 2.

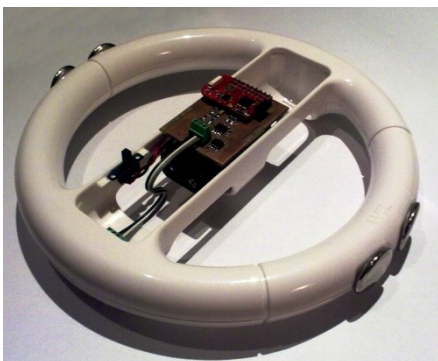


Figure 2. Handheld device for fast in-home ECG acquisition

A system for the simultaneous acquisition of the ECG and IPG has been developed. This system is particularly interesting because it only requires four electrodes meanwhile typical systems require up to

seven. Besides being useful to perform diagnoses based on the ECG shape and rhythm, ECG and IPG can be used to calculate the arrival time of the pulse wave (PAT) to the hands which is a parameter used to assess fast changes in blood pressure.

A bathroom scale intended for bioimpedance measurement has been modified to simultaneously acquire the ECG, BCG and IPG at the feet. ECG signals acquired with this system are typically masked by EMG noise but a signal processing algorithm based on ensemble averaging has been developed to obtain clear signals. This signal processing prevents the use for beat-to-beat tracking of hemodynamic changes but the signals are still useful to assess long-term trends.

A handheld bar has been added to a second bathroom scale to enable beat-to-beat tracking of cardiovascular parameters. This system allows simultaneous acquisition of BCG, IPG and three ECG leads. The system is shown in Fig. 3.



Figure 3. Modified bathroom scale for the acquisition of ECG (leads I, II and III), IPG and BCG

The assessment of trends it is still on early stages, but some studies have already been performed. The time interval between the R peak of the ECG and the J wave of the BCG has proven to be highly correlated (>0.85) to beat-to-beat changes on systolic blood pressure. Fig. 4 shows a record of beat-to-beat blood pressure and an estimate obtained from the RJ interval.

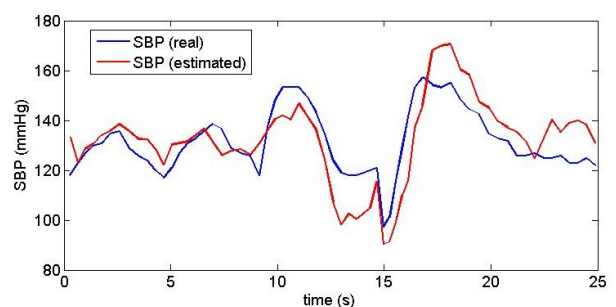


Figure 4. Changes in systolic blood pressure recorded and estimated from the RJ interval

IV. Acknowledgments

This thesis is supported by grant BES-2010-032893 from the Spanish Ministry of Science and Innovation under the project TEC2009-13022.

Fault Tolerant Vector Control of Five-Phase Permanent Magnet Motors

Author: Ramin Salehi Arashloo, Thesis Advisor: Prof. José Luis Romeral Martinez

ramin.salehi@mcia.upc.edu, luis.romeral@upc.edu

I. Introduction

The development of power electronics and digital microcomputers has created powerful tools in the field of motor controllers. On the other hand, by increasing the importance of Permanent Magnet (PM) machines in industries, proper control of these devices to provide good dynamic behavior is gaining more importance.

Comparing with 3-phase machines, multiphase systems, especially 5-phase machines are distinguished with several advantages which make them proper candidates in applications where safety and reliability is important. They have more abilities to work after fault occurrence in one (or even two) of the phases.

Field Oriented Control (FOC) and Direct Torque Control (DTC) are the main standards in the field of PM controlling methods. Comparing with DTC, FOC has more capabilities under faulty conditions. In this thesis, FOC of five-phase permanent magnet synchronous machine (PMSM) will be considered under healthy and faulty conditions.

II. Work Description and Methodology

Fig. 1 illustrates the basic structure of PMSM FOC. Optimal control strategies while missing one or two phases have been developed in several studies for five phase PM motors [1] [2]. Assuming isolated neutral point, all of these studies have focused on postfault torque improvement by controlling the current of remaining healthy phases. In all of these studies, it is tried to satisfy the following three conditions while computing the reference current phasors of remaining healthy phases:

- 1) To maintain the average of pre-fault generated torque
- 2) To have symmetric rearrangement of the healthy phases with respect to the faulty phase
- 3) To have zero amplitude of homopolar currents due to an isolated neutral point:

$$\sum_{A,B,C,D,E} i = 0 \quad (1)$$

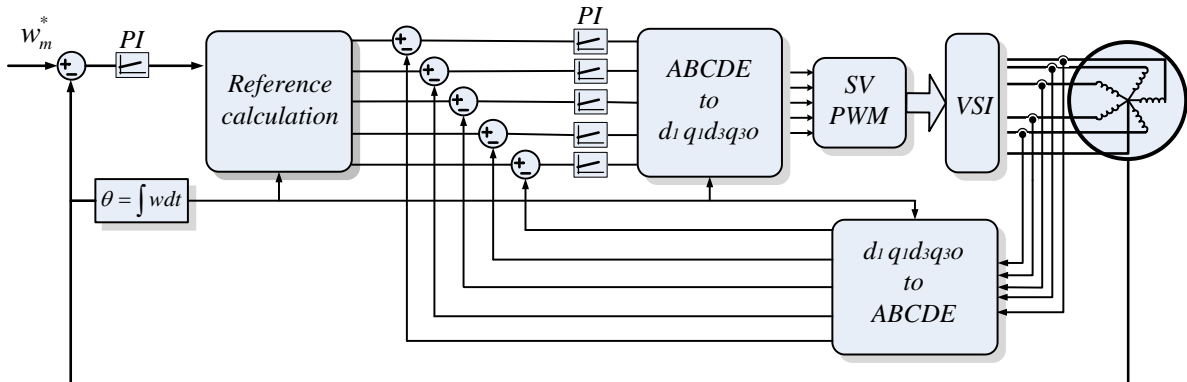


Fig.1 General block diagram of five-phase PMSM FOC

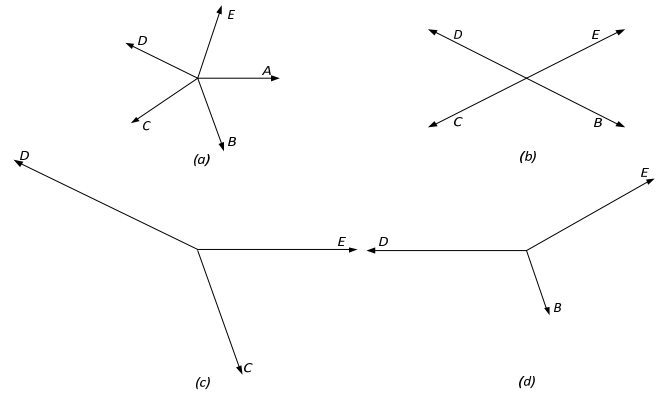


Fig. 2. Current phasor diagrams while neutral point is isolated, (a) healthy mode operation, (b) one phase open circuit fault, (c) two adjacent faulty phases, (d) two nonadjacent faulty phases

Following these limits, the appropriate current reference phasors under faulty conditions can be summarized in Fig. 2 for different conditions. While having one faulty phase, the current amplitudes should increase up to 1.38 their initial value to generate the same electrical torque.

The situation is more critical while having two faulty phases. In this case, depending on the mechanical position of the faulty windings, the current amplitudes of healthy phases should increase up to 3.62 their initial value to maintain the pre-fault electrical torque.

In this project, the availability of neutral point has also been considered in five phase PM drives. Taking the advantage of having control on neutral point voltage, new control strategies are being developed to reduce the current amplitude in the remaining healthy phases.

Operational temperature can be mentioned as the main limiting factor under faulty conditions. This leads to limited amplitude of currents in the remaining healthy phases. On the other hand, the main objective can be mentioned as the improvement of torque quality, and increasing the machine's dynamics speed.

As a brief summary, the general steps of this project can be summarized as controlling method proposal, simulation, experimental verification, and documentation.

III. Completed Thesis Steps

III.A. Evaluation of Accessible Neutral Point Effect in Fault Tolerant Five Phase PMSM Drives

In the first step, the importance of neutral connection under faulty conditions has been studied for five phase PMSM drives. Open circuit fault has been considered for both one and two phases, and fault tolerant field oriented control of five phase PMSM has been developed under healthy and faulty conditions. It is shown that by having access to the neutral point under faulty conditions, it is possible to have less torque ripple, and less current amplitudes in the remaining healthy phases. Comparing with isolated neutral case, this current reduction reaches to 51% in the case of two adjacent faulty phases. In table.1, the effect of available neutral point on motor amplitudes is summarized.

Table. 1: The effect of available neutral point on current amplitudes under different faulty conditions

condition	Reduction in Maximum peak Current
One Faulty Phase	6.5%
Two adjacent faulty phases	51%
Two nonadjacent faulty phases	5%

III.B. Ripple Free Fault Tolerant Control of Five Phase Permanent Magnet Machines

In this study, it is tried to reduce the generated torque ripple under faulty conditions. Different operational conditions are considered including healthy motor, one faulty phase, two adjacent faulty phases, and two nonadjacent faulty phases. Under each operational condition, optimized current patterns are obtained to achieve maximum available power, zero torque ripple, and nominal copper losses. It is shown that by having access to neutral point the output power can be increased up to 65% in the case of two adjacent faulty phases (Fig. 3).

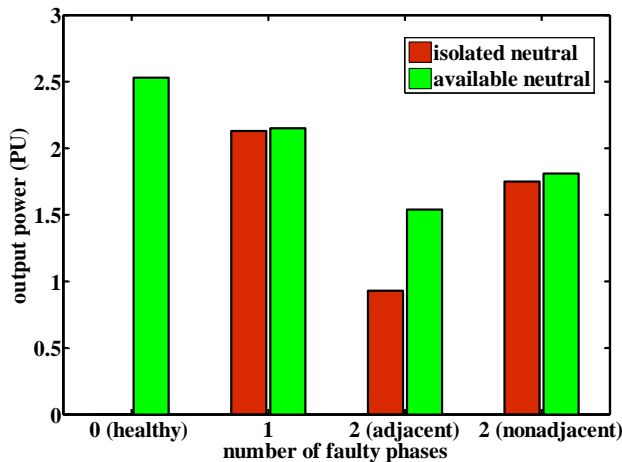


Fig. 3 motor output power under healthy and faulty conditions

III.C. Title: Model Predictive Current Control of Five Phase Permanent Magnet Motor

Model Predictive Control (MPC) is developed to achieve faster dynamics, and more reliability in this project (illustrated in Fig. 4). Comparing to conventional cascade configuration, MPC has faster dynamics in transients. On the other hand, due to the lack of integrators in MPC structure, the steady state error is not guaranteed to be zero. This weak point can be covered by using an integrator in the speed loop controller. Moreover, in high speeds and while pushing DC bus voltage limit, MPC is more stable than conventional cascade structure. This work is developed and documented for healthy condition; the next step will be to implement MPC advantages for improving the stability and motor dynamics under faulty conditions.

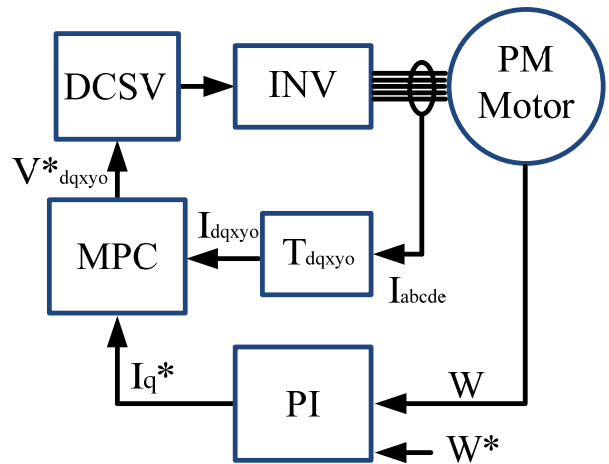


Fig. 4: MPC general block diagram

IV. Acknowledgments

All of the works are supported by Ministry of Economic Affairs and Competiveness under the Research Project TRA 2010-21598-C02-01 and CD2009-00046 Consolider Project

V. References

[1] L. Parsa, H. A. Toliyat, "Fault-tolerant five-phase permanent-magnet motor drives," in Proc. IEEE IAS Annu. Meeting, Oct. 2004
 [2] A. G. Jack, B. C. Mecrow, J. A. Haylock, "A comparative study of permanent magnet and switched reluctance motors for high-performance fault-tolerant applications," IEEE Trans. Ind. Appl., vol. 32, no. 4, Jul./Aug. 1996.

Satellite for Health: An architecture to provide E2E quality of service guarantees

Author: Elizabeth Rendón-Morales, Thesis Advisors: Jorge Mata-Díaz and Juanjo Alins

Contact email: elizabeth.rendon@entel.upc.edu

I. Introduction

Satellite systems are used to monitor specific situations, such as natural disasters, military operations, health care support in planes and boats etc. In such scenarios, satellite communication infrastructures are the only technology that remains available to maintain the link between affected sites and the authorities. Taking this in to account, it is mandatory to guarantee the transfer of time critical data to end users when this communication is done by means of satellite systems.

Moreover, when the satellite capacity is reduced due to the presence of atmospheric events, it is necessary to classify and prioritize high priority data to guarantee its transfer over the reduced satellite capacity.

Considering such aspects, for the provision of Quality of Service (QoS) guarantees over satellite systems, it is desirable to have a complete End-to-End (E2E) satellite architecture based on the standards such as the DVB-S2/RCS. This architecture must take in to account the drawbacks posed by GEO satellite systems (the delay, losses and principally the presence of bandwidth variations in an E2E satellite path), while implementing algorithms to provide enhanced QoS support.

One of the main reasons for designing an E2E architecture with the support of QoS, it is that organizations such as the European Space Agency (ESA), which manages satellite infrastructures in Europe, requires the continuous exploitation of their current assets, as launching a new communication satellite is associated with expensive costs. Therefore, it is required the support of IP services with QoS guarantees over current satellite communication systems, taking advantage of new proposals developed for the earth segment.

In this paper we propose an architecture to provide health care support based on QoS guarantees over DVB-S2/RCS satellite systems.

Our architecture provides low complexity on its implementation and can seamlessly inter-operate with terrestrial IP networks. Our solution is designed in compliance with the ETSI-BSM-QoS framework and provides a detailed design at the Satellite Independent-Satellite Dependent (SI-SD) layers in order to provide QoS guarantees by means of traffic priorities. Particularly, the SI layers are defined to deal with QoS differentiation based on the DiffServ framework. Conversely, the SD layers are proposed for applying different DVB-S2 channel adaptations. Finally, our solution is compatible with IP-based technologies and protocols and it specifies the requirements for the forward and the return channel based on the DVB-S2/RCS standards

The E2E scenario for the proposed architecture is shown in Figure 1. It considers a broadband satellite system in the Ka band (30/20 GHz) in a multi-beam architecture. It represents the typical scenario, in which remote users demand Internet applications by the intensive use of the forward channel.

In particular, an emergency remote vehicle requires accessing critical applications and data allocated at the regional hospital to provide the first medical aid during an emergency situation (i.e. earthquake, tsunami, etc.), where the satellite system is the only technology that remains available.

Here, three sources, with different QoS levels, send data to a remote destination by means of the broadcast GEO satellite channel. This channel represents the communication link between the ground gateway and return channel satellite terminal (RCST). Particularly, in the proposed scenario, a heavy rain event is affecting the available bandwidth in the DVB-S2 forward channel.

In particular the Expedited Forwarding (EF) class supports a real-time VoIP application, simulating a constant-rate traffic, which is transferred over the User Data Protocol (UDP) to strictly guarantee bandwidth reservation. The Assured Forwarding (AF) traffic class bears a HTTP application while the BE traffic class bears a persistent File Transfer Protocol (FTP) transaction server. Both, the AF and BE traffic classes are transported using the TCP protocol.

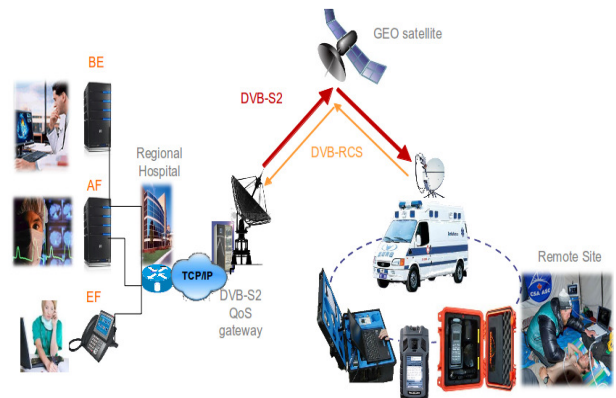


Figure 1. Satellite for health architecture.

II. Architecture Design

For the provisioning of QoS guarantees, the satellite architecture design is based on the DiffServ framework. The main goal of the proposed architecture is to guarantee different QoS levels for IP traffic over the DVB-S2 channel while reducing latency and jitter values, considering the fact that the available bandwidth present in the satellite system is constantly changing.

The DVB-S2 gateway design including its separation between high SI layers and low SD layers is shown in Figure 2. The main elements in the proposed architecture design are:

(i) A cross-layer optimization between the physical layer and the network layer, to provide E2E QoS guarantees considering the fact that the DVB-S2 forward channel is affected by the presence of rain events.

(ii) A complete Active Queue Management (AQM) system that considers Token Buckets (TBs) as rate limiters to regulate and guarantee a minimum

transmission rate for each traffic class according to the priority levels established by the satellite operator.

(iii) A modified queuing policy called Re-Queuing Mechanism (RQM) to reduce delay and jitter while improving the user's QoE for the Expedited Forwarding (EF) and the Assured Forwarding (AF) traffic classes. This mechanism follows the philosophy of the DVB-S2 design, in which retransmissions are avoided because the two-way propagation delay is significantly high. In our case, the RQM mechanism prevents dropping packets that do not fulfill the DiffServ specification.

(iv) A dynamic IP scheduler to allocate bandwidth resources for prioritizing those flows with high QoS requirements. The IP scheduler uses an algorithm that adjusts its internal values considering the capacity present in the system. This dynamic adaptation considers the cross-layer information sent by the physical layer to provide enhanced priority for specific flows when a reduced and limited channel capacity is experienced in the satellite system.

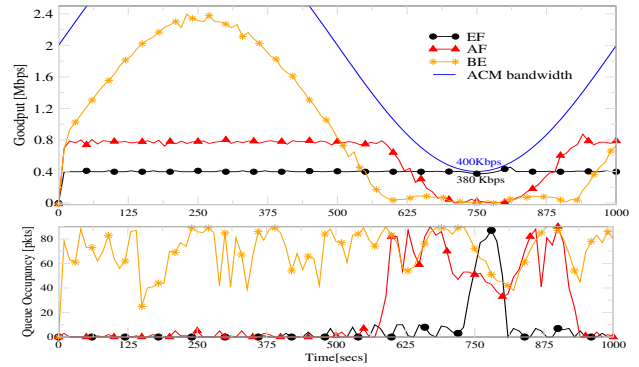


Figure 3. Simulation Results.

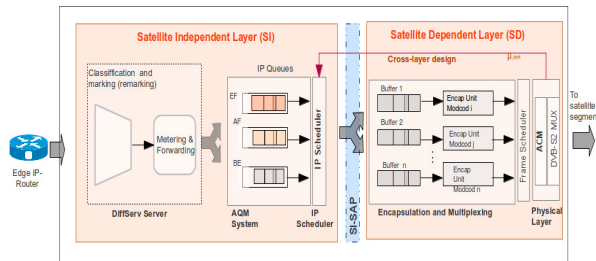


Figure 2. DVB-S2 gateway design

III. Simulation Results

Fig. 3 shows the goodput and queue occupancy results for the EF, AF and BE traffic classes working simultaneously. It includes the ACM sinusoidal function representing a rain event reducing the bandwidth availability up to 400 Kbps.

Here, it is possible to see that the EF traffic class (symbol •) is totally guaranteed during the whole rain event. In contrast to the AF traffic class (see symbol Δ) which is guaranteed only if the resources for the EF traffic class have been assigned. This is an expected result according to the QoS requirements defined for a DVB-S2 satellite system. Finally, the BE traffic class (symbol *) is able to use the remaining link bandwidth during all the simulation, taking advantage of the resources that the other classes are not using.

In addition Table 1 shows the mean and the standard deviation (Std Dev) parameters for the EF delay and jitter experienced at the application layer. As it is observed, these values are highly reduced when using the proposed architecture compared to those results obtained by using either static or weighed configurations. Using the proposed architecture, it is possible to guarantee lower delay values (330 msec) during almost all the simulation, which is a suitable result considering the fact that the available capacity present in the satellite systems is reduced to a critical point in which the priority of the EF traffic class requires to be guaranteed.

Parameter (seconds)	Static Configuration	Weighted configuration	Satellite for Health architecture
Mean Delay	3.71	2.45	0.33
Delay Standard Deviation	1.7	1.56	0.24
Mean Jitter	6.55	0.017	0.016
Jitter Standard Deviation	3.81	1.9	0.029

Table 1. E2E delay and jitter parameters for the EF traffic class.

IV. Conclusions

The adoption of the proposed satellite architecture allows an enhanced distribution of bandwidth resources while guaranteeing the QoS requirements for specific traffic flows in a satellite for health scenario. By means of the proposed cross-layer optimization, it is possible to continuously update the bandwidth availability to keep the QoS requirements for the high priority traffic classes.

Finally, the proposed architecture design allows enforcing the QoS specifications to guarantee the support of health services when an extreme reduction of bandwidth occurs in the satellite system

V. Acknowledgments

This work is supported by the Spanish Ministry of Science and Education under the projects TEC2011-26452 (SERVET) and CONSOLIDER-ARES (CSD2007-00004). E. Rendón wants to thank FPI-UPC grant and R. Aviles-Espinosa for his valuable comments and suggestions to improve this paper.

VI. References

[1] Rendon-Morales E, Mata-Díaz J, Alins J, Muñoz JL, Esparza O, "Performance evaluation of selected Transmission Control Protocol variants over a DVB-S2 BSM satellite systems with QoS". International Journal of Communication Systems 2012. [http://dx.doi.org/10.1002/dac.2333]
 [2] Rendon-Morales E, Mata-Díaz J, Alins J, Muñoz JL, Esparza O, "QoSAr: a cross-layer architecture for E2E QoS provisioning over DVB-S2 broadband satellite systems". EURASIP Journal on Wireless Communications and Networking. 2012.

Contribution to develop a communication framework for vehicular ad-hoc networks in urban scenarios

Author: Carolina Tripp Barba, Thesis Advisor: Mónica Aguilar Igartua

Contact email: *ctripp@entel.upc.edu*

I. Introduction

During the last 5 years the automobile industry interest has shown an interest in vehicular ad-hoc networks (VANETs) [1]. An exponentially growing interest in this area, both from academia and automobile industry, has embraced this new research area and technology. At the present moment, the number of potential applications have quickly expanded beyond road safety and now includes other types of applications as well, e.g. Infotainment, Internet access, video streaming.

Nowadays, the huge amount of vehicles in transit has arisen a big interest in developing vehicular communication technologies. In this respect, several innovative and cost-effective mobile services and applications for traffic networks are under investigation, emerging as the basis of the so called intelligent transportation systems (ITS). ITS have become an attractive research field for several years. Among many technologies proposed for ITS, wireless vehicular communication, covering vehicle-to-vehicle (V2V) and vehicle-to-infrastructure (V2I) communication, aims to increase road safety, transport efficiency, reduction of pollution emission as well as to provide ubiquitous wireless connectivity to the Internet and to offer infotainment services to passengers.

This type of network has the advantage to warn the driver and the co-pilot of any event occurred in the road ahead, such as traffic jam, accidents, bad weather, etc. This way, the number of traffic accidents may decrease and many lives could be saved. Besides, a better selection of non-congested roads will help to reduce pollution. Transportation in roads and highways will be easier, safer and more comfortable for passengers.

In this thesis we aim at designing a framework to deploy multimedia services over vehicular ad hoc networks in urban environments. To achieve this goal, an efficient routing protocol specially designed for vehicular environments is needed.

II. Objective

After analyzing the characteristics of previous proposals we decided to include in ours some features that are adequate to design any routing protocol for VANETs. For instance, our framework should assume the knowledge of maps. That is, vehicles are map-aware. With this, vehicles in the VANET know the environment, e.g. where intersections, buildings, traffic lights and other traffic signals are located.

On the other side, we will design new metrics and algorithms to improve the performance of the routing operation. Besides, we will design an algorithm to assist the routing protocol to select between carrying or forwarding the packets. Also, we assume vehicles have a global positioning system (GPS) and a driver assistant device.

The main objective of this thesis is to design a communication framework for VANETs in urban scenarios. We aim at designing a routing protocol that improves the selection of forwarding nodes in VANETs.

To carry out our objectives, we defined the following tasks:

- Design of a routing protocol adequate for VANETs, including different metrics to design the routing protocol: vehicle density, distance, velocity vector, link lifetime and available bandwidth.
- Include privacy capabilities in the routing protocol to protect users' identities.
- Include in the routing an analytical model to estimate the available bandwidth in the wireless link.
- Algorithm to make vehicles be aware of the buildings to take proper forwarding decisions.
- Algorithm to switch between carry and forward modes depending on the current network conditions.
- Adaptation of the designed algorithms specifically for video-streaming services.
- Performance evaluation of the different proposals compared to other routing protocols in realistic urban scenarios.

These characteristics are requirements that may improve significantly a general good routing protocol for VANETs. These improvements will be included in our routing protocol to be adequate for VANETs. Besides, the new routing proposal will be tested in realistic scenarios using the simulator NCTUns 6.0 [2] and the mobility generator CityMob [3] which will allow us to add traffic signals, car accidents and different scenarios varying the speed, number of vehicles, network dimensions and other configuration settings.

III. Traffic density

We assume a smart city scenario that includes intelligent traffic lights (ITL) which will gather traffic statistics to be used by the routing protocol and by the driver assistant device to take proper decisions.

In this work we focus on the analysis of traffic density, although similar analysis can easily be done for other traffic statistics (e.g. number of passengers, trip time). Traffic messages are sent by each vehicle to the closest ITL every 2 sec. This way, a vehicle moving at $v=40$ km/h would send 4 messages while it crosses a 100 m. street. The procedure to gather traffic statistics is shown in Fig. 1. Each vehicle sends a statistic message (SM) to the nearest ITL. The SM includes the current number of neighbours of that vehicle. ITLs will receive SMs and update traffic density statistics (TDst) by using an exponential weighted moving average (EWMA) to average current and historical traffic density values. ITLs will store the results and will share their statistics throughout time with the other ITLs in the smart city through a sub-network they form.

The network scenario was designed in NCTUns 6.0 [2] and the mobility generator was Citymob [3]. It represents a Manhattan-style city like Barcelona, Spain. We carried out simulations varying the number of vehicles in the city throughout time, so that the density of vehicles increases during the morning (TDst₉₋₁₂),

reaches its maximum at rush hours (TDst₁₂₋₁₅) and decreases during the afternoon (TDst₁₅₋₂₁), see Fig. 2.

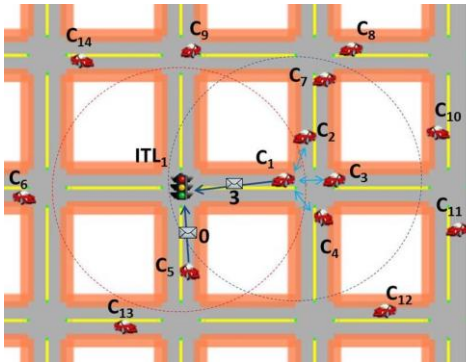


Figure 1. Intelligent traffic light (ITL) obtaining traffic statistics in its crossroads.

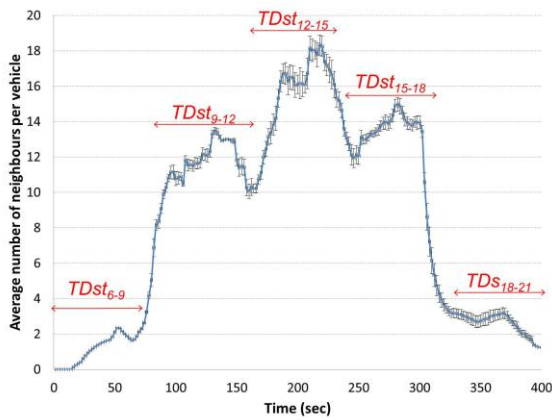


Figure 2. Average number of neighbours per vehicle measured in the city entrance (90% confidence intervals).

IV. Warning messages

We have implemented a simple warning service to prevent accidents and further collisions by alerting drivers about accidents and dangerous road conditions. Warning messages include a field with the location of the initial place where the warning message was generated. Nearby vehicles that receive such message will reduce their speed depending on the warning message, according to Table 1.

Traffic density (2-bit)	Weather (2-bit)	Warning message: reduce speed
Free road segment 	Sun	U
	Rain	$85\% \cdot U$
	Storm	$65\% \cdot U$
	Ice	$40\% \cdot U$
Semi-congested road segment 	Sun	$75\% \cdot U$
	Rain	$50\% \cdot U$
	Storm	$25\% \cdot U$
	Ice	$10\% \cdot U$
Very congested road segment 	Sun	$50\% \cdot U$
	Rain	$40\% \cdot U$
	Storm	$30\% \cdot U$
	Ice	$10\% \cdot U$
Accident 	Sun	0
	Rain	0
	Storm	0
	Ice	0

Table 1. Warning messages: traffic and weather conditions.

The use of warning messages helps to avoid collisions among other vehicles and the broken vehicle, thanks to this scheme that makes vehicles brake

beforehand. For example, in case of very congested road segment and rain, the speed of the vehicle should be reduced to 40% of the initial driver speed (U in Table 1).

In Table 2 we can see simulation results that show the effectiveness of this scheme since it is able to reduce the braking distance until stop and the driver's reaction time. Using our framework the vehicles's total distance travelled after a vehicle accident would be reduced from 18.63 m to 8.45 m, which may help to avoid further collision with a broken vehicle. This way road safety improves.

	Use of ITLs	Non use of ITLs
Driver/vehicle's reaction time	0.084 sec	1 sec
Distance travelled till reaction	0.93 m	11.11 m
Braking period of time	1.355 sec	1.355 sec
Distance travelled during braking	7.52 m	7.52 m
Total distance travelled	8.45 m	18.63 m

Table 2. Driver's reaction time and distance travelled after receiving a warning message.

V. Conclusions and future work

We have designed a smart city framework for VANETs that includes intelligent traffic lights (ITLs) that gathers, updates and transmits traffic statistics (see Fig. 1). Besides, our smart city framework includes warning messages sent by broken vehicles to make approaching vehicles brake beforehand to thus avoid more collisions. The goal is that the driver's assistant device uses updated traffic statistics to take proper trip decisions, for instance avoiding congested roads, to therefore reduce the trip time and also pollution as a consequence. Besides, warning messages alerting about accidents and dangerous road conditions may help to avoid further collisions and to improve road safety.

Currently, we are developing a routing protocol that considers vehicles' density to take better packet forwarding decisions seeking to reduce packet losses and delay in infotainment services such as video-streaming.

VI. Acknowledgments

This work was partly supported by the Spanish Government through projects TEC2010-20572-C02-02 Consequence, FI-AGAUR grant of the "Comissionat per a Universitats i Recerca del DIUE" from the Generalitat de Catalunya and the Social European Budget. Also, by the "Universidad Autónoma de Sinaloa (Programa Doctores Jóvenes en Áreas Estratégicas)", Mexico.

VII. References

[1]. Hartenstein, H., Laberteaux, K. "VANET Vehicular Applications and Inter-Networking Technologies (Intelligent Transportation System)". Wiley, 2010. ISBN: 978-0470740569.
 [2]. Wang, S.Y., Chou, C.L. "NCTUns tool for wireless vehicular communication network researches". *Simulation Modelling Practice and Theory*. 2009. pp. 1211-1226.
 [3]. Martínez, F. J., Cano, J. C., Calafate, C. T., Manzoni, P. "CityMob: a mobility model pattern generator for VANETs". IEEE International Conference in Communications (ICC'08). 2008. pp. 370 - 374

Layer Discovery in the Recursive InterNetwork Architecture

Author: Eleni Trouva, Thesis Advisors: Eduard Grasa, Xavier Hesselbach Serra
contact email: eleni.trouva@i2cat.net

I. Introduction

It is well accepted in traditional networks, such as the Internet, that for an application to find the application it wants to communicate with, they must both have access to the same address space or in other words, they both should have access to the same layer. However, by exploring the properties of a complete network architecture, such as the Recursive InterNetwork Architecture (RINA), it became clear that this commonly accepted view is not the case. Although it is required that for two applications to communicate they must belong to the same layer, there is no requirement for discovering the requested application to be in the same layer. Application discovery in networks involves two steps, first discovery of the requested application and next finding a supporting layer for the communication by using an existing one or by creating one from scratch. To support these operations a directory service is required. The research of this thesis is focused on the component that is responsible to provide the functions that comprise the directory service in RINA.

II. The Directory

A simple case that illustrates the problem under research is given in Fig. 1. In the scenario shown the web browser (application A) residing in host H3 requests to communicate with the web page (application B) on host H2. The first step is to find the requested application B. Then, the question is which layers support application B and which one should be chosen for the communication. The need for a directory service -a database that maintains mappings of application names to list of supporting layers- is becoming apparent.

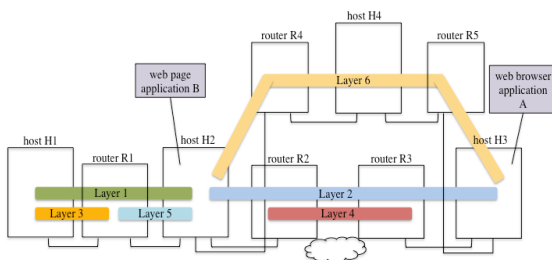


Figure 1. Application discovery involves also discovering which layers support the requested application.

There are several architectural decisions that define the design and the function of a directory. The directory structure may be centralized or decentralized (distributed, replicated or cached). It might follow a hierarchical organization or be flat. A combination of these is possible, as well as a directory that has an evolving structure according to the number of applications registered, the usage and the load and availability requirements. Two protocols are required for the directory service, the first is a request/response protocol to query the database and the other, an update

protocol to distribute updates to the database in the case it is replicated or in the case that caches exist. Moreover, a decision on how the members of the directory are queried has to be taken. When a query is made to a member of the directory, the directory might respond back with the best local information it has, might be responsible to query other databases and then return a response according to the information it acquired or simply return a reference of the next directory to ask. In addition, a policy for the creation of the supporting layer has to be decided. In reality, there is a set of policies that decide on several operations that need to be done when creating a new layer such as the selection of the path that connects the source and the destination systems, whether an existing layer is used or a new one is created and the communication and the coordination between the systems along the path.

III. The Inter-DIF Directory in RINA

The goal of this thesis is to propose a framework for the directory service in RINA. The Recursive InterNetwork Architecture (RINA) is a novel network architecture proposed by John Day in his book "Patterns in Network Architecture: A return to fundamentals" [1], [2]. It is based on the view that networking is only inter-process communication (IPC) and only IPC. For this networking can be seen as a set of recursive layers that provide distributed IPC over different scopes. Each of these layers, Distributed IPC Facility (DIF) as it is called in RINA, performs a coordinated set of policy managed functions to achieve the desired IPC service. The Directory framework for RINA encompasses distinct subtopics, the directory structure, the search/query mechanism, the update mechanism and the strategy to follow for creating the supporting layer. A study of the different approaches on these topics and the conditions under which each approach works best will be the outcome of this work.

The Directory in RINA is called InterDIF Directory (IDD). The IDD is a distributed application, which is simply a collection of two or more cooperating application processes in one or more processing systems, which exchange information using IPC and maintain shared state. Each processing system has an instance of the IDD that enables the system to register its applications and make them discoverable by other applications and also, to search for other applications. The application processes that belong to the same IDD are called peer IDs and are able to exchange messages for the discovery of other applications. An example of an IDD distributed application is shown in Fig.2.

When an application wants to communicate with another application, first all the DIFs (layers) of the source system will be examined to see if the requested application can be reached through them. If the result is negative then the IDD is used to first find the requested application and then attempt to create a supporting DIF between the two systems for the communication. The peer IDs will forward a request from one to another asking for the requested application. Forwarding begins at the IDD that resides in the same system with the

requesting application and will be based on the forwarding policies decided for the specific IDD. The forwarding will continue until the IDD of the system that the requested application is registered is found or if a pre-defined termination condition is met to avoid infinite search. If the destination system is reached, using the information carried in the request, the IDD will have to check whether an instance of the requested application is available and if yes, whether the requesting is allowed to access it. If both checks are positive, the next step for the IDD is to create the DIF that will span between the source and the destination systems and will support the communication. This either involves creating a new DIF from scratch or expanding (joining) an existing one.

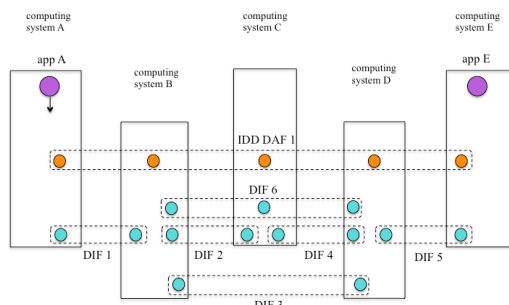


Figure 2. An example of an IDD distributed application.

As we saw, the IDD function can be tuned through several different policies. It is clear that there is no perfect choice of policies in general but only policies that work best for a specific environment and under specific conditions. One of the goals of this work is to provide guidelines that indicate which approaches to follow for specific cases. For this reason performance metrics, such as the time to the discovery of the application, the hit rate of the caches, the number of messages exchanged, the number of systems contacted, the mean look-up time, the time to distribute updates in caches, etc. are of interest. Analytical modeling and formal methods allow an estimation of these quantities and then a comparison between the different approaches. However, the feasibility of the IDD functionality has to be proven especially in large scale networks. For this, computer-based modeling and simulations with plugged-in policies is the method to follow to perform large-scale experimentation. Experimental evaluation will also be an option, as a RINA prototype is being developed.

IV. Conclusions, on-going and future work

The work in this research is novel as it is the first effort to explore the properties of the IDD function in RINA. Partial validation of the IPC model theory [1] will be one of the results with the completion of this thesis and also refinement of the current IDD specifications. There is no a comparable function to the IDD in the Internet today. The only Directory-like service in the current architecture is DNS which provides IP addresses where an application protocol might be found if the requesting application knows the well-known port to connect to. If different applications are available using the same application protocol, the application protocol must be able to determine how to find them, e.g. http. In the Internet, applications must belong to the same layer. The IDD can span across a sequence of layers, allowing the discovery of all the applications registered.

Applications do not have to be on the same layer as with the current Internet architecture. The implications of the IDD in network architectures seem profound. So far it appears that it eliminates the need for layers with large address spaces and creates greater security by better compartmentalization without impairing reachability. Moreover, the IDD makes it clear that the scope of the application name space is the set of IDD's that can be queried by any one IDD. Other implications are expected to emerge with further exploration and study the IDD's properties. A more detailed description of the IDD and its function can be found at [3].

Since the IDD is a component of the RINA architecture, a few of the implications of that follow its adoption should also be named. RINA is surprisingly simple compared to today's protocol complexity and provides a structure that allows network designers to solve the problems identified in the current Internet. It addresses mobility, multi-homing and Quality of Service support inherently without the need of extra mechanisms, provides a more secure and configurable environment comparing to the current structure, while remaining scalable, and motivates for a more competitive marketplace. At the same time, RINA allows for a seamless adoption. Some readers might wish to look at [4] for more information on RINA.

Current work involves the development of a prototype that implements the RINA architecture, including an IDD implementation. Further research is on-going on exploring how existing DIFs between the source and the destination systems can be used to our advantage and in which cases expanding an existing DIF is preferred over creating a new one from scratch. Future work includes experimentation, measurements and performance comparisons using the developed IDD implementation under a choice of different routing, updating and caching strategies.

V. Acknowledgments

This research has been partially supported by the Spanish Government, MICINN, under research grant TIN2010-20136-C03.

VI. References

- [1] J. Day, *Patterns in Network Architecture: A Return to Fundamentals*, Prentice Hall, 2008.
- [2] E. Trouva, E. Grasa, J. Day, I. Matta, L. T. Chitkushev, P. Phelan, M. Ponce de Leon and S. Bunch, Is the Internet an unfinished demo? Meet RINA!, in *TERENA Networking Conference*, 2011.
- [3] E. Trouva, E. Grasa, J. Day, S. Bunch, Layer Discovery in RINA networks, in *17th International Workshop on Computer Aided Modeling and Design of Communication Links and Networks*, 2012.
- [4] Pouzin Society - <http://www.pouzinsociety.org/>

Privacy Protection of User Profiles in Personalized Information Systems

Author: Javier Parra-Arnau, Thesis Advisors: Jordi Forné, David Rebollo-Monedero
contact email: xparna@gmail.com

I. Introduction

Recent years have witnessed the accelerated growth of a rich variety of personalized information systems (PISs) of unprecedented sophistication, which have been integrating seamlessly into our daily lives. Examples of these systems comprise personalized Web search and news, resource tagging in the semantic Web and multimedia recommendation systems. The key enabling technology of such systems is *personalization*, a research area that has received great attention lately and whose aim is to tailor information-exchange functionality to the specific interests of their users. To accomplish this functionality, most personalized information systems capitalize on, or lend themselves to, the construction of *profiles*, either directly declared by a user, or inferred from past activity, not only of the user in question, but also from the profiles of users with whom social relationships are known to the information system.

Personalized services therefore allow users to deal with the overwhelming overabundance of information, but inevitably at the expense of *privacy*, especially when profiling is conducted across several information systems. Besides, the enrichment of these services with data from social networks creates additional opportunities with respect to information sharing but, at the same time, increases the user privacy risks. Figure 1 shows an example of user profile modeled as a list of categories of interest.

II. Measuring the Privacy of User Profiles

A variety of privacy-enhancing technologies (PETs) have been proposed to enable the provision of new services and functionalities aimed at mitigating those privacy threats. Unfortunately, these technologies have not yet gained wide adoption. This is because it remains unclear whether their overall benefits outweigh their typically costly deployment and/or integration, as well as the operational cost that arises due to the fact that PETs typically come with penalties in terms of utility and performance, when compared to more privacy-invasive alternatives [1]. Assessing the privacy provided by a PET is, therefore, crucial to both determine its overall benefit and compare its effectiveness with other technologies. In other words, privacy metrics, accompanied with utility metrics, provide a quantitative means of contrasting the suitability of two or more privacy-enhancing mechanisms.

Building upon well-established principles of information theory and statistics, we make a first contribution in this direction by proposing Kullback-Leibler (KL) divergence as a criterion for quantifying the privacy of user profiles. Our metric, which encompasses Shannon's entropy as a special case, is examined, on the one hand, under the beautiful perspective of the method of types and large deviation theory, and on the other, under Jaynes' rationale behind entropy-maximization methods. The proposed privacy measure contemplates a user profile modeled as a normalized histogram of user data, e.g., tags, ratings or queries,

across a predefined set of categories of interest. In addition, we consider two distinct adversary models—an attacker aimed at targeting users who deviate from the average profile of interests; and another attacker whose objective is to classify a given user into a group of users.

III. Privacy-Enhancing Technologies in Personalized Information Systems

Equipped with a quantitative measure of privacy and utility, we investigate PETs providing *hard privacy*. By hard privacy, the privacy research literature refers to the case in which users mistrust communicating entities, e.g., the personalized information provider or the network operator, and thus strive to reveal as little private information as possible. This is in contrast to those privacy-preserving systems that build upon the assumptions of *soft privacy*, what means that users entrust their private data to these systems, which are therefore responsible for the protection of their data.

Under the assumptions of hard privacy, this thesis contemplates two conceptually-simple strategies that capitalize on the principle of data perturbation. First, we consider the *suppression* of tags in the scenario of the semantic Web, and secondly, the combination of the *forgery* and suppression of ratings in personalized recommendation systems. Figure 2 provides a depiction of one of these approaches. Specifically, we illustrate the case of tag suppression, whereby users may wish to refrain from tagging certain resources. In doing so, the actual user profile q , that is, the profile capturing the user genuine interests, is observed from the outside as a perturbed profile; we refer to this profile as the apparent user profile s . Consequently, the adoption of our approach enables users to avoid being accurately profiled by the service provider, or in general, by any attacker capable of collecting the tags posted by users.

Our second strategy contemplates the submission of false information, together with the aforementioned suppression technique, but in the scenario of

Below you can edit the interests and inferred demographics that Google has associated with your cookie:

Category	
Beauty & Fitness - Fitness - Yoga & Pilates	Remove
Books & Literature - Children's Literature	Remove
Food & Drink - Cooking & Recipes - Fruits & Vegetables	Remove
Hobbies & Leisure - Water Activities - Surf & Swim	Remove
Home & Garden - Home Improvement - House Painting & Finishing	Remove
News - Health News	Remove
People & Society - Family & Relationships - Family - Baby & Pet Names	Remove
People & Society - Family & Relationships - Family - Parenting - Baby Care	Remove
People & Society - Social Sciences - Psychology	Remove
People & Society - Women's Interests	Remove
Shopping - Toys	Remove
Sports - Individual Sports - Cycling	Remove
Sports - Individual Sports - Gymnastics	Remove
Demographics - Age - 25-34	Remove
Demographics - Gender - Female	Remove

Figure 1. Example of user profile, as shown by Google [2]. The interest of this user in the categories highlighted in red might reveal she is pregnant or planning to get pregnant. In this information ended up in the hands of her employer, her job might be at risk.

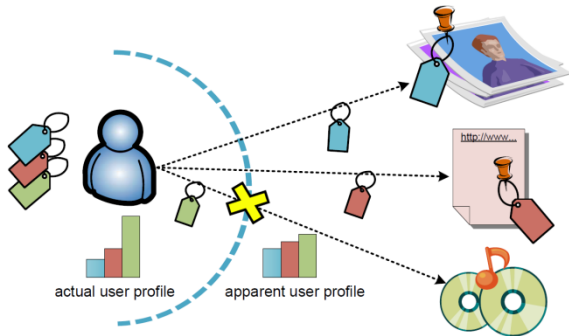


Figure 2. Tag suppression in the semantic Web.

recommendation systems. More precisely, in our approach, users rate items, e.g., movies, music or books, as they normally do. However, when their privacy is being compromise, users may want to submit some ratings to items that do not reflect their actual interests.

IV. On the Trade-Off between Privacy and Utility

By adopting our strategies, users enhance their privacy to a certain extent, without having to trust an external entity or the network operator. Nevertheless, this is inevitably at the expense of a loss in data utility. For example, in the case of tag suppression, privacy comes at the cost of a degradation in the semantic functionality of the Web, since tags has the purpose of associating meaning with resources. On the other hand, the forgery and suppression of ratings in recommendation systems come with penalties in terms of the accuracy of the prediction generated by the recommender. In a nutshell, data-perturbative mechanisms pose an inherent trade-off between privacy and utility.

One of the objectives of this thesis is precisely to investigate the trade-off posed by such PETs. For this purpose, first we formulate mathematically the compromise between these two contrasting aspects; and secondly we tackle the issue in a systematic fashion by applying the methodology of multiobjective optimization. Our extensive theoretical analysis includes a close-form solution to the mathematical problem of tag suppression on the one hand, and to the problem of the forgery and suppression of ratings on the other. In addition, we characterize the optimal trade-off between the aspects of privacy and utility. Figure 3 illustrates the trade-off between privacy, measured as the Shannon entropy of the apparent user profile $H(s)$, and the tag suppression rate $\sigma \in [0,1)$, i.e., the proportion of tags a user is willing to eliminate. Figure 4 shows the contours of the function modeling the trade-off among privacy risk, forgery rate ρ and suppression rate σ .

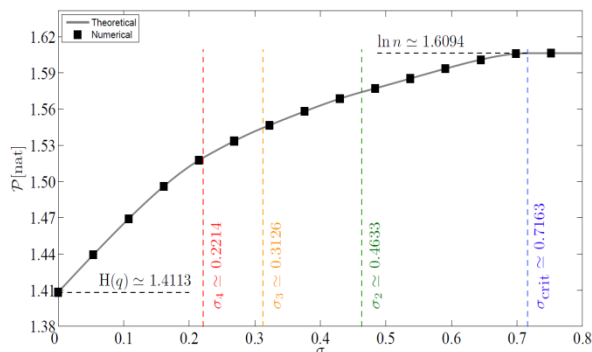


Figure 3. Privacy-utility trade-off in tag suppression.

V. Experimental Evaluation of our Privacy-Enhancing Technologies

Having investigated the privacy-utility trade-off posed by such PETs, we study the impact of those mechanisms on a real world application scenario. In particular, we assess the level of privacy attained by those users suppressing tags, and also how this mechanism may affect a parental control filter that enforces blocking conditions on resources (e.g., Web pages, videos or pictures), on the basis of the tags associated with them. More accurately, we contemplate an enhanced collaborative tagging system that consists of a “traditional” bookmarking service, such as Delicious (<http://delicious.com>), and two main additional services built on top of it. Such services address two main issues. The former allows users to specify certain policies to control the access to the browsed data, and the latter features our tag suppression mechanism.

Our experimental evaluation shows how our PET allows users to enhance their privacy to a certain extent. In addition, we assess the impact that suppression has on utility, by considering the percentage of tags that each bookmark loses as a result of elimination of tags. Lastly, we quantitatively evaluate the degradation in the classification of Web content, in terms of false negatives, false positives, precision and recall. Our results indicate that our technique does not have a significant impact on the accuracy of a parental control filter.

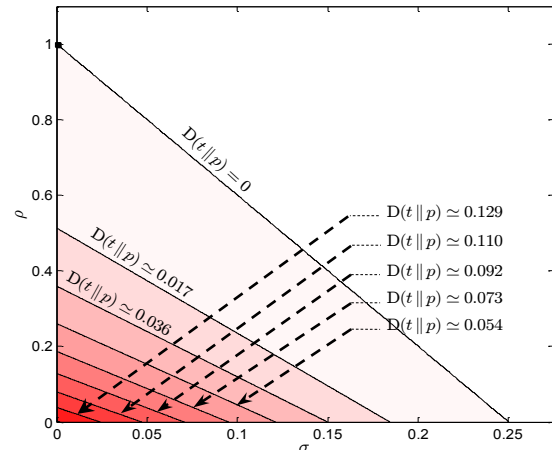


Figure 4. We measure privacy risk \mathcal{R} as the KL divergence between the apparent user profile t , resulting from the addition of false ratings and the suppression of genuine ratings, and the population’s distribution of ratings p , that is, $\mathcal{R} = D(t||p)$. This figure plots the contours of the privacy risk function for different values of forgery rate ρ and suppression rate σ .

VI. Acknowledgments

This work was partly supported by the Spanish Government through projects Consolider Ingenio 2010 CSD2007-00004 “ARES”, TEC2010-20572-C02-02 “Consequence”.

VII. References

[1] J. Borking, “Why adopting privacy enhancing technologies takes so much time, in: S. Gutwirth, Y. Poulet, P. Hert, R. Leenes (Eds.), Proc. Comput. Priv., Data Prot. (CPD), Springer-Verlag, 2011, pp. 309-341.
 [2] Google Ads Preferences. Available at <http://www.google.com/ads/preferences>.

Analytical Models for Architectural Exploration of Many-core Chip Multiprocessors

Author: Nikita Nikitin, Thesis Advisor: Jordi Cortadella

I. Introduction

The performance of microprocessors has improved drastically in the last few decades. Rapid downscale of the CMOS technology has led to higher operating frequencies and performance densities, facing the fundamental issue of power dissipation. *Chip Multiprocessors* (CMPs) have become the latest paradigm to improve the power-performance efficiency of computing systems by exploiting the parallelism inherent in applications [1, 2].

CMP architects are challenged to take many complex design decisions. What should be the ratio between the core and cache areas on chip? Which core architectures to select? How many cache levels should the memory subsystem have? Which interconnect topologies provide efficient on-chip communication? These and many other issues create a *complex multidimensional exploration space* for future generation on-chip architectures with hundreds or thousands of cores. *Design Automation* tools become essential to make the architectural exploration feasible under the hard time-to-market constraints.

The objective of this thesis is to establish the theoretical basis for efficient modeling of many-core CMPs and develop a usable and extensible software framework for automated architectural exploration. The major theoretical contribution of this work is the design of analytical models, capable of rapidly and accurately predicting CMP performance to avoid costly simulation. Another contribution is the design of the flow for efficient exploration of the next generation CMPs. The practical contribution of the work is the creation of flexible software tool for architectural exploration.

II. The CMP Architectural Exploration

Industrial and prototype implementations have already demonstrated the benefits achieved by CMPs with tens and hundreds of cores. Intel SCC chip is one of the examples, incorporating 48 cores [2]. The chip is organized into 24 dual-core tiles, each having two L2 cache modules and an on-chip router (Fig. 1). A 6x4 mesh-based on-chip network provides communication between the tiles as well as access to DDR memory controllers and I/O interface.

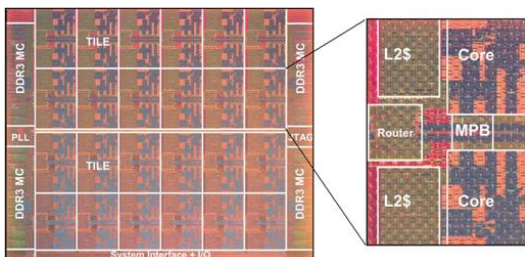


Figure 1. Layout of the 48-core Intel SCC chip [2].

The problem of architectural exploration for CMPs can be formulated as an optimization problem, aiming at the efficient usage of chip resources. Given the budgets for silicon area, power, temperature and other physical and design constraints, the problem is to maximize the

CMP performance for a selected set of workloads. The discrete nature of the design space makes it a very complex combinatorial problem. The issue is aggravated by the fact that simulation techniques are typically used to estimate the cost of one particular configuration. Simulation times of minutes and hours per configuration make the efficient exploration of large design spaces intractable.

Analytical models are of key importance for this work, since they are capable of estimating the configuration cost orders of magnitude (10^3 - 10^6 times) faster than simulation. The design of analytical models constitutes the most important part of the thesis. The works in [3] and [4] have already proposed analytical methods for exploration of CMP architectures. However, these models are too high-level and generic to capture certain aspects of hierarchical many-core architectures, such as the interconnect contention or cache-coherency protocols. Section IV summarizes the contributions of this thesis in the field.

III. The Exploration Framework

The developed exploration framework provides the CMP designer with a tool which, given the description of design space and cost metrics, returns the parameters of optimal configurations that fit the design space.

Figure 2 shows the structure of the framework. The design space is described using a comprehensive set of parameters and models for the cores, cache memories, interconnect fabrics, memory controllers, workloads and the expected cache-coherence protocol. The user can set constraints for the chip area, throughput and power or specify them as the optimization metrics. The output from the tool is a set of parameters, describing the optimal architectures.

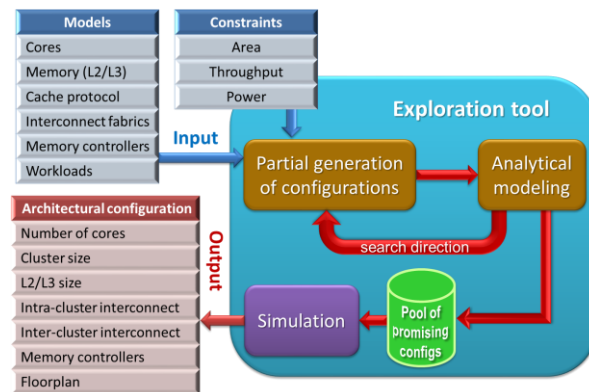


Figure 2. The tool interface and the exploration flow.

The basis of the exploration algorithm is an iterative procedure that generates a configuration from the design space, estimates its cost using fast analytical modeling and decides on the direction in which the exploration has to be continued. The loop is executed using an iterative metaheuristic search. The outcome from this process is a moderate pool of promising configurations which are further exhaustively simulated to find the best architecture with high accuracy.

IV. Analytical Modeling of CMP Performance

The core of the framework is the analytical model that estimates the cost of a given CMP configuration. The first contribution in this field was the proposal of a performance analytical model for the on-chip interconnects [5].

Using queuing theory, a comprehensive performance model for CMP has further been designed, capturing the behavior of the cores, interconnects and the memory subsystem for selected workloads [6]. During the model development, an important observation was made, which is the cyclic dependency between the traffic and latency of memory requests in a CMP. This dependency primarily defines the overall CMP performance and was shown to form a complex system of non-linear equations. Several numerical methods (fixed-point iteration, bisection, subgradient optimization) were proposed to efficiently resolve this dependency. This enabled the estimation of the performance of a CMP with hundreds of cores in several milliseconds.

The model was further extended to work with in-order, out-of-order and multithreaded core architectures. Another recent extension is the introduction of a queuing model and bandwidth for memory controllers. The work on analytical models is continued by investigating the impact of the cache coherence protocols on modeling.

Another contribution of the research is the application of *metaheuristic search* for speeding-up the exploration. Several metaheuristics based on probabilistic hill climbing have been analyzed and two of them (Simulated Annealing and Extremal Optimization) were finally adopted. The results show that the usage of metaheuristics on top of the analytical models delivers immense runtime savings and makes possible exploration of huge design spaces ($>10^9$ of configurations) in just a few seconds.

One of the directions in which the research is continued is the design of analytical models for heterogeneous CMPs. These systems incorporate different types of computing cores, including general-purpose, graphical and digital signal processors. Heterogeneous systems were shown to improve power efficiency of the computation and their design imposes novel challenging problems for architectural exploration.

V. Results

To demonstrate the functionality of the developed analytical framework, this section presents results of the exploration in the design space, comprised of about 10^9 configurations. The description of the design space is given in Fig. 3. Exploration is performed subject to the area (350mm^2) and power (130W) constraints with the objective to maximize CMP throughput in *instructions per cycle, IPC*. Three types of cores are considered, with the characteristics shown by Fig. 3b. This plot reproduces the square root dependency between the core area and IPC (Pollack's rule). The cache model is presented in Fig. 3c. The workload model mimics the behavior of SPEC2006 applications. It is given by the number of Memory references Per Instruction (MPI) and the dependency of miss rate on cache size (Fig. 3d).

Figure 4 shows the architecture and parameters of the best configuration discovered by the framework. Due to the fast analytical modeling and intelligent sensing of the design space using metaheuristics, the search

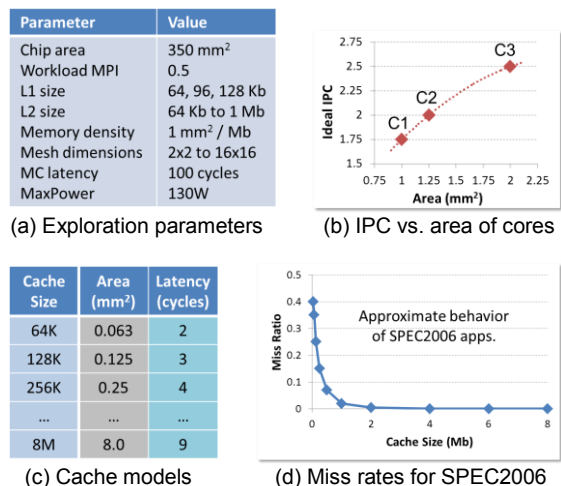


Figure 3. Models and parameters of exploration.

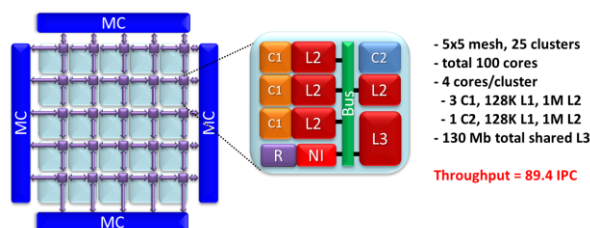


Figure 4. Best configuration for the design space in Fig. 3.

algorithm managed to discover the solution in *less than 10 seconds!* Even fast probabilistic simulation-based exhaustive exploration of the design space would take hundreds of years to finish, making the search prohibitively expensive.

These results emphasize the importance of the methodology developed in this thesis for accelerating the power-performance efficient design of the future many-core CMPs. The proposed analytical methods and the framework are extensible and highly flexible to incorporate novel architectural solutions and constraints.

VI. Acknowledgments

This research has been funded by a grant from Intel Corporation, FPI grant BES-2008-004612 and project CICYT TIN2007-66523.

VII. References

- [1] J. Flich, D. Bertozzi, *Designing Network-on-Chip Architectures in the Nanoscale Era*, CRC Press, 2010.
- [2] J. Howard et al., "A 48-Core IA-32 Processor in 45 nm CMOS Using On-Die Message-Passing and DVFS for Performance and Power Scaling," in *IEEE Solid-State Circuits*, vol. 46, no. 1, pp. 173-183, January 2011.
- [3] T. Oh, H. Lee, K. Lee, S. Cho, "An analytical model to study optimal area breakdown between cores and caches in a chip multiprocessor," in *ISVLSI*, 2009, pp. 181-186.
- [4] A. Cassidy, A. Andreou, "Beyond Amdahl's Law: An Objective Function That Links Multiprocessor Performance Gains to Delay and Energy," *IEEE Trans. on Computers*, vol. 61, no. 8, pp. 1110-1126, August 2012.
- [5] N. Nikitin, J. Cortadella, "A performance analytical model for Network-on-Chip with constant service time routers," in *ICCAD*, 2009, pp. 571-578.
- [6] N. Nikitin, J. de San Pedro, J. Carmona, J. Cortadella, "Analytical Performance Modeling of Hierarchical Interconnect Fabrics," in *NOCS*, 2012, pp. 107-114.

SPECTRAL FEATURE DETECTION FOR SPECTRUM SENSING

Author: Eva Lagunas, Thesis Advisor(s): Montse Nájjar

contact email: eva.lagunas@upc.edu

I. Introduction

In 2002, the Federal Communications Commission (FCC) proved two very important facts [1]: (i) the availability of unlicensed spectrum is getting scarce mainly due to the recent rapid growth of wireless devices and (ii) the licensed part of the radio spectrum is poorly utilized in the sense that many licensed bands are only used sporadically. The spectrum scarcity together with the inefficiency of the licensed spectrum has resulted in an innovative way of thinking known as Cognitive Radio (CR).

The idea of CR [2] is to solve the spectrum allocation problem by allowing spectrum sharing, i.e., allowing opportunistic unlicensed access to the unused licensed frequency bands insofar as the unlicensed users do not degrade the service of the original license holders. To protect the primary (licensed) systems from the opportunistic secondary users' interference, spectrum holes should be reliably identified. The identification procedure of available spectrum is commonly known as spectrum sensing. Spectrum sensing involves making observations of the radio frequency spectrum and reporting on the availability of unused spectrum for use by the CR users.

Recently, the idea of CR has evoked much enthusiasm. Particularly, there has been much work on designing sensing algorithms. There are several sensing methods proposed in the literature. Focussing on each narrow band, existing spectrum sensing techniques are widely categorized in two families: blind sensing and feature-based sensing techniques. One of the most popular blind detection strategy is energy detector (ED) [3]. However, ED is unable to discriminate between the sources of received energy.

On the other hand, the most famous feature-based method is the matched filter. If the full structure of the primary signal is known (together with time and carrier synchronization), the optimal detector is matched filter detector. Unfortunately, the complete knowledge of the primary signal is not usually available. If only some features of the primary signal are known, feature-based detectors such cyclostationary detector [4] are more suitable. A survey of the most common spectrum sensing techniques, both non-feature and feature-based detectors, has been published in [5].

The conventional spectrum sensing algorithms usually exploit two dimensions of the spectrum space: frequency and time. In other words, they look for bands of frequencies that are not being used at a particular time. Fortunately, there are other dimensions that need to be explored further for spectrum opportunity. With the recent developments of beamforming technology, a new dimension emerges: the angle dimension. If a primary user is transmitting in a specific direction, the secondary user can transmit in other directions without interfering on the primary user. Thus, the spatial diversity brings extra spectrum opportunities [6].

Here, a new spectral estimation procedure for monitoring the radio spectrum which exploits frequency, time and angle dimension is presented. The procedure is a feature-based method able to detect predetermined

spectral shape, providing at the same time an estimate of its power level, an estimate of its frequency location and an estimate of its angle of arrival. The specific spectral shape is called the candidate spectrum and gives name to the different methods.

II. System Model

The space-time-frequency spectrum sensing will be computed using multiple snapshots of measurements from a uniformly spaced linear array:

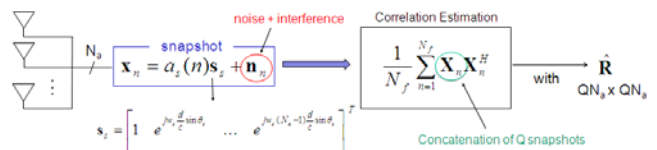


Figure 1. First stage of the receiver: Correlation estimation.

The objective is to determine the frequency ω_s and the angle θ_s , and an estimation of the received power γ . The proposed approach is based on a correlation matching procedure, changing the traditional single frequency scan to a spectral scan with a particular shape (called candidate spectral shape).

III. The Candidate Spectrum and Autocorrelation Matrix

A frequency scanning and an angle scanning is developed using the candidate spectral shape:

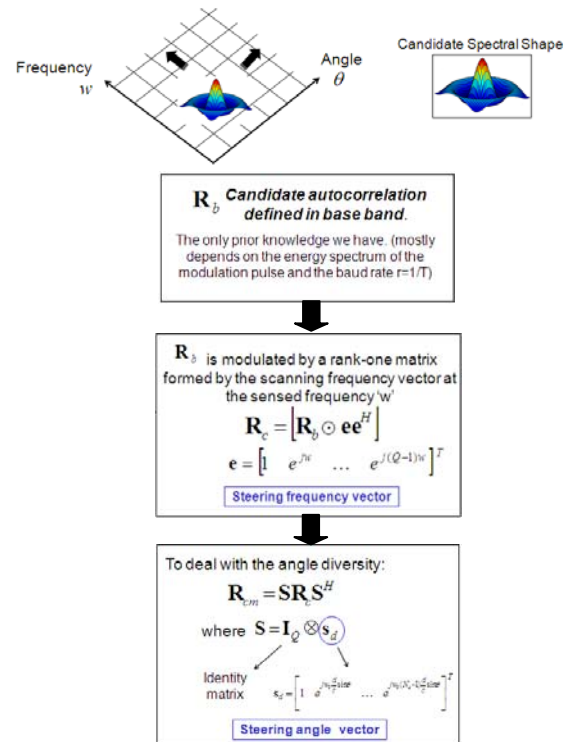


Figure 2. Generation of candidate correlation matrix.

IV. Candidate-based Spectrum Sensing

The proposed procedure is based on a spectral scan which reacts only when the candidate's spectral shape is present. Therefore, some similarity function is required to measure how much candidate spectrum power is contained in the given autocorrelation data matrix:

$$\min_{\gamma} \Psi(\hat{\underline{R}}, \gamma \underline{R}_{cm})$$

The different estimates result from the proper choice of the aforementioned similarity function can be decided in two groups: (1) similarity functions based on the distance between the two matrices and (2) similarity functions based on the positive definite character of the difference.

IV.A. Candidate-F

A detector based on the traditional Euclidean metric (Frobenius norm of the difference between matrices), can be directly applied to the current 2D scanning (CANDIDATE-F).

$$\min_{\gamma} \left| \hat{\underline{R}} - \gamma \underline{R}_{cm} \right|_F$$

However, this estimate does not preserve the positive definite property of the difference.

IV.B. Candidate-G

The second alternative is a detector based on the geodesic distance (CANDIDATE-G) that best suits the space generated by hermitian matrices. The set of autocorrelation matrices is a convex cone because they are hermitian and positive semidefinite matrices. Therefore, a more proper distance for the space generated by the semidefinite positive matrices is the geodesic distance.

$$\min_{\gamma} \left| \hat{\underline{R}} - \gamma \underline{R}_{cm} \right|_G$$

IV.C. Candidate-M

Finally, a third power level estimate (CANDIDATE-M) can be derived by forcing a positive definite difference between the data autocorrelation matrix and the candidate matrix.

$$\begin{aligned} & \max_{\gamma \geq 0} \gamma \\ & \text{s.t. } \hat{\underline{R}} - \gamma \underline{R}_{cm} \succ 0 \end{aligned}$$

V. Simulation Results

The general performance of the three candidate methods proposed before will be discussed in this section. The scenario for this study considers a desired user with binary phase shift keying (BPSK) using a rectangular pulse shape (with 4 samples per symbol) and an interference. For simplicity and as baseline, we assume that the interference is a pure tone. In practice, the interference signal is due to the presence of a secondary user, which is rarely going to use the same modulation or physical support as the primary user. The scenario characteristics have been summarized in Table 1. The data record for the following plots is 1000 snapshots and $Q=16$. The array is composed of 6 antennas with an antenna separation equal to $\lambda/2$ resulting into a total array length of 37.5cm. Fig. 3 shows the performance of the Candidate-F under the

proposed scenario. It can be observed that Candidate-F presents low resolution and significant leakage when interferences are present.

	Desired	Interference
Modulation	BPSK	Pure Tone
Frequency	2MHz	3MHz
DOA	30°	60°
SNR	10dB	10dB

Table 1. Scenario Characteristics

In Fig. 4(a) is shown the performance of Candidate-M, which provides a clear estimate of the frequency and angle location, and produces a power level of 8.74dB, which implies some bias. The interfering tone has disappeared due to the feature-based nature of the estimate.

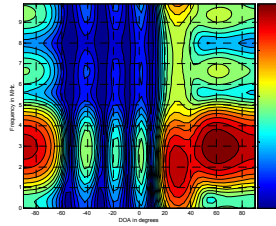


Figure 3. Contour lines of Candidate-F result.

Finally, the best power estimate in terms of resolution is given by Candidate-G which provides a power level of 9.99dB for the same scenario. The inverse of the geodesic distance is shown in Fig. 4(b). These plots show higher resolution compared with Candidate-M and an accurate estimation of the frequency and angle location.

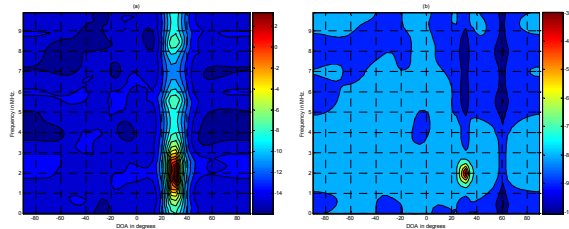


Figure 4. Contour lines: (a) Candidate-M, (b) Candidate-G.

VI. Acknowledgments

This work was partially supported by the Catalan Government (AGAUR) under grant 2009 SGR 891 and by the Spanish Ministry of Science and Innovation under project TEC2011-29006-C03-02 (GRE3N-LINK-MAC).

VII. References

- [1] Federal Communications Commission, "Tech. Report," *TR 02-155*, Nov 2002.
- [2] S. Haykin, "Cognitive Radio: brain-empowered wireless communications" *IEEE J. Sel. Areas in Commun.*, vol. 23, no. 2, pp. 201-220, 2005.
- [3] H. Urkowitz, "Energy Detection of Unknown Deterministic Signals", *Proc. IEEE*, vol. 55, pp. 523-531, Apr 1967.
- [4] W. Gardner, "Signal Interception: A Unifying Theoretical Framework for Feature Detection", *IEEE Trans. Commun.*, vol. 36, pp. 897-906, Aug 1988.
- [5] T. Yucek and H. Arslan, "A Survey of Spectrum Sensing Algorithms for Cognitive Radio Applications", *IEEE Commun. Surveys Tuts.*, vol. 11, no.1, pp. 116-130, 2009.
- [6] W. Wang and K.J. Ray Liu, "Advances in Cognitive Radio Networks: A Survey", *IEEE J. Sel. Topics Signal Process.*, vol. 5, pp. 5-23, 2011.

GNSS Array-based Acquisition: Theory and Implementation

Author: Javier Arribas Lázaro Thesis Advisor: Carles Fernández-Prades

contact email: jarribas@cttc.es

I. Introduction and Motivation

Global Navigation Satellite Systems (GNSS) is the general concept used to identify those systems that allow user positioning and timing based on a constellation of satellites. Specific GNSSs are the well-known American GPS, the Russian GLONASS or the forthcoming European Galileo. All those systems rely on the same principle: the user computes its position by means of measured distances between the receiver and the set of in-view satellites. These distances are calculated estimating the propagation time that transmitted signals take from each satellite to the receiver. Nowadays, GPS (often combined with an augmentation system) is used in a myriad of applications such as geodesy and surveying, Earth observation, piloted and autonomous aircraft landing, or distributed synchronization of radio communication links and electric power networks.

Radio Frequency Interferences (RFI) are widely recognized to be one of the most jeopardizing sources of accuracy degradation, and even denial-of-service, of GNSS receivers. This performance degradation is especially important in conventional receivers equipped with minimal or basic level of protection towards RFIs. A growing concern of this problem has appeared in recent times as reported in [1,2].

Focusing our attention on the GNSS receiver, it is known that signal acquisition has the lowest sensitivity of the whole receiver operations, and, consequently, it becomes the performance bottleneck in the presence of interfering signals [3]. A single-antenna receiver can make use of time and frequency diversity to mitigate interferences, even though the performance of these techniques is compromised in low Signal-to-Noise Ratio scenarios or in the presence of wideband interferences.

On the other hand, antenna arrays receivers can benefit from spatial-domain processing, and thus mitigate the effects of interfering signals. Spatial diversity has been traditionally applied to the signal tracking operation of GNSS receivers. However, initial tracking conditions depend on signal acquisition, and there are a number of scenarios in which the acquisition process can fail as stated before. Surprisingly, to the best of our knowledge, the application of antenna arrays to GNSS signal acquisition has not received much attention.

This Thesis pursues a twofold objective: on the one hand, it proposes novel array-based acquisition algorithms to protect the receiver from the interferences threat, and on the other hand, it demonstrates both their real-time implementation feasibility and their performance in realistic scenarios.

The main contributions and the possible applications of the developed technology in the industry are briefly discussed in this document. It is organized as follows: Section II introduces the proposed array-based signal processing solution to mitigate the RFIs effects in the acquisition stage and presents the performance simulations results, comparing it to the existing solutions. Section III presents the design and the implementation of a real-time GNSS array-based

receiver platform intended to be a proof-of-concept prototype of our solution, as a previous step towards a possible industrialization of the product. Moreover, in Section IV we present an open-source GNSS Software Defined Receiver (SDR) that works in real-time in a Personal Computer and contributes with several novel features.

II. Novel array-based acquisition algorithm for interference mitigation

We propose a statistical detection approach for the antenna array-based GNSS signal acquisition problem. We obtained a new GNSS detector algorithm which is able to mitigate temporally uncorrelated point source interferences even if the array is unstructured and moderately uncalibrated. The key feature is the capture of the statistical behavior of the interferences and other non-desirable signals, while exploiting the spatial dimension provided by antenna arrays. Figure 1 shows the array-based acquisition concept. The antenna array is connected to a multi-channel RF front-end and the baseband output is digitized using a multi-channel Analog-to-Digital Converter (ADC) board. The digital array baseband signal is processed directly by the proposed test function to acquire GNSS satellites. The result is compared to a threshold and a decision is made (the presence or the absence of a satellite signal).

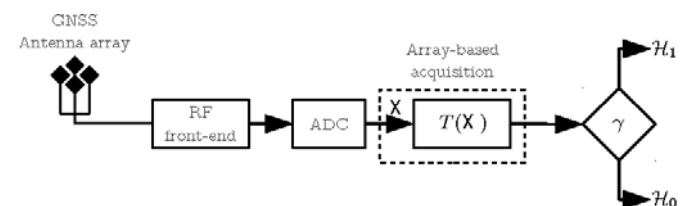


Figure 1 Array-based acquisition concept.

The obtained detector has constant false alarm rate property, which is highly valuable in a cold acquisition situation where there is neither information of the satellites' Direction Of Arrival (DOA), which prevents from applying spatial-based beamforming, nor the receiving signals power, that makes difficult to set an acquisition threshold. Using our detector, it is possible to fix a specific acquisition threshold value to obtain the maximum performance in a variety of radio electric scenarios. Theoretical expressions and simulations results show that the detector offers a superior interference protection in both wideband and narrowband interference cases. Figure 2 shows the performance obtained by simulations in a Galileo E1 acquisition scenario with the presence of an in-band wideband interference impinging into the array with an Interference-to-Noise density ratio (IN0) of 85 dB-Hz and random DOA. Results show that the proposed acquisition (so named GLRT colored) outperforms the existing solutions. We included in the comparison conventional acquisition techniques performed after DOA-driven beamformers, such as the Minimum Variance Distortionless Response (MVDR) beamformer, and blind null-steering beamformer approaches, such as the power minimization algorithm. In addition, the

performance upper bound obtained by the optimum detector was also plotted (known as *the clairvoyant detector*). The reader is referred to [4] for complete information on the developed algorithm.

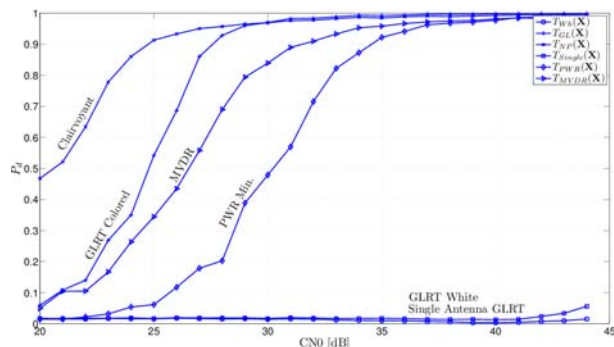


Figure 2 Galileo E1 acquisition detection probability (P_d) vs. satellite Carrier-to-Noise density ratio (CNO) in the presence of an interference for different algorithms, considering 20° of DOA error in the MVDR beamformer.

III. Proof-of-concept prototype

The implemented GNSS Smart Antenna proof-of-concept platform automatically adapts to the electromagnetic scenario and cleans the signals to be processed by a GNSS receiver, mitigating possible interferences to a great extent (including dynamic multi-jammer scenarios), and thus contributing to enhance the robustness, availability and reliability of the receiver, and hence the quality of the positioning/timing system. Figure 3 shows a possible case of use for time dissemination / distributed synchronization in power transport networks.

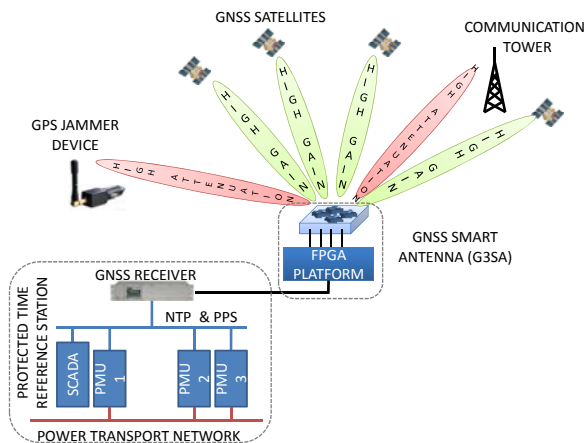


Figure 3 Example of use of the GNSS Smart Antenna for distributed synchronization.

Internally, the platform is composed of eight antenna chains that are downconverted in frequency by a RF front-end, translated into the digital domain and processed using the algorithms described in Section II, implemented using Field Programmable Gate Array (FPGA) technology. Those algorithms provide assistance to the GNSS receiver in two basic steps: *i) signal acquisition*, which consists of the detection of in-view satellites and, a coarse estimation of their synchronization parameters, and *ii) signal tracking*, that performs a fine tuning of the estimations and allows the computation of the navigation solution (thus obtaining position, velocity and time of the user's receiver). The information obtained by the algorithms is used to filter

the incoming signals, allocating more gain to the directions of arrival of satellite signals. The output is a spatially-filtered version of the incoming signal, in which the desired signals have been amplified while other nuisance signals such as interferences and multipath have been greatly attenuated. This signal can be brought back to the analog domain and upconverted to the system carrier frequency for its use by a wide range of legacy GPS receivers and legacy GPS-based synchronizers.



Figure 4 GNSS smart antenna proof-of-concept prototype.

In addition, the platform can be connected to a SDR receiver processing in real-time the spatially-filtered signal sample stream coming from the platform using a Gigabit Ethernet bus data link. In the last section we present a novel open source receiver that can be used tightly-coupled with this platform.

IV. GNSS-SDR: a real-time open-source GNSS Software Defined Receiver (SDR)

The proposed receiver targets multi-constellation/multi-frequency architectures, pursuing the goals of efficiency, modularity, interoperability, and flexibility demanded by user domains that require non-standard features, such as intermediate signals or data extraction and algorithms interchangeability. This makes possible rapid prototyping of specific receivers intended, for instance, to geodetic applications, observation of the ionospheric impact on navigation signals, GNSS reflectometry, signal quality monitoring, or carrier-phase based navigation techniques. In this context, we introduce an open-source, real-time GNSS software defined receiver (so-named GNSS-SDR) that contributes with several features such as the use of software design patterns and shared memory techniques to manage efficiently the data flow between receiver blocks, the use of hardware-accelerated instructions for time-consuming operations, and the availability to compile and run on multiple software platforms and hardware architectures. The source code and the documentation are available on-line in the GNSS-SDR project website www.gnss-sdr.org.

V. References

- [1] M. Thomas, "Global Navigation Space Systems: reliance and vulnerabilities". Tech. rep., The Royal Academy of Engineering, London, UK, 2011.
- [2] Federal Communications Commission (FCC), "LightSquared Technical Working Group final report", Tech rep., Washington DC, June 2011.
- [3] E.D. Kaplan, C. Hegarty, Understanding GPS. Principles and Applications, Second Edition, Artech House Publishers, Norwood, MA, 2005.
- [4] J. Arribas, GNSS Array-based Acquisition: Theory and Implementation, PhD Dissertation, Universitat Politècnica de Catalunya, June 2012.

Elastic transponders for optical direct detection OFDM systems based on the FHT

Author: Laia Nadal Reixats, Thesis Advisor(s): Michela Svaluto Moreolo and Gabrient Junyent

contact email: laia.nadal@cttc.es

I. Introduction

The rapid growing of IP traffic and the new emerging applications and services such as cloud computing and high quality IP services (VoIP, IPTV, etc.) require a high capacity optical backbone network. Operators main purpose is to find different ways to provide all these services in a cost-effective manner. Conventional fixed-grid and rigid-bandwidth wavelength division multiplexing networks lead to an inefficient utilization of bandwidth resources. In order to efficiently deal with the current and future demand, elastic optical networks have been proposed [1]. They introduce flexibility in the system and increase the overall spectral efficiency allowing network reconfigurability. Optical orthogonal frequency multiplexing (O-OFDM) is one of the key enabling technology for elastic optical networks which allows software defined optical transmission (SDOT). The transponders can be dynamically adapted depending on the traffic demand to different modulation formats using adaptively modulated O-OFDM (AMO-OFDM) [2] and achieving different bit rates [3]. In optical communications direct detection (DD) and coherent detection are two different optical implementations. The first one allows cost-effective optical transmitter and receiver architecture at expenses of receiver sensitivity and spectral efficiency. A real signal must be transmitted through the channel. Our purpose is to analyze DD OFDM based elastic optical systems enhancing the performance of the system in terms of bit error rate (BER). We evaluate the use of an alternative transform to the fast Fourier transform (FFT): the fast Hartley transform (FHT) [4] as it doesn't need the implementation of the Hermitian symmetry constraint (HS) required for real-valued FFT based O-OFDM systems. Moreover, we propose the design of low complexity (LC) bit rate variable transponders with peak-to-average power ratio (PAPR) capabilities. The PAPR is a major problem of OFDM systems that can lead to large distortions of the optical signal due to the fiber and nonlinearities of system devices such as Mach-Zehnder modulator (MZM), digital-to-analog converter (DAC), analog-to-digital converter (ADC). Hence, it must be mitigated.

II. DD O-OFDM for software-defined optical transmission

Figure 1 shows a DD O-OFDM system where the transponder digital signal processing (DSP) can be adapted or reconfigured by software depending on the traffic demand and the available resources. As the FHT is implemented, real constellations such as Binary Phase-Shift Keying (BPSK) or Pulse Amplitude-Modulation (PAM) must be used in order to transmit real data. The subcarriers can be modulated with different formats for varying the bit rate with a fine step. For an electrical signal bandwidth of 10GHz and using BPSK, 4PAM and 8PAM formats, bit rates from 10Gbits/s to 30Gbits/s can be obtained. In the particular case of Figure 1 the bit rate is 23Gbits/s as 20% of the subcarriers are modulated with BPSK, 30% with 4PAM

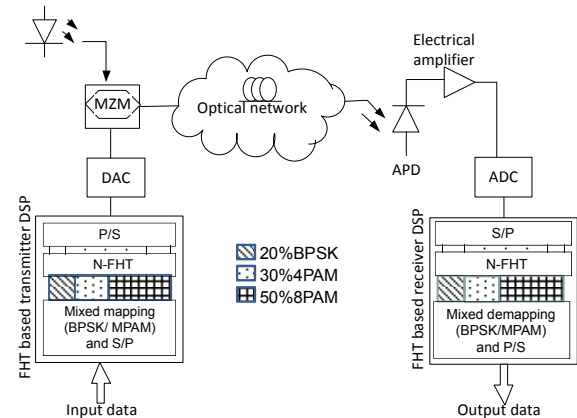


Figure 1. Example of bit rate variable DD O-OFDM system based on the FHT.

and 50% with 8PAM. The OFDM signal is symmetrically clipped and digital to analog converted. It is then modulated with a MZM, sent through the optical channel and photodetected. Finally, in order to reconstruct the original signal it is converted to digital domain and processed in the receiver DSP.

Symmetrically clipping is performed to mitigate the PAPR of the signal. However, it causes signal distortion and results in clipping noise which degrades the system performance. The signal is clipped at a fixed clipping level, which is related to the allowed maximum amplitude level of the signal. Increasing the value of the clipping level reduces the clipping noise at expenses of the power efficiency as it is demonstrated in [3].

Additionally, the limited bit resolution of the converters introduces quantization noise to the system. Our purpose is to mitigate the PAPR, the quantization noise and the clipping noise in order to enhance the system performance in terms of BER and power efficiency.

III. Proposed solution and simulation results

III.A. Low complexity PAPR reduction techniques based on the FHT

Different distortionless PAPR reduction techniques are analyzed in [5] when the FHT is used. Applying these techniques implies the use of additional transform blocks in order to create different signal representations of the original signal and transmit the one with lower PAPR.

PAPR reduction	1 FHT	2 FHT	3FHT	4FHT
SLM	-	1.5 dB	-	2.4 dB
Interleaver	-	1.5 dB	-	2.4 dB
PTSadj	-	0.7 dB	-	2.6 dB
PTSrand	-	1.5 dB	2.4 dB	3.1 dB
LC-SLM	1.5 dB	2.4 dB	-	-
LC-PTSadj	0.7 dB	2.6 dB	-	-
LC-PTSrand	1.5 dB	3.1 dB	-	-

Table 1. PAPR reduction comparison varying the number of FHT blocks in transmission.

Selective mapping (SLM), interleaving and partial transmit sequence with adjacent (PTSadj) and random partitions (PTSrand) are distortionless techniques used to reduce the PAPR of the OFDM signals. In our work, we have proposed a LC scheme that can be used with all these techniques halving the required number of FHT blocks. Thanks to the properties of the FHT we can parallel process two different signal representations with a single FHT [3].

Table 1 shows the PAPR reduction at a complementary cumulative distribution function (CCDF) of 0.1% applying and without applying the proposed PAPR reduction techniques in the system of Figure 1. It is seen that the highest reduction is obtained when LC-PTSrand or standard PTSrand are applied. LC-SLM achieves a PAPR reduction of 1.5 dB with a single FHT block.

III.B. System performance

We analyze the performance of the proposed bit rate variable transponder in additive white Gaussian noise (AWGN) channel for a fixed clipping level of 7 dB [3].

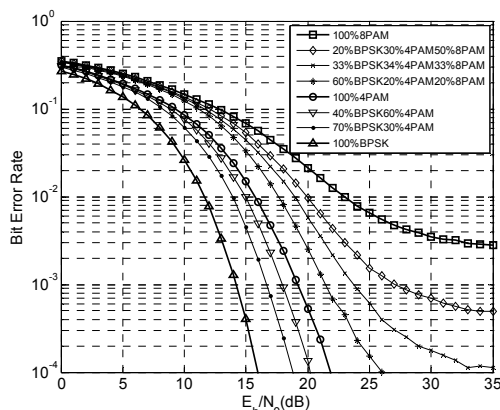


Figure 2. BER performance of adaptive DC biased O-OFDM system based on the FHT.

Figure 2 shows that a target BER of 10^{-3} cannot be ensured when a high percentage of the subcarriers are modulated with 8PAM due to the clipping noise. Therefore, a higher clipping level must be fixed in order to transmit all the possible formats that the transponder supports.

In order to mitigate the system impairments, we propose to introduce LC schemes in the analyzed software defined transponders without using additional transform blocks. Figure 3 shows the BER performance of the system of Figure 1 varying the clipping level at fixed receiver sensitivity. The optical channel is replaced by a variable optical attenuator (VOA) [6]. Different DAC bit resolutions are considered in order to take into account the quantization noise. Applying the LC-SLM scheme the quantization and clipping noise are mitigated. Moreover, when the proposed technique is applied, lower values of clipping level can be used for achieving the same BER performance as in the case of not using PAPR reduction techniques. Therefore, the power efficiency is enhanced.

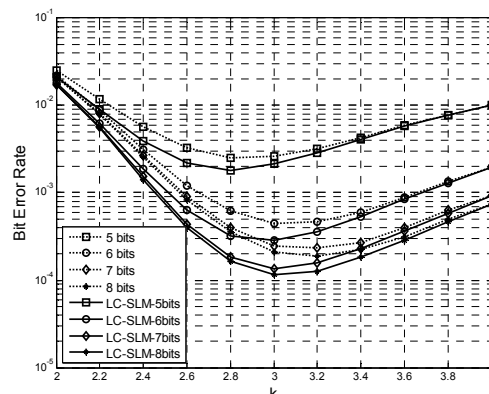


Figure 3. BER performance versus clipping level k (in lineal scale) at fixed receiver sensitivity, for 100% of subcarriers modulated with 8PAM format and 256 subcarriers with and without LC-SLM technique.

For example with a clipping level of $k=2.45$ (corresponding to 7.7 dB) the modulation format supported by the different subcarriers can be arbitrary varied by software up to uniform bit loading with 8PAM ensuring a target BER of 10^{-3} .

IV. Conclusions

We have proposed cost effective adaptive transponders with LC PAPR reduction capabilities to mitigate the impairments that arise in DD OFDM based elastic optical systems. The use of the FHT allows simplifying the DSP. With adaptive transponders, variable bit rates can be supported depending on the traffic demand. The spectral and power efficiency is enhanced and the available resources of the network are optimized.

V. Acknowledgments

This work was funded by the MICINN (Science and Innovation Ministry of Spain) through the project DORADO (TEC2009-07995) and the FPI research scholarship grant BES-2010-031072.

VI. References

- [1] M. Jinno, et al, "Distance-adaptive spectrum resource allocation in spectrumsliced elastic optical path" IEEE Comm. Magazine, vol.48, no.8, pp.138-145, 2010.
- [2] J.M.Tang, K.A.Shore, "Maximizing the Transmission Performance of Adaptively Modulated Optical OFDM Signals in Multimode-Fiber Links by Optimizing Analog-to-Digital Converters," J. of Light. Tech., vol.25, no.3, pp.787-798, 2007.
- [3] L.Nadal, M.Svaluto Moreolo, J. M. Fàbrega, G. Junyent, "Low Complexity Bit Rate Variable Transponders Based on Optical OFDM with PAPR Reduction Capabilities", in Proc. In Conf.on Netw. and Optical Comm., 2012.
- [4] M. Svaluto Moreolo, R. Muñoz and G. Junyent, "Novel Power Efficient Optical OFDM Based on Hartley Transform for Intensity-Modulated Direct-Detection Systems", J. Lightw. Technol., pp. 798 -805, 2010.
- [5] L. Nadal, M. Svaluto Moreolo, J. M. Fàbrega and G. Junyent, "Comparison of Peak Power Reduction Techniques in Optical OFDM Systems Based on FFT and FHT", in Proc. Int. Conf. on Transp. Opt. Netw., 2011.
- [6] L. Nadal, M. Svaluto Moreolo, J. M. Fàbrega and G. Junyent, "Clipping and quantization noise mitigation in intensity-modulated direct detection O-OFDM systems based on the FHT", in Proc. Int. Conf. on Transp. Opt. Netw., 2012.

Characterization and design of coherent optical OFDM transmission systems based on Hartley Transform

Author: Marcin Chochoł, Thesis Advisor(s): Josep M. Fàbrega, Gabriel Junyent
contact email: mchochol@cttc.es

I. Introduction

Orthogonal frequency division multiplexing (OFDM) has emerged in the optical communications field because of its promising capabilities for transmission link reconfiguration and its unique flexibility [1]. Since the OFDM-based transceivers have a strong digital signal processing (DSP), they can be easily reconfigured (even defined by software) and their implementation becomes straightforward and repeatable, with reduced hardware tuning processes. Among the existing optical OFDM techniques, those combining coherent detection with digital signal processing are the most promising to cope with the network requirements while improving spectral efficiency, as they can fully recover a signal in phase, amplitude and polarization [1].

However, coherent optical OFDM systems still are quite sensitive to the system non-linearities, related to the peak-to-average power ratio (PAPR) of the signal [2]. Also, the phase noise related to the optical sources is a critical parameter, which is mitigated by means of employing low linewidth lasers in combination with enhanced DSP. Furthermore, their implementation is still complex, not only in terms of the specific devices needed, but also in terms of the DSP algorithms used.

Hence, the objective of the present paper is to propose a new alternative solution that copes with OFDM advantages while simplifying DSP and hardware. Additionally it solves this critical issue regarding high PAPR. To cope with that, a DSP based on Fast Hartley Transform (FHT) is proposed, as it has been demonstrated to be more efficient than those based in the Fourier transform [3]. Also, it is proposed to modulate the optical phase with the FHT-based OFDM signal at the transmitter side [4]. So, it is delivering a constant output power with extremely low PAPR. Furthermore, the optoelectronic front-end at the transmitter gets reduced to a laser and a simple phase modulator.

In addition, the potential deployment of transceivers based on the proposed transmission system is assessed by means of simulations for two scenarios: a metropolitan transport network of about 100km reach, and an access network of less than 50km reach.

II. System description

The proposed transmission scheme is given on Figure 1. In general, the idea of OFDM scheme is to transmit a data bit rate on several subcarriers at lower rate. To afford this, first, the data are parallelized and mapped into real binary phase shift keying (BPSK) symbols. A training symbol sequence is then inserted for using it as a reference for the equalization process at the receiver side. Next, OFDM modulation applying self-inverse real FHT (IFHT) and serialization are performed. Next, the analog base-band OFDM signal is fed into the optoelectronic front-end. Here, electrical OFDM signal drives phase modulator (PM) properly excited by a laser. Optically modulated signal in phase is then transmitted over the optical channel and detected at receiver. Please note that, unlike the Fourier transform related DSP, here no Hermitian symmetry is needed for generating a real (non-complex) output. So, BPSK signal mapping is allowed for obtaining spectral efficiencies near 1 b/s/Hz.

At receiver side, a coherent detection is performed. This means that an incoming optical OFDM signal interferes with local oscillator (LO) signal. Thanks to the combination of a 90° optical hybrid and photo-detectors, signal is downconverted while translating it to the electrical domain. LO laser is here frequency locked to the received optical signal. The resulting complex signals on I and Q branches, are then digitized at analog-to-digital converter (ADC) and fed into the DSP block. Here, carrier recovery is executed. Subsequently, the argument is retrieved featuring electrical phase demodulation. The resulting samples are parallelized and the OFDM signal is demodulated using FHT. Finally, the training symbols are removed and equalization applied. Then, demapping and serialization of incoming symbols are conducted resulting in the data reconstruction.

A more detailed system description, modeling and optimization can be found in [5].

Although, the scheme of an optical OFDM system with constant envelope is reviewed, some facts related to its practical implementation are worth to be noted.

First, a tunable laser can be used for dynamically adapting the optical carrier frequency. This feature becomes especially relevant when using the proposed intradyne detection, as no optical filters are needed at

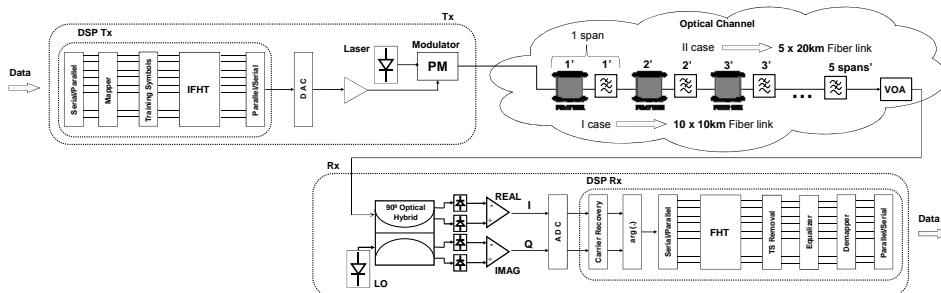


Figure 1. Transmission scheme for testing the filter's cascading effects in a metro network environment.

the receiver. So, for each channel the central wavelength corresponds to the one provided by the local laser. The transceiver can be tuned from one channel to another by only modifying the wavelength of the local laser. Therefore, the transceivers could be reconfigured if needed.

One of the main properties of the proposed transmission system is that the phase noise only affects the central OFDM carriers of the transmitted/received signal [4]. So, if these subcarriers are suppressed, the effects of lasers phase noise are mitigated without any specific digital processing. Nevertheless, subcarriers suppression leads to an increase of the overall signal overhead (6.3% per 1dB penalty at linewidth of 12MHz).

Since the changes in the state of polarization of the optical signals are expected to be very slow in a controlled environment, they are not taken into account in the scheme of Fig. 1 for the sake of simplicity. Nevertheless a dual-polarization receiver configuration can be used for a polarization insensitive detection with almost no changes in the expected performances. These optoelectronic front-ends with polarization diversity are commercially available, as they match with the OIF 100G implementation agreement.

III. Case studies

Two case study applications for the system proposed are analyzed by means of simulations. The first is a flexible metropolitan area network of up to 100km, on which the traffic is aggregated/dropped by means of wavelength division multiplexing [6]. The second studies the options for deploying a decomposed radio access network over an optical access network [7].

Regarding the first (Fig.1), effects while cascading optical filters are investigated. As a small bandwidth granularity will be allowed in the new flexible grid on which the ITU-T works, the cases are studied for a system featuring a standard data rate of 10Gb/s, which occupies a total bandwidth of 10GHz. The optical filters are modeled as low-pass equivalent Gaussian. First a back-to-back (no fiber) case is investigated. Simulations show a 3dB sensitivity penalty after a single filter of only 6.8GHz (68% of the signal bandwidth). For this case, 10 filters of bandwidth 21.6GHz can be cascaded for a 3dB penalty. The cases including fiber spans between filters are also analyzed for distances up to 100km. Precisely, inserting 10km spans, a maximum of 7 filters (with 26GHz bandwidth) could be cascaded for a 3dB power penalty. When inserting 20km spans, the 3dB penalty point has been found after 3 filters of 15.4GHz.

Another relevant case study is their use for radio access network (RAN) signals delivery by means of a WDM overlay in deployed optical access networks. Precisely, it is proposed to reuse the deployed infrastructure by overlaying a decomposed radio access network by means of WDM, avoiding interference with PON signals. So, a distribution based on exclusive wavelengths per each pair of radio resource management (RRM) units and remote radio units (RRU) can be achieved, providing a virtual private network connection from the central office to each radio unit. As shown in Fig.2, C-band (1530-1565nm) is used, avoiding interferences and crosstalk from/to the fixed network users. In order to cope with that while minimizing the power budget impact onto the performance of legacy equipment, a transceiver based on the transmission system described in section II is

used. Thanks to it, the losses introduced in the path of deployed infrastructure are reduced to the range of 0.04-3dB and the decomposed RAN can be massively deployed in urban environments while ensuring the compatibility with standard PONs and achieving narrow channel spacings (11.6GHz per 11.4Gb/s gross data rate). For the case of a practical implementation using CPRI, simulations show that for TDM-PON path losses of only 0.96dB, a maximum of 188 RRUs can be served at the same time, together with the PON customers and within a reach of 23km.

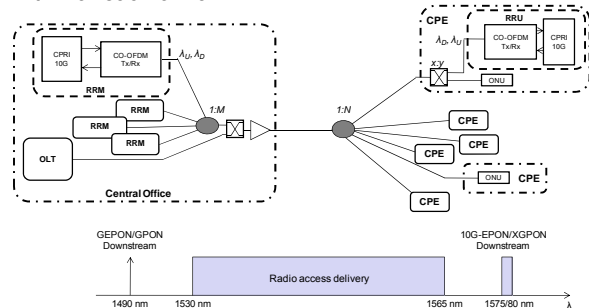


Figure 2. Network scheme and wavelength plan for the RAN signals delivery over deployed access network infrastructure.

IV. Conclusion

A novel coherent optical OFDM transmission system is proposed and discussed. As it is based on the phase modulation of the optical field, it features reduced PAPR and an improved laser linewidth tolerance. Furthermore, it is implemented using the Hartley transform, simplifying the associated digital signal processing.

Two examples of a practical use are analyzed by means of simulations. The first consists on a metropolitan area network of up to 100km, where concatenation of add/drop filters over the transmission path shows to have a trade-off between no. of channels and span length between filters. The second is for radio access signals delivery over deployed optical access infrastructure. For this last case, the proposed system exhibits a narrow channel spacing, while reducing losses introduced in the access equipment path.

The work reported in this paper was fully supported by the project DORADO (TEC2009-07995) and grant PTQ-11-04805, both sponsored by Spanish MICINN.

V. References

- [1] W. Shieh et. al, *OFDM for Optical Communications*, Elsevier, 2010.
- [2] S.L. Jansen et al, "Coherent Optical 25.8Gb/s OFDM Transmission Over 4160km SSMF," *J. Lightwave Technol.*, vol. 26, no. 1, Jan. 2008.
- [3] M. Svaluto Moreolo et. al, "Novel Power Efficient Optical OFDM Based on Hartley Transform for IM-DD Systems," *J. Lightwave Technol.*, vol. 28, no. 5, March 2010
- [4] J.M. Fàbrega, et. al, "Constant Envelope Coherent Optical OFDM based on Hartley Transform," in *Proc. Int. Conf. on Transparent Optical Networks (ICTON) 2011*, paper We.A.1.5.
- [5] M. Chochol, et. al, "Novel Power Efficient Optical OFDM Based on Hartley Transform for IM-DD Systems," in *Proc. Network and Optical Comm. 2012*, paper
- [6] M. Chochol, et. al, "Optical Filter Cascading Effects in a PM CO-OFDM system based on Hartley Transform," in *Proc. ICTON 2012*, paper We.P.4
- [7] J. M. Fàbrega, et. al, "WDM overlay of distributed base stations in deployed PONs using CO-OFDM transceivers," in *Proc. ICTON 2012*, paper We.D3.3

MULTI-ANTENNA DIVERSITY TECHNIQUES FOR FBMC/OQAM SYSTEMS IN WIRELESS COMMUNICATIONS

Author: Màrius Caus López, Thesis Advisor: Ana I. Pérez Neira
 contact email: *marius.caus@upc.edu*, *ana.isabel.perez@upc.edu*

I. Motivation

Due to the popularity of wireless communications the users' demand on multimedia content combined with mobility is increasing. To satisfy the ever increasing throughput goals the state-of-the-art cellular systems such as: Worldwide Interoperability for Microwave Access (WiMAX) and third generation partnership project long term evolution (3GPP-LTE) have considered the utilization of multicarrier modulations and multiple-input-multiple-output (MIMO) techniques in the physical layer specifications. The general trend is to employ the orthogonal frequency division multiplexing (OFDM) technique, which is the most prominent multicarrier modulation. The use of OFDM is widespread because efficiently combats the multipath fading by partitioning the channel bandwidth into several narrowband subchannels. Besides the OFDM technique enables transforming the end-to-end system model as set of parallel flat fading channels, which drastically simplifies the MIMO applicability to multicarrier modulations. Actually the same MIMO techniques studied in single carrier communications can be straightforwardly tailored to OFDM.

However there are some studies, such as [1], that reveal that OFDM is outperformed in several areas by a more advanced technique called filter bank based multicarrier (FBMC). The first improvement is that unlike OFDM, FBMC does not need to transmit redundancy in the form of a cyclic prefix (CP). Then, the spectral efficiency can be increased. The second advantage has to do with the fact that the subcarrier signals, which stand for the low-rate signals transmitted among the narrowband subchannels, are not shaped with a rectangular pulse. By contrast it is possible to employ well-frequency localized pulses that decay much faster in the frequency domain than the rectangular window. As a result, FBMC systems are more robust to time and frequency misalignments and narrowband interferences than OFDM. To illustrate this we have depicted in Fig. 1 the power spectral density of one subcarrier signal centered at the tenth subchannel. The FBMC potentials are of paramount importance in the multiple access channel (MAC) where several users communicate with a base station (BS). If perfect synchronization between the users and the BS cannot be achieved then it is customary to leave empty some subcarriers between users. This measure allows the BS to successfully detect the information transmitted by different users. Note that this entails that some subcarriers remain unused. Since the frequency localization is better in FBMC than it is in OFDM the number of subcarriers that are used as a guard can be substantially reduced.

In light of this discussion it seems reasonable to think that a better performance with respect to OFDM can be achieved if the FBMC system is extended to accommodate multi-antenna configurations. However, the MIMO applicability to FBMC systems is not a straightforward task. In fact this is an active research area that has not been fully explored yet. In order to

make progress in this direction our aim is to study how to take advantage of spatial diversity in FBMC.

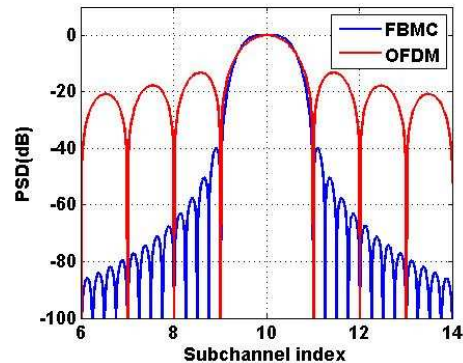


Figure 1. Power spectral density of one subcarrier in OFDM and FBMC.

II. Subband processing

Under ideal propagation conditions the FBMC systems are capable of recovering a delayed version of the information conveyed on each subcarrier. This implies that the waveforms used to multiplex the low-rate signals both in time and frequency domain are indeed an orthogonal basis. It is worth mentioning that the orthogonality is only satisfied in the real field. For this reason the symbols are modulated according to the offset quadrature amplitude modulation (OQAM) scheme.

In wireless communications the transmitted signal is degraded by multipath fading. Then it is deemed necessary to equalize the channel to restore the orthogonality. Since the subcarrier signals are well-confined in the frequency plane the equalization can be done on a per-subcarrier basis. If the channel frequency response (CFR) can be modeled flat in the subcarrier pass band region, then the design of the equalization stage is straightforward. In this sense, the same single tap linear processing used in OFDM succeeds in restoring the orthogonality of FBMC. Note that the flatness assumption strongly relies on the coherence bandwidth of the channel and the subcarrier spacing. It must be mentioned that in some occasions the selectivity of the channel imposes a minimum number of carriers that is too high, thus impractical. Then, the OFDM solution cannot be directly applied to FBMC/OQAM. Focusing in this more challenging scenario, several authors have proposed different solutions. Most of them can be found in the deliverables of the European project Phydys [2].

To highlight that the flatness assumption may not always be satisfied, we have plotted in Fig. 2 the channel frequency response of two different scenarios. Obviously when the propagation conditions obey the ITU-VehB channel model the flatness assumption will no longer be true. Although this is an extreme case, the cellular systems with large inter-site distances may have the same problem.

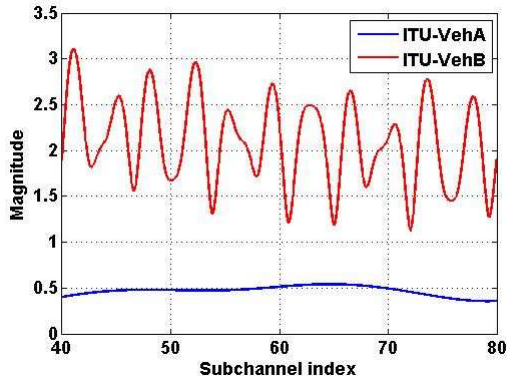


Figure 2. Magnitude of the channel frequency response of ITU-Veh.A and ITU-VehB channel models.

III. MIMO transmit and receive processing

If channel state information (CSI) is perfectly known at both ends of the link, then the transmitter and the receiver can be adapted to the channel conditions, which enable making an efficient use of the spectrum. Keeping this in mind we have proposed a new scheme that combines the MIMO scheme with the FBMC concept. The block diagram is depicted in Fig. 3. While the synthesis filter bank (SFB) is in charge of frequency multiplexing the low-rate signals the analysis filter bank (AFB) demodulates the received signal to recover the data transmitted on each subcarrier. Note that several replicas of the symbols are transmitted over all the antennas by feeding the symbols to the precoding stage. At the receiver the outputs of the AFB are combined by means of the equalization stage.

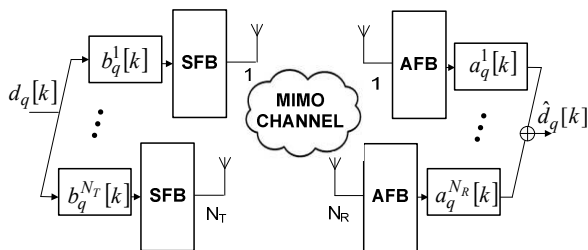


Figure 3. Transmultiplexer block diagram.

The jointly design of the transmit filters $b_q^i[k]$ ($i=1, \dots, N_T$) and the receive filters $a_q^j[k]$ ($j=1, \dots, N_R$) is definitely challenging. The subindex q accounts for the subcarrier index. The total number of subcarriers in which the band is partitioned is usually a power of two. Typical values are 512 and 1024. In the literature we can find several criteria to devise multi-antenna diversity techniques. In this work we have selected the maximization of the signal to interference plus noise ratio (SINR). This figure of merit is directly related to the bit error rate (BER) and the system capacity.

When no assumption about the flatness of the channel is made the system takes into account that the signal transmitted on a given subcarrier may leak through the adjacent subcarriers. Under this assumption we have devised in [3] a new subband processing that enables achieving diversity gains in FBMC systems, which is one of limitations of the existing techniques. Although the proposed solution is not optimal it provides

satisfactory results in terms of BER as the next section illustrates.

IV. Numerical results

In this section FBMC and OFDM are compared in terms of BER. As a benchmark we have compared the technique of [3] with the OFDM solution devised in [4]. As for the system parameters we have considered a system that partitions the 10MHz of the transmission bandwidth into $M=512$ subcarriers. The frequency sampling is set to 11.2MHz and the subcarrier spacing is equal to 21.88 KHz. The power delay profile of the channel obeys the ITU-VehB model.

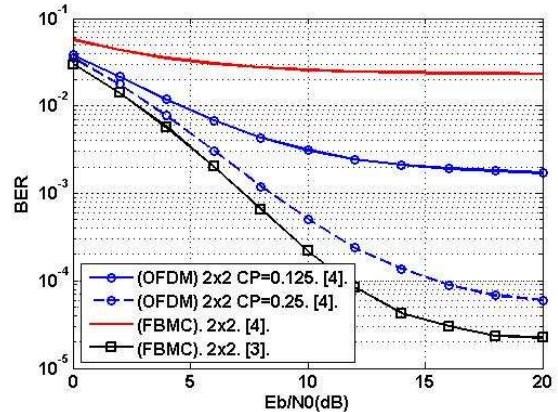


Figure 4. BER against E_b/N_0 for MIMO 2x2. The channel obeys the ITU-VehB model. The symbols are 16QAM.

In this scenario the channel is highly frequency selective and for this reason the error is pushed down in OFDM by increasing the CP length. If the CP length was higher than 25% of the block, then the performance would be improved. However, the spectral efficiency might be unacceptable. As Fig. 4 shows the solution proposed in [3] is able to deal with the multipath fading without transmitting redundancy. That is, FBMC operates on a higher information rate. In addition the BER is substantially reduced in comparison to OFDM. It is worth emphasizing that when the technique of [4] is directly applied to FBMC, the BER curve exhibits an error floor. The reason is because the flat fading condition is not satisfied.

V. Acknowledgments

The research leading to these results has received funding from the Spanish Ministry of Science and Innovation under projects TEC2011-29006-C03-02 (GRE3N-LINKMAC), TEC2008-06327-C03-01 and the Catalan Government (2009SGR0891).

VI. References

- [1] Farhang-Boroujeny, B.; "OFDM Versus Filter Bank Multicarrier," *Signal Processing Magazine, IEEE*, vol.28, no.3, pp.92-112, May 2011.
- [2] "Physical layer for dynamic access and cognitive radio," European Project ICT 211887, PHYDYAS, <http://www.ictphydyas.org>.
- [3] Caus, M.; Perez-Neira.; "Transmitter-Receiver Designs for Highly Frequency Selective Channels in MIMO FBMC Systems," *Signal Processing, IEEE Transactions on*, status: Accepted with Mandatory Revisions.
- [4] Kai-Kit Wong; Cheng, R.S.-K.; Letaief, K.B.; Murch, R.D.; "Adaptive antennas at the mobile and base stations in an OFDM/TDMA system," *Communications, IEEE Transactions on*, vol.49, no.1, pp.195-206, Jan 2001.

On the resource abstraction, partitioning and composition for virtual GMPLS-controlled multi-layer optical networks

Author: Ricard Vilalta, Thesis Advisor: Raül Muñoz (CTTC)

contact email: ricard.vilalta@cttc.es

I. Introduction

In the last years, virtualization of optical networks is receiving a lot of attention by network infrastructure providers in order to support dynamic provisioning of dedicated networks over the same network infrastructure. Optical network virtualization technologies allow the partitioning/aggregation of the network infrastructure (i.e., physical optical nodes and links) into independent virtual resources, where each virtual resource has the same functionality as the physical resource. The composition of these virtual resources allows deploying multiple Virtual Optical Networks (VONs). The deployment of dynamic infrastructure services to build ad-hoc VON services is known as infrastructure as a service (IaaS), and allows supporting the heterogeneous and stringent network infrastructure requirements of the emerging bandwidth-hungry and dynamic applications such as high-definition video streaming (e.g., telepresence, television, remote surgery, etc.), and cloud computing (e.g., real-time data backup, remote desktop, etc.).

Network service providers can request, on a per-need basis, a dedicated VON for each application and have full control over it. In order to provide the required independent and full control functionalities (i.e., optical connection provisioning, traffic engineering, protection/restoration, etc.), a VON must be composed of not only a virtual transport plane (i.e., a set of virtual optical switches interconnected by virtual optical links) but also of a virtual control plane. A virtual GMPLS control plane is a distributed entity composed of Virtual Connection Controllers (VCC), one VCC per virtual optical switch, executing several collaborative processes, and a Data Communication Network (DCN) based on virtual IP Control Channels (IPCC) to allow the exchange of control messages between the VCCs.

The first objective of the presented PhD Thesis is the design and experimental evaluation in the ADRENALINE Testbed of a VON Resource Broker for dynamic GMPLS-controlled WSON infrastructure services, whose task is to dynamically deploy GMPLS-controlled VONs from service provider requests[1][2]. To the best of our knowledge, all works dealing with VON composition are focused on the allocation of virtual transport resources, (i.e., optical switches and links), but do not consider the allocation of virtual control resources (i.e., GMPLS controllers and IPCC) to dynamically configure and set-up independent instances of GMPLS control plane for each requested VON. In our approach, the service provider becomes a virtual operator, having complete access to the configuration of the protocol parameters of the virtual control plane processes. For example, a VON operator may consider its own and independent routing policies within its virtual network.

The second objective of the PhD Thesis is the design of architecture for virtual MPLS-TP networks over WSON. With this purpose, the PhD Thesis also

focuses on the design and development of an MPLS-TP/WSON node [3] which has been deployed for the proposed virtual MPLS-TP over virtual WSON. There also appears the necessity to provide resource management techniques and algorithms for optimal usage of this physical infrastructure.

II. Virtual Optical Network Resource Broker

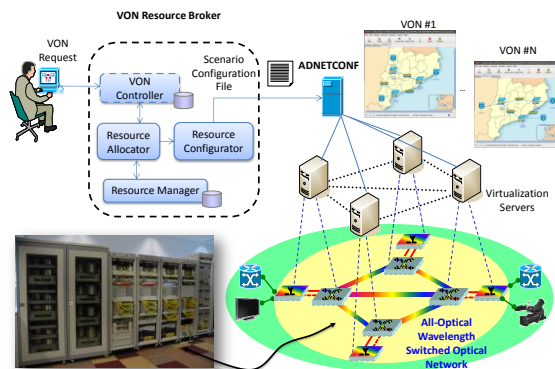


Figure 1. VON Resource Broker Architecture.

Fig. 1 describes the proposed architecture for a VON Resource Manager, which is responsible for deploying on-demand GMPLS-controlled VONs. The four main components are described as follows.

The Resource Manager handles both the virtual control and transport resources. As for the virtual control resources, it manages the available IP subnetworks that shall be used to establish the virtual IPCC to later deploy dedicated DCN for each virtual transport plane. Transport plane resources are described as optical links and switches. Each optical switch has a determined number of input and output ports and a maximum number of partitions are feasible. The specific partitioning of an optical switch is performed dynamically, based on the requirements of the requested VON. Each optical link stores the information about the edge optical switches the link is connected to, the number of supported wavelengths and their identifiers, as well as any link parameter (i.e. optical impairments). The partitioning of an optical link is on a wavelength granularity basis [5].

The VON Controller accepts incoming TCP sessions, which include VON requests, and handles these requests asynchronously and dynamically. Once the VON identifier, which is a unique identifier per each VON, is assigned, the VON controller triggers the resource allocator in order to process the VON request, which consists on the allocation of the new VON, the modification of resources assigned to an existing VON or the releasing of the resources in case a VON is torn down. A VON request is modeled as a graph that describes a set of virtual optical switches and links for the virtual transport plane, specifying for each one the number of requested input and output optical ports, and the number of wavelengths respectively. The VON

request also includes some requirements for the virtual control plane, such as the needed capacities for the virtual GMPLS controllers, or the configuration values for the control processes of the virtual GMPLS controllers, which can be later modified by the service provider.

The resource allocator assigns the virtual transport and control resources to the requested VON. For the virtual control plane, it allocates the virtual GMPLS controllers, and assigns the GMPLS router address. It also assigns IP addresses and GRE tunnels for the required IPCC. For the virtual transport plane, the target is to assign the requested number of available wavelengths (N) for each virtual optical link of the requested VON. The algorithms which run on the core of the resource allocator are a central objective of the presented PhD Thesis. Some simple wavelength allocation algorithms have been studied (e.g., First-Fit Random, WC First-Fit, WC Random) [4], and results are provided in Section 3.

The resource configurator generates the virtual transport and control plane configuration XML file, which describes a VON scenario model that can be set up, modified or torn down by means of ADRENALINE Network Configurator (ADNETCONF), which is a software tool in charge of scenario model management in ADRENALINE Testbed.

III. Experimental Results

The experimental demonstration consists in validating the VON Resource Broker and Composer architecture by requesting different VONs to be deployed on the ADRENALINE Testbed. We also provide simulation results of the performance of different VON Resource Allocation algorithms in an European Optical Network (EON) scenario.

The ADRENALINE Testbed is a GMPLS-based Intelligent Optical Network composed of an all-optical WSON with 2 ROADMs and 2 OXCs providing reconfigurable (in space and in frequency) end-to-end lightpaths, deploying a total of 610 km of G.652 and G.655 optical fiber, with six DWDM wavelengths per optical link. Each optical node is also equipped with a virtualization server (i.e., physical GMPLS controller) running in a Linux-based router. The virtualization of the GMPLS control plane of the ADRENALINE Testbed to partition the physical control plane into multiple virtual control plane instances has been previously addressed by the authors in [4].

The performance values are obtained when dynamically provisioning VONs, in which the inter-arrival (IAT) process is Poisson, and the holding time (HT) follows a negative exponential distribution. The average VON-holding time is set to 1000 s, and the mean inter-arrival time will be varied during all different experimentations, yielding an offered traffic load from 1 to 10 Erlangs. The topology for each VON request is randomly selected from the space of feasible topologies, which is determined by the physical optical network infrastructure (Fig. 1). For the ADRENALINE Testbed, we consider a set of 28 topologies.

The number of wavelengths requested for each VON is set to one, and the wavelength assignment algorithm used is First-Fit. 10^4 VONs have been requested for measuring the blocking probability. For the rest of figures of merit, 100 requests have been performed for each data point. The provided results are

request processing time (T_{req}) at the VON resource broker and compositor, the VON setup and tear down average delays employed by ADNETCONF to configure both the control and data plane (T_{up} and T_{down} , respectively). Finally, we provide the Blocking Probability (P_b). The obtained results are shown at Table 1. We observe that the VON setup and tear down delay for our testbed is around 11 and 5 seconds respectively, whilst the request processing time is of the order of few ms per request. As for the blocking probability, we can observe that it increases significantly up to 34.5% with a requested load of 5Er.

VON req. load (Er.)	T_{req} (us)	T_{up} (s)	T_{down} (s)	P_b (%)
1	131	11.76	5.18	0.79
5	126	10.13	5.68	34.5
10	111	11.04	4.78	60.3

Table 1. VON deployment results.

With the purpose to evaluate the performance of the different presented algorithms (i.e., First-Fit, Random, WC First-Fit and WC Random), we present the simulation results performed in an scenario which consists of 14 physical optical nodes connected using an EON topology, consisting of 24 bidirectional links. Each of the considered optical nodes included in the proposed scenarios contains 32 virtual GMPLS controllers and 8 wavelength converters. For each physical optical link of the considered scenarios 32 different wavelengths are available.

In Figure 2, we observe the blocking rate of VON requests in the EON topology scenario. The different blocking rate results have been obtained for the four proposed algorithms (First-Fit, Random, WC First-Fit and WC Random).

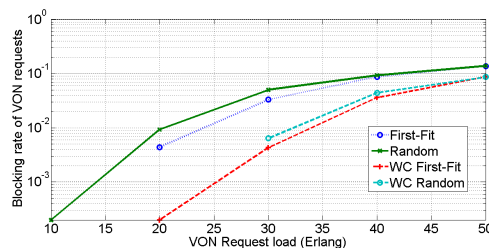


Figure 2. Blocking rate of VON Request in EON scenario.

IV. Acknowledgments

This work was partially funded by the MICINN through the project DORADO (TEC2009-07995).

V. References

- [1] R. Vilalta et al., "Experimental demonstration of a Virtual Optical Network Resource Broker and Composer for dynamic GMPLS WSON infrastructure services", in *OFC/NFOEC*, 2012.
- [2] R. Vilalta et al., "Dynamic Virtual GMPLS-controlled WSON Using a Resource Broker with a VTN Manager on the ADRENALINE Testbed" in *ECOC*, 2012.
- [3] R. Vilalta et al., "GMPLS-enabled MPLS-TP/PWE3 node with integrated 10Gbps tunable DWDM transponders: design and experimental evaluation", *Communication Networks*, 2012.
- [4] R. Muñoz et al., "Virtualizing ADRENALINE testbed for deploying dynamic GMPLS-controlled WSON as a service", in *OFC/NFOEC*, 2011.
- [5] R. Vilalta et al., "Dynamic Wavelength Allocation Algorithms for On-Demand Deployment of GMPLS-controlled Virtual WSON Using a VON Resource Broker," in *NOC*, 2012.

Automatic representative keyframe selection for video by using a Random Walk algorithm

Author: Carles Ventura Thesis Advisor(s): Verónica Vilaplana, Xavier Giró-i-Nieto, Ferran Marqués
contact email: carles.ventura@upc.edu

I. Introduction

Television broadcasters have large amounts of video data in their local archives from TV producers and news agencies. Generally, these companies upload their audiovisual contents on the Web, where every video clip is pre-visualized as an image by the users. The selection of this representative keyframe is a challenging process since the keyframe should be representative for the user who is searching for a video. The representativeness of a frame depends on its semantics with respect to the semantics of the whole clip. Currently, we are working in a project with *Televisió de Catalunya* (TVC), where this selection task is manually developed by their documentalists. In some cases, this process is not manually performed and a random frame is selected as representative. Therefore, broadcasters require a system which allows the automatic selection of one representative keyframe for any video clip.

The main objective of this work is the automation of the representative keyframe selection process. Two different scenarios have been considered: (i) the intra-clip mode, and (ii) the inter-clip mode. The intra-clip mode consists on selecting the representative keyframe by using only the input video clip and its metadata. The inter-clip mode allows using not only the input data (video and metadata) but also a video database in which each video has its own metadata and its own representative keyframe. The idea is that these keyframes can be used in the selection process.

II. Representative keyframe selection algorithm

This section describes how the automation of the representative keyframe selection has been designed. It uses the Random Walk [1], an algorithm which computes the probability of a walker of being located in each of the vertices of a graph (with a random starting point), where the decision to take a particular path is defined by the weights at the edges. One of the most successful applications of the Random Walk is PageRank [2], a Web page ranking technique that has been the key stone of the Google search engine. The main idea behind the PageRank is to determine the importance of a Web page in terms of the importance assigned to the pages hyperlinking to it. This algorithm is computed over a directed Web graph which has the Web pages as nodes and the hyperlinks as directed edges.

Sections II.A and II.B show how Random Walk has been adapted for the two scenarios considered: intra and inter modes, respectively.

II.A. Intra mode for representative keyframe selection

In our context we have a similarity graph instead of the Web graph. The nodes of the similarity graph represent the images of a dataset and the edges represent how similar are the two connected images. In order to compute these similarity values, some MPEG-7 visual descriptors, which are based on features such as

the spatial distribution of color and texture, are previously computed. Each descriptor has a similarity measure also defined in MPEG-7 standard which has been used to assign the weights to the edges of the graph. Fig. 1 shows an example of similarity graph.

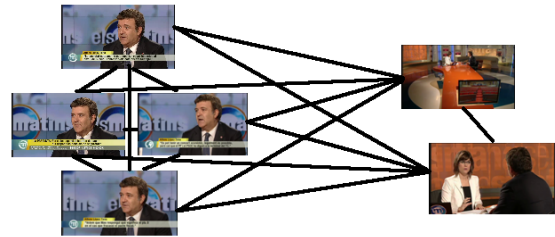


Figure 1. Visual similarity graph (intra mode)

Our work proposes a Random-walk-based ranking algorithm to rank the images and to select the most representative keyframe. Intuitively, applying this algorithm in the case represented by Fig. 1, the ranking scores obtained by the four frames on the left would be larger than the two other ranking scores. The reason is that the probability of visiting one frame from another one is directly proportional to their visual similarity. Therefore, the four similar images reinforce themselves. As a consequence, one of them will achieve the highest score and will be selected as the representative keyframe.

The Random Walk algorithm can be formulated in the following way:

$$x(k+1) = \alpha \cdot P \cdot x(k) + (1 - \alpha) \cdot v$$

where $x(k)$ is the normalized vector which contains the probabilities for each node at iteration k , P is the similarity or transition matrix, v is the initial ranking score vector, and α is a weighting factor. In our case, vector v is set according to a uniform distribution since no a priori information is used. The whole process is illustrated in Fig. 2.



Figure 2. Intra-clip mode scheme

II.B. Inter mode for representative keyframe selection

In the inter-clip scenario, the representative keyframe selection does not only depend on the input video clip, but also on the representative keyframes previously selected for videos stored in the database. First, the title and category fields from the metadata are used to retrieve the most related videos from the database. The words of the title are inserted in a textual

searcher and the retrieved videos are filtered by category. The textual search tool is based on the Lucene index. Fig. 3 illustrates the representative keyframes of the videos retrieved by the textual searcher (bottom part) related to the input video (its keyframes are showed in the upper part).

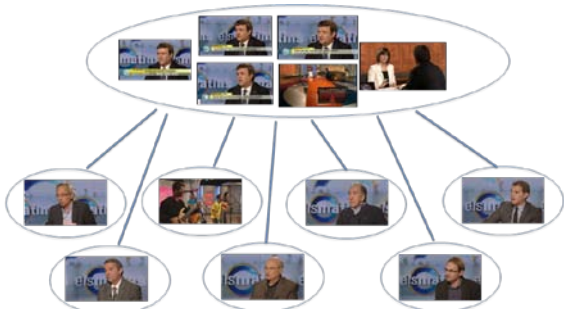


Figure 3. Input video's keyframes and representative keyframes retrieved from related videos

Once these related videos have been retrieved, the visual features are extracted from their representative keyframes. Then, the keyframe extractor is applied over the input video clip and the visual features are also computed from them. Then, the visual similarity graph is built by taking into account the similarity values obtained when each pair of images is compared.

Next, the Random Walk algorithm is applied on the similarity graph. A new parameter β , which modulates the influence of the retrieved videos on the representative keyframe selection, has been introduced. Therefore, the initial ranking score vector v is not set uniformly. The components related to the input video's keyframes are set to β/M and the ones related to the retrieved videos' representative keyframes are set to $(1-\beta)/N$, where M is the number of keyframes extracted from the input video clip and N is the number of related videos retrieved from the dataset. Therefore, if $\beta = 1$ the configuration is equivalent to the intra mode, since the retrieved videos are not considered. On the other hand, if $\beta = 0$ the input video's keyframes do not reinforce themselves since their visual similarities are not taken into account. Finally, the keyframe belonging to the input video with the highest score is selected as the representative keyframe. The whole process is illustrated in Fig. 4.



Figure 4. Inter-clip mode scheme

III. Experimental Results

Some experimental results have been performed to analyze the performance of the representative keyframe selection process. Fig. 5 shows the ranking score vector given by the Random Walk algorithm used in the inter mode (with $\beta=0.3$) for an interview video clip. The first 9

images (marked by a red rectangle) are the representative keyframes of the retrieved videos related to the input video (different interviews from the same TV program). The first image after these marked frames is the input video's keyframe with the highest score, so it is selected as the representative keyframe. In Fig. 6, the representative keyframes from the retrieved videos have been manually modified to analyze the influence of the dataset representative keyframes. The results show that the input video's representative keyframe has also changed.



Figure 5. Ranking scores in inter-clip mode ($\beta=0.3$) with original representative keyframes



Figure 6. Ranking scores in inter-clip mode ($\beta=0.3$) with modified representative keyframes

IV. Future Work

The proposed representative keyframe selection process is still an open work line. One of the unfinished tasks is the objective evaluation of this system. We plan to carry out it through a blind test in which the users will have to guess if a set of representative keyframes have been selected manually by TV employees or automatically by our system.

V. Acknowledgments

This work is partially funded by TVC through the Spanish project CENIT-2009-1026 BuscaMedia, by TEC2010-18094 MuViPro project of the Spanish Government, and by FPU-2010 Research Fellowship Program of the Spanish Ministry of Education.

VI. References

- [1] L. Lovász, "Random Walks on Graphs: A Survey," *Combinatorics, Paul Erdős is Eighty*, János Bolyai Mathematical Society, vol. 2, pp. 1-46, 1993.
- [2] S. Brin, L. Page, "The Anatomy of a Large-Scale Hypertextual Web Search Engine," *Computer Networks and ISDN Systems*, vol. 30, nos. 1-7, pp. 107-117, 1998.

Context Discovery in Cognitive Radio Networks

Author: Liliana Bolea, Thesis Advisors: Ramon Agustí Comes, Jordi Pérez-Romero
contact email: lilianab@tsc.upc.edu

I. Introduction

Cognitive Radio (CR) has emerged as a promising solution to exploit the existence of spectrum holes through opportunistic spectrum access. In these techniques, secondary users (SUs) are allowed to access in an opportunistic and non-interfering manner some licensed bands temporarily unoccupied by primary users (PUs).

A proper estimation of context is essential for an efficient operation of CR networks. This context includes features such as path loss model, transmitter positions, radiation pattern, transmission power and shadowing characterization among others. Once acquired, such context information should be stored in a database system, locally or globally, to be used during the secondary network operation.

The goal of this thesis is to explore the characterization of the relevant PUs context features by combining a number of sensed samples at different geographical positions collected by SUs, without making any a priori considerations regarding the radiation patterns of the PUs and propagation model.

II. Problem formulation

A generic scenario is considered, presented in Fig. 1, which is characterized by a number of primary transmitters that operate at different frequencies and have different coverage areas. A secondary network will rely on the information measured by a number of sensors, which are randomly distributed in the scenario, and also on the appropriate post-processing of this information, in order to estimate different context parameters of the primary network. The sensors cooperate with each other in a centralized manner, where a central entity plays the role to gather all sensing information from the sensors and to detect the positions and coverage areas of the primary transmitters.

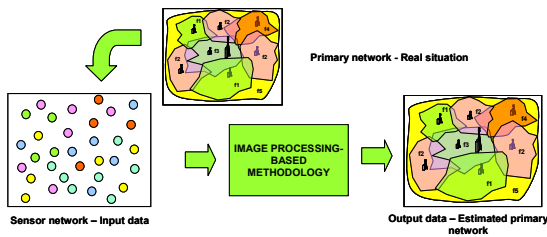


Figure 1. General problem formulation [1].

A sensor measures the received power in a number of N specific frequencies in its geographical position. It is assumed that frequency f_i ($i = 1, \dots, N$) is detected by the sensor at position (x, y) when the received power is above a given threshold $P_{th}(f_i)$. The value detected by a sensor for each frequency is quantified to a set of 2^n values with quantization step Δ . Then, this value will be encoded as a word of n bits and sent to the central entity.

Different measurements at random positions associated to the sensors represent a partial vision of the scenario. The problem considered here consists in defining a methodology to smartly combine these

measurements in order to get a full vision in which the primary transmitter networks are estimated.

III. Proposed methodology

The proposed methodology characterizes the radio environment by an image, where each pixel (i.e., a rectangular area of dimensions $\Delta x \times \Delta y$) contains the information of the Received Signal Strength (RSS) levels associated to the frequencies measured in this area. It is assumed that a pixel can only have the result of one sensor. Then these values will be combined using image interpolation and processing techniques in order to reconstruct the overall image and to discover context features such as transmitter positions, antenna patterns and directions and propagation model. The main steps of the procedure are shown in Fig. 2 and explained in the following.

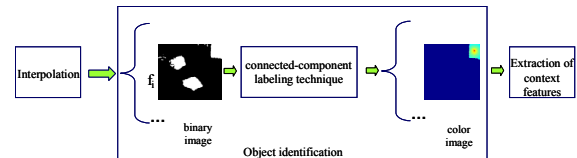


Figure 2. Overall steps of the proposed methodology [1] [2].

III.A. Interpolation

This step intends to determine the RSS associated to those pixels without any sensor based on the pixels available. Three methods of interpolation are used:

- Nearest neighbor interpolation: assign the value of the closest point.
- Linear interpolation: estimate a new value by connecting two adjacent known values with a straight line.
- Natural neighbor interpolation: it is a weighted average method that constructs the interpolant by using natural neighbor coordinates based on Voronoi tessellation of a set of positions.

III.B. Object identification

This step identifies the different transmitters existing in the scenario.

- From the resulting image, a set of N binary images is built, one per each frequency. Each pixel of a binary image takes the value 1 if frequency f_i is detected (i.e., it is above $P_{th}(f_i)$) and 0 otherwise.
- For each binary image, an object identification mechanism is applied where an "object" is a contiguous region where frequency f_i is detected.
- Then, the binary images will be converted into color images, one per each object identified, using the quantified values from the received power at each frequency f_i after the interpolation.

III.C. Extraction of context features

For each of the objects identified in the previous step a set of context features are extracted.

- Transmitter position estimation: It is initially estimated as the centroid of the pixels with the highest value. For directive antennas, a further refinement is introduced using an estimation of the antenna pattern.
- Antenna orientation estimation: the antenna direction ρ is estimated as the angle with maximum received power averaged over the different distances.
- Antenna pattern radiation estimation: is based on the average over the distances of the received power for each azimuth angle φ , relative to the average for the antenna direction ρ .
- Propagation model estimation: is based on correlation between distance and received power for the available sensors through regression analysis

IV. Results and future work

To test the interpolated data accuracy, a framework was built to perform the proposed methodology. A scenario with a transmitter equipped with a directive antenna is analyzed. Scenario size is 3780 m x 3780 m with pixel size $\Delta x = \Delta y = 20$ m. The EIRP is 55 dBm, and power threshold $P_{th}(f_i)$ is -85 dBm. The number of bits used to encode the RSS measurements is $n = 5$ bits, and the quantization step is $\Delta = 1.5$ dB. Based on the propagation model used in the area of the transmitter, the expected received power in dBm at distance 1 m should be $P_0 = 24.5$ dBm and the path loss exponent $\alpha = 3.552$.

Three different situations are analyzed: the case with no shadowing, the case with 6 dB non-correlated shadowing, and the case with spatially correlated shadowing with 6 dB shadowing standard deviation. Results (Fig. 3, 4, Table 1, 2) show that the proposed methodology is able to extract the transmitter position, the antenna pattern, and propagation model features adequately regardless the considered interpolation technique. The case of correlated shadowing in general exhibits better estimation errors than the case of non-correlated shadowing for all parameters with the only exception of the antenna direction. In general, linear and natural neighbor interpolations present better results than the nearest neighbor.

Future work is devoted to combine the proposed methodology together with Maximum Likelihood approach presented in [3]. This enables to keep the benefits of the optimality of ML performance but yet reducing dramatically the computational complexity.

V. Acknowledgments

The support from the Spanish Ministry of Science and Innovation (MICINN) under FPU grant AP2008-02291 is hereby acknowledged.

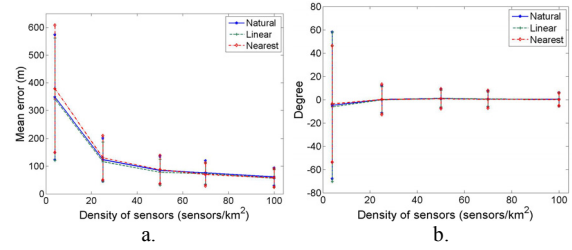


Figure 3. Mean error and standard deviation in transmitter position estimation (a) and in antenna direction estimation (b), for different sensor densities, case without shadowing [2].

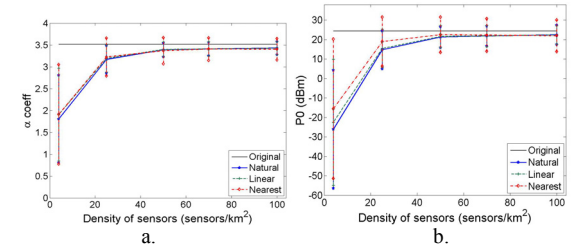


Figure 4. Estimated propagation factor α (a) and estimated P_0 (b), as a function of the sensor density, case without shadowing [2].

	Natural	Linear	Nearest
Standard Deviation (dB)	4.0763	4.0574	8.4599

Table 1. Standard deviation in horizontal antenna radiation pattern, for the case $D = 50$ sensors/km², case without shadowing [2].

	Pos. error - Avg (m)	Dir. error- Avg (°)	α (avg)	P0 Avg (dBm)
<i>Natural neighbor interpolation</i>				
Non corr. sdw	111	0.21	2.57	-0.54
Corr sdw	99.9	3.83	2.74	6.13
<i>Linear interpolation</i>				
Non corr. sdw	105	0.30	2.66	2.57
Corr sdw	93.2	4.03	2.79	7.62
<i>Nearest neighbor interpolation</i>				
Non corr. sdw	123	-0.41	2.37	-0.34
Corr sdw	98.6	4.40	2.84	12.0

Table 2. Simulation results for the case of density of sensors $D = 50$ sensors/km², correlated shadowing [2].

VI. References

- [1] L. Bolea, J. Pérez-Romero, R. Agustí, and O. Sallent, "Context discovery mechanisms for cognitive radio," in *IEEE VTC Spring*, 2011, pp. 1-5;
- [2] L. Bolea, J. Pérez-Romero, R. Agustí, "Received signal interpolation for context discovery in Cognitive Radio," in *WPMC*, 2011, pp. 1-5;
- [3] R. K. Martin and R. Thomas, "Algorithms and bounds for estimating location, directionality, and environmental parameters of primary spectrum users", in *Wireless Communications, IEEE Transactions on*, vol. 8, no. 11, pp. 5692 – 5701, Nov. 2009.

Network Stability Assurance in the Context of Autonomic Management.

Author: Antonio Astorga, Thesis Advisor(s): Joan Serrat

Contact email: {aastorga, serrat}@tsc.upc.edu

I. Introduction

It is common to accept that one of the main obstacles currently faced in the IT industry is system complexity. The need to integrate several heterogeneous environments in one or more systems is partially causing this complexity. To face these problems the Autonomic Computing paradigm [1] has been proposed. In addition, Future networks will become more and more complex because they will deal with real and virtual resources. These will imply that systems will become massive and complex enough to render almost impossible their configuration and management tasks by means of traditional approaches.

The Autonomic Network Management paradigm is a descendent of Autonomic Computing conceived to cope with the problems associated to the management of future networks. Autonomicity is about self-management; that means that the autonomic systems will maintain and adjust their operation in changing environments.

Nevertheless, one of the main risks faced in multiple autonomic network management systems is the instability of the global network under its control.

Stability could be defined as the property of a system to return to the original condition after a disturbance. The instability could be defined as the opposite where the disturbance tends to increase.

Stability problems will be analyzed through different network instability scenarios. For our approach we will start modelling the autonomic control loops intervening in a network scenario as policy-based systems making use of Finite State Transducers [2]. The challenge here is not the modelling of systems as if they were isolated but to include in this model the side effects (i.e. the interactions between systems) that are usually the cause of instabilities.

A model such the above will be then analyzed by means of the Hybrid Systems approach. This representation will facilitate the analysis to determine the regions of the space where the system is stable. These regions will be characterized by constraints on the policies that as said before are responsible of the system's behaviour. Thus we expect to derive guidance for policy authors so that the networks deployed and driven by these policies are in fact stable networks.

The main goal here is to maintain the target network working in an equilibrium point just to maintain the stability and to fix it in case of some disturbance affects the behaviour of the systems.

Through the achievement of this goal we expect to contribute to the development of Autonomic Networking.

II. Proposed Solution

The main problem that we want to address in our research is the stability of autonomic managed networks. This goal will be fulfilled through the adoption of different techniques as described hereafter.

Our ongoing work started establishing a networking scenario where we can create instability problems to

make evident the consequences and impact on the supported service.

The current scenario consists of two wireless access points. Each of these access points has some policies that govern its behaviour, and maybe we will have a situation where both Base Transceiver Station (BTS) are close enough and they have the same policies applied to their respective domains. The policies enforced by each BTS are meant to implement the access control mechanism of the access point. The policy is characterized by a threshold above which no more connections are accepted.

Policies are rules governing the behaviour of a system. Then, one of the first steps we plan to do is to have this behaviour represented as a Finite State Machine applying techniques based on [2]. In-depth information about finite state machines can be found in [3, 4].

The model developed will be an abstract tool based on Finite State Machines representing the rules inside the Event-Condition-Action (ECA) paradigm of a policy. Our approach will model the scenario as two policy-driven systems. Nevertheless, the main challenge of our approach here is to deal with the modelling of the interaction of the two systems obtaining only one Finite State Machine (FSM).

Let's suppose that we have each BTS represented as a FSM as we can see in Figure 1.

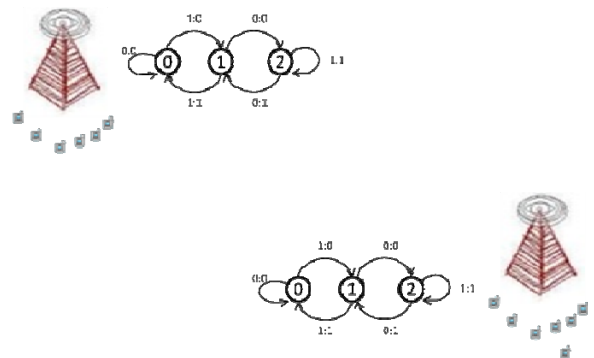


Fig. 1. - Model Based on Finite State Machines for each BTS.

The second step is to obtain the same representation based on FSM but including the interaction of the two systems working side to side to capture all behaviour of the global system (i.e. when the interaction between the two BTS occurs). Figure 2 is a representation of what we expect to obtain when this interaction occurs, just one model based in FSM for the hall system.

To study the stability in the systems we have different approaches that can help. One of these approaches is making use of Control Theory to provide a framework to analyze stability. Nevertheless, Control Theory is usually dealing with the continuous dynamics of the problem. On the other hand, our investigation lends us to a different approach dealing with

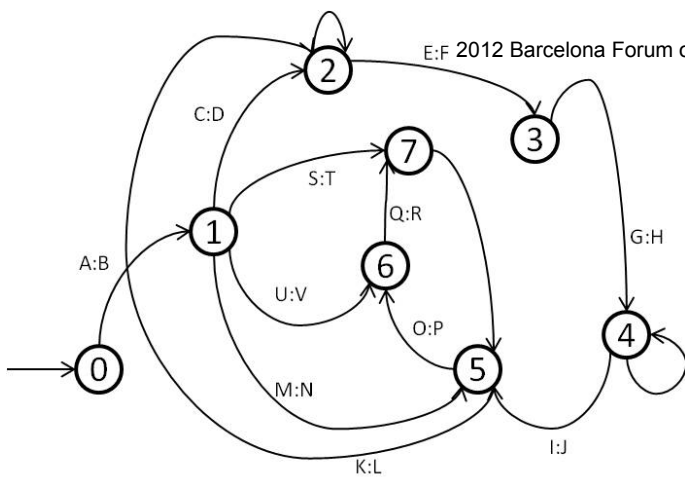


Fig. 2. - Expected Model based on Finite State Machines representing the interaction of the two BTS.

Finite State Machines. This approach is part of a paradigm called Hybrid Systems. An interesting abstraction of Hybrid Systems is the Hybrid Automaton, which is a representation of the discrete and continuous dynamics in the system. The motivation found to apply Hybrid Control to the scenario above described is because we are dealing with a system characterized by both a continuous and a discrete dynamics. In fact, policies governing the behaviour of the BTS represent the continuous part of our system; these policies will be enforced along the continuous time domain. On the other hand, the events that trigger these policies and the events that may be generated as a consequence of the enforcement of our policies are discrete in nature (e.g. they occur at a given random epoch in the time domain) thus constituting the discrete part in our model.

Being more specific, the main problem in the stability analysis of hybrid systems is the complicated interplay between discrete and continuous dynamics. To get this complication under control it is proposed to view the hybrid automaton as a discrete system in which the continuous dynamics has been eliminated by abstraction. From a stability point of view all that matters is the continuous state behavior at the transition times.

Finally, once our system is characterized by means of a Hybrid System we will have to determine the regions of the space where it is stable.

Last, it is worthy to mention that the above mentioned stability regions will be expressed in terms of the parameters characterizing the system's driving policies. Stability is fundamental in control theory [5]. It basically states that small perturbations in operating conditions lead to small changes in the system behaviour. In generalizing the notion of stability to hybrid systems, one needs to pay attention not only to the evolution of the continuous state but also to the discrete state. An equilibrium point of a hybrid system can either be in the interior of a domain or on the boundary between two or more domains. A simple example that illustrates stability of hybrid systems is discussed in [6]. This means that we expect, as the main outcome of our research work, to obtain boundaries and constraints on policies to grant the stability of multiple autonomous control loops. These constraints will then be used at the policy authoring stage and distributed to the autonomous management systems by means of a distributed orchestration plane

III. Innovativeness and Contributions

In the Future Networks, the level of complexity will increase because the networks going to deal with real and virtual resources. The Autonomous Computing paradigm is proposed as a solution to face this

increasing level of Complexity. Nevertheless, one of the major problems faced in the Autonomous Computing is the stability problems in networks managed by multiple control loops.

This paper highlights the ideas and directions we are currently investigating on a methodology based in Finite State Machines and Control theory to prevent instabilities caused by multiple Autonomous Management Systems caused by their mutual interactions. The final aim is to find or determining the regions of the space where the system is stable and the associated constraints to ensure the system is operating inside those regions. When we have these regions the Orchestration plane is able to guarantee the stability in the Autonomous Systems. The Orchestration plane with the help of these stability techniques will enable the cooperation of the various autonomous control loops in the network to ensure the operation within the boundaries set by the business goals defined by the operators.

Once we achieve this goal by applying these stability techniques we are able to deploy a system that recognizes the policies that are running in different autonomous systems, either because they have been deployed in situ by their respective managers or because they have evolved over time through self-learning techniques. This system models the global network and in particular the interactions between systems. This determines the potential instability of the global system and solved by creating new policies and / or modifying the existing ones, which are properly deployed. Before this policies are being sent, the stabilization system (orchestration plane) finds that the system is stable with the policies that are added / modified. This concept may have applications to other systems, not necessarily in the domain of telecommunication networks, which can be modeled as systems of rules determined by independent but requiring that the systems are globally stable

IV. Acknowledgments

This work has been started within the project TEC2009-14598-C02-02 granted by the MEC Spanish Ministry, partially funded with FEDER.

V. References

- [1] IBM, "An Architectural Blueprint for Autonomous Computing", v7, June 2005, <http://www.ibm.com/developerworks/autonomic/librariy/ac-summary/ac-blue.html>
- [2] Javier Baliosian, "Finite State Transducers for Policy Evaluation and Conflict Resolution in Autonomous Communications Systems", unpublished PhD Thesis, Universitat Politècnica de Catalunya, Barcelona, Spain. 2005.
- [3] J. E. Hopcroft and J. D. Ullman. *Introduction to Automata Theory, Languages and Computation*. AddisonWesley, 1979
- [4] Emmanuel Roche and Yves Schabes. *Finite-State Language Processing*. Technical report, MIT Press, Cambridge, Massachusetts., 1997.
- [5] A.B. Kurzhanski / I.F. Sivergina. *Stability Concepts*. Encyclopedia of Life Support Systems [EOLSS], 6.43.2].
- [6] M.S. Branicky. *Stability of Hybrid Systems*. Encyclopedia of Life Support Systems [EOLSS], 6.43.28.3]

Multi-Agent based Reinforcement Learning for Dynamic Resource Allocation in Next Generation Virtual Networks

Author: Rashid Mijumbi. Thesis Advisors: Joan Serrat and Juan-Luis Gorricho

Contact email: rashid@tsc.upc.edu, serrat@tsc.upc.edu, juanluis@entel.upc.edu

I. Introduction

The Internet is ossified. However, the demands of the users continue to increase such that resource and protocol stack specialization is a must for service providers. However, it would be economically unfeasible for each service provider to deploy physical resources for each service context.

Network Virtualization – which enables the building of multiple virtual networks over a shared physical network – has recently received attention from both academia and industry. One of the challenges to Virtualization is efficient resource allocation. Even in the offline case where all the requirements of the different Virtual Networks are known, this problem is NP hard, such that its optimization is computationally intractable. For this reason, most solutions to this problem have not only been based on heuristics, but have also made many simplifying assumptions such as availability of unbounded resources in the substrate network. In this paper, we propose to apply techniques from Artificial Intelligence to the resource allocation problem. Our objective is to propose a solution that is dynamic and online (including topology optimization); to allow for cooperation and negotiation between substrate and virtual networks; and to achieve a distributed and context aware resource management solution. In general, our ideal solution is an Autonomic Management of the Substrate Resources, implying that the networks are self-configuring, self-optimizing, self-healing and context aware.

II. Proposed Solution

To achieve the objectives of our work, our proposal is to apply Reinforcement Learning and Multi-Agent Systems to the resource allocation problem. Our idea is to represent each of the networks by an intelligent agent. Each agent that represents a virtual network is responsible for customizing its resources to the needs of its users while at the same time minimizing the costs incurred in using the substrate resources. Each of these agents has independent objectives. Similarly, each of the physical networks is represented by an intelligent agent whose main objective is to ensure that the overall resources are efficiently used. In the end, our proposal is for the different agents to not only learn from the decisions they make, but also to cooperate and negotiate with each other so as to achieve both local level as well as system level objectives.

In Fig. 1, we present a scenario of our proposed solution. While in this figure we represent two virtual networks sharing resources of a single network, our ultimate solution will be a general one with many virtual networks, and possibly many substrate networks.

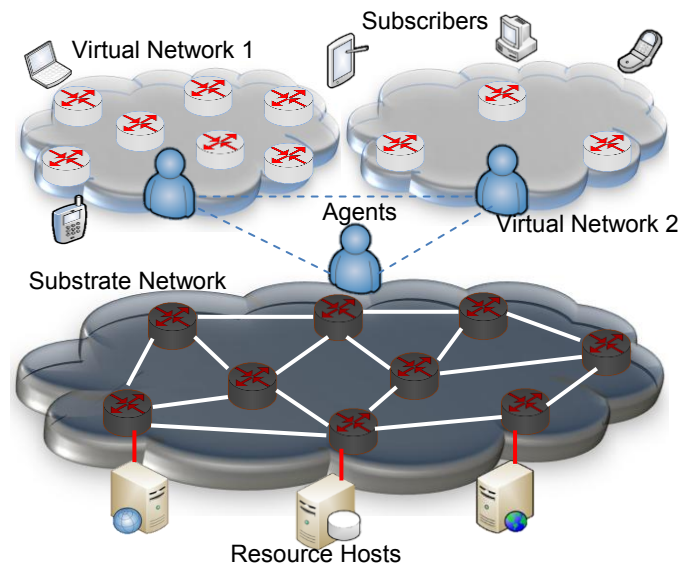


Fig. 1: Virtual Network Environment Proposed Framework

With this representation, some of the objectives of our work can be achieved as follows:

- I) *Self-Configuration*: As users make requests for resources, the virtual network agents continuously evaluate their network topologies searching for possibilities of re-configuration. Whenever they find these possibilities, they can make requests for this to the substrate agents. Virtual network agents can also negotiate and cooperate amongst themselves so as to agree on the usage of substrate resources and achieve the best utility both on individual and system levels.
- II) *Self-Optimization*: As the conditions of the substrate network change, substrate agents should exhibit proactive as well as reactive characteristics. For example, if a physical node and/or link is added to the network, or if their capacities are changed, the substrate agent should re-evaluate the network loadings to establish possibilities for re-allocation of resources. While this would ideally not require any action on the part of the agents, in our solution we require that these agents always look out for possibilities of optimizing their resource usage whenever there are changes to the substrate network.
- III) *Self-Healing*: If for any reason a node and/or link becomes unavailable, the substrate agent – in collaboration with virtual network agents – should make decisions so as to cause the minimal possible disruptions in customer service. This situation is different from II) in a way that while self-optimization is mainly aimed at optimizing costs, and possible

improvements in customer service levels, self-healing is much more urgent as in such cases there are possibilities of violating agreements with customers. Therefore, if the virtual network agents have to cooperate and/or negotiate in one of these two cases, an agent will adjust its objectives considering the possible conflict between utility optimisation and customer satisfaction.

IV) Context Awareness: The above three cases generally consider context awareness with respect to the network. However, we also require user context awareness. For example, with respect to a mobile virtual network, whenever users are connected to the network, they will send periodic updates about their location. Based on these locations, virtual agents will determine not only the exact location of the customer, but may also reason about the actual state of the user, for example; the agent can know if a user is walking, driving or stationary. Based on this user context information, the virtual network may take decisions about the resources being used by the user. For example, a user whose location is near a Wi-Fi hot spot **AND** this user is stationary **AND** this user is occupying a high bandwidth – say for a video on demand service – could be offloaded to the Wi-Fi and if there are necessary changes to the nodes for this specific customer, these changes can be effected by substrate agent.

III. Innovativeness and Contributions

The demands of users towards service providers continue to be conflicting in a way that they require better quality and highly customized services, but are only willing to pay less. It is inevitable that service providers have to specialize smaller quantities of resources so as to meet the diverse user needs. However, meeting users' price requirements and still remaining profitable means that service providers cannot feasibly deploy specialized physical resources for each user group or business context. For this reason, Network virtualization is very important as an enabling solution to this impasse. In fact, especially on the mobile front, as of May 2011 there were 645 virtual network operators worldwide, and 205 of these had become operation in one year [1].

Efficient Resource Allocation is one of the practical challenges to network virtualization. Most of the current approaches make some assumptions – such as unbounded resources – which cannot be achieved practically. While these could give solutions to specific instances of this problem, the possibility to make improvements is a major motivation of this work. Our work involves making the resource allocation task autonomic, which is a vital characteristic especially considering the complexity of current and future networks.

By the end of this work, we will have a dynamic resource allocation algorithm based on reinforcement learning. A solution based on Reinforcement Learning allows for incorporation into our proposal, economic costs to enable not only projects in the area of pricing for substrate network resources, but also practical development of resource pricing models between infrastructure providers and service providers.

Our proposed consideration of network and users' context will not only enhance decision making and

hence improve resource utilization efficiency but would also help service providers in enhancing customers Quality of Experience.

We will also propose a Cooperation framework for the multi-agent system that represents the different networks. To this end, a Negotiation protocol based on network and user context will be proposed. This would allow for the coordinated and profitable use of resources whenever it is applicable.

IV. Acknowledgments

This work has been started within the project TEC2009-14598-C02-02 granted by the MEC Spanish Ministry and partially funded with FEDER funding. We also acknowledge the EVANS EU project funded under contract PIRSES-GA-2010-269323.

V. References

[1] The MVNO Directory 2011, Mobile virtual network operators and major resellers (5th Edition), Blycroft Ltd, May 2011.

Atmospheric compensation experiments on advanced free-space optical coherent communication systems

Author: Esdras Anzuola, Thesis Advisor(s): Aniceto Belmonte
contact email: eanzuola@tsc.upc.edu

I. Introduction

As a result of ever-increasing requirements for high data rate wireless communications in space, sensing, and security applications, lasers are used to extend radio-frequency atmospheric communication techniques to the optical-frequency band. However, even under clear-weather conditions, the earth's atmosphere is not a quiescent propagation channel.

Atmospheric turbulence restricts the received power levels in optical systems and degrades their overall performance [1]. Optical communications systems exhibit severe temporal fading associated with the turbulence-induced optical amplitude fluctuations which increases the error in the communication link and decreases its capacity.

Significant advances in the technology for fiber-optic communication components at 1.5-micron wavelength, that can be applicable to free-space optical communications systems, are motivating a transitioning to coherent (synchronous) optical communication systems addressing modulation and detection techniques for high spectral efficiency and robustness against transmission impairments. It is necessary to develop and demonstrate the coherent optical infrastructure necessary to produce robust high-capacity free-space optical communication links over the 1.5-micron wavelength spectral band.

New, affordable adaptive compensation methods and technologies can help to improve substantially the performance and reliability of coherent optical communication systems in the atmosphere. The use of adaptive optics to mitigate turbulence-induced phase fluctuations in links employing coherent detection is poised to reduce performance penalties enabling a more capable next generation of free-space optical communications.

II. Work description and methodology

The objective of the project is to address experimentally two intertwined research problems that are instrumental in the development of the next generation of advanced free-space optical communication systems.

The first is the use of coherent systems in links where clear air turbulence impairs communication efficiency so coherent processing can be used to reduce atmospheric interference significantly. The second is the use of affordable adaptive optics and diversity combining to mitigate turbulence-induced signal fluctuations on both coherent and incoherent atmospheric communication systems [2]. The different steps in our research can be summarized as:

II.A. Implementation of a first engineering prototype for a fully functional optical coherent transceiver:

This task will assess the benefits and drawbacks of them. We will perform a detailed investigation of the optical technologies and techniques that could enable

the transmission of high data rates at optical frequencies through the atmosphere, with regard to all kinds of atmospheric phenomena.

II.B. Design and implementation of a free space optical adaptive system:

Adaptive optics technology, currently primarily used in astronomical imaging, needs to be adapted to the requirements of free-space optical communication systems and their specific challenges. In particular, we will investigate a non-conventional adaptive optics approach that has certain advantages with respect to its incorporation into free-space optical communication terminals.

MOEMS-based electrostatic micro-deformable mirrors are promising for future AO systems. As electrostatic MDM are well-suited for open-loop operation, we define, implement, and test working adaptive systems able to compensate turbulence-induced phase fluctuations in our free-space optical communication receiver [Figure 1].

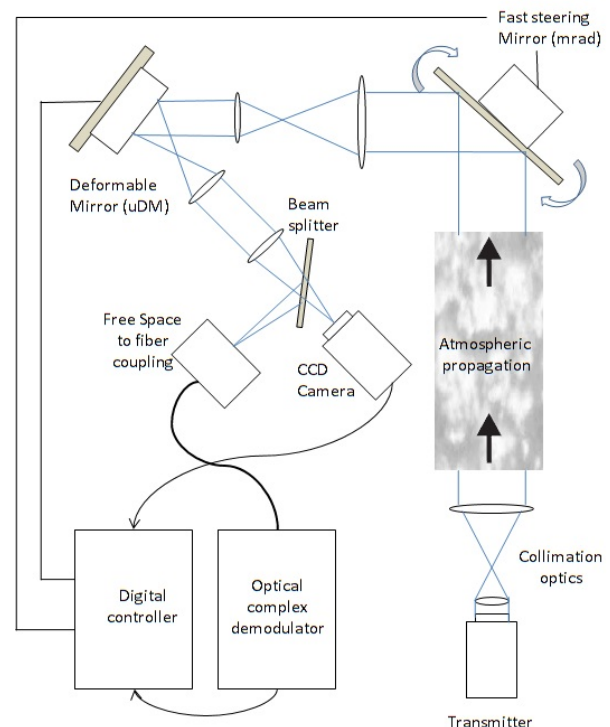


Figure 1. Wavefront sensorless adaptive optics experimental set-up.

II.C. Performance analysis and algorithm development:

Finally, we establish, through analysis and active experimentation, how the addition of adaptive optics architectures and receive diversity to the transmitter or receiver can reduce the effects of atmospheric

propagation and discuss systems which circumvent this performance degradation by effectively exploiting field diversity (spatial and temporal).

We evaluate and quantify experimentally the performance achievable in free-space coherent optical systems using atmospheric compensation techniques and describe the performance limitations, with regard to atmospheric conditions, of binary modulation formats (ASK, DPSK, and PSK).

III. Results

In this work a study and implementation of an optical coherent transmission system has been made and demonstrated. A practical system has been designed, implemented and tested. The coherent system implementation has shown the viability of optical communications using complex modulation formats, which improves the spectral efficiency and provides better sensitivity at the receiver.

Our system is able to compensate the most influential effects that appear in practical systems. The IQ diagram obtained after different compensation techniques are presented [Figure 2].

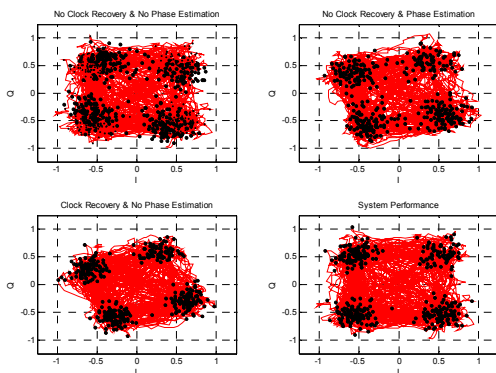


Figure 2. IQ diagrams of a QPSK transmission (SNR=10dB) after compensation

When compensation techniques are not applied, data demodulation becomes random. By introducing a frequency offset estimator, a clock recovery system and a phase offset estimator the system is able to demodulate data correctly.

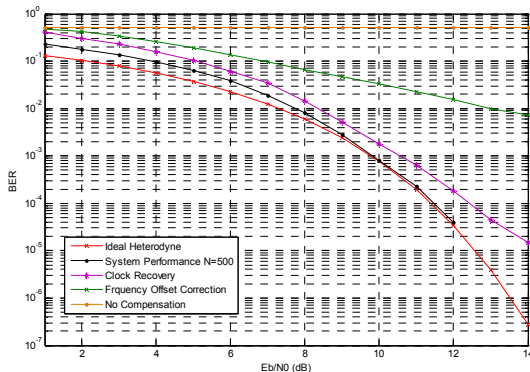


Figure 3. Bit error rate as a function of signal to noise ratio for different compensation modules.

In this situation, for SNRs higher than 8 dB the sensitivity penalization is around 0.1dB in compare to the theoretical limit [Figure 3], which can be considered negligible.

By using the implemented prototype, we study the viability of optical coherent technology in free-space communications using compensation techniques and we try to achieve the theoretical limits [3]. Particularly, we study the limits imposed for different atmospheric conditions, aperture sizes and number of compensations modes applied at the receiver [Figure 4]

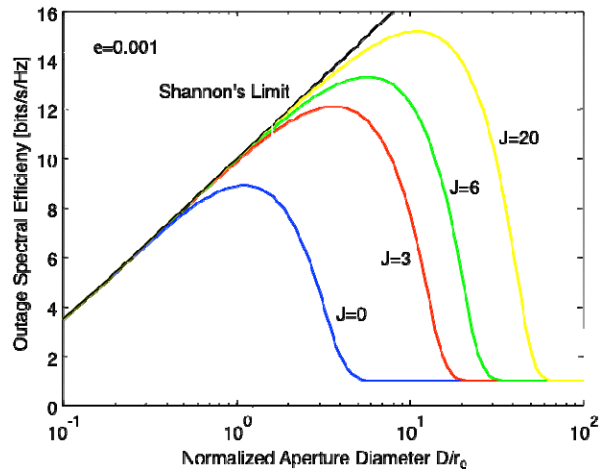


Figure 4. Outage spectral efficiency limit versus normalized aperture diameter for different number of compensation modes (J).

IV. Acknowledgments

This project is funded by the Spanish Department of Science and Innovation MICINN Grant No. TEC 2009-10025. The research of Esdras Anzuola is supported by a Spain MEC Secretary of State for Universities and Research Grant Fellowship.

V. References

- [1] L. C. Andrews, R. L. Philips, "Laser beam propagation through random media". Bellingham, SPIE Press, 2005.
- [2] R. K. Tyson, "Introduction to Adaptive Optics". Bellingham: SPIE Press, 2000.
- [3] A. Belmonte and J. Khan, "Performance of synchronous optical receivers using atmospheric compensation techniques," *Opt. Express* 16, 14151-14162, 2008.

Contributions to Radio Frequency Interference Detection and Mitigation in Earth Observation

Author: Giuseppe Francesco Forte, Thesis Advisor: Adriano Camps Carmona

contact email: giuseppe.forte@tsc.upc.edu

I. Introduction

Radio Frequency Interference (RFI) is the effect of unwanted energy due to one or a combination of emissions, radiations, or inductions upon reception in a system, manifested by any performance degradation, misinterpretation, or loss of information which could be extracted in the absence of such unwanted energy [1]. Sources of RFI may be artificial (generated by an electrical circuit) or natural (such as the Solar storms).

In order to mitigate these errors, RFI detection and mitigation systems and algorithms have been developed, thus more reliable measurements can be expected. In general, those algorithms require a lot of processing power, and the data needs to be stored for to be processed. The objectives of this Ph.D. thesis are to develop algorithms and implement them in real-time processing hardware to mitigate the RFI.

II. RFI Detection and Mitigation

RFI affects any kind of measure. While these effects range from a simple degradation of data to total signal corruption, in general it is necessary to remove those effects or at least detect them. One of the main applications is in radiometry because are very sensible instruments. RFI sources affect the radiometric data, leading to erroneous geophysical parameters. Communication and navigation systems are also affected. Almost all of RFI mitigation methods used in the radiometry field have been previously used in radio astronomy as described in [2].

The time variability of most interferences demands analysis on short time scales, implying a large amount of data to handle, and becoming especially true in case of surveys where several millions of spectra have to be analyzed for RFI mitigation.

The proposed Ph.D. thesis consists of the study of algorithms suitable for implementation in a real-time RFI detection and mitigation hardware system. In order to design and test the performance of some of these algorithms, they have been implemented first in software with synthetic signals, then tested with real data acquired with different instruments deployed in field experiments (e.g. PAU-SA [3], LAURA [4, 5] and MERITXELL [6]), and finally a few selected algorithms implemented in a FPGA.

III. RFI Detection and Mitigation Hardware

Previous studies [7, 8] have shown that not a single algorithm performs well in front of different types of RFI. Actually, a combination of several algorithms is required to improve the detection performance. Therefore the hardware to be developed will include Normality Tests, Spectrogram Analysis, and Wavelet Denoising Algorithms.

For wavelet denoising method [9] in which I am working [10], the interfering signal $\hat{s}(t)$ (RFI) is estimated without any a priori knowledge of it. This signal is then

subtracted from the received signal $x(t)$, to obtain a quasi RFI-free noise signal $\hat{n}(t) = x(t) - \hat{s}(t)$ from which the power is detected (Figure 1).

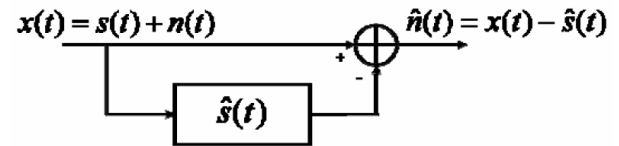


Figure 1. RFI mitigation technique: an estimate of the RFI signal $\hat{s}(t)$ is subtracted from the received signal $x(t) = s(t) + n(t)$, so as to obtain a quasi RFI-free noise signal

$$\hat{n}(t) = x(t) - \hat{s}(t)$$

Wavelet denoising algorithm is composed of three sequential steps:

1. Calculate wavelet transform of data as enters,
2. Calculate threshold coefficients, and
3. Calculate the inverse transform with the remaining components after thresholding.

To have a system operating in continuous mode without collapsing the memory, data must be processed before the next data block comes in. To achieve this, a three stage pipeline method has been devised, meaning that output data rate is the same as input data rate, with a latency.

At this moment, the Haar wavelet has been tested with results shown on Fig. 2. Also more wavelets will be tested to increase RFI mitigation, but only the ones that can be implemented on an FPGA and its computation can be done in real time will be ultimately implemented.

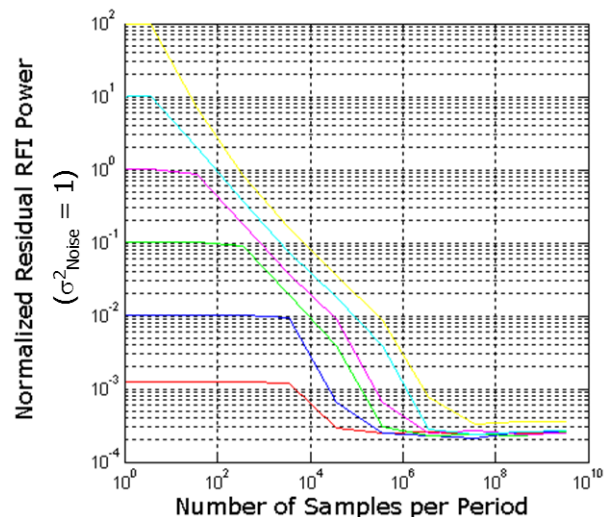


Figure 2. Normalized Residual RFI Power ($\sigma^2_{\text{Noise}} = 1$) vs. number of samples per period for with different INR: +20 dB (yellow), +10 dB (cyan); 0 dB (magenta); -10 dB (green); -20 dB (blue), and -30 dB (red). Sinusoidal RFI.

As an example result, to estimate the interference with an INR of -30dB, a sequence of 2^{21} sequence length with at least 36000 samples per period are needed for effective threshold estimation as shown in Figs. 3 and 4. Calculating again with 2^{21} samples: (2^{21}

samples) • (3 pipeline levels) • (9 ns) \approx 57 ms is now the latency. To obtain this, the data must be stored on internal block RAM for speed reasons.

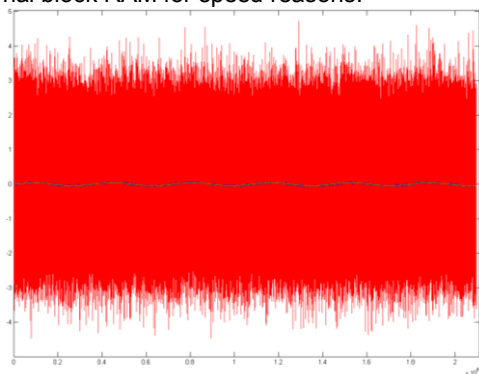


Figure 3. -30 dB Interference to Noise Ratio. Red=(Noise + interference) signals. Green=Interference signal (Sinusoidal at 360 Kilosamples per period). Wavelet estimated interference in blue.

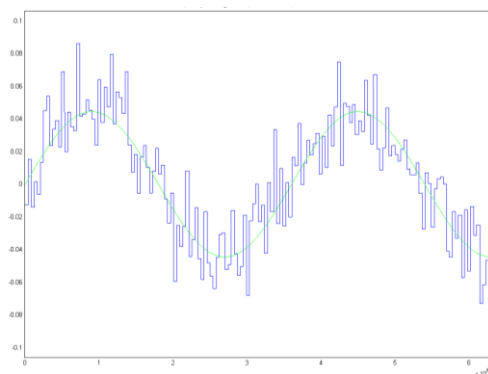


Figure 4. Zoom of Fig. 1. Interference signal in green. Wavelet estimated interference in blue. Red removed to enhance visibility.

IV. Acknowledgments

This work was supported by funds from the Spanish projects AYA2008-05906-C02-01/ESP, AYA2010-22062-C05-05 and AYA2011-29183-C02-01 from the Spanish Ministry of Science and Innovation and EU Feder.

V. References

- [1] "Handbook of Frequency Allocations and Spectrum Protection for Scientific Uses", Panel on Frequency Allocations and Spectrum Protection for Scientific Uses, Committee on Radio Frequencies, National Research Council, ISBN: 0-309-10301-0, 2007.
- [2] P. A. Fridman and W. A. Baan, "RFI mitigation methods in radio astronomy", *Astronomy and Astrophysics*, Vol. 378(1), pp. 327-344, Oct. 2001.
- [3] Ramos-Perez, I.; Forte, G.; Bosch-Lluis, X.; Camps, A.; Valencia, E.; Rodriguez-Alvarez, N.; Park, H.; Vall-llossera, M.; , "First results of the PAU-SA synthetic aperture radiometer," *Geoscience and Remote Sensing Symposium (IGARSS)*, 2011 IEEE International , pp.3633-3636, 24-29 July 2011
- [4] Camps, A.; Font, J.; Vall-llossera, M.; Gabarro, C.; Corbella, I.; Duffo, N.; Torres, F.; Blanch, S.; Aguasca, A.; Villarino, R.; Enrique, L.; Miranda, J.J.; Arenas, J.J.; Julia, A.; Etcheto, J.; Caselles, V.; Weill, A.; Boutin, J.; Contardo, S.; Niclos, R.; Rivas, R.; Reising, S.C.; Wursteisen, P.; Berger, M.; Martin-Neira, M.; , "The WISE 2000 and 2001 field experiments in support of the SMOS mission: sea surface L-band brightness temperature observations and their application to sea surface salinity retrieval," *Geoscience and Remote Sensing, IEEE Transactions on* , vol.42, no.4, pp. 804- 823, April 2004

- [5] Villarino, R.; Fernandez, J.; Camps, A.; Vall-llossera, M.; Corbella, I.; Duffo, N.; Torres, F.; , "Design and test of the L-band automatic radiometer (LAURA) temperature control," *Geoscience and Remote Sensing Symposium, 2005. IGARSS '05. Proceedings 2005 IEEE International*, vol.7, pp. 4902-4905, 25-29 July 2005
- [6] Tarongi, J.M.; Camps, A.; , "Multifrequency experimental radiometer with interference tracking for experiments over land and littoral: Meritxell," *Geoscience and Remote Sensing Symposium, 2009 IEEE International, IGARSS 2009* , vol.4, pp.IV-653-IV-656, 12-17 July 2009
- [7] Tarongi, J.M.; Camps, A.; , "Normality analysis as a radio frequency interference detection," *Microwave Radiometry and Remote Sensing of the Environment (MicroRad)*, 2010 11th Specialist Meeting, pp.288-293, 1-4 March 2010
- [8] Depau, V.; Tarongi, J.M.; Forte, G.; Camps, A.; "Preliminary performance study of different Radio-Frequency Interference detection and mitigation algorithms in microwave radiometry", *Proceedings of the IEEE, MICRORAD 2012*, March 2012
- [9] Walker, J.S. "A Primer on Wavelets and Their Scientific Applications," 2nd ed.; Chapman & Hall/CRC: Boca Raton, FL, USA, 2008
- [10] Forte, G.F.; Tarongi, J.M.; Camps, A.; , "Hardware implementation of a wavelet-based radio frequency interference mitigation algorithm for microwave radiometers," *Geoscience and Remote Sensing Symposium (IGARSS)*, 2011 IEEE International , pp.2241-2244, 24-29 July 2011

Simulation, detection and classification of vessels in maritime SAR images

Author: Luis E. Yam Ontiveros, Thesis Advisor: Jordi J. Mallorquí

contact email: {eduardo.yam,mallorqui}@tsc.upc.edu

I. Introduction

Synthetic Aperture RADAR (SAR) is a wide spread technique used in the microwave remote sensing community for acquiring images of the Earth's surface on any location. Its success resides on its capability of synthesizing a large antenna (aperture) based on the flight path of the sensor. In this way, the azimuth (cross-track) resolution is greatly enhanced in comparison with a real aperture RADAR system. Moreover, the frequencies deployed by SAR systems are in the range of the microwaves in which the radar signal can pass through the clouds and precipitations with little or no deterioration. Thus, the SAR images can be acquired virtually under any weather condition and independently of the present of natural illumination.

Nowadays, the orbital-based SAR sensor (Figure 1) is a mature technology. Through the last 30 years, the evolution of this system has provided each time better image resolutions. In the early years, the first SAR orbital sensors worked on a single polarization mode and offered image resolutions up to tens of meters, which was suitable for the acquisition of geophysical data in large areas. Current civilian systems such as TerraSAR-X or COSMO-SkyMed Constellation are able to provide polarimetric images and resolutions of about 1 meter. These improvements provide a wide range of possibilities in the development and analysis of algorithms for extracting special features from the SAR data, allowing the detection and classification of targets of different sizes and shapes.

In recent years, the characteristics of the orbital SAR sensors have been considered to be exploited as a part of vessel surveillance systems because: 1) these type of sensor can obtain images on any location of the sea surface regardless of the weather conditions and natural illumination, and 2) they are non-cooperative detection systems, i.e. the detection is performed independently of any acknowledgment from the targets. In this way, the orbital SAR sensors may complement traditional monitoring systems by expanding their covering area far from the coastal line and correlating data with cooperative systems such as AIS (Automatic Identification System) and VMS (Vessel Monitoring System) to highlight suspicious activity.

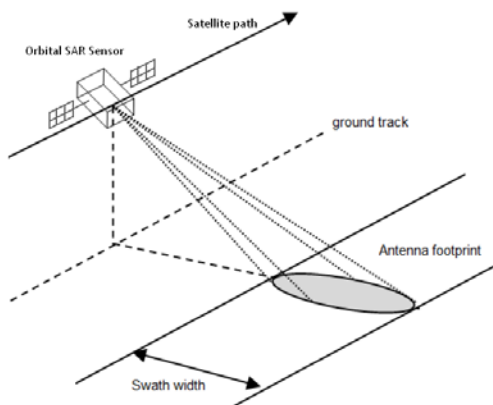


Figure 1. Diagram of orbital SAR system.

The main progress in the application of SAR technology to the vessel surveillance systems resides on the detection. Different algorithms have achieved a level of refinement which allows successful detection of vessels with low false alarm rates [1-3]. In contrast, the classification part still requires tackling great challenges related with the complex behavior of vessel's SAR images (signatures) in real maritime scenes:

- The vessels are complex targets regarding their scattering properties.
- The backscattering signatures are expected to change as a function of the angle of observation.
- The SAR technique assumes a static scene, but the vessels would not be, in general, static targets.
- Distortions and focusing aberrations of the SAR image due to the movement of the vessel.

Vessel classification is an emerging technology, and only few works have addressed the problem [2-9]. The classification still requires more improvements to achieve a level of robustness and refinement as we can find in the detection part. In this sense, our research project is focused on the development of new techniques to process high-resolution SAR signatures of vessels to extract characteristic features before the classification stage.

In this paper, Section II is devoted to the description of the methodology to follow in this research project, while its expected contributions are described in Section III.

II. Methodology

II.A. GRECOSAR: a SAR simulator of complex targets

Due to the approach of this project, working with SAR images requires a complete control of the scene that generates the signature of the vessel (e.g. type of vessel, its dynamics, sea state); it can be costly or even not always possible for SAR images from real orbital SAR sensors. Nevertheless, a practical solution is the use of flexible SAR simulators. In our case, we employ the numerical tool GRECOSAR [9], developed by the Universitat Politècnica de Catalunya (UPC). It is able to provide SAR raw data from virtually any target (including its dynamics) based on the corresponding 3D CAD models. Additionally, all radar parameters of the sensor can be adjusted for the simulations. These features make GRECOSAR a suitable tool to use throughout this project for the generation of the SAR images.

II.B. Autofocus processing and feature extraction

The core part of the project is the processing of the SAR signatures to extract a vector of characteristic features for the classification stage. In this sense, the project contemplates the implementation of an autofocus stage in order to increase robustness in identifying the desired features. This preprocessing will compensate focusing aberrations introduced by the dynamics of the vessels [9]. Thus, high-quality SAR signatures will be obtained. However, special

characteristics of the maritime scenes

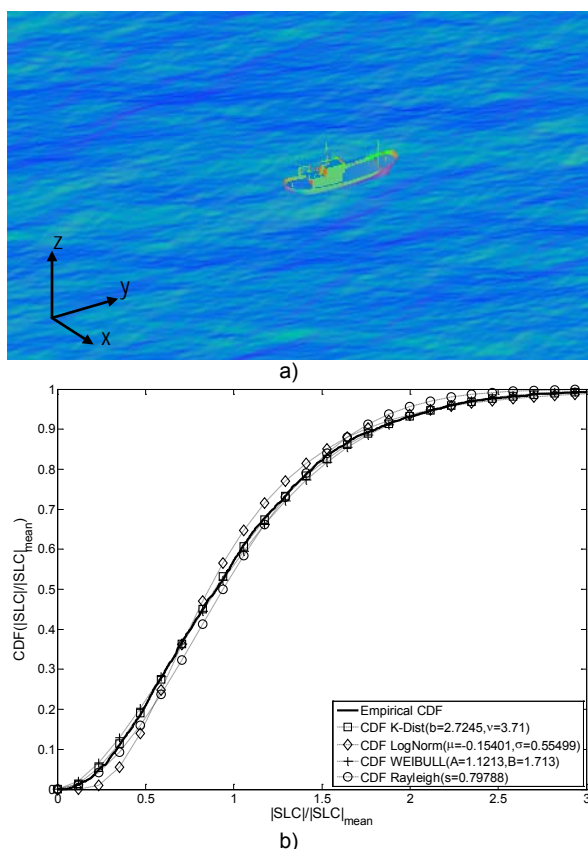


Figure 2. a) Detail of a maritime scene in GRECOSAR with the multi-harmonic model of the sea surface. b) Cumulative Distribution function (cdf) of the magnitude of the simulated sea surface model (empirical data) and theoretical cdfs related to the statistics of real sea clutter (K, Log-normal, Weibull and Rayleigh distributions); X-Band Sensor, HH channel of the simulated SAR image.

have to be considered. Many autofocus techniques assume that the scene is static and the causes of focusing error are the same over the whole SAR image. In general, that is not the case in maritime scenes: the target of interest (i.e. the vessel) has different dynamics than the surrounding area (i.e. the sea surface), which implies different focusing errors for the target and the background.

The applicability of classical autofocus algorithms to maritime scenes is being studied in the current stage of the project. A proper adaptation of these processes must focus the vessel's signature and ignore the focusing errors from the background due to the movement of the sea surface. In this sense, a merge of the best characteristics of the different classical autofocus techniques is being considered to obtain a process that suits the requirements of the SAR images from maritime scenes.

After the autofocus step, the SAR signature is suitable for the extraction of feature vectors related to its qualities. As a first approach, these feature vectors will consist of a combination of information regarding the physical dimensions of the SAR signature, the nature of the scatters and their distribution.

III. Expected contributions

This research project is yet in an early stage and the main advances have been done in the improvement

of the processing and modeling of the maritime scenes in GRECOSAR's simulations. In particular, it has been adapted a more realistic model of the sea surface (figure 2a). The statistics of its simulated SAR image presents a similar trend as the probabilistic distributions expected in real SAR images (figure 2b) [3]. These results suggest that this model is suitable for the simulations of real maritime scenes with GRECOSAR.

In a long-term perspective, through this research project we expect to provide the details about the best practices in processing the vessels' SAR signatures to improve their classification. Then, strategies can be established to take advantage of the existing space infrastructure in applications for maritime surveillance systems. Finally, this will have a direct impact on the development of the signal processing toolbox of the NEREIDS Project (FP7-SPACE-2010-1 contract 263468), which our research project is part of.

IV. Acknowledgments

This research work is being supported by the Spanish MICINN under project TEC2011-28201-C02-01 and the European Community under project NEREIDS (FP7-SPACE-2010-1 contract 263468).

V. References

- [1] D. J. Crisp, *The state-of-the-art in ship detection in synthetic aperture radar imagery*, Intell., Surveillance and Reconnaissance Div., Inf. Sci. Lab., Def., Sci. Technol. Org. Edinburgh, S.A., Australia, Res. Rep. DSTO-RR-0272, May 2004.
- [2] M. Tello, C. Lopez-Martinez, J.J. Mallorqui, "A novel algorithm for ship detection in SAR imagery based on the wavelet transform," *Geoscience and Remote Sensing Letters, IEEE*, vol. 2, no. 2, pp. 201-205, April 2005.
- [3] G. Ferrara, M. Migliaccio, F. Nunziata, A. Sorrentino, "Generalized-K (GK)-Based Observation of Metallic Objects at Sea in Full-Resolution Synthetic Aperture Radar (SAR) Data: A Multipolarization Study," *Oceanic Engineering, IEEE Journal of*, vol. 36, no. 2, pp. 195-204, April 2011.
- [4] S. Estable, F. Teufel, L. Petersen, S. Knabe, G. Saur, T. Ullmann, "Detection and classification of offshore artificial objects in TerraSAR-X images: First outcomes of the DeMarine-DEKO project," *OCEANS 2009 - EUROPE*, pp. 1-8, 11-14 May 2009.
- [5] G. Margarit, A. Tabasco, "Ship Classification in Single-Pol SAR Images Based on Fuzzy Logic," *Geoscience and Remote Sensing, IEEE Transactions on*, vol. 49, no. 8, pp. 3129-3138, Aug. 2011.
- [6] S. Brusch, S. Lehner, T. Fritz, M. Soccorsi, A. Soloviev, B. van Schie, "Ship Surveillance With TerraSAR-X," *Geoscience and Remote Sensing, IEEE Transactions on*, vol. 49, no. 3, pp. 1092-1103, March 2011.
- [7] G. Margarit, J.J. Mallorqui, "Scattering-Based Model of the SAR Signatures of Complex Targets for Classification Applications," *International Journal of Navigation and Observation*, vol. 2008, Article ID 426267, 11 pages, 2008.
- [8] R. Touzi, R.K. Raney, F. Charbonneau, "On the use of permanent symmetric scatterers for ship characterization," *Geoscience and Remote Sensing, IEEE Transactions on*, vol. 42, no. 10, pp. 2039-2045, Oct. 2004.
- [9] G. Margarit, J.J. Mallorqui, J. M. Rius, J. Sanz-Marcos, "On the Usage of GRECOSAR, an Orbital Polarimetric SAR Simulator of Complex Targets, to Vessel Classification Studies," *Geoscience and Remote Sensing, IEEE Transactions on*, vol. 44, no. 12, pp. 3517-3526, Dec. 2006.

Contributions to Free-Space Optical Communications through the Turbulent Atmosphere

Author: Ricardo Barrios, Thesis Advisor: Federico Dios

I. Introduction

For many decades the search for a probability density function (PDF) in free-space optical links capable to model the irradiance fluctuations has been exhaustive. Although many distributions have been proposed, the most widespread models nowadays are the Lognormal (LN) and Gamma-Gamma (GG) distributions. Albeit these models comply with the actual PDF data most of the time, neither of them works in all scenarios and, depending on the conditions, one of the two have to be chosen, depending on the particular link conditions. In this work, a new model is presented resulting in the exponentiated Weibull (EW) distribution. Particularly, it is shown how the proposed EW distribution offers an excellent fit to simulation and experimental data under all aperture averaging conditions, under weak-to-strong turbulence conditions, as well as for point-like apertures.

Expressions have been found to relate the defining parameters of the EW distribution to atmospheric parameters. Moreover, a new closed-form expression is derived for bit-error rate (BER) of on-off keying (OOK) modulation under EW fading.

II. New atmospheric turbulence fading model

II.A. Exponentiated Weibull fading

Let us first assume a very simple fading model. An optical wave propagating in the turbulent atmosphere, can be regarded as a circular complex Gaussian random field $U=X\exp(-j\varphi)$. Now let the received irradiance to be obtained from a nonlinear function of the squared modulus of the wave's amplitude. Such a nonlinearity is manifested in terms of a power parameter $\beta>0$, therefore, the received random irradiance $I=X^{2\beta}$ follows a Weibull distribution.

Models in which the fading is characterized by a single PDF are only valid for stationary conditions, where the statistics of the channel are somehow invariant over the observation time period. On the other hand, if the process of interest is nonstationary and the signal statistics vary significantly over the interval of interest, a mixture model is better suited, where a weighted summation of several statistical distributions can be used.

Let us now, extent the simple Weibull fading channel model. Assume an optical wave propagating in the turbulent atmosphere, with multiple scatterers and random refractive-index. As the wave travels through this medium, multipath scattering components start to appear and cause irradiance random fluctuations of the signal-carrying laser beam. The observed field at the receiver is, thus, composed by a line-of-sight (LOS) component and a weak multipath term, composed by scattered components via different independent non-LOS paths. The physical reason for this partition of the received optical field is supported by the high directivity inherent to laser beams sources.

By taking into account the above physical justification, the observed field irradiance I is assumed to be a weighted summation of several mutually independent ir-

radiance random variables

$$I^p = \sum_{i=1}^m w_i I_i^p, \quad (1)$$

where I_i are independent and identically distributed Weibull random variables (RV), and w_i are weighting factors accounting for the mean attenuation of each path. The line-of-sight component is denoted by I_1 , and there are $m-1$ non-LOS terms. Moreover, instead of a summation of linear components it is assumed the existence of a nonlinear relationship manifested in terms of a power parameter $p>0$. Now, supported by the fact that the LOS term is on average greater than the multipath component one can try to make an approximation of the summation in Eq. (1). The naive alternative would be to drop all the non-LOS, but this would led to the simple Weibull fading model derived above. Then, in order to approximate such summation to the LOS component, but still considering the non-LOS terms the maximum function can be introduced as

$$I = \lim_{p \rightarrow \infty} \left(\sum_{i=1}^m w_i I_i^p \right)^{1/p} = \max_{1 \leq i \leq m} \{ I_i \}, \quad (2)$$

Therefore, using the property of ordered statistics for the maximum of a sample the cumulative distribution function (CDF) of the irradiance is given by $F(I)=[F_w(I)]^m$, where $F_w(I)$ is the CDF of the Weibull RV. This type of distributions are referred in the literature as exponentiated distributions, where m is a nonnegative integer number. Nevertheless, it is a natural assumption to define $\alpha>0$ as the real valued extension of m . This allows for a less stringent model, where noninteger values may account for nonzero correlation among the components of different propagation paths [1].

Physical intuition tell us that the α parameter should be low for weak turbulence, as there are few scatterers lowering the probability of non-LOS components to appear, increasing to a maximum value somewhere in the moderate turbulence regime, as the number of scatterers increases too. Nevertheless, when approaching the strong turbulence regime this value should decrease as—although, there are a higher number of scatterers in the optical path—the non-LOS components easily deviate in such a way that the probability of missing the receiver increases. Moreover, the value of α can be lower than unity denoting deep fading events where, during the observation time period, on average even the LOS component can not reach the receiver.

II.B. Exponentiated Weibull PDF and CDF

The PDF and CDF of a random variable I described by the exponentiated Weibull (EW) distribution are given by

$$f_{EW}(I) = \frac{\alpha \beta}{\eta} \left(\frac{I}{\eta} \right)^{\beta-1} e^{\left(\frac{I}{\eta} \right)^\beta} \left[1 - e^{\left(\frac{I}{\eta} \right)^\beta} \right]^{\alpha-1}, \quad (3)$$

and

$$F_{EW} = \left[1 - e^{\left(\frac{I}{\eta} \right)^\beta} \right]^\alpha, \quad (4)$$

respectively; where $\beta > 0$ and $\alpha > 0$ are shape parameters related to the scintillation index σ_I^2 , and $\eta > 0$ is a scale parameter.

In a previous work [2], the expression for the shape parameter α as found to approximately follow

$$\alpha \simeq \frac{7.220 \sigma_I^{2/3}}{\Gamma(2.487 \sigma_I^{2/6} - 0.104)} \quad (5)$$

The shape parameter β as found to be related with Eq. (5) as

$$\beta \simeq 1.012 (\alpha \sigma_I^2)^{-13/25} + 0.142 \quad (6)$$

Finally, the scale parameter η is given by

$$\eta = [\alpha \Gamma(1 + 1/\beta) g_1(\alpha, \beta)]^{-1} \quad (7)$$

where $g_1(\alpha, \beta)$ is defined in [3, Eq. (18)].

II.C. Closed-form expression for BER under exponentiated Weibull fading

Assuming OOK modulation, the bit-error probability under atmospheric turbulence is given by

$$P_b = \frac{1}{2} \int_0^\infty \operatorname{erfc}\left(\frac{SNR_0 I}{2\sqrt{2}}\right) f(I) dI \quad (8)$$

where SNR_0 is the signal-to-noise ratio in the absence of atmospheric turbulence, $\operatorname{erfc}(\cdot)$ is the complementary error function, and $f(I)$ is the PDF of irradiance fluctuations.

In order to provide a closed-form solution to the integral in Eq. (8) the $\operatorname{erfc}(\cdot)$ can be expressed in terms of the Meijer's G-function $G_{p,q}^{m,n}[\cdot]$ [4, Eq. (8.2.1.1)]. Thus, the above integral can be solved leading to Eq. (9) (shown at the bottom of this page), where $\omega = 1 + j$, $\sigma = (\eta SNR_0)^2 / 8$, and l and k are integer numbers that satisfy the relationship $l/k = \beta/2$; and $\Delta(k, a)$ is defined in [5, Eq. (22)]. The particular implementation of the Meijer G-function used here correspond to the open source library for multiprecision floating-point arithmetic `mpmath` [6].

III. Experimental data analysis

In Fig. 1 the PDF, CDF and BER for an experimental testbed of 1.2km and receiver aperture diameter of 60mm are presented. The detailed conditions of the experimental scenario can be found in [7]. For the sake of comparison LN and GG curves are also shown. Here, the dash-dotted line corresponds to the EW model using the parameters derived from Eq. (5) through Eq. (7). Nevertheless, the rest of curves were plotted with parameters obtained using a Levenberg-Marquardt least-square fitting algorithm, for the corresponding distribution.

For the analysis of the probability of fade a fade threshold parameter F_T is introduced, and defined as the number of decibels below the mean irradiance.

It is readily seen how the EW offer a better fit to the experimental data, in moderate turbulence conditions. This good fitting have been also confirmed in weak and strong turbulence regime, and even outperforming—in some scenarios—the most widespread distribution in literature nowadays, i.e. the LN and GG distributions.

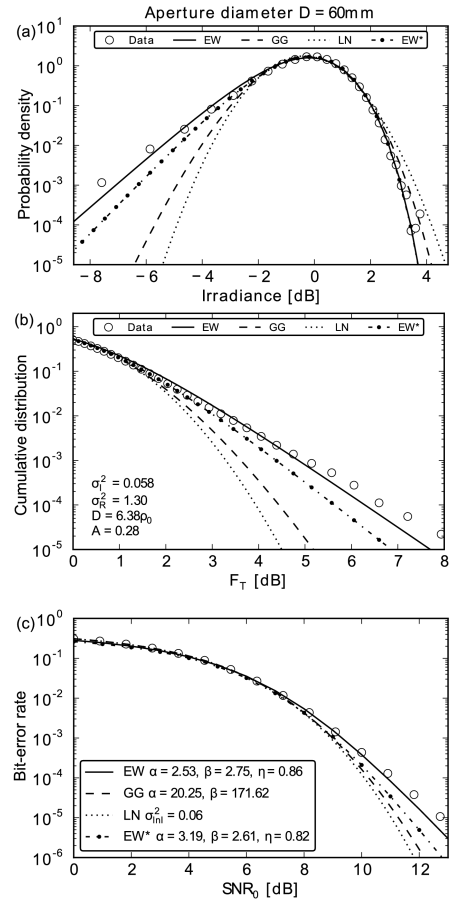


Figure 1. PDF, CDF and BER for experimental data, of a 1.2km testbed. The distribution parameter for the dash-dotted line (EW*) were obtained with the expressions derived in Sec. II.B.

IV. Acknowledgments

This work is supported with funding from the Spanish Ministry of Science and Innovation under contracts TEC2006-12722 and TEC2009-10025.

V. References

- [1] M. D. Yacoub, "The α - μ distribution: a physical fading model for the Stacy distribution," *IEEE Trans. Veh. Technol.*, vol. 56, no. 1, pp. 27–34, 2007.
- [2] R. Barrios, F. Dios, "Exponentiated Weibull model for the irradiance probability density function of a laser beam propagating through atmospheric turbulence," *unpublished*, 2012.
- [3] R. Barrios, F. Dios, "Exponentiated Weibull distribution family under aperture averaging for Gaussian beam waves," *Opt. Express*, vol. 20, no. 12, pp. 13055–13064, 2012.
- [4] A. P. Prudnikov, U. A. Brychkov, O. I. Marichev, *Integrals and Series Vol. 3*, 1990.
- [5] V. S. Adamchik, I. O. Marichev, "The algorithm for calculating integrals of hypergeometric type functions and its realization in REDUCE system," *Symp. Sym. Algebraic Comp.*, pp. 212–224, 1990.
- [6] F. Johansson, "mpmath: a Python library for arbitrary-precision floating-point arithmetic (version 0.17)," 2011.
- [7] R. Barrios, F. Dios, J. Reolons, A. Rodríguez, "Aperture averaging in a laser Gaussian beam: simulations and experiments," *Proc. SPIE*, vol. 7814, pp. 78140C, 2010.

$$P_b = \frac{\alpha \beta \sqrt{k \pi}}{2 \sigma (2 \pi)^{(l+k)/2}} \left(\frac{l}{\sigma}\right)^{\beta-1} \sum_{j=0}^{\infty} \frac{(-1)^j \Gamma(\alpha)}{j! \Gamma(\alpha-j)} G_{21, k+l}^{k, 21} \left[\left(\frac{\omega}{k}\right)^k \left(\frac{l}{\sigma}\right)^l \middle| \begin{matrix} \Delta(l, 1-\beta/2), \Delta(l, (1-\beta)/2) \\ \Delta(k, 0), \Delta(l, -\beta/2) \end{matrix} \right] \quad (9)$$

A Framework for the Design of Pilot Sequences and Precoders in Multiple-Antenna Systems

Author: Adriano Pastore, Thesis Advisor: Javier Rodríguez Fonollosa
contact email: {adriano.pastore,javier.fonollosa}@upc.edu

I. Introduction

Some seminal works from the end of nineties and beginning of the last decade sparked a strong interest in multiple-antenna systems for modern wireless communication systems, by showing that the use of multiple antennas at both transmitting and receiving user terminals can strongly potentiate data transmission speeds and link reliability [1][2]. The term "multiple-input multiple-output" (MIMO) systems was coined to designate such transmission systems. The benefits of MIMO technology apply to virtually any communication scenario, ranging e.g. from decentralized cooperative communications and device-to-device relaying to cellular radio systems, femtocells and indoor connectivity, etc.

The early theoretical results, however, rely on the somewhat overidealized assumption that the receiving terminals have immediate and perfect knowledge of the time-varying channel coefficients at no cost. In subsequent years, some research groups attempted to back off from this assumption, and extend the analysis of MIMO systems to more realistic scenarios. Though the multiple-antenna paradigm has already found its way into the mobile communication standards (e.g. IEEE 802.11n, HSPA, LTE, 4G), to the date of today, a full understanding is still a long way ahead.

In fact, the realistic assumption that the receiver has no a priori perfect and up-to-date knowledge of the time-varying channel coefficients entails a far more involved mathematical description. The information-theoretic treatment of such realistic communication conditions poses great challenges: the system behavior is not properly understood, and optimal coding schemes are known only for rare special cases.

To cope with these difficulties, a very common and popular approach is to insert a known pattern (so-called *pilot* symbols, or *training* symbols) into the transmit signal. The receiver knows when these known patterns are transmitted, and exploits them to deduce approximate values of the channel gains. Pilot-aided schemes achieve near-optimal performance results, while at the same time offering a simple decoding.

The main contributions of this PhD thesis consist in

- improving theoretical bounds and mathematical tools describing the system performance
- improving practical training-based transmission schemes for wireless communications
- gaining new insights into the couplings between decoding and estimation problems
- establishing a mathematical framework that allows to compute optimal resource tradeoffs between data transmission and channel parameter estimation

- trying new ways to transmit data fast and reliably with implicit channel estimation

II. Summary of contributions

II.A. System model

We typically consider a linear system model, in which a single transmitter encodes a message into a Gaussian signal vector X , that is sent over a channel with transfer matrix H . At the receiver side, the impinging signal HX is corrupted with thermal additive Gaussian noise N due to the amplifiers. The overall signal that the receiver observes is thus

$$Y = HX + N$$

From this noisy observation, the receiver infers which codeword was sent by the transmitter, and thus reconstructs the message encoded in the input signal X .

As said previously, the assumption that the value of H is perfectly known to the receiver greatly simplifies the analysis of such systems. However, in mobile communications, either the transmitter or the receiver is not static. Also, reflecting obstacles and scatterers (e.g., persons, vehicles) may be in permanent motion. This leads to random fluctuations of the value of the transfer matrix H . When the receiver totally ignores the current value of H , we say that the receiver tries to decode the input signal X *noncoherently*. By contrast, if the receiver knows H , the setting is said to be *coherent*.

The information-theoretic limits of noncoherent decoding are very difficult to investigate, and exact and constructive results are scarce. Additionally, the optimal decoding strategy would require a very high receiver complexity that cannot be handled by current technology. Therefore, in practical systems, the decoding task is decomposed into a two-stage approach: first, the transmitter sends pilot symbols, which the receiver knows. From its observation, the receiver generates an estimate of the transfer matrix H , which we shall call \hat{H} . Second, the transmitter sends data, and the receiver attempts to decode it as if the channel transfer matrix had the (approximate) value \hat{H} . In other words, the channel H is the sum of an approximation \hat{H} and an error term E , so that the receiver observes

$$Y = (\hat{H} + E)X + N$$

while knowing \hat{H} , but not E . This situation lies midway between the *coherent* and *noncoherent* settings.

There is a number of performance metrics that the system designer may wish to achieve: reliability, transmission speed, user fairness, etc. Depending on

which of these metrics is chosen, the designer may try to optimize several system parameters, namely:

- number of data streams to encode simultaneously
- number of pilot symbols at each training phase
- power levels of data and pilots
- precoding matrix used to generate the input X
- sequence of pilot symbols

Note that these parameters present mutual couplings, in the sense that changing one will affect the values of others. Previous works (e.g. [3][4][5]) have tackled part of these optimizations from different angles. The framework developed in this thesis proposes comprehensive methods to tackle the joint design of all or part of the above parameters.

II.B. Main results

Though in its full generality, the joint optimization problem is extremely involved and ambitious, one can still derive some essential properties of the jointly optimal solutions that drastically simplify its treatment. Among these, we point out three main results:

1. The directions of the pilot symbol vectors should be equal to the directions of the channel eigenmodes. Intuitively, one can understand this as follows: due to the presence of scatterers, the channel may present preferential transmit directions, and the pilot symbols should be chosen in alignment with these preferential directions
2. The number of pilot symbols should be always equal to the number of data streams transmitted simultaneously. Otherwise, one would waste transmit power
3. The highly complex joint optimization problem can be decomposed into different partial problems, which can be efficiently solved with numeric methods

II.C. Simulations

Figures 1 and 2 illustrate the performance gains that can be achieved when jointly optimizing the pilot symbols and the data precoder. On the y-axis, a performance metric known as the input-output mutual information is plotted against the signal-to-noise ratio (SNR). The mutual information is an information-theoretic quantity that can be assimilated to the transmission speed (in bits per symbol duration) or the spectral efficiency (in bits per second per Hertz).

Figure 2 shows the plots of Figure 1 normalized with respect to the case of no optimization, and over a lower SNR range. We can see that a low SNR values, joint optimization can yield strong relative improvements (approx. 3.5-fold increase at low SNR in this special case).

III. Conclusion

These contributions are of fundamental importance for paving the road towards a deep understanding of realistically operating MIMO systems and exploiting their full potential. The mathematical tools developed in this

thesis and related work, may, at some point, trickle down to practical applications and be transferred to wireless communication standards.

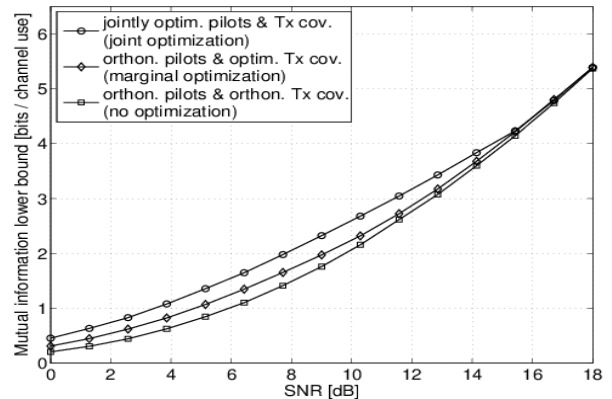


Figure 1. Mutual information as a function of the SNR, for three different systems: 1) jointly optimized pilots and precoder, 2) optimized precoder, 3) no optimization

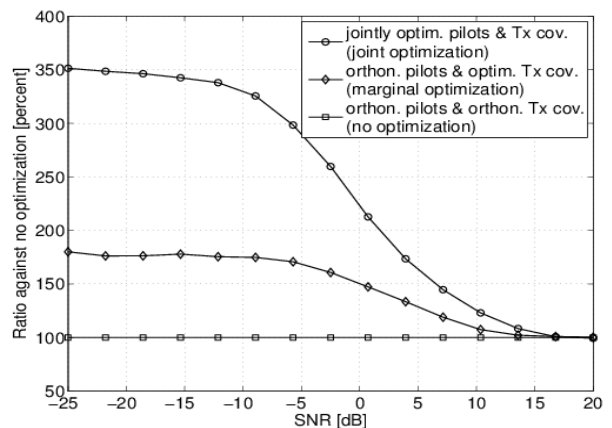


Figure 2. Same as Figure 1, but normalized with respect to the non-optimized case

IV. Acknowledgments

This work was supported by the Spanish Science and Technology Commissions and FEDER funds from the EC (TEC2006-06481/TCM, TEC2010-19171/TCM and CONSOLIDER INGENIO CSD2008-00010 COMONSENS) and 2009SGR1236 of the Catalan administration.

V. References

- [1] G. J. Foschini, "Layered space-time architecture for wireless communications in a fading environment when using multi-element antennas," *Bell Labs Technical Journal*, vol. 1, no. 2, pp. 41–59, 1996.
- [2] E. Telatar, "Capacity of multi-antenna Gaussian channels," *European Transactions on Telecommunications*, vol. 10, pp. 585–595, 1999.
- [3] B. Hassibi and B. Hochwald, "How much training is needed in multiple-antenna wireless links?" *IEEE Transactions on Information Theory*, vol. 49, no. 4, pp. 951–963, April 2003.
- [4] T. Yoo and A. Goldsmith, "Capacity and power allocation for fading MIMO channels with channel estimation error," *IEEE Transactions on Information Theory*, vol. 52, no. 5, pp. 2203–2214, May 2006.
- [5] A. Lozano, "Interplay of spectral efficiency, power and Doppler spectrum for reference-signal-assisted wireless communication," *IEEE Transactions on Wireless Communications*, vol. 7, no. 12, pp. 5020–5029, Dec. 2008.

Demand-Side Management via Distributed Energy Generation and Storage Optimization

Author: Italo Atzeni, Thesis Advisors: Javier R. Fonollosa, Luis G. Ordóñez
 contact email: italo.atzeni@upc.edu

I. Introduction

Demand-side management (DSM), distributed energy generation (DG), and distributed energy storage (DS), are considered increasingly essential elements for implementing the smart grid concept and balancing massive energy production from renewable sources.

We focus on a smart grid in which the demand-side comprises traditional users as well as users owning some kind of distributed energy sources and/or energy storage devices. By means of a day-ahead optimization process regulated by an independent central unit, the latter users aim to reduce their monetary energy expense by producing or storing energy rather than just purchasing their energy needs from the grid.

Considering the selfish nature of the users, a game theoretical approach is particularly suitable in order to calculate the optimal production and storage strategies of the demand-side users. For this reason, we model the day-ahead optimization problem as a noncooperative Nash game and we analyze the existence of the solutions, which correspond to the well-known concept of Nash equilibria. Assuming a practical pricing model, we devise a distributed algorithm to be run on the users' smart meters, which provides the optimal production and/or storage strategies, while preserving the privacy of the users and minimizing the required signaling with the central unit.

Simulations on a realistic situation show that the demand curve resulting from optimization is sensibly flattened, reducing the need for carbon-intensive and expensive peaking power plants. Finally, the approach presented here, being directly applicable to end users like households and small businesses, can also be extended to larger contexts, such as small communities or cities. In fact, flattening the energy demand along time is clearly beneficial at any layer or scale of the energy grid. The work illustrated in the following sections is presented in detail in [1].

II. Day-ahead Optimization

II.A. Smart Grid Model

The modern power grid is a complex network comprising several subsystems (power plants, transmission lines, substations, distribution grids, and consumers), which can be conveniently divided into: (i) *Supply-side*: it includes the utilities (energy producers and providers), the energy transmission network, and the energy distribution networks; (ii) *Central unit*: it is the regulation authority that coordinates the grid optimization process; (iii) *Demand-side*: it incorporates the end users (energy consumers), eventually equipped with distributed generation and/or distributed storage.

In particular, demand-side users adopt a control device, commonly known as smart meter, which communicates with the supply-side and manages their energy demand. Hence, each user is connected not only to the power distribution grid, but also to a communication infrastructure that enables two-way communication

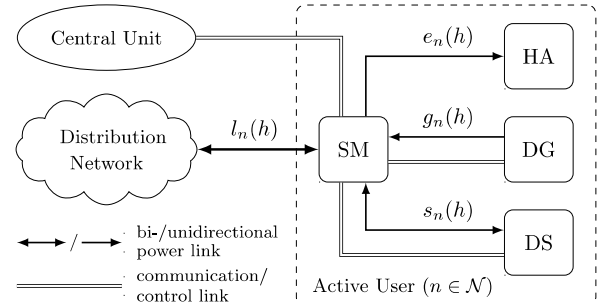


Figure 1. Connection scheme between the smart grid and one active user consisting of: smart meter (SM), home appliances (HA), distributed energy generation (DG), and distributed energy storage (DS).

between his smart meter and the central unit (as shown in Figure 1).

II.B. Energy Production and Storage Model

Energy producers can generate energy either to power their own appliances, to charge a storage device, or to sell it to the grid during peak hours. We distinguish between non-dispatchable energy producers (using, e.g., renewable resources of intermittent nature such as solar panels or wind turbines) and dispatchable energy producers (using, e.g., internal combustion engines, gas turbines, or fuel cells). The former have only fixed costs, which implies no strategy regarding energy production, whereas the latter have also variable production costs (such as the fuel cost) and, therefore, they are interested in optimizing their production strategies.

On the other hand, distributed energy storage allows to adapt renewable energy production to energy consumption, both of which can vary randomly over time. Additionally, it helps to alleviate the peak of the users' demand by maintaining energy consumption at a more constant level.

II.C. Energy Cost and Pricing Model

Traditionally, residential users have always paid a fixed price per unit of electricity representing an average cost of power generation over a given time interval, regardless of the actual generation cost. In contrast, in our model, the retail prices are connected with the generation costs, which vary quadratically according to the aggregate energy load at each time-slot. A more comprehensive model employing generalized grid cost functions is analyzed in [2]. Furthermore, at a given time interval, an eventual energy surplus is fed through the transmission system into the supply-side.

The cumulative expense over the time period of analysis represents the cumulative monetary expense incurred by the end user to consume, produce, and store the desired amount of energy over the time period of analysis. Note that, in general, the amount of money paid/received by a demand-side user to purchase/sell the same amount of energy from/to the grid is different

during distinct time-slots due to the fact that the grid cost function and the aggregate per-slot energy load are variable along the day.

II.D. Game Theoretical Formulation

By participating in the day-ahead optimization process, demand-side users commit to follow strictly the resulting consumption pattern. Moreover, we suppose that users know exactly their energy requirements at each time-slot in the time period of analysis in advance, neglecting any real-time fluctuation of such demand. A day-ahead bidding system that allows real-time deviations of the end users' consumption, together with a pricing system with penalties that aims at limiting these deviations, is presented in [3].

Our day-ahead optimization process works as follows. First, the grid energy prices for the time period of analysis are fixed by the supply-side in the day-ahead market-clearing process. Then, each demand-side user reacts to the prices provided by the central unit through iteratively adjusting his generation and storage strategies and, thus, his day-ahead energy demand, given the aggregate energy loads.

One could consider to solve the previous optimization problem in a centralized fashion, with the central unit imposing every active user how much energy he must produce, charge, and discharge at each time-slot. However, this represents a quite invasive solution, since it requires each user to provide detailed information about his energy production and/or storage capabilities. Indeed, these privacy issues may discourage the demand-side users to subscribe to the optimization process. Besides, a centralized approach is not scalable and cannot account for an unpredictably increasing number of participants.

In consequence, we are interested instead in a fully distributed solution and, hence, a game theoretical approach is remarkably suitable to accommodate our optimization problem. In this regard, each user is a player who competes against the others by choosing the production and storage strategies that minimize his cumulative expense over the time period of analysis. Since these individual strategies impact the grid energy price of all users, this leads to a coupled problem where the desired solution is an equilibrium point where all users are unilaterally satisfied. Note that the individual strategies are not revealed among the users in any case, and only the aggregate energy load, which is determined at the central unit adding the individual day-ahead energy demands, is communicated by the central unit to each active user.

III. Results

We consider a smart grid comprising 1000 demand-side users, with 18% of active users equally distributed among dispatchable energy producers, energy storers, and dispatchable energy producers-storers. Moreover, each demand-side user has a random energy consumption curve with daily energy consumption ranging between 8 kWh and 16 kWh.

As expected, energy storers charge their battery at the valley of the energy cost, resulting in a substantially more flattened demand curve. Contrarily, they discharge it at peak hours, shaving off the peak of the load. Likewise, dispatchable producers generate few energy dur-

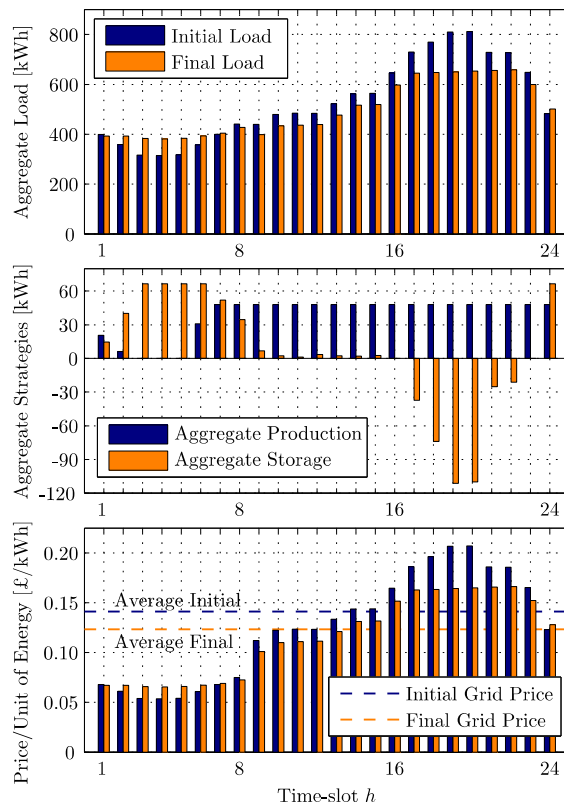


Figure 2. Aggregate per-slot initial and final energy loads; aggregate per-slot energy production and storage; initial and final grid prices per unit of energy.

ing night-time hours, when they rather purchase it from the grid.

The average grid price per kWh reduces from 0.1412 £/kWh to 0.1234 £/kWh (12.6% less). Moreover, the total expense of all demand-side users reduces from 1704 £ to 1426 £ (16.3% less). Lastly, the peak-to-average ratio decreases from 1.5223 to 1.3129 (13.8% less) resulting in a generally flattened demand curve. The comparison between the initial and the final aggregate loads and grid prices, as well as the aggregate production and storage strategies, are illustrated in Figure 2.

IV. Acknowledgments

This work was supported in part by the Spanish Ministry of Economy and Competitiveness (CONSOLIDER CSD2008-00010 COMONSENS, and TEC2010-19171 MOSAIC), the Catalan Government (2009 SGR-01236 AGAUR).

V. References

- [1] I. Atzeni, L. G. Ordóñez, G. Scutari, D. P. Palomar, and J. R. Fonollosa, "Demand-side Management via Distributed Energy Generation and Storage Optimization," *IEEE Trans. on Smart Grid*, 2012. DOI: 10.1109/TSG.2012.2206060
- [2] I. Atzeni, L. G. Ordóñez, G. Scutari, D. P. Palomar, and J. R. Fonollosa, "Optimization of Distributed Energy Generation and Storage in the Demand-side of the Smart Grid: A Variational Inequality Approach," *IEEE Trans. on Signal Proc.* (Submitted), 2012.
- [3] I. Atzeni, L. G. Ordóñez, G. Scutari, D. P. Palomar, and J. R. Fonollosa, "Day-Ahead Bidding Strategies for Demand-Side Expected Cost Minimization," *IEEE Int. Conf. on Smart Grid Comm. (SmartGridComm)* (Submitted), 2012.

MOSAIC: Multilateral agreements for clinical data exchange

Author: Magí Lluch-Ariet and Albert Brugués de la Torre

Thesis Advisors: Josep Pegueroles-Vallés and Francesc Vallverdú-Bayes

contact email: magi.lluch@upc.edu

I. Introduction

Worldwide collaboration is a fact in most areas of activity and often implies some exchange that is facilitated when the items to transfer correspond to knowledge or information, easily transmitted digitally. Local repositories of data are growing and growing and the search of valuable information becomes very complex or impossible to be managed manually in certain frameworks. We can find an example of this in the healthcare domain.

Clinicians often need to compare the information collected from the experiments performed to their patients with information from similar patients in other places. This is needed for accurate diagnosis, theragnosis, effective management of the diseases and efficient use of drugs.

Ethical and legal regulations that apply to personal data, and the associated data access authorisations to be provided by ethical committees, must be integrated in any negotiation process for data exchange. Under the assumption that the access rights to a certain dataset are given, a clinician may also add some additional constrain and give access to the data only if another dataset is given. However, bilateral agreements between two clinical centres will not always solve those constrains and involving a set of centres in multilateral agreements for data exchange would increase the amount of data potentially accessible in the network.

The problem of solving multilateral agreements can be mapped to the problem of finding the shortest path to connect a set of nodes in a network, that could be rapidly solved using the Dijkstra algorithm [1], but this is possible only if the links between the nodes are known and the topology of the whole network available in a centralised place. In many scenarios neither the information of the network topology is available in a single place nor this information is complete. As an example of this, a clinician may accept to publish the reference of which datasets are available from his local repository, but the specific constrains to give access to them may not be informed before a explicit data access request from a specific centre is received. Thus, a centralised approach to solve this problem is not feasible and distributed and dynamic mechanisms for the exploration of the paths associated to possible multilateral agreements are needed.

II. The MOSAIC System

II.A. A Use Case to illustrate the system

An example that illustrates how a system for clinical data sharing may work is the following. Consider a clinical framework in which patients are classified in different classes (A, B, C, ...) and for each class there is a set of possible diagnoses (A1, A2, ...).

- **Node-I** Hosts a Data Mart (local database of the node, part of the federated data warehouse of the whole network) of cases 'class A' (including all

possible diagnoses in the class). Exceptionally a new patient 'class B' needs to be diagnosed and the clinician wants to compare it with some other cases (class B) from some external nodes, already diagnosed as B1.

- **Node-II** Hosts a Data Mart of patients 'class B' with an exceptional considerable number of cases diagnosed as B1. A new patient 'class B' needs to be diagnosed and the clinician wants to compare it with some other cases from external nodes already diagnosed as B2.
- **Node-III** Hosts a Data Mart composed by data of class B, with an exceptional considerable number of cases diagnosed as B2, but without a single case diagnosed as B1. A new case 'class A' needs to be diagnosed and the clinician wants to compare it with other cases already diagnosed as A1 in other centres.

There is not any bilateral agreement for data interchange from the three nodes that solves the data access needs. However, as shown in Figure 1, the agreement is possible among the three nodes as follows:

- Node-III gives the access rights to Node-II for accessing to the cases already diagnosed as B2
- Node-II gives access rights to its cases diagnosed as B1 to Node-I
- Node-I gives access rights to its cases diagnosed as A1 to Node-III



Figure 1. Example of multilateral agreement for data exchange.

II.B. The MOSAIC Architecture

The mechanisms to implement the negotiation process to achieve multilateral agreements fit with the Intelligent Agents framework. The following Agents compose the ecosystem of MOSAIC:

Multicast Contributor Agent (MCC). Activated by the user to offer a certain dataset to the network, with or without constrains.

Unicast Contributor Agent (UCC). Activated by the MCC to negotiate a specific data access request sent by a MCP.

Multicast Petitioner Agent (MCP). This Agent is activated by the user or by a Unicast Petitioner Agent. The user launches it in order to explore the network looking for a certain data set. The UCP launches it in order to solve a constrain from a UCC when the dataset requested is not available at the node of the UCP.

Unicast Petitioner Agent (UCP). Activated by the MCP in order to negotiate a specific data access request with a UCC.

Yellow Pages Agent (YP). This Agent provides the directory service and hosts the list references of MCC active in the network.

III. The MOSAIC negotiation process

From the launch of a data set request by the User to the data delivery and all the corresponding intermediate steps to solve the possible constrains, the MOSAIC protocol follows a process with the following five stages:

- **Stage 1:** Network exploration
- **Stage 2:** Agreement proposal notification
- **Stage 3:** Agreement selection and notification
- **Stage 4:** Data transfer
- **Stage 5:** Transaction completion

During the Network Exploration the MCP asks the YP to obtain the list of MCC to whom the data access requests can be addressed. The reference of the MCC delivered by the YP, are those hosting a dataset of the type requested by the MCP. For each MCC three situations may arise:

- **No constrain:** The MCC offers the requested data set with no constrains to fulfill through a UCC. The UCP receives the notification of the data set availability and notifies this to the MCP.
- **Constrain solved locally:** The constrain of the MCC can be solved locally at the requesting node of the MCP. The UCP asks to its MCP to look for the MCC active in its node in order to collect the data from its DataMart. The UCP sends the notification of the dataset availability at the UCC and after the potential fulfillment of the constrain, the UCC sends the agreement for the possible dataset transfer initially requested to the UCP. Both UCC and UCP notify to their MCC and MCP their agreement for the potential exchange of the corresponding datasets.
- **Constrain to be solved externally:** The MCC constrain cannot be solved locally at the requesting node of the MCP. If the length of the path does not exceed the limit (monitored through a Time To Live -TTL- parameter), the UCP launches a new MCP to look for the data set needed in order to solve the constrain.

IV. Evaluation and results

The scenario evaluation used corresponds to a set of nodes (cities) hosting each of them a number of datasets with clinical cases of brain tumour (see Table1). While some datasets are freely offered to the network without any restriction, most of them have a constrain associated, requiring the delivery of some other dataset from some other node.

Brain and CNS Tumors		USA network 205 Nodes	
Class	Histology	Datasets	Cases
A	Tumors of Neuroepithelial Tissue	859	41.360
B	Tumors of Cranial and Spinal Nerves	201	12.750
C	Tumors of Meninges	238	54.380
D	Lymphomas and Hematopoietic Neoplasms	95	2.690
E	Germ Cell Tumors and Cysts	14	240
F	Tumors of Sellar Region	227	20.360
G	Local Extensions from Regional Tumors	1	10
H	Unclassified Tumors	189	6.720

Table 1. Dataset of the scenario evaluation. Brain tumors by major histology groupings.

The evaluations have considered two criteria for the MCC selection among those offering the requested data: i) A random selection; and ii) A selection based on the data set size on the MCC node.

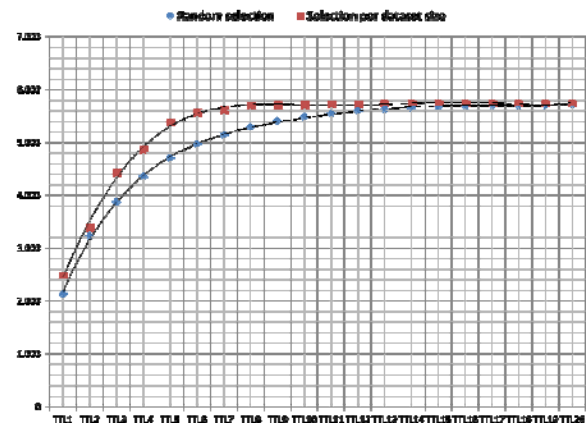


Figure 2. Number of agreements with different TTL values.

The results show an increase in the total number of agreements when the selection of the MCC is based on the dataset size (see Figure 2).

V. Acknowledgments

We would like to thanks our colleagues from the Telematics Engineering department, for the inspiring discussions we had with them, and the Central Brain Tumor Registry of the United States for the possibility to use the CBTRUS database in this research.

VI. References


- [1] E. W. Dijkstra. A note on two problems in connexion with graphs. *Numerische Mathematik*, 1:269-271, 1959. 10.1007/BF01386390.
- [2] Central Brain Tumor Registry of the United States. Statistical report: Primary brain tumors in the united states (2004-2008). web site. <http://www.cbtrus.org/>

The Doctoral Programme in Computer Architecture

2011/2012 academic year

This Ph.D. program is managed by the Computer Architecture Department (DAC) and its main objective is to train researchers with international competence in some of the areas covered by the programme: computer architecture, operating systems, communications and networks of computers, and microelectronic design. These researchers will be called on to contribute, within their fields of experience, to scientific, technical, social and economic progress, with the industries and institutions in which they will perform their professional tasks. In the field of teaching, the doctoral programme will also have the objective of training the lecturers who will be responsible for university teaching in the areas of knowledge covered by the programme. To achieve these objectives, the program defines two specializations: 1) High-performance Computing and Technology and 2) Communication Networks and Distributed Systems.

The Ph.D. program on Computer Architecture at UPC has obtained the so called "Mención de Calidad" from the Spanish Ministry of Education and Culture, recognizing its quality and relevance, reference MCD2003-00126 (resolution published in the Spanish BOE -- May 28, 2003) and renewed for academic years 2004/05, 2005/06, 2006/07, 2007/08, [2008/09 and until 2009/10](#), and the Excellence Mention for academic years 2011/12, 2012/12 and 2013/14 (MEE2011-0361). The program has been awarded on September 2012 with the *Verifica* stamp by the National Agency for Quality Assessment.

The program in numbers (2011/2012 academic year)	UPC 
New students	28
Students in the training period	11
Students in the research period	148
Thesis proposals	15
Ph.D. thesis presented	20
Total number of students 11/12	159

Ph.D. students will carry out their training and research activities strongly linked to one of the 8 research groups at DAC and may be also candidates to join some of the research teams working at any of the research labs hosted by the DAC's research groups.

Research groups	Contact person
ANA – Advanced Network Architectures	Dr. Xavi Masip, xmasip@ac.upc.edu
ARCO – Architectures of Compilers	Dr. Antonio González, antonio@ac.upc.edu
CAP – High Performance Computing	Dr. Mateo Valero
CBA – Broadband Communications Systems	Dr. Jordi Domingo
CNDS – Computer Networks and Distributed Systems	Dr. Jorge García
DAMA – Data Management	Dr. Josep Lluís Larriba
DMAG – Distributed Multimedia Applications Group	Dr. Jaime Delgado
ICARUS – Intelligent Communications and Avionics for Robust Unmanned (Aerial) Systems	Dr. Enric Pastor

The Computer Architecture Department leads the following research centers at the Universitat Politècnica de Catalunya:

CCABA: Advanced Broadband Communications.

<http://www.ccaba.upc.edu/>

CRAAX: Advanced Network Architectures Lab.

<http://www.craax.upc.edu>

CRAE: Centre de Recerca de l'Aeronàutica I de l'Espai

<https://recerca.upc.edu/crae>

Some of the DAC's research groups are also actively working with the following research institutions :

BSC : Barcelona Supercomputing Center – Centro Nacional de Supercomputación

<http://www.bsc.es>

Es-CERT-UPC : Spanish Computer Emergency Response Team.

<http://escert.upc.edu>

Intel-Labs Barcelona.

<http://www.intel.com/jobs/spain/sites/barcelona.htm>

The Doctoral Programme in Computing 2011/2012 academic year


Since 1985 the Department of Software (LSI) offers a PhD Program oriented to the research areas related to the analysis, design and use of software. This means, in particular, research areas such as: information systems and databases, software engineering, programming methodology, formal methods, computational complexity, analysis and design of algorithms, bioinformatics, computer-aided geometric design, virtual reality and synthesis of realistic images. In order to focus scientific and methodological skills on specific topics, the programme has been structured around three core areas:

- Algorithms and Programming,
- Information Systems, and
- Visualization, Virtual Reality and Graphic Interaction.

Each research area offers a set of courses and seminars and in addition research projects within the corresponding research groups.

The research work is developed within international networks and European and national projects with a great number of national and international partners. These collaborations always involve directly or indirectly PhD students, as the research that is carried out is supported by the established research network and connections. At present the program has the distinctions of quality and internationality of the Spanish and Catalan administrations.

In this context, the department of LSI has led the starting of a master of research in Computing which addresses specialized teaching in the three core research areas.

The program in numbers (2011/2012 academic year)	UPC 
New students	18
Students in the training period	4
Students in the research period	43
Thesis proposals	5
Ph.D. thesis presented	6
Total number of students 09/10	61

Research work in the PhD in Computing program is carried out inside of different autonomous Research Groups which develop basic as well as applied research.

Research groups	Contact person
<u>ALBCOM</u> : Algorithms, Bioinformatics, Complexity and Formal Methods	Dr. Josep Díaz, diaz@lsi.upc.edu Dr. Fernando Orejas, orejas@lsi.upc.edu
<u>GESSI</u> : Software Engineering for Information Systems Research Group	Dr. Pere Botella, pere.botella@upc.edu Dr. Xavier Franch, franch@essi.upc.edu
<u>GIE</u> : Computer Science in Engineering	Dr. Robert Joan, robert@lsi.upc.edu Dr. Lluís Solano, lluis@lsi.upc.edu
<u>LARCA</u> : Laboratory for Relational Algorithmics, Complexity and Learnability	Dr. Ricard Gavaldà, gavald@lsi.upc.edu
<u>LOGPROG</u> : Logic and Programming	Dra. Maria Lluïsa Bonet, bonet@lsi.upc.edu Dr. Robert Nieuwenhuis, roberto@lsi.upc.edu
<u>MOVING</u> : Research Group on Modelling, Interaction and Visualization in Virtual Reality	Dra. Isabel Navazo, isabel@lsi.upc.edu
<u>MPI</u> : Information Modeling and Processing	Dr. Ernest Teniente teniente@essi.upc.edu Dr. Antoni Urpí, urpi@essi.upc.edu

The staff involved in the Doctoral Programme in Computing leads or participates in the following multi-disciplinary research centers or spin-off companies originated at the Universitat Politècnica de Catalunya:

Barcelogic, <http://barcelogic.com>

CTO and founder: Roberto Nieuwenhuis

CEBIM - Centre de Biotecnologia Molecular, <http://algggen.lsi.upc.edu/cebim/>

Director: Pere Garriga, pere.garriga@upc.edu

CREB - Centre de Recerca en Enginyeria Biomedica, <http://www.creb.upc.edu/>

Director: Pere Caminal, pere.caminal@upc.edu

CRNE - Centre de Recerca en Nanoenginyeria, <https://www.upc.edu/crne/>

Director: Ramón Alcubilla, ramon.alcubilla@upc.edu

CRG - Centre for Genomic Regulation, <http://pasteur.crg.es/portal/page/portal/Internet/>

Contact: comunicacio@crg.es

CRV: Centre de Realitat Virtual de Barcelona <http://moving.lsi.upc.edu/>

Director: Pere Brunet



Contact: crv@lsi.upc.edu

The Doctoral Program in Electronic Engineering

2011/2012 academic year

This Doctoral Program is jointly organized by the Electronic Engineering Department of the Universitat Politècnica de Catalunya (UPC) in Barcelona and the Physics Department of the Universitat de les Illes Balears (UIB) in Palma de Mallorca. The goal of the program is to offer highly motivated graduated students the possibility to extend their education in the various fields of research related with Electronic Engineering. The academic activities of the program are designed both to introduce the students to highly specialized research topics and to extend their skills with methodologies oriented to the tasks, tools and procedures required to develop a high quality innovative research activity. The Doctoral Program is closely linked with the Electronic Engineering Master, which is jointly organized by the TelecomBCN School at UPC and the Physics School at UIB. The courses and other activities offered in the framework of the Electronic Engineering Master provide the students enrolled in the Doctoral Program the necessary academic background for efficiently perform the research work in their Ph.D. Thesis.

The program has been awarded the Quality Mark (Mención de Excelencia) MEE2011-0690 by the Spanish Ministry of Education for the period 2011-2014.

The program in numbers (2011/2012 academic year)	UPC 	UIB 
New students	19	5
Students in the training period	18	11
Students in the research period	89	5
Thesis proposals	23	4
Ph.D. thesis defended	12	1
Total number of students 11/12	107	16
Professors of the Program	77	5

Please visit the web page for more detailed information:

<http://eel.postgrau.upc.edu>

During their Ph.D. thesis research at UPC the students are hosted in one of the 13 research groups with more than 16 research laboratories and facilities that cover a wide range of specialties in four main fields of investigation: Integrated Circuits and Systems, Industrial and Power Electronics, Measuring and Instrumentation, and Semiconductor Devices and Microsystems.

<http://www.eel.upc.edu/research>

Research groups	Contact person
Semiconductor Devices and Microsystems	
MNT- Micro and Nanotechnologies	Dr. Luis Castañer, luis.castaner@upc.edu
Integrated Circuits and Systems	
HIPICS- High Performance Integrated Circuits and Systems	Dr. Antonio Rubio, antonio.rubio@upc.edu
AHA- Advanced Hardware Architectures	Dr. Joan Cabestany, joan.cabestany@upc.edu
QINE- Low Power Design, Test, Verification, and Fault Tolerance	Dr. Joan Figueras, joan.figueras@upc.edu
Measuring Circuits and Biomedical Instrumentation	
GSS- Sensor Systems Group	Dr. Miguel García, miguel.j.garcia.hernandez@upc.edu
IEB- Electronic and Biomedical Instrumentation	Dr. Xavier Rosell, javier.rosell@upc.edu
SARTI- Remote Acquisition and Data Processing Systems	Dr. Antoni Manuel, antoni.manuel@upc.edu
ISI- Instrumentation, Sensors and Interfaces	Dr. Ramon Pallas, ramon.pallas@upc.edu
Industrial and Power Electronics	
EPIC- Energy Processing and Integrated Circuits	Dr. Alberto Poveda, alberto.poveda@upc.edu
MCIA- Motion Control and Industrial Applications	Dr. Luis Romeral, luis.romeral@mcia.upc.edu
TIEG- Terrassa Industrial Electronics Group	Dr. Josep Balcells, josep.balcells@upc.edu
SEPIC- Power and Control Electronics Systems	Dr. J.L. García de Vicuña, vicuna@eel.upc.edu
GREP- Power Electronics Research Group	Dr. Josep Bordonau, josep.bordonau@upc.edu

The Electronic Engineering Department leads the following multi-disciplinary research centers at the Universitat Politècnica de Catalunya:

CETpD: Technical Research Center for Dependency Care and Autonomous Living.

Contact person: Dr. Joan Cabestany (joan.cabestany@upc.edu), web: <http://www.upc.edu/cetpd/>

CRNE: Center for Research in NanoEngineering.

Contact person: Dr. Ramon Alcubilla (ramon.alcubilla@upc.edu), web: <http://www.upc.edu/crne/>

PERC: Power Electronics Research Centre.

Contact person: Dr. Josep Bordonau (josep.bordonau@upc.edu).

CREB: Center for Research in Biomedical Engineering.

Contact person: Dr. Pere J. Riu (pere.riu@upc.edu), web: <http://www.creb.upc.es/>

CRAE: Center for Research in Aeronautics and Space.

Contact person: Dr. J. Oscar Casas (jocp@eel.upc.edu), web: <http://recerca.upc.edu/crae>


The Doctoral Programme in Telematics Engineering

2011/2012 academic year

The PhD program in Telematics Engineering covers within the Information Technologies arena the necessity to provide a postgraduate instruction to study in depth the fundamental concepts of the telematics systems from the three basic points of view: networks, systems and services.

The objective of the Doctoral Programme is the formation of researchers with international recognition in the following research areas:

- **Telematic Services.** Development and proposal of services in terrestrial, wireless and VSAT communication networks. Audiovisual services, multimedia distributed systems, and corporative services in Internet and Intranet frameworks. Security services and e-business.
- **Wireless communications.** Cellular communications. Modelling of the user's behaviour from the mobility and traffic point of view. Mobility functions analysis (access, actualization, research and transferring). Study of enhancements to the protocols mainly used in Internet, for all kinds of environments, especially in wireless environments.
- **Design and Evaluation of Networks and Broad-Band Services.** Access and transport protocols. Analytic modeling of sources and protocols. Traffic analysis. Management of Networks. IP based networks, including routing, control and management. Multimedia services over broadband platforms, to be used for teleeducation, telemedicine, telework... Integration of the existent technologies at present (fixed, mobile or mixed) in a high velocity environment. Active networks and Agents.

The program in numbers (2011/2012 academic year)	UPC 
New students	8
Students in the training period	13
Students in the research period	43
Thesis proposals	11
Ph.D. thesis presented	7
Total number of students 11/12	56

During their Ph.D. thesis research the students are hosted in one of the research groups where the students are fully integrated.

Research groups	Contact person
BAMPLA - Design and Evaluation of Broadband Networks and Services	Dr. Sebastià Sallent, sallent@entel.upc.edu
GIRCEL - Cellular Networks and Location	Dr. Francisco Barceló, barcelo@entel.upc.edu
ISG - Information Security Group	Dr. Miquel Soriano, soriano@entel.upc.edu
MAPS - Management, Pricing and Services in Next Generation Networks	Dr. Joan Serrat, serrat@tsc.upc.edu
SERTEL - Telematic Services	Dr. Francisco Jose Rico, f.rico@entel.upc.edu
WNG - Wireless Networks Group	Dr. Josep Paradells, josep.paradells@entel.upc.edu Dr. Jordi Casademont, jordi.casademont@entel.upc.edu

The Department of Telematics Engineering leads or participates in the following multi-disciplinary research centers at the Universitat Politècnica de Catalunya:

CTTC: Centre Tecnològic de Telecomunicacions de Catalunya, <http://www.cttc.es/>

Director: Miguel Ángel Lagunas, m.a.lagunas@cttc.es

CCABA: Advanced Broadband Communications Center, <http://www.ccaba.upc.edu/>

Contact: info-ccaba@ac.upc.edu

I2CAT Foundation, <http://www.i2cat.net/>

Director: Sebastià Sallent i Ribes, sebastia.sallent@i2cat.net

The Doctoral Programme in Signal Theory and Communications

2011/2012 academic year


Since 1987 the Department of Signal Theory and Communications offers a PhD Program oriented to the scientific formation in the following areas:

- Communications with physical and radio support
- Study of phenomena associated to the generation, propagation and radiation of electromagnetic signals at frequencies ranging from RF/microwave to optical wavelength
- Basic techniques of the signal processing and its applications in communications, voice and image processing
- Telecommunication systems

There is a close connection between teaching contents and research carried out at the department, and makes intense use of the department's experimental facilities.

The research areas are developed within international networks and European projects with a great number of national and international partners. These collaborations always involve directly or indirectly the PhD students, since the research that they carry out is integrated into these projects. At present the program has the distinctions of quality and internationality of the Spanish and Catalan administrations.

In this context, the department of TSC has led the starting of a master of research on Information Technologies and Communications (MERIT Master) that has been selected by the prestigious European program Erasmus Mundus.

The program in numbers (2011/2012 academic year)	UPC 
New students	39
Students in the training period	6
Students in the research period	139
Thesis proposals	32
Ph.D. thesis presented	21
Total number of students 11/12	145

Research at the Signal Theory and Communications Department covers many different topics related to the information processing and transmission. Research is carried out by means of different autonomous Research Groups which develop basic as well as applied research.

Research groups	Contact person
Anntena Lab - Antennas and Radio Systems	Dr. Àngel Cardama, cardama@tsc.upc.edu
Array & Multichannel Processing	Dr. Lluís Jofre, jofre@tsc.upc.edu
Control, Monitoring and Communications Group	Dra. Ana Isabel Pérez, anuska@tsc.upc.edu
Optical Communications Group	Dr. Eduard Bertran, bertran@tsc.upc.edu
	Dr. José A. Delgado, delpen@tsc.upc.edu
	Dr. Josep Prat, jprat@tsc.upc.edu
	Dr. Sergio Ruiz, sruiz@tsc.upc.edu
Image and Video Processing Group	Dr. Jaume Comellas, Comellas@tsc.upc.edu
Mobile Communications Research Group	Dr. Josep Ramon Casas, josep@tsc.upc.edu
	Dr. Ramón Agustí, ramon@tsc.upc.edu
	Dr. Ferran Casadevall, ferranc@tsc.upc.edu
MAPS - Management, Pricing and Services in Next Generation Networks	Dr. Joan Serrat, serrat@tsc.upc.edu
Radio Frequency and Microwave Systems, Devices and Materials Group	Dr. Joan O'Callaghan, joano@tsc.upc.edu
Remote Sensing Research Group	Dr. Lluís Pradell, pradell@tsc.upc.edu
	Dr. Adriano Camps, Camps@tsc.upc.edu
	Dr. Jordi Mallorquí, mallorqui@tsc.upc.edu
	Dr. Francesc Rocadenbosch, roca@tsc.upc.edu
Signal Processing and Communications Group	Dr. Javier R. Fonollosa, fono@tsc.upc.edu
	Dr. Josep Sala, alvarez@tsc.upc.edu
Speech Processing Group	Dr. Francesc Vallverdú, sisco@tsc.upc.edu
	Dr. Javier Hernando, javier@tsc.upc.edu
WiComTec	Dra. Silvia Ruiz, silvia@tsc.upc.edu
	Dr. Joan Olmos, olmos@tsc.upc.edu
Audio Visual Technologies Group	Dr. Francesc Tarrés, tarres@tsc.upc.edu
High/Low Altitude Platforms Stations Group	Dr. José A. Delgado, delpen@tsc.upc.edu
	Dr. Eduard Bertran, bertran@tsc.upc.edu

The Department of Signal Theory and Communications leads or participates in the following multi-disciplinary research centers at the Universitat Politècnica de Catalunya:

ICFO: The Institute of Photonic Sciences, <http://www.icfo.es/>

Director: Lluís Torner, lluis.torner@icfo.es

CTTC: Centre Tecnològic de Telecomunicacions de Catalunya, <http://www.cttc.es/>

Director: Miguel Ángel Lagunas, m.a.lagunas@cttc.es

CCABA: Advanced Broadband Communications Center, <http://www.ccaba.upc.edu/>

Contact: info-ccaba@ac.upc.edu

TALP: Research Center for Technologies and Applications in Language and Speech, <http://www.talp.upc.edu>

Director: José Adrián Rodríguez Fonollosa, adrian@talp.upc.edu

I2CAT Foundation, <http://www.i2cat.net/>

Director: Sebastià Sallent i Ribes, sebastia.sallent@i2cat.net

The Doctoral Programme in Artificial Intelligence


2011/2012 academic year

Since 1985 the Software Department offers a PhD Program oriented to the scientific formation in the following areas:

- Knowledge Representation and Machine Learning
- Natural Language Processing
- Softcomputing
- Autonomous Agents

The main goal of the programme is to motivate students to take-up their research in the Cognitive Sciences and/or the Knowledge Engineering related areas. The emphasis in Cognitive Sciences suggests a basic interest in understanding the phenomena associated with Learning mechanisms, Natural Language Understanding, Mind and Intelligence, Perception, *etc.*

The Ph.D. program in Artificial Intelligence aims to provide the basis for a solid and strong research profile. Students completing the program are typically well qualified for teaching and research positions with colleges and universities as well as with national and international industries and laboratories. The program covers many topics of research related to the design, analysis and use of Artificial Intelligence systems. The doctoral program is designed to allow a full-time student entering with a Master of Science in Artificial Intelligence or Computer Science or any other equivalent Master to complete all degree requirements within four years. However, it is not uncommon for doctoral programs to take somewhat longer.

The program in numbers (2011/2012 academic year)	UPC 
New students	7
Students in the training period	2
Students in the research period	47
Thesis proposals	6
Ph.D. thesis presented	8
Total number of students 11/12	49

Research in Artificial Intelligence at the Software Department is a multi-discipline enterprise that covers many different topics related with including the understanding and reproduction in a computer of human problem solving as symbolic reasoning, knowledge representation, and learning. Research activities are organized around a number of semi-autonomous research groups, each of which is headed by one or more Professors or research scientists that develop basic as well as applied research.

Research groups	Contact person
<i>Knowledge Engineering and Machine Learning</i>	Dr. Javier Vázquez-Salceda, jvazquez@lsi.upc.edu Prof. Ulises Cortés, ia@lsi.upc.edu
<i>Softcomputing</i>	Dr. Àngela Nebot, angela@lsi.upc.edu
<i>Natural Language Processing Group</i>	Dr. Núria Castell, castell@lsi.upc.edu Dr. Lluís Padró, padro@lsi.upc.edu
<i>Logic and Programming</i>	Prof. Ma Lluïsa Bonet bonet@lsi.upc.edu Prof. Robert Nieuwenhuis, roberto@lsi.upc.edu

The staff involved in the Doctoral Programme in Artificial Intelligence leads or participates in the following multi-disciplinary research centers or spin-off companies originated at the Universitat Politècnica de Catalunya:

3Scale <http://www.3scale.net>

Co-Founder and CEO: Steve Willmott, steve@3scale.net

BSC: Barcelona Supercomputing Center, <http://www.bsc.es>

Director: Prof. Mateo Valero, mateo.valero@bsc.es

SISLtech, Sanejament Intel·ligent, S.L. <http://www.sisltech.net/en>

Co-Founders: Prof. Ulises Cortés, ia@lsi.upc.edu, Dr. Miquel Sànchez-Marrè, miquel@lsi.upc.edu

TALP: Research Center for Technologies and Applications in Language and Speech, <http://www.talp.upc.edu>

Director: José Adrián Rodríguez Fonollosa, adrian@talp.upc.edu